Proneural Protein Specificity in *Drosophila melanogaster*

Saw Myat Thanda Win Maung

A thesis presented for the degree of Ph.D.

University of Edinburgh

2004

Declaration

I declare that this thesis is my own work unless otherwise stated in the text, and that this work has not been submitted for any other degree or qualification.

Saw Myat Thanda Win Maung

September 2004

Acknowledgements

'In great darkness, remain true, dawn will come again' – the I Ching.

I'd like to thank the members of the Jarman lab, Petra zur Lage, Emma Rawlins, Davy Prentice, Lynn Powell, Eimear Holohan, Ivan Clark and Sebastian Cachero. You have given me support and made my time spent in the lab enjoyable.

Thank you to all my friends in Edinburgh and The Pond, especially big thanks to Ollie and 'Magic' Bob. I'd also like to thank my long-term buddies Ahmed, Graeme, Derek and Pete.

Thanks Mum and Dad for everything you've done for me, without your love and support I wouldn't be where I am today. Another big thanks to my brothers' Thura and Sithu who underline the importance of staying cool. And to Ali, you've seen me through all the way; it wouldn't have been the same without you.

Lastly but foremost, I'd like to thank my supervisor Dr. Andrew Jarman. Thanks Andy for giving me the biggest opportunity of my life and believing in me. Your patience and strength have been a huge inspiration and lifted me up at my lowest points.

'You can't always get what you want, but if you try sometimes, you might just find, you get what you need' –M. Jagger and K. Richards.

Abstract

Neural specification in *Drosophila melanogaster* requires the function of the proneural genes *achaete-scute*, *atonal* and *amos*. These genes encode transcription factors of the basic-helix-loop-helix (bHLH) family. The proneural genes are generally expressed in small groups of ectodermal cells called proneural clusters. One cell from this cluster is selected to become a sense organ precursor cell. This precursor cell subsequently divides and differentiates into the cells that make up a peripheral sense organ. Although any one of the proneural genes are sufficient for sense organ precursor selection, the fate of the sense organ precursor cell is determined by the specific proneural gene expressed. For example *achaete-scute* genes are required for the specification of external sense organs, *atonal* is required for specification of internal stretch-responsive organs and *amos* is required for the specification of olfactory organs. Thus proneural genes are required for neural competence and subtype specification.

I have investigated the nature of this subtype specificity by analysing the number, type and pattern of ectopic sense organ precursors produced by proneural gene misexpression in transformant flies. The bHLH domains of Atonal and Amos share 88% identity, however these proneural proteins have very different wildtype functions. Moreover, I show that they have abundantly distinct misexpression phenotypes. Importantly, I show that an apparent overlap in function is actually due to cross-activation of *atonal* by *amos*. I have investigated the functional specificity of *amos* with regard to *atonal* and *scute* by constructing chimeric proteins of Amos and Atonal, and also Amos and Scute. All previously published studies concerning sub-type specificity have concluded that the bHLH domain is the determining factor in all bHLH proteins. However, no chimeric studies have investigated the specificity between highly related proneural proteins such as Atonal and Amos.

Contrary to published studies, I found that Atonal specificity is determined to a large extent by its non-bHLH sequence. Reciprocally, the non-bHLH region of Amos can also facilitate Amos functions. However these results are only valid in the context of an Atonal-like bHLH

domain. Phenotypic analysis of Amos and Scute chimeras has reiterated the requirement for the Amos bHLH domain for Amos-like function and correspondingly the Scute bHLH domain for Scute-like function. In synopsis I conclude that subtype information is contained within the bHLH domains of highly divergent proneural proteins such as Amos and Scute; however closely related proneural proteins such as Amos and Atonal require elements outside the bHLH domain for complete subtype specification. I propose a model in which these sequence elements function via interaction with specificity co-factor proteins.

TABLE OF CONTENTS

List of Figures and Tables

Chapter 1. Introduction

Chapter 3. Comparison of the functional specificities of *atonal* and *amos*

Chapter 6. Conclusion

Abbreviations

ac	*-achaete*	g	-grams
amos	*-absent md neurones and olfactory sensilla*	gal	-galactosidase
AS-C	*-Achaete Scute-Complex*	GFP	-green fluorescent protein
ase	*-asense*	hrs	-hours
ato	*-atonal*	HRP	-horse radish peroxidase
boss	*-bride of sevenless*	*hs*	*-heatshock*
bHLH	-basic helix-loop-helix	l	-litre
bp	-base pairs	L-broth	-Luria broth
BSA	-bovine serum albumin	*l'sc*	*-lethal of scute*
°C	degrees Celsius	M	-molar
cato	*-cousin of atonal*	mAB	-monoclonal antibody
cDNA	-complimentary DNA	Mb	-megabase
ch	-chordotonal	mg	-microgram
cho	-chordotonal organ	mins	-minutes
CNS	-central nervous system	ml	-millilitre
CyO	*-Curly of Oster*	mM	-millimolar
da	*-daughterless*	mRNA	-Messenger RNA
DER	*-Drosophila epidermal growth factor receptor*	MW	-molecular weight
Dl	*-Delta*	*N*	*-Notch*
DNA	-deoxyribonucleic acid	N^{ICD}	-Notch intracellular domain
DNAse	-deoxyribonuclease	*OrR*	*-Oregan R*
dNTP	-deoxyribonucleoside triphosphate	p	-plasmid
ds	-double stranded	PBS	-phosphate buffered saline
EDTA	-diaminoethanetetra-acetic acid	PBTx	-PBT with Triton X-100
Egfr	*-epidermal growth factor receptor*	PCR	-polymerase chain reaction
emc	*-extramacrochaete*	pers. Comm.	-personal communication
EMS	-ethyl methyl sulphonic acid	pH	-$\log_{10}$ (hydrogen ion concentration)
ES	-external sensory	PNC	-proneural cluster
E(spl)C	*-Enhancer of split Complex*	PNS	-peripheral sense organ
pnt	*-pointed*	R	-photoreceptor

RCF	-relative centrifugal force
RNA	-ribonucleic acid
RNAse	-ribonuclease
RPM	-rotations per minute
rt	-room temperature
secs	-seconds
sc	-*sc*
sca	-*scaberous*
sens	-*senseless*
SOP	-sense organ precursor
Tris	-tris (hydroxymethyl) amino methane
UAS	-upstream activation sequence
μg	-microgram
μl	-microlitre
V	-volts
v	-volume
v/v	-volume for volume
y	-*yellow*

Chapter 1

Introduction

1.1. Neurogenesis

The development of the nervous system, i.e. neurogenesis, is complex and difficult to elucidate in higher vertebrates, but in evolutionary terms the same basic concepts are present today in the simplest metazoans through to the highest vertebrates. For this reason neurogenesis has been extensively studied in lower vertebrates such as the *Xenopus laevis* and the zebrafish, and also in invertebrates such as *Caenorhabditis elegans* and *Drosophila melanogaster*. These species are very good models for developmental biology because they are relatively inexpensive to keep, are easily manipulated genetically, and have a short life cycle.

Genetic research in *D. melanogaster (Drosophila* for short*)* has been on going since the early twentieth century. *Drosophila* has all the aforementioned advantages for the study of neurogenesis, and also has a very well defined nervous system. In particular, its peripheral nervous system is an excellent model for understanding fate determination and patterning in neurogenesis. This is further enhanced by the identification of cell specific markers such as 22C10 (Zipursky et al., 1984) and horse-radish peroxidase (Jan and Jan, 1982), which recognise epitopes on the surface of neurons. Furthermore enhancer trap lines such as A37 (Ghysen and O'Kane, 1989) and A101 (Ray and Rodrigues, 1995) have also been identified to recognise neural cell precursors and their subsequent cell types.

1.2. *Drosophila* sense organs

The adult peripheral nervous system (PNS) in *Drosophila* comprises of sense organs for various sensory modalities. Many of these consist of small organs know as sensilla (singular: sensillum). These include the external sense organs (sensory bristles) for touch and taste, internal chordotonal organs for proprioception, and three subtypes of olfactory sensillum for smell (Fig.1.1). In addition, vision and light detection is achieved via the compound eye and ocelli, which contain photoreceptors and support cells. The sense organs are made up of a limited number of cell types, which are mostly related by a

strictly regulated cell lineage. This makes location and cell composition of the sense organs very stereotyped, so they form an excellent model for identifying and studying the genes involved in their development.

1.2.1 External sense organs

The external sense (ES) organs are usually bristles or hairs with open tips to sense chemical stimuli or closed pointed tips for mechanoreception (McIver, 1985). The majority of external sense organs are the chaetae, located almost all over the surface of the fly and larvae. The chaetae can be large singular macrochaetae in tightly regulated stereotypical locations such as the notum and scutellum or small microchaetae, which are evenly spaced all over the cuticle. Their main job is to sense the environment by touch. This of course being extremely important for organisms with an exoskeleton. The chaetae are made up of the socket cell (tormagen), shaft cell (trichogen), sheath cell (thecogen), and are innervated by a solo neuron (Fig.1.1A). There are also other types of external sense organ such as the sensilla campaniformia of the wings. These organs are modified to sense not touch but cuticular strain and hence their sensilla are short and surrounded by a raised socket cell.

1.2.2 Chordotonal organs

The chordotonal organ is a homologous structure to the external sense organ however chordotonal organs are located internally (Moulins, 1976). Thus they do not require a trichogen cell; instead the main sensory structure is the scolopale. The scolopale is an elongated tube like structure consisting of microtubules, which can detect body movements and stretch. Accordingly, chordotonal organs are found in the hemisegments of the embryo and larvae and in the moving parts of the adult fly such as the wing hinge and leg joints. The scolopale is supported by a cap cell, attachment cell and ligament cell (Fig.1.1B). Like the external chaetae, each chordotonal unit is innervated by a single neuron. Unlike chaetae however, chordotonal organs are not required for spatial information and are generally found in clusters. An example of a large chordotonal array

is the Johnston's organ of the second antennal segment. This organ responds to more subtle stretch, i.e. vibration and functions as the fly ear (Fig.1.8).

1.2.3 Multiple dendtritic neurons

External sensory organs and chordotonal organs make up the major types of sensillum in the embryo. However a third type of sensory neurons exist, the multiple dendritic neurons. Very little is know about these types of internal organ however they are innervated by three neurons and can be classified by their position in the embryo. The multiple dendritic neurons with sub epidermal arborisations are known as the da neurons, those which innervate tracheal branches are known as td neurons and those with two opposing dendrites are known as bd neurons (Bodmer and Jan, 1987).

1.2.4 Olfactory organs

The olfactory sensilla are specialised chemoreceptors, located on the third antennal segment (funiculus) and maxillary palp (review (Stocker, 2001). They are composed of a trichogen and support cells. The shafts of these sensilla are very different from external mechanoreceptors. Firstly there are three morphologically distinct types; the trichodea, which are long and pointed, the basiconica that, are intermediate in size with rounded tips and the coeloconica, which are short and sharp (Fig.1.1D-F). Furthermore the shaft cell is perforated by microscopic holes, which allow the passage of chemical odours. The innervation of olfactory sensilla is rather complicated and dependent upon a number of factors such as shaft type, surface location and the combination of odorant binding receptors expressed (Clyne et al., 1997; de Bruyne et al., 1999; de Bruyne et al., 2001).

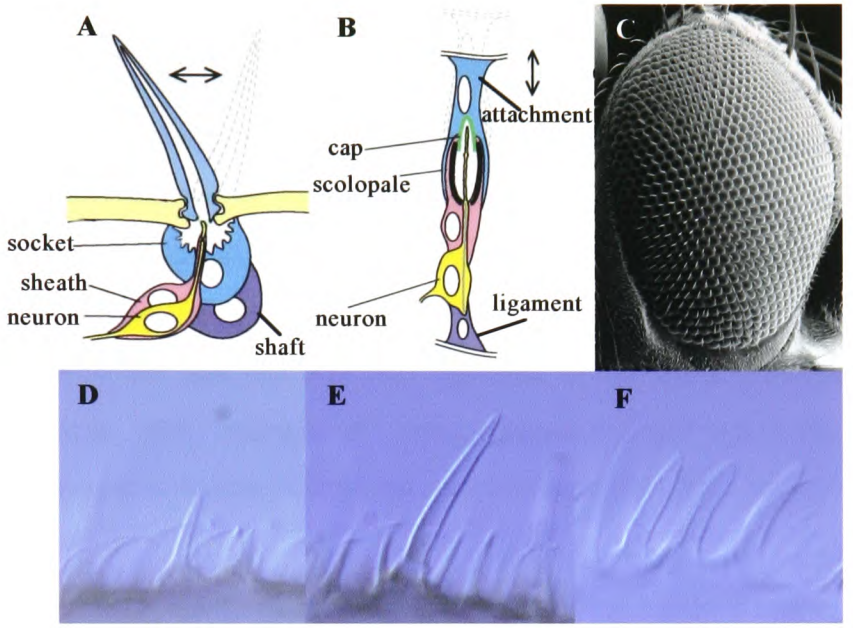

Figure 1.1 Sense Organs of *Drosophila melanogaster*

(A) External sensory bristle. **(B)** Internal chordotonal organ (**A** and **B** adapted from (Jarman, 2002). **(C)** Compound eye (*courtesy of K. Moses*) made up of 800 ommatidial units, each unit consisting of 8 photoreceptors and their support cells. **D-F** Olfactory sensilla, **(D)** Sensilla coeloconica, **(E)** Sensilla trichodea, **(F)** Sensilla basiconica.

1.3. Sense organ development

Drosophila is a holometabolous organism and as such, neurogenesis occurs in two separate stages. For the larval PNS, it occurs in mid embryogenesis; for the adult PNS it occurs in the imaginal discs of the late third instar larval and pupal stages. For sensilla, neurogenesis begins with the selection of sense organ precursor cells (SOPs) from undifferentiated ectodermal cells (Doe and Goodman, 1985; Jan and Jan, 1993). These SOPs divide and differentiate to form neuron(s) and support cells of the sensillum. This process appears to be similar, with variations, for all sensilla. This suggests that all sensilla derive from a common ancestral sensory structure. The process begins in a similar way in the eye, where the first event is selection of R8 photoreceptor precursors.

However, these cells do not divide like SOPs; instead they recruit surrounding cells to form the remaining photoreceptors and support cells of an ommatidium.

1.3.1 Sense organ lineage

Microchaetae were the developmental model for the first detailed investigation of cellular composition and cell lineage. The cell composition and structure of the external sense organ was determined using the electron microscope (Hartenstein and Posakony, 1989). The microchaete was observed as a unit of cells comprising of one neuron and three support cells. A fifth glial cell was later identified by the *LacZ* enhancer trap A101 (Boulianne et al., 1991; Huang et al., 1991). However the glial cell of the microchaete lineage undergoes apoptosis shortly after birth (Fichelson and Gho, 2003).

Cells of the sensory lineage have been identified with the neuronal marker MAb 22C10 and the mitotic divisions of the SOP have been followed using BrdU-labelling, organ specific GFP labelling and time-lapse confocal microscopy (Bodmer et al., 1989; Gho et al., 1999). From such studies, the most recent model of ES organ lineage has been developed (Fig.1.2).

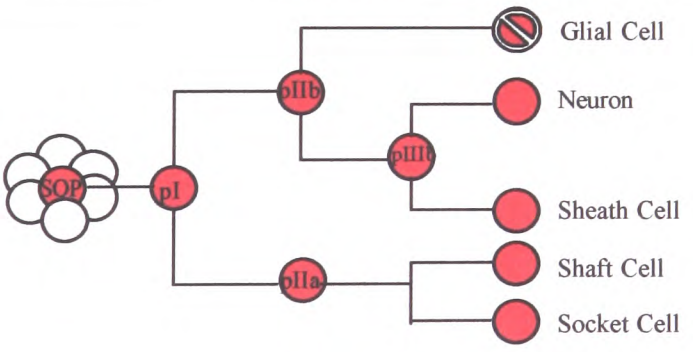

Figure 1.2 Model of External sense organ lineage. The external sense organ develops from three asymmetric divisions of the SOP (a.k.a the pI cell). The pI cell divides into two daughter cells; pIIa and pIIb. pIIa divides to produce the shaft/trichogen cell and socket/tormorgen cell. The pIIb cell divides to produce the pIIIb cell and a glial cell ,which undergoes programmed cell death. The pIIIb cell divides to produce the neuron and sheath/thecogen cell.

1.3.2 A common sense organ lineage

The external sense organs, internal chordotonal organs and embryonic and larval MD neurons were once thought to be derived from distinct classes of cell lineages. More recently however, the use of cell specific enhancer trap lines and cell markers have indicated that all sense organs may develop from variations of a common lineage program. For example, the enhancer trap marker A1-2-29 is expressed in shaft and sockets cells of the ES organ, however it is also expressed in the cap and attachment cells of the chordotonal organ (Blochlinger et al., 1991; Hartenstein et al., 1992). The sheath cell marker Prospero is also expressed in the scolopale (Doe et al., 1991; Vaessin et al., 1991) and the ligament cell is found to express glial specific markers. Thus the chordotonal organ is composed of equivalent cells to those of the ES organ (Fig.1.3); identified by the expression of daughter specific markers.

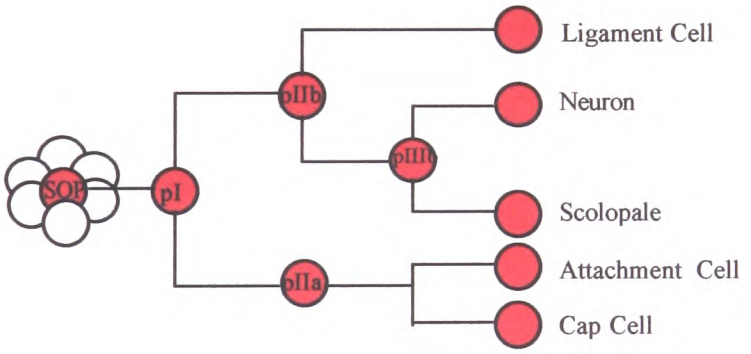

Figure 1.3 Model of adult chordotonal lineage. The chordotonal organ develops from three asymmetric divisions of the pI cell, akin to the ES organ lineage. To produce the cells of a chordotonal organ, there are changes in terminal cell fate. The pI cell divides into two daughter cells; pIIa and pIIb. pIIa divides to produce the attachment cell and cap cell. The pIIb cell divides to produce a ligament cell and the pIIIb cell. The pIIIb cell divides to produce the neuron and scolopale.

The olfactory lineage is the least investigated of all sense organs; however there is evidence that olfactory organs also originate from asymmetric divisions similar to those followed by chordotonal and ES organs. Olfactory organs are derived from cells of a presensillum cluster (Ray and Rodrigues, 1995). Clonal analysis suggests that the cells which make up an individual olfactory unit are composed of cells from distinct lineages (Reddy et al., 1997). The cells of the olfactory unit are derived from asymmetric divisions of unrelated pIIb-like and pIIa-like cells of the presensillum cluster. Like the ES organ lineage, the pIIb-like cell undergoes two asymmetric divisions to produce a glial cell, neuron and sheath cell (Sen et al., 2004). Similarly, the pIIa-like cell undergoes a single division to generate a shaft and socket cell. The olfactory organ is made up of further neurons derived from a pIIc cell, which has no equivalent in the ES lineage.

1.3.3 lineage specific cell death and cell proliferation

Some sense organs are derived from lineages, which have evolved further proliferative divisions such as the wing campaniformia and also lineages, which have incorporated apoptosis as an essential feature of neural lineage, such as the embryonic/larval md neurons. Sensilla campaniformia of the wings are composed of four sensory daughter cells from asymmetric division of the pI cell (Van De Bor and Giangrande, 2001). Unlike the microchaete lineage the glial cell does not under go apoptosis, but proliferates into a further 6 glial cells (Fig.1.4.).

Md neurons were recently found to derive from an ES-type lineage where pIIa and pIIIb cells specifically express the pro-apoptotic genes *reaper* and *grim* (Orgogozo et al., 2002). The cell lineage utilised here is similar to the ES organ lineage, however the glial cell does not undergo apoptosis but differentiates into the md neuron, the sibling cells pIIa and pIIIb do not undergo further divisions but are programmed to die (Fig.1.5).

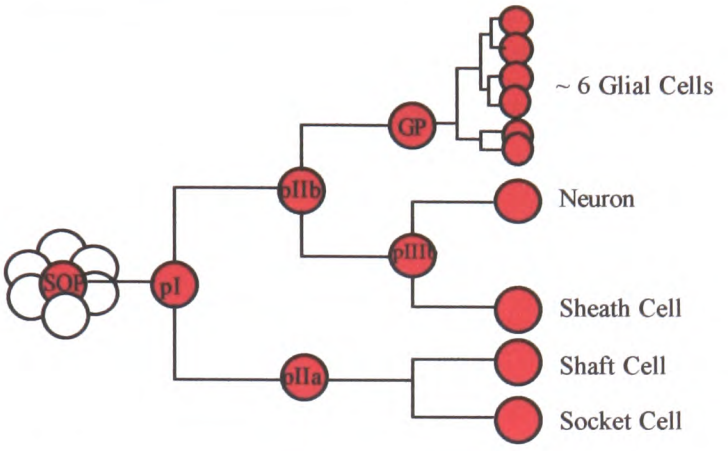

Figure 1.4 Model of wing campaniform sensilla lineage. The campaniform sensilla lineage is akin to the ES organ lineage. The glial cell however does not undergo apoptosis but becomes the glial precursor (GP) and divides to produce 6 further glia.

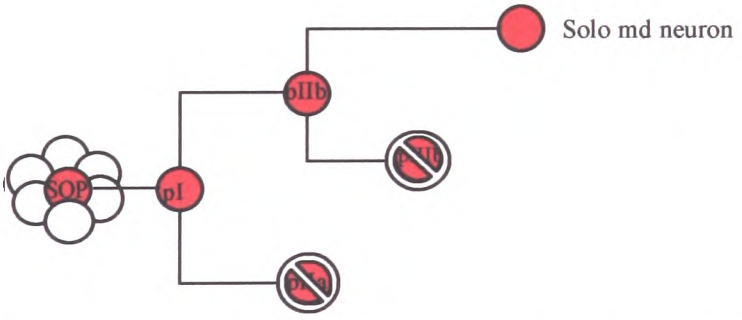

Figure 1.5 Model of embryonic/larval md lineage. The development of md neurons utilise the common lineage program. However this program is modified to include apoptosis of pIIIb and pIIa. The sibling cell of pIIIb is no longer a glial cell destined for apoptosis but becomes the md neuron.

1.4. Specification of sense organ precursors

Proneural genes are required for the specification of sense organ precursor (SOP) cells and R8 photoreceptors. This specification is thought to involve a common mechanism regardless of sense organ subtype. Proneural genes encode related transcription factors *atonal* (*ato*), *amos*, and the *achaete* (*ac*) and *scute* (*sc*) genes of the *achaete-scute* complex (*AS-C*). These genes are transiently expressed in specific areas of the developing ectoderm of the embryo or larval imaginal discs. The SOP is selected from within these groups of cells transiently expressing the proneural genes. This involves the interplay of the proneural genes with the neurogenic genes in a process of lateral inhibition (see Fig.1.7).

1.5. Defining features of proneural genes

Proneural genes are the primary drivers of neurogenesis and are the subject of this thesis. Apart from sequence (which will be addressed later), they are defined by three criteria. These are summarised here and then expanded upon subsequently.

(a) Expression pattern: proneural genes are expressed in groups of undifferentiated ectodermal cells, and then expression becomes refined to SOPs.

(b) Mutant phenotype: loss of proneural gene function results in loss of specific subsets of sense organs, due to failure in SOP selection.

(c) Misexpression phenotype: experimental misexpression of proneural genes results in ectopic sense organ formation, due to selection of supernumerary SOPs in inappropriate locations and numbers.

(d) Sequence: proneural genes encode transcription factors of the basic-helix-loop-helix (bHLH) family.

Only the proneural genes show all these characteristics, although several other genes may show one or more of them. For instance, the bHLH gene *asense* can cause ectopic

SOP formation when misexpressed, but it is not expressed prior to SOP formation and mutants do not general lack SOPs (Brand et al., 1993; Jarman et al., 1993a).

1.6. SOP formation by *achaete-scute* genes

Much of our knowledge for SOP specification is originally based on studies of the *AS-C*. This is summarised here. The *AS-C* comprises the genes: *ac*, *sc*, *asense* and *lethal of scute* (*l'sc*) (Campuzano and Modolell, 1992). The *AS-C* genes have been known and studied since the 1940's. Although there are four genes, only *ac* and *sc* are required for SOP formation in the PNS (Campuzano and Modolell, 1992). *asense* and *l'sc* play more minor roles in development, *asense* is the proneural gene for wing margin bristles and is also expressed downstream of all proneural genes (Brand et al., 1993; Jarman et al., 1993a). *l'sc* is required for muscle and CNS development (Carmena et al., 1995; Martin-Bermudo et al., 1993; Younossi-Hartenstein et al., 1996).

Loss-of-function studies of *ac* and *sc* show that the SOPs, which give rise to external bristles are lost (Dambly-Chaudière and Ghysen, 1987). *ac-sc* deficient mutant flies lack the majority of touch and gustatory bristles (Fig.1.6). Similarly in embryos, *AS-C* mutants lack all external sense organs, but other sense organs are unaffected.

The formation of solitary external sense organs begins with the expression of the *ac/sc* genes in a cluster of competent neural cells called the proneural cluster (PNC). One cell from the PNC is selected to become the SOP, which subsequently divides to form the different cells that make up the external sense organ. The process of precursor selection is regulated by the neurogenic genes such as *Notch* (*N*) and *Extramacrochaetae* (*EMC*) and the further division and differentiation of daughter cells is regulated by other genes known as asymmetric division and neural selector genes.

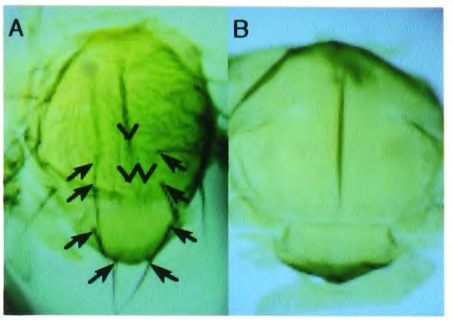

Figure 1.6. Loss of *achaete* and *scute* results in loss of all external sense organs. **(A)** wildtype thorax showing stereotypical number and position of microchaetae (arrowheads) and macrochaetae (arrows). **(B)** The double mutant for *achaete* and *scute* (sc^{10-1}) shows no development of macrochaetae or microchaetae on the fly mesothorax. (Images adapted from Brand et al., 1993)

1.6.1 Defining domains of proneural gene expression

The master control genes (homeobox genes) and prepattern genes mark out certain areas of undifferentiated ectodermal cells to become competent to express the proneural genes. For example *decapentaplegic*, *wingless*, *pannier*, the *Iroquois* complex and *u-shaped* are prepattern genes expressed in the wing imaginal discs and are required for the spatial expression of *ac* and *sc* (Cubadda et al., 1997; Gomez-Skarmeta et al., 1996; Haenlin et al., 1997; Ramain et al., 1993; Sato and Saigo, 2000). In the embryo, segment polarity genes and pair-rule genes outline areas for the expression of *ac* and *sc* (Skeath et al., 1992). In this way prepattern genes control where and when proneural gene expression occurs (Jan and Jan, 1993).

1.6.2 Precursor selection

The following process of sense organ precursor (SOP) cell selection has been most clearly and extensively investigated in the wing imaginal discs of third instar larvae (Cubas et al., 1991; Huang et al., 1991; Skeath and Carroll, 1991). In discs, expression of *ac* and *sc* are restricted to groups of around 10-30 ectodermal cells which make up the PNC (Cubas et al., 1991; Romani et al., 1989; Skeath and Carroll, 1991). It is from

the PNC that the SOP cell is derived (Fig.1.7). The location of bristle formation on the epidermis is stereotypically arranged due to factors, which regulate SOP selection.

ac/sc expression in each cell of the PNC is directly inhibited by surrounding adjacent cells by a process of lateral inhibition mediated by the Notch-Delta signalling mechanism (Ghysen et al., 1993; Simpson, 1997). *Notch* is involved in many cell fate decisions in many different organisms and as such, much work continues on its functions and interactions. However for the purpose of SOP selection, *Notch* is required for the singling out of one cell from a group of competent cells.

Notch encodes a type I transmembrane receptor which is responsive to type I transmembrane ligands encoded by *Delta* (*Dl*) and *Serrate,* however *Serrate* is not involved in neurogenesis but is required for wing morphology (Parks and Muskavitch, 1993; Parody and Muskavitch, 1993; Speicher et al., 1994). When the Notch receptor is activated by its ligand Delta, Notch is cleaved and the intracellular portion of the receptor (N^{ICD}) sequesters the Suppressor of Hairless [Su(H)] transcription factor and translocates to the nucleus (Fortini and Artavanis-Tsakonas, 1994; Jennings et al., 1995). Once sequestered into the nucleus, Su(H) binds to upstream activating sequences of the *Enhancer of split* [*E(spl)*] group of genes (Bailey and Posakony, 1995). The E(spl) proteins generally act as transcriptional repressors with the product of the neighbouring gene *Groucho* (Heitzler et al., 1996). In this way, proneural gene expression in that competent cell is inhibited.

Both Notch and Delta are expressed on the cell surface of all competent cells and thus inhibitory signals are sent between all the cells of the proneural cluster. Some cells of the PNC become dominant over others and are then less affected by inhibitory signals from adjacent cells. This may occur as a consequence of high Delta : low Notch ratios and the initial expression levels of the proneural genes, in this case *Dl* transcription is activated by Ac/Sc (Cubas et al., 1991; Goriely et al., 1991; Heitzler et al., 1996; Kunisch et al., 1994). Eventually one or a few cells of the PNC retain and then increase their proneural

gene expression to become committed to the neural lineage. The dominant cell(s) delaminates from the ectoderm and becomes the SOP (Hartenstein et al., 1994) (Fig.1.7). Neural competence in the remaining cells of the PNC is lost, as proneural gene expression in these cells is inhibited and they return to ectodermal fate.

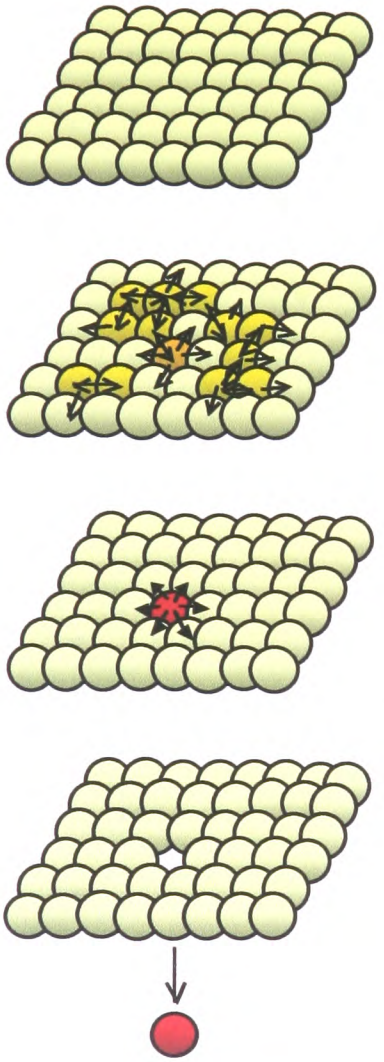

Step 1. Undifferentiated ectodermal cells.

Step 2. *AS-C* expression (orange) in uncommitted proneural cluster cells and lateral inhibition via *Notch* and *Delta* cell signalling.

Step 3. One cell gains dominance and continues proneural gene expression, the rest of the cells in the proneural cluster return to ectodermal fate.

Step 4. Dominant cell becomes committed and becomes the SOP cell, then delaminates from the ectoderm.

Figure 1.7. Sense organ precursor formation. Proneural gene expression begins in a group of undifferentiated cells to form the proneural cluster. Lateral inhibition restricts proneural expression to one cell, which subsequently delaminates from the ectoderm and becomes the sense organ precursor cell.

1.6.3 Maintenance of the sense organ precursor cell

After SOP selection, proneural gene expression within the SOP continues and activates a range of pan-neural precursor genes before being switched off (Jarman and Jan, 1995). The pan-neural precursor genes (as indicated by their name) are thought to be universally required for the maintenance and further development of all SOPs. The pan-neural genes represent a diverse group of regulatory proteins whose functions are still being assessed. Some pan-neural genes such as *deadpan* (*dpn*), *scratch* (*scrt*), and *senseless* are thought to be required for maintenance of the SOP and their deletion results in a significant loss of neurons (Bier et al., 1992; Emery and Bier, 1995; Jafar-Nejad et al., 2003; Roark et al., 1995). Other pan-neural genes such as *asense* provide neural information for further differentiation (Campuzano and Modolell, 1992). Interestingly, *asense* is also part of the *AS-C*. However *asense,* like *dpn* and *scrt*, act downstream of the proneural genes as indicated by the presence of cis regulatory elements which are activated by *ac* and *sc* (Jarman et al., 1993a).

Some pan-neural genes function by regulating the activity of other pan-neural genes, for instance *prospero* (*pros*) inhibits the expression of *dpn* and *scrt* and is required for neuronal development in the CNS (Doe et al., 1991; Li and Vaessin, 2000; Vaessin et al., 1991). Other pan-neural genes such as *scabrous* (*sca*) (Mlodzik et al., 1990) repress surrounding undifferentiated cells from taking on the neuronal fate.

As well as the pan-neural genes, there are also specific down stream target genes, required for specific neuronal lineages. *atonal* downstream target genes include *cousin of atonal* (*cato*) which is required for determination of chordotonal precursor cells (Goulding et al., 2000a) and TAKR86C (Powell et al., 2004).

1.6.4 Asymmetric division and neural selector genes

After SOP selection and delamination, the SOP undergoes a series of asymmetric divisions which give rise to the neurons and support cells of the sense organ. Many of the pan-neural genes expressed in the SOP are also expressed in the daughter cells, revealing their potential to influence asymmetric cell division. In addition to the pan-neural genes, asymmetric cell division genes are also expressed in subsets of daughter cells. These asymmetric division genes generally influence the expression of Notch. The activity of Notch is a determining factor in asymmetric division as well as SOP selection. (Schweisguth et al., 1996). In sister cells, one cell becomes the net N sender and the other the net Notch receiver.

In cases where Notch is misexpressed or in mutants of Notch antagonists such as *numb*, the daughter cells adopt the non-neural fate i.e. socket cells (Hartenstein and Posakony, 1990). *numb* is required in the neural precursor cell and without its expression, neurons fail to develop (Uemura et al., 1989), as such *numb* is an asymmetric division gene. Overexpression of *numb* or loss of Notch causes the opposing phenotype, all daughter cells become neural and sheath cells (Rhyu et al., 1994). Other asymmetric division genes such as *tramtrack* (*ttk*) act down stream of *numb* and are involved in glial versus neuronal fate in the CNS (Guo et al., 1995). *ttk* also inhibits *asense* and *deadpan* (Badenhorst, 2001).

The neural selector genes control the terminal fate choice of the lineage program. For example the homeobox gene *cut*, controls the terminal fate choice between the chordotonal and external sense organ. The component cells of the ES organ require expression of *cut*, but if *cut* is inhibited, chordotonal component cells differentiate in their place (Bodmer et al., 1987; Jarman and Ahmed, 1998; Merritt, 1997; Merritt et al., 1993). It is thought that *cut* represents the molecular switch for the formation of external sensory cells, and in its absence, only internal sensory cells develop (Blochlinger et al., 1990). In support of this theory, *cut* is found to determine the fate choice between ES and md neurons (Brewster et al., 2001). However in this case asymmetric division genes such as

numb, *inscuteable* and *Hamlet* are also required for the md fate choice (Moore et al., 2002; Orgogozo et al., 2001; Vervoort et al., 1997). Thus the SOP (pI) cell has certain multipotent properties and the final type of sensory organ produced is influenced by expression of the selector genes.

1.7. SOP formation by *atonal*

Loss of the entire *AS-C* leaves chordotonal organs, photoreceptors and olfactory organs unaffected (Dambly-Chaudière and Ghysen, 1987). It was suggested that related gene(s) must be responsible for SOP formation for other sense organs. In the early 1990's a related gene was identified and cloned on the basis of sequence homology to the *AS-C* genes; this gene was named *atonal* (*ato*) (Jarman et al., 1993b).

1.7.1. *ato* and chordotonal organ specification

During development, *ato* is expressed during neurogenesis in both the embryo and imaginal discs. In general, expression is as expected for a proneural gene. Expression begins in groups of ectodermal cells (PNCs) and becomes refined to SOPs. *ato* PNC expression prefigures the appearance of chordotonal organ SOPs in the embryo and leg, wing and antennal imaginal discs (Jarman et al., 1995)

Loss-of-function evidence was initially provided by the loss of chordotonal SOPs and organs in deficiencies spanning the genomic region of *ato* (Jarman et al., 1993b). Subsequently, direct and unequivocal evidence that *ato* is the proneural gene for chordotonal organs came by the isolation of *ato* point mutants (Jarman et al., 1995). ato^{1} has mutations in its bHLH domain and is possibly a null. ato^{3} is a truncation that removes the entire bHLH domain. In both cases, mutant embryos lack all chordotonal organs except for one that sometimes remains in the embryonic lateral cluster (Jarman et al., 1995). Some multiple dendritic neurons which are closely associated with the ventral chordotonal organs are also missing (Jarman et al., 1993b; Jarman et al., 1995). Despite this loss, mutant ato^{1} flies are viable. They lack all chordotonal organs including the

Johnston's organ in the antenna – the fly's ear (Fig.1.8). This results in flies being deaf and lacking negative geotaxis.

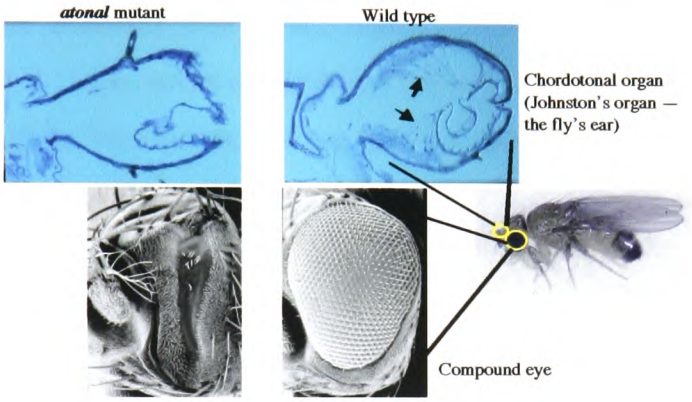

Figure 1.8. *ato* is required for chordotonal organs (Johnston's organ of second antennal segment depicted) and photoreceptors of the compound eye. The *ato*[1] mutant results in loss of chordotonal organs (arrows) and the R8 photoreceptors and subsequently the entire compound eye. (Images adapted from (Jarman et al., 1995)

1.7.2. *ato* and eye development

The most visibly striking phenotype of *ato* mutant flies is their loss of the compound eye (Fig.1.8) and ocelli. This loss is because *ato* is required for the specification of R8 photoreceptors (Jarman et al., 1994). The compound eye is made up of around 800 units of cells called ommatidia. Each ommatidium comprises of eight photoreceptors and their support cells. The ommatidial units are arranged into a hexagonal structure to form the *Drosophila* compound eye. The R8 photoreceptor is the first cell of each ommatidium to be specified and is required for the further development of the ommatidium. The precursor cells that differentiate into R8 photoreceptors are specified in the eye imaginal discs within the morphogenetic furrow. The morphogenetic furrow is a band of gene expression that moves posterior to anterior across the undifferentiated ectoderm of the eye disc.

During R8 selection, *ato* is expressed in a band of cells immediately preceding the morphogenetic furrow. As the furrow moves on, *ato* expression in the furrow becomes restricted to groups of around 12 cells called the intermediate groups (Jarman et al., 1995). The intermediate groups of cells expressing *ato* are evenly spaced due to the secreted protein Scabrous (Lee et al., 1996). Lateral inhibition further resolves *ato* expression to 2 or 3 cells, which are known as the equivalence group (Baker et al., 1996; Dokucu et al., 1996). Very quickly, one cell from the equivalence group is selected as the R8 founder cell (Baker and Yu, 1998).

1.7.3. *ato* and local neural recruitment

The R8 photoreceptor is required for the recruitment of local undifferentiated cells, which subsequently differentiate into the other 7 photoreceptors and 12 support cells of the ommatidia (Cagan, 1993; Freeman, 1996; Tomlinson and Ready, 1987). This local recruitment is achieved by receptor tyrosine kinase signalling mediated via *sevenless* and epidermal growth factor receptors (Egfr), in *Drosophila* known as DER (Domínguez et al., 1998; Freeman, 1994; Kumar et al., 1998; Tio et al., 1994; White and Jarman, 2000; Yang and Baker, 2001). Consequently, in ato^1 mutants the entire eye is missing since no recruitment occurs in the absence of R8 cells.

Local recruitment also occurs during chordotonal organ formation. Notch signalling restricts chordotonal SOP numbers, but DER signalling promotes recruitment of further SOPs in both the embryo and the leg imaginal disc (zur Lage et al., 1997; zur Lage and Jarman, 1999). Thus an organised array of chordotonal organs results. Interestingly, Egfr signalling also plays a role in *AS-C* dependent bristle patterning (Culi et al., 2001), but is not involved in the formation or recruitment of the SOPs. Thus a major difference in neurogenesis between *AS-C* and *ato* is that the former leads to the formation of solitary SOPs and *ato* expression promotes groups or clusters of SOPs/photoreceptors, attributable to *DER* dependent recruitment.

1.7.4. *ato* and olfactory sensilla

More recently, it was discovered that *ato* is also required in olfactory sense organ development. Olfactory sensilla comprise three main classes based on morphology: sensilla coeloconica, trichodea and basiconica (Fig.1.1 D-F) (Shanbhag et al., 1999). The arrangement of the olfactory sensillum in the antenna is organised into large bands on the third segment. The sensilla trichodea occupy the lateral surface and the sensilla basiconica occupy the medial surface of the third segment. The sensilla coeloconica occupy the remaining areas. Whilst the sensilla trichodea and basiconica are unaffected in ato^1 mutant flies, sensilla coeloconica are drastically reduced (Gupta and Rodrigues, 1997; Reddy et al., 1997). This suggests that *ato* is the proneural gene for sensilla coeloconica in addition to chordotonal organs and R8 cells. In the antennal disc, *ato* is expressed in many small PNCs consisting of 3-4 cells. Expression in each PNC becomes refined to single SOPs, and there is no apparent recruitment of further SOPs (Gupta and Rodrigues, 1997).

1.8. SOP formation by *amos*

Embryos mutant for both *AS-C* and *ato* lack almost all sensory neurons (Huang et al., 2000b; Jarman et al., 1993b). However, a few do remain. These include the dorsal bipolar dendritic neuron (dbd) and an adjacent multiple dendritic neuron (dda), and also many neurons in the head. Moreover, two important classes of adult olfactory sensilla are unaffected in *AS-C* or *ato* mutants (Reddy et al., 1997). This led to the search for and discovery of the last proneural gene, *amos* (*absent multidendritic neurons and olfactory sensilla*). *amos* is closely related to *ato*. Disruption of *amos* expression in the embryo by *amos* RNAi results in the loss of dbd and dda neurons, corroborating the requirement of *amos* for their development (Huang et al., 2000b). More recently, specific *amos* point mutations have been isolated that confirm this requirement. $amos^1$ is a truncation of the bHLH domain and is likely to be a null (zur Lage et al., 2003). Consistent with its proneural function, in the embryonic PNS *amos* is expressed in a small PNC in each abdominal segment at stage 9. By late stage 11, *amos* expression is refined to a single

SOP before being switched off (Goulding et al., 2000b; Huang et al., 2000b). This suggests that SOPs defined by *amos* utilise lateral inhibition in the refinement of proneural gene expression, just as *AS-C* and *ato*.

amos mutants are viable. The mutant adults are largely normal except for loss of olfactory organs from the third antennal segment (zur Lage et al., 2003). Here, the mutants lack all sensilla basiconica and trichodea, whilst the sensilla coeloconica are unaffected. Interestingly, in place of the missing olfactory sensilla, there appears ectopic external sense organs (Fig.1.9). This is thought to be due to inappropriate *AS-C* function which must normally be suppressed by *amos* (zur Lage et al., 2003).

In the antennal disc, *amos* is expressed at a later developmental stage from *ato* (zur Lage et al., 2003). Initially, expression is in three broad swathes of cells. Unusually, SOPs seem to delaminate from these giant PNCs continuously over a long period of time during pupal development.

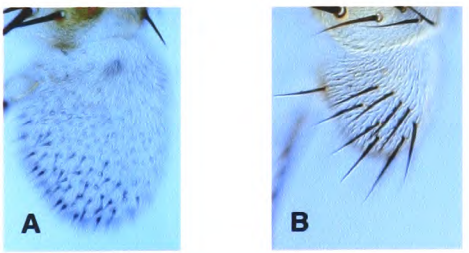

Wild type

***amos*^{1}**

No sensilla basiconica
No sensilla trichodea
Ectopic sensory bristles

Figure 1.9 *amos* is required for sensilla trichodea and basiconica. The *amos*^{1} mutant **(B)** results in loss of all *amos* dependent olfactory sensilla and shrinkage of the third antennal segment, compared to wildtype **(A)**. (Images adapted from (zur Lage et al., 2003)

1.9 Summary of wildtype proneural gene functions

With the discovery of *amos*, the origin of the entire PNS could be explained (Table 1.1). *AS-C* is required for the formation of external sense organs, *ato* for chordotonal organs, R8 photoreceptors and a subset of olfactory sensilla. *amos* is required for the embryonic and larval bipolar dendritic md neurons and the remaining classes of olfactory sensilla.

Table 1.1. Summary of proneural gene function in adult sense organ specification

ac, sc	*ato*	*amos*
External sense organs	Chordotonal organs	ddb and dda neurons
	R8 precursors	Sensilla basiconica
	Sensilla coeloconica	Sensilla trichodea

1.10 Proneural genes can provoke ectopic SOP formation

One of the defining features of proneural genes is that their misexpression is sufficient to promote SOP formation in ectopic ectodermal locations. On this basis, it has been said that proneural genes are both necessary and sufficient to drive neurogenesis (e.g. (Jan and Jan, 1993).

1.10.1 Misexpression experiments

The evidence for this characteristic originally came from gain-of-function mutations of the *AS-C* that are known as *Hairywing* (*Hw*) (Campuzano et al., 1986). In such flies, *ac/sc* are ectopically expressed in the wing disc, which results in supernumerary sensory bristles on the wing and thorax. Subsequently, evidence has come from experimentally induced misexpression of proneural transgenes. Induction of *sc* under the control of a heatshock promoter results in extensive ectopic bristle formation (Rodriguez et al., 1990). The pattern of ectopic bristles depends on the time of development at which induction takes

place. More recently, ectopic expression of all proneural genes is routinely performed using the Gal4/UAS system (Brand and Perrimon, 1993; Chien et al., 1996; Huang et al., 2000b; Jarman and Ahmed, 1998; Jarman et al., 1993b).

1.10.2 Misexpression experiments provide evidence for subtype specificity

In early models of SOP formation, it was proposed that proneural genes make SOPs whereas a second layer of 'neural selector' genes, such as *cut*, endows these SOPs with specific subtype fates (Blochlinger et al., 1990; Blochlinger et al., 1991; Bodmer et al., 1987; Jack, 1985; Merritt, 1997). An assumption was that proneural genes themselves did not take part in this process. However, misexpression experiments have shown that proneural genes do influence SOP subtype fate. The range of ectopic sense organs produced after misexpression under identical conditions differs for the three types of proneural gene (Table 1.2).

Table 1.2. The Effect of Proneural Gene Misexpression on Ectopic Sense Organ formation

	ac, sc	*ato*	*amos*
External sense organs	+++	(+)	(+)
Chordotonal organs	-	+++	++
Olfactory organs	-	-	+++

(+) Represents positive effect on ectopic sense organ formation, (-) represents no effect on sense organ formation. *AS-C* misexpression produces ectopic bristle formation but has no effect on the other sense organ subtypes. Both *ato* and *amos* misexpression can also induce ES organs but have a stronger affect on other sense organ subtypes. *ato* has a strong positive effect on the formation of ectopic chordotonal organs. *amos* induces the formation of ectopic olfactory sensilla. Interestingly, *amos* can also specify ectopic chordotonal organs. (Adapted from Jarman and Ahmed, 1998).

1.11 Subtype specificity

To some extent, the proneural capabilities in misexpression experiments correlate with their wildtype functions (deduced from mutants), but there are several complications that lead to an apparent loss of specificity after misexpression. For instance misexpression of *amos* accordingly leads to the formation of ectopic olfactory-like sensilla and extra sensilla trichodea and basiconica, however some *ato* dependent sense organs are also affected. The number of sensilla coeloconica formed on the funiculus is increased and furthermore chordotonal organs are specified in ectopic locations (Goulding et al., 2000b). This is the first example where misexpression of a proneural gene produces phenotypes discordant with its wildtype function. This loss of specificity by *amos* requires further investigation if phenotypic analysis of proneural misexpression is to be used as a reliable method to investigate protein specificity. Clearly, misexpression experiments can produce artefactual results, and they must be interpreted with caution. On the other hand, they have also proved invaluable for defining new functions of the different proneural proteins. This will be explored further in Chapter 3.

Subtype specificity has led to the 'two function' model (Fig.1.10). All proneural genes share a basic SOP selection function, which is achieved through regulation of a common set of target genes. However, other target genes are differentially regulated and lead to different subtypes of SOP fate. There is much interest in determining

(a) what these target genes are, and
(b) how they are differentially regulated

The latter is particularly the focus of this thesis. I wish to understand how the structures of the proneural proteins relate to their differing subtype determining roles in SOP formation. As mentioned, proneural genes encode transcription factors of the bHLH family. What is known of this family is summarised next.

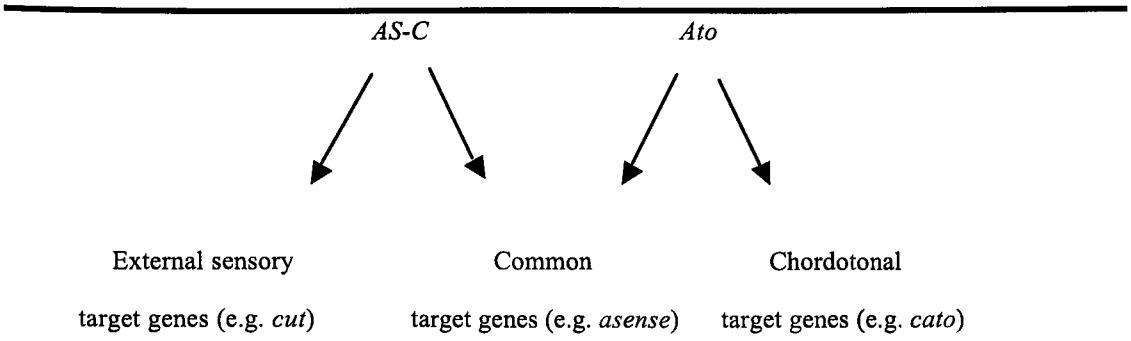

Figure 1.10. The two function model of proneural genes. The proneural genes are required for the development of sense organs and function in two ways. Firstly they provide neural competence to uncommitted cells and subsequently this competence is maintained by the activation of common target genes. Secondly the proneural genes provide neural subtype identity by activation of sense organ specific target genes.

1.12 bHLH transcription factors

The proneural genes encode transcription factors of the basic helix-loop-helix (bHLH) superfamily of transcription factors. The transcription factors of this superfamily contain a conserved sequence of around 60 residues; the bHLH domain. This conserved motif is thought to fold into a helix-loop-helix structure when adjacent to highly charged regions (Murre et al., 1989). The structure of this motif can be divided into two functional regions; the basic or binding (b) region and the dimerisation helix-loop-helix (HLH) region. The b domain consists of around 12-15 hydrophilic residues, half of which contact DNA, this is followed by two hydrophobic α-helices separated by a non-conserved flexible region of amino acids termed the loop.

1.12.1 bHLH proteins are important regulators of development and cell fate

Proteins of the bHLH family have functions in cell proliferation, subtype determination and differentiation. In fact bHLH proteins are found in plants and metazoans. For vertebrate and invertebrate organisms, these factors play a role in divergent developmental pathways such as haematopoiesis (Bain et al., 1994; Porcher et al.,

1999; Porcher et al., 1996), myogenesis (Davis et al., 1987) and neurogenesis (DamblyChaudiere and Vervoort, 1998; Lee, 1997a; Vetter and Brown, 2001). In all cases, the bHLH domain is the structural motif that is critical for protein function.

1.12.2 Classification of bHLH proteins

The bHLH domain was initially defined based upon sequence homologies shared between the immunoglobulin enhancer-binding proteins, *myc* oncogenes, myogenic determination genes and proneural genes. The superfamily of bHLH proteins consist of four distinct groups; A, B, C and D (Atchley and Fitch, 1997).

Group B includes functionally unrelated proteins such as *Myc*, *Max*, *MITF*, *SREBP*, *USF* and Enhancer of Split related proteins (HER) (Fisher and Caudy, 1998; Goding, 2000; Henriksson and Luscher, 1996). Group B proteins bind to sequences known as N-boxes (Akazawa et al., 1992) and may have additional functional domains such as the Leucine Zipper (Thiem and Miller, 1989) and WRPW domain (Fisher et al., 1996).

Group C includes the family of bHLH-PAS proteins, so named according to the first three proteins identified with this motif; *Drosophila* Period, human ARNT and *Drosophila* Single-minded. The PAS motif is around 260-310 residues long and allows specific dimerisation with other PAS proteins (Crews, 1998).

Group D proteins only contain the HLH region of the bHLH motif and act as negative regulators of bHLH protein function. This group includes the Id's (inhibitors of differentiation) (Benezra et al., 1990) and Extramacrochaetae (Ellis et al., 1990; Garrell and Modolell, 1990). The HLH proteins sequester bHLH proteins by dimerising with them. Because these proteins have no b-domain, the heterodimer formed is unable to bind to DNA or other bHLH proteins and becomes functionally inert (Van Doren et al., 1991; Van Doren et al., 1992).

Group A includes tissue-specific proteins such as MyoD and the proneural proteins as well as their ubiquitously expressed partner proteins. Group A bHLH proteins have functions in development and can be subdivided into two further classes; I and II. Expression patterns and dimerisation properties govern sub-class determination of the group A bHLH proteins.

Other classifications of the bHLH proteins do exist, however they are generally the same groups of proteins given different group names (Ledent and Vervoort, 2001; Massari and Murre, 2000). The more recent classifications of the bHLH proteins, are similar to the original classification by Atchley and Fitch (1997). For example Ledent and Vervoort (2001) have added two further groups; E which includes *Enhancer of split* genes and group F, furthermore they have grouped together A and D proteins based on phylogenetic evidence. No doubt these classifications will continue to develop as more bHLH proteins are found.

1.12.2.1 Group A bHLH proteins

Class I proteins, also known as E-proteins, are ubiquitously expressed, whilst class II proteins have tissue specific expression patterns. In most cases class I proteins form functional heterodimers with class II proteins (review (Massari and Murre, 2000), however in some instances, the bHLH homodimer is the functional form (Choi et al., 1996; Shao et al., 1997; Zhang et al., 1999; Zhuang et al., 1996; Zhuang et al., 1994).

Most class II proteins do not readily form homodimers with themselves or other class II proteins but rely upon heterodimerisation with E-proteins for function (see Fig.1.11) (Gradwohl et al., 1996; Hsu et al., 1994b; Lassar et al., 1991; Van Doren et al., 1992; Wendt et al., 1998). When heterodimerisation occurs, the DNA binding domains of both partner proteins are brought together to form a new DNA binding interface. The bHLH heterodimer complex is then able to recognise and bind to DNA residues called E-boxes to initiate transcription (Dang et al., 1992; Murre et al., 1989; Voronova and Baltimore, 1990).

Class II proteins bind universally to E-protein partners (Hsu et al., 1994a) however the functional specificity of the heterodimer is governed by the class II protein. For example, the *Drosophila* E-protein Daughterless, is required for dimerisation with the Achaete-Scute complex, Atonal and Amos (Cabrera and Alonso, 1991; Goulding et al., 2000b; Jarman et al., 1993b), all of which specify the developmental pathways of different neural lineages. For this reason, the E-proteins are generally regarded as adapter proteins and are unlikely to be involved in functional specificity.

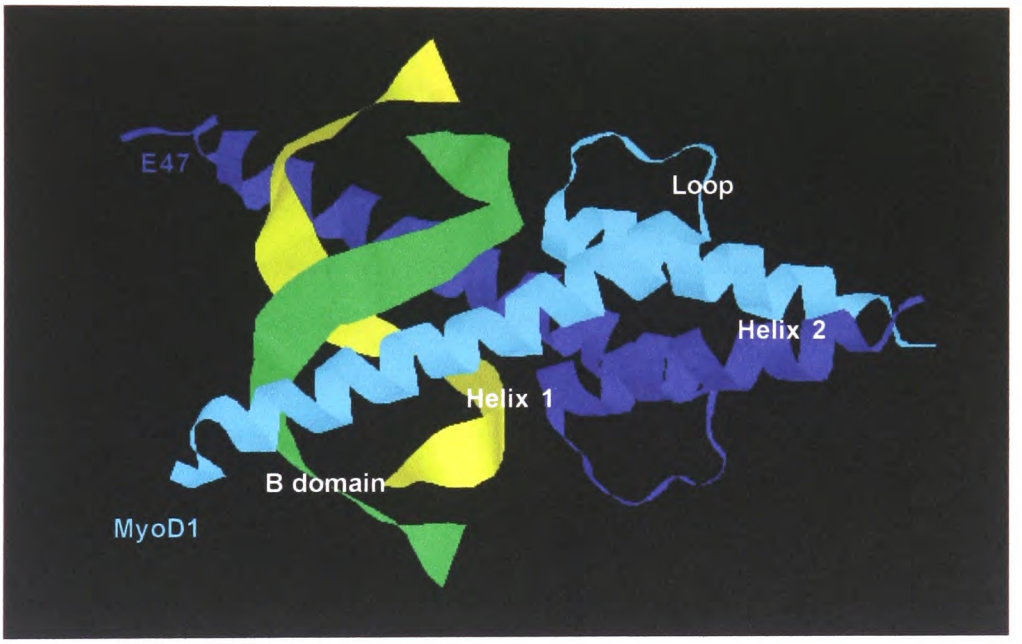

Figure 1.11. Heterodimerisation of Group A bHLH transcription factors, represented by MyoD and E47. This computerised image was obtained by the x-ray crystalline structure of the mammalian MyoD bHLH protein (turquoise) and partner protein E47 (blue) (Ma et al., 1994). The heterodimer is then able to bind to DNA (green and yellow strands). The structure of the bHLH motif is highly conserved and computerised structures can be altered to represent heterodimerisation of all group A proteins.

1.13 Proneural proteins as bHLH transcription factors

The *Drosophila* proneural proteins fall into the group A, class II bHLH category. Their basic regions interact with the DNA binding sites of the enhancers of downstream developmental genes. Their HLH regions form heterodimers with the corresponding region of the *daughterless* (*da*) gene product (Caudy et al., 1988; Vaessin et al., 1994). The proneural/Da heterodimer is then able to bind to consensus E-box sequences (gCAGSTGK) (Cabrera and Alonso, 1991) and activate pan-neural precursor genes and neuronal type selector genes (Jan and Jan, 1993). More recently there is evidence of proneural specific e-boxes for Scute and Ato (Powell, 2004).

1.13.1 Sequence and structural relationships between the proneural proteins

If proneural proteins impart sense organ specificity, where does this specificity lie? All the proneural proteins share some identity between their bHLH domains but no homology out with these domains has been found. Sequence analysis of the bHLH domains of the AS-C family show that they share 70% identity. However bHLH sequence homology between Ato and Sc is only 42%. *amos* and *ato* being part of the same subfamily show 88% bHLH identity (Fig.1.12). Together, *amos* and *ato* are known as the Ato-like proneural genes.

The bHLH regions are so conserved that the computerised model of MyoD-E47 heterodimer interaction with DNA (Fig.1.11) can be manipulated to show the Daughterless- Ato or Scute heterodimer interaction with DNA (Ma et al., 1994). Substitution of the divergent residues of MyoD and E47 with those of Ato-Da and Sc-Da show that the DNA contacting residues and dimerisation residues are conserved between Ato (also Amos) and Scute (Chien et al., 1996). This suggests that differences in bHLH function must be down to the non-conserved residues. Interestingly most of the non-conserved residues point away from the DNA and HLH interaction interfaces suggesting that they may be available for interaction with specific cofactors. Indeed

pointed has been recognised as a putative cofactor for femoral chordotonal organs. (zur Lage et al., 2004).

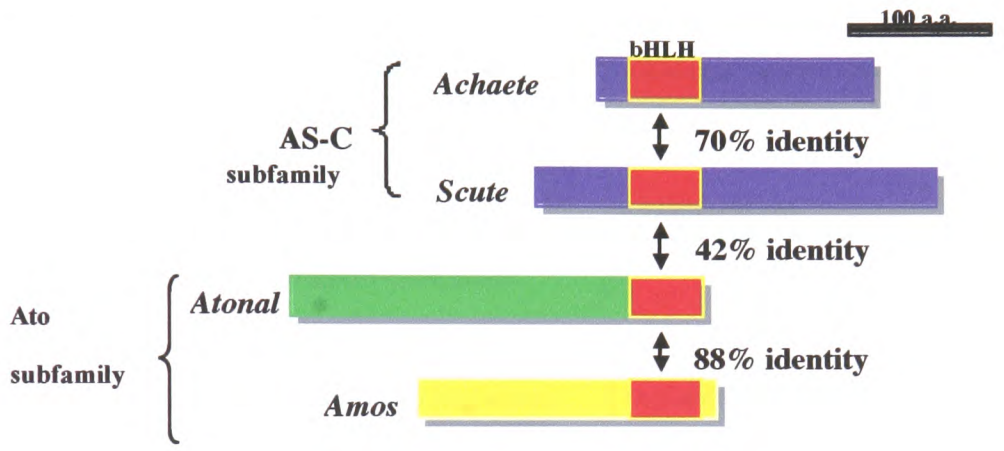

Figure 1.12. Sequence identity between the bHLH regions of proneural proteins. The highest identities are found within bHLH family groups. Ac and Sc belong to the AS-C subfamily and share high sequence identity. The Ato subfamily proteins Ato and Amos also show high identity. However between the Ac-Sc subfamily and Ato subfamily, the shared identity is much lower.

1.14 Vertebrate homologues of proneural genes

After the importance of the *AS-C* and *ato*-like genes in *Drosophila* neurogenesis was established, many laboratories have worked on finding proneural homologues in vertebrates. Since then a range of *Xenopus*, zebrafish, murine, chick and human homologues have been isolated on the basis of their sequence homology to the bHLH domain of Sc or Ato (Akazawa et al., 1995; Brown et al., 2002; Brown et al., 1998a; Kanekar et al., 1997; Kay et al., 2001; Park et al., 2003). As shown in the summary tree (Fig. 1.13), proneural homologues fall into a number of subfamilies.

The vertebrate homologues of *Drosophila* proneural proteins generally fall into two broad categories; those with homology to AS-C such as Mash, Xash and Cash (Henrique et al., 1997; Johnson et al., 1990; Lo et al., 1991; Sommer et al., 1996) and those

homologous to Ato the Ato-like proteins such as the Ato-homologues (ath's), Neurogenins (Ngn's) and NeuroD (Akazawa et al., 1995; Anderson, 1995; Ben-Arie et al., 1996b; Lee, 1997b; Lee et al., 1995; Ma et al., 1996a; Shimizu et al., 1995b; Sommer et al., 1996).

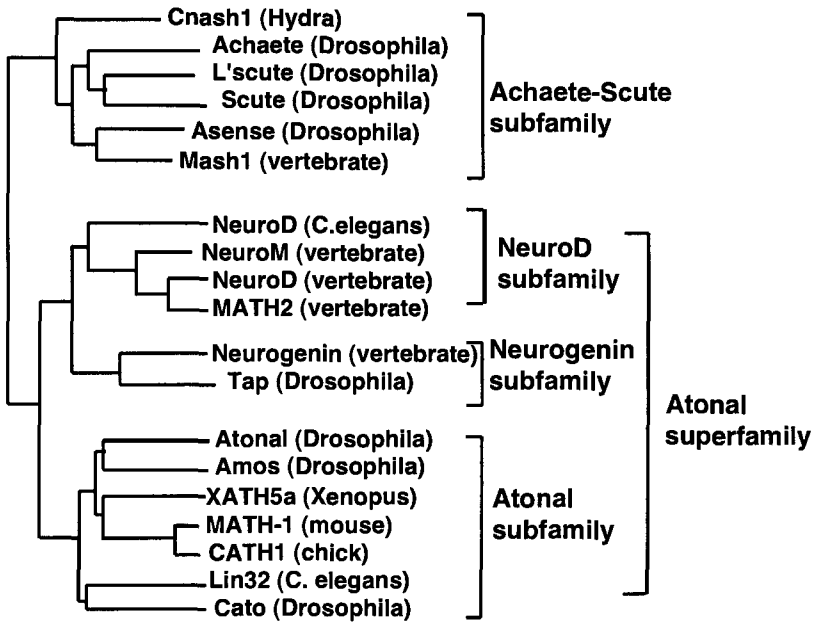

Figure 1.13. Family tree of sequence homology of the bHLH domains. Neuronal specific bHLH genes are grouped into subfamilies according to sequence identity using the Clustal X programme. This bHLH family consists of the Ato superfamily and the Ac-Sc subfamily. The Ato superfamily is subdivided into the NeuroD subfamily, the Neurogenin subfamily and the Ato subfamily.

1.14.1 AS-C homologues

Mash1 has activities reminiscent if AS-C function, it is transiently expressed in spatially restricted neural cells (Lo et al., 1991) and seems to utilize some of the same neurogenic genes for neural development such as *Notch* and *Egfr* (Ahmad et al., 1998; Casarosa et al., 1999). Mash1 is expressed in olfactory epithelium, autonomic neurons, the neural tube and also the retina (Anderson, 1994; Guillemot et al., 1993; Hirsch et al., 1998; Tomita et al., 1996). It is yet to be decided if *Mash1* behaves like a proneural gene in

vertebrates, in most cases, *Mash1* does not commit multipotent cells (like true proneural genes) but promotes proliferation and differentiation of committed neural precursors (Sommer et al., 1995). However in the vertebrate telencephalon *Mash1* mutants result in a severe loss of neural progenitors (Casarosa et al., 1999). Also the AS-C homologue in chickens (Cash1) can substitute for AS-C function in flies and also promote the formation of neural precursors in vertebrate CNS (Henrique et al., 1997).

In general, the activity of Mash1 for the specification of neuronal fate in different neural lineages is dependent upon other determinants of neural identity. For example Mash1 acts in co-ordination with the Ngn's and ath's for neural development in the CNS, olfactory epithelium and retina (Akagi et al., 2004; Cau et al., 1997; Gowan et al., 2001; Gradwohl et al., 1996; Lo et al., 2002; Nieto et al., 2001). In addition Mash1 can activate other bHLH genes and cell determinants such as *NeuroD* and *Phox2a* (Cau et al., 1997; Hirsch et al., 1998).

1.14.2 Ato homologues

The vertebrate homologues of Ato have been identified and mapped in fish birds and mammals (Akazawa et al., 1995; Ben-Arie et al., 1996b; Brown et al., 1998b; Isaka et al., 1996; Kanekar et al., 1997; Kim et al., 1997). The bHLH domains of all Ato homologues share high identity, Math1 (mammalian Ato homologue) and Ato share 67% identity whilst Math2 and Ato share 51% identity. Between the vertebrate species, the ath's are even more similar, Math1 and Cath1 (chicken homologue) share 95% identity whilst Cath1 and Hath1 (human homologue) share 97% identity (Ben-Arie et al., 1996b). Furthermore the entire bHLH domain is the same size in all Ato homologues (Ben-Arie et al., 1996b) and the b-region is identical between Math1, Math5, Ato and Amos, this suggests that they encode proteins with similar regulatory properties.

Indeed the vertebrate ath's are expressed in neuroblasts of the developing neural tube where they influence neuronal cell type (Ben-Arie et al., 1996a; Helms and Johnson, 1998; Kim et al., 1997). Math in particular seems to have functions in analogous

structures to that of fly Ato. Math1 is expressed in cerebellar granule cells and hair cells which are required for geotaxis, hearing, limb and eye movements (Ben-Arie et al., 1997; Bermingham et al., 1999). In addition, Math1 is expressed in mechanosensory touch receptors and Math5 in retinal-ganglion cells (Bermingham et al., 1999; Brown et al., 1998b; Brown et al., 2001).

Although the expression profiles of the ath's are conserved in both the fly and vertebrate nervous systems, there appears to be clear distinctions in the functions of ath's compared to Ato. In *Drosophila ato* is required for both neural competence and subtype specification of chordotonal organs, photoreceptors and a subtype of olfactory sensilla. However in the vertebrate systems, these functions are assigned to orthologues of the Ato-related proteins, for instance Math1 has analogous functions in hearing, locomotion and balance, whilst Math5 is required for retinal ganglion cell specification. Like the *ac-sc* homologues, there is no clear evidence to suggest that the ath's actually confer neural competence to uncommitted cells, instead they seem to function as regulators of differentiation.

1.14.3 Neurogenins

The Ngn's constitute a family of Ato-related genes involved in vertebrate neurogenesis (Ma et al., 1996a; Sommer et al., 1996). The encoded proteins share on average 53% bHLH identity with Ato making them the most distantly related Ato-like proteins. However, these proteins seem to possess Ato-like like functions not present in the ath's. Ngn's are involved in the early stages of neurogenesis not determined by the ac-sc homologues and ath proteins.

The Ngn's define distinct progenitor populations in the PNS and CNS, where their expression precedes that of NeuroD and the *ac-sc* homologues and ath's (Ma et al., 1996a; Ma et al., 1996b; Ma et al., 1997). Ngn expression is sensitive to *Notch* and is required for selection and delamination of at least some precursors of sensory neurons derived from the epibrachial placode (Fode et al., 1998; Ma et al., 1998). This suggest

that the neurogenins may be vertebrate neural determination factors with analogous functions to the proneural proteins for precursor selection.

Unlike the proneural proteins, expression of the Ngn's is not terminated after precursor selection, but continues to be involved in fate determination steps such as inhibition of the glial fate (Nieto et al., 2001; Sun et al., 2001). Ngn's also influence neuronal sub-type identity however this function seems to be very sensitive to cellular context (Lo et al., 2002). For example Ngn1 has cross-inhibitory interactions with Math1, resulting in the formation of distinct neural domains in the neural tube. These distinct domains ultimately determine the sub-type identity of neurons (Gowan et al., 2001). The requirement for Ngn in co-ordination with other bHLH proteins is also demonstrated in the determination of retinal cell type; combinations of Mash1, Math3/NeuroM and NeuroD, are required for retinal cell sub-type, however this can only be achieved in concert with glial lineage inhibition by Ngn2 (Akagi et al., 2004).

Even though the neurogenins share the least identity with Ato compared to the Atonal homologues (review (Hassan and Bellen, 2000), the neurogenins carry out analogous functions to Ato and indeed AS-C in early neurogenesis. It would appear that proneural function in vertebrates has been subdivided; the Ngn's taking the role of neural determination and precursor selection, whilst the *ac-sc* homologues and ath's influence later stages of neuronal differentiation and subtype determination. Interestingly, the *Drosophila* Ngn *Biparous* (a.k.a. *Tap*) does not have proneural function, as it is not expressed in early progenitors, but seems to be involved in glial versus neuronal fate in the CNS (Bush et al., 1996).

1.14.4 NeuroD

The NeuroD group of proteins was first identified in hamster and *Xenopus* (Lee et al., 1995; Naya et al., 1995). Other NeuroD proteins were subsequently identified in *Drosophila*, chick, mouse and human developmental systems (Bartholoma and Nave, 1994; Roztocil et al., 1997; Shimizu et al., 1995a; Takebayashi et al., 1997; Wang et al.,

2003; Yan and Wang, 1998). NeuroD is expressed in a variety of tissues in the CNS and PNS, including the olfactory bulb, pancreas and developing retina (Hitchcock and Kakuk-Atkins, 2004; Inoue et al., 2002; Liao et al., 1999; Miyachi et al., 1999; Miyata et al., 1999; Morrow et al., 1999; Yan and Wang, 2004) (review (Vetter and Brown, 2001).

NeuroD has transient expression in a subset of neurons in the PNS and CNS at the time of terminal differentiation, accordingly overexpression causes premature differentiation and conversion of non-neural cells into neurons (Lee, 1997b; Lee et al., 1995; Takebayashi et al., 1997). Overexpression in the retina leads to the *de novo* induction of photoreceptors. Although, the NeuroD group of proteins have evolved to play a number of roles in different cell lineages, *NeuroD* is not expressed in progenitor cells and cannot be proneural. *NeuroD* expression is affected by changes in *Ngn* expression, this suggest that it is a target gene of *Ngn* (Fode et al., 1998; Huang et al., 2000a; Ma et al., 1998).

1.14.5 Summary of vertebrate neural bHLH proteins

Neurogenesis in vertebrates is much more complex than in the fly; the vertebrate neural homologues seem to be involved in a huge variety of roles in many different tissue types, implicating tissue specific functions. In addition some functions require the co-ordination of many different genes. Thus it seems that the all-in-one function of *ato* (and *AS-C* to some extent) in sense organ specification is divided up between all the different ac-sc homologues and Ato-like proteins in the vertebrate nervous system (Fig.1.14) (reviews Bertrand et al., 2002; Brunet and Ghysen, 1999b).

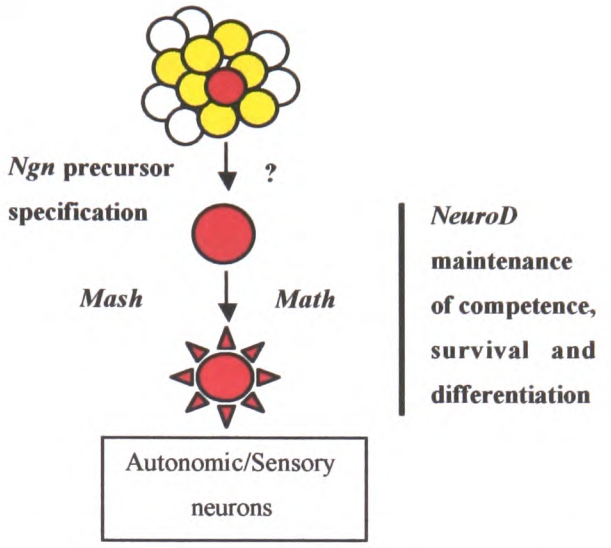

Fig 1.14 Vertebrate neurogenesis. The process of neurogenesis in flies require the proneural genes from precursor selection to sense organs subtype specification. However, in vertebrates, each step of the process is divided amongst a number of genes.

1.15 Relation of structure to function

It is plausible that variations in the bHLH domains confer functional specificity, and this is supported in structure-function experiments for Sc and Ato (Chien et al., 1996). However, if the bHLH domain is important, it is not clear how. One possibility is that variations in the bHLH domain cause different proteins to bind to different DNA sequences (variant E-boxes). A more favoured possibility is that different bHLH proteins interact with different 'specificity cofactor' proteins, and the resulting complexes then recognise different target gene enhancers (Bertrand et al., 2002; Brunet and Ghysen, 1999a; Chan and Jan, 1999; Chien et al., 1996). Supporting this idea, modelling of the bHLH domain has suggested that all DNA-contacting residues are conserved between Sc and Ato (Chien et al., 1996).

In support of this theory, cofactor involvement has been shown to play an important role in the specificity of other bHLH proteins involved in myogenesis, haematopoiesis and the vertebrate Hox selector proteins (Chan and Mann, 1996; Li et al., 1999; Molkentin and Olson, 1996; Porcher et al., 1999). More recently, *pointed* has been proposed as a putative Ato cofactor for femoral chordotonal organs (zur-Lage et al., 2004).

1.16 Overall goal of this thesis: how is Amos functionally distinct from Ato?

Amos and Atonal are structurally very similar within their bHLH domains. However, these proneural proteins are required for the development of distinct sense organ subtypes. I aim to explore the basis of Amos and Atonal functional specificity. I aim to determine to what extent the functional differences are due to different expression patterns versus differences in the proteins' ability to function.

In this thesis, I compare more thoroughly the functional capability of Amos relative to Ato (and Sc) in order to better define shared and unique functions. I then explore whether these functions are encoded within or out with the bHLH domains of these proteins.

Chapter 2

Materials and Methods

2.1 Acquisition of *D. melanogaster* genomic sequences

cDNA sequences of proneural genes *scute*, *ato* and *amos* were acquired from Flybase sequences (http://flybase.bio.indiana.edu/). These were used to design primers for the construction of chimeric proneural DNA sequences (see appendix A). These chimeras were then constructed and amplified by Polymerase-chain reaction (PCR) from fly genomic DNA templates.

2.2 Preparation of genomic DNA from adult flies

D. melanogaster genomic DNA was prepared using the following procedure. 25 wildtype *Oregon R* flies were frozen in 200μl lysis buffer (100mM Tris-HCl pH 9, 100mM EDTA pH 8, 1% SDS) at –20 °C, thawed and homogenised. A further 200μl of lysis buffer was added and incubated at 70°C for 30 minutes. 150μl of 8M potassium acetate was added, thoroughly mixed and the tube was incubated on ice for 20 minutes. The tube was centrifuged at 20817 rcf, for 20 minutes at 4 °C. The supernatant was drawn off, split equally between two tubes and 0.9 total supernatant volume (v/v) of isopropanol added. The tubes were centrifuged for 5 minutes at 20817 rcf, following which the supernatants were drawn off and the pellets were washed in 70% ethanol and allowed to dry at room temperature (RT). The pellets were resuspended in 50μl of TE (10mM Tris-HCl, 1mM EDTA, adjusted to pH8) and pooled together.

Purification of DNA was carried out by phenol-chloroform extraction. An equal volume of phenol-chloroform ($PhOH/CHCl_3$) was added and the solution was vortexed for 1 minute. The sample was then centrifuged for 8 minutes at 20817 rcf, and the aqueous phase was transferred to a new eppendorf. Traces of phenol were removed by a further extraction with chloroform:Isoamyl alcohol (24:1) using the same method described above for phenol/chloroform extraction.

The purified DNA was precipitated with 0.05 (v/v) of sodium acetate (3M pH 5.2) and 2 v/v 100% ethanol. The solution was mixed and left at –20°C overnight. The DNA was pelleted at 20817 rcf for 10-15 minutes. The supernatant was discarded and the pellet washed with 70% ethanol and allowed to dry at RT. The pellet was resuspended in 50µl TE or double distilled (dd) H_2O. Genomic DNA was used as template for PCR of DNA fragments.

2.3 Polymerase Chain Reaction (PCR)

PCR was used to amplify each chimeric fragment from genomic DNA. The fragments were then used as templates for PCR construction of larger chimeric fragments. The primers for each PCR are listed in the appendix B and details of each PCR in appendix C. In all cases primers were initially tested using appropriate positive control template DNA. Roche and Stratagene *Taq* and their supplied buffers (a standard magnesium chloride concentration of 1.5mM was used). 10pmol of each primer and 2.5 nmol of dNTPs were used for each 50µl PCR reaction. Negative controls (without DNA) were performed in parallel for each primer set. Variations of a standard PCR program (on Biometra) were used for amplification of each fragment (see appendix D). The standard PCR program is as follows: lid temperature 100°C, denaturing step 94°C for 2 minutes, followed by 30 cycles of 94°C for 30 seconds, 55°C for 30 seconds and 72°C for 2 minutes, the end of the cycles followed by the final elongation step at 72°C for 10 minutes. The PCR reactions were then held at 4°C until purification and analysis.

2.4 Analysis of DNA fragments by gel electrophoresis

Restriction enzyme digested plasmid DNA and PCR-amplified double stranded DNA fragments were analysed by gel electrophoresis. Standard 0.8% agarose in 1xTAE (made from 50x stock: 242g Trizma base, 18.6g EDTA, pH8 with glacial acetic acid) containing 0.5 µg/ml EtBr were run in 1xTAE buffer. For separation of low molecular weight fragments, 1.6% agarose gels were used. DNA was mixed with loading dye (0.17 v/v 150g/l ficoll 400;

2.5g/l bromophenol blue) before running on the gel. Gels were run for appropriate lengths of time at 80V or 100V depending on the size of the gel tank and concentration of agarose.

2.5 Clean up of DNA

DNA from PCR reactions and restriction digests were purified to remove enzymes and primers by commercially available spin columns (GFX, Amersham Biosciences). The manufacturer's recommended protocol was adhered to. DNA fragments were separated by gel electrophoresis and cut out using a sterile razor blade and purified using commercially available gel band purification columns (GFX, Amersham Biosciences). The manufacturer's recommended procedure was adhered to.

2.6 Estimation of nucleic acid concentration

The concentration of nucleic acid solutions was determined either by gel electrophoresis with reference to known molecular weight standards (Bioline) or by spectrophotometry. Absorbance of double-stranded DNA samples were read at 260nm in a quartz cuvette.

2.7 Restriction digests of plasmid vectors pBluescript and pUAST

Restriction endonucleases (Roche) were used according to the manufactures instructions for p-vector subcloning of chimeric constructs (appendix E) and screening of plasmid minipreps for the appropriate insert and orientation (appendix F), approximately 3 units of enzyme were used per μg of DNA and incubated in the appropriate buffer for up to one hour at 37°C.

2.8 5' dephosphorylation of plasmid vectors pBluescript and pUAST

EcoR1 cloning sites of plasmid vectors were used to insert chimeric constructs. Restriction digest of plasmid DNA yields blunt or sticky ends, which may re-circularise especially if only

one enzyme is used. To prevent this, restriction digested plasmids were dephosphorylated at their 5' ends using calf intestinal phosphatase (CIP) before further ligation reactions. 1μl of CIP was added to DNA in digestion buffer at 37 °C for 15 minutes and a further 1μl of CIP was added for another 15 minute incubation period. The enzymes and phosphatase were removed using a purification column (GFX, Amersham Biosciences) using the manufacturer's standard protocol.

2.9 Ligation

In order to maximise the ligation between vector and insert fragments, a standard formula was used to predict the best fragment vector ratios.

[vector (ng) x fragment size (bp)/ vector size (bp)] x3 = ng of insert needed

T4 DNA ligase (NEB) was used according to the manufacturer's instructions. Ligations were performed at 16°C overnight.

2.10 Transformation of *E. coli*

Competent cells used for transformation were prepared using a $CaCl_2$ procedure (David Prentice). Lab made cells gave adequate transformation efficiencies for the purpose of subcloning (~10^5/μg DNA). Cells were used within 1 hour of preparation or from aliquots stored at -80°C in 50% glycerol. Commercially available Xl-10 Gold cells (Stratagene) were also used in some instances. In these cases the appropriate transformation protocol was followed according to the manufacturers instructions.

10-100ng of DNA in ligation buffer (2-5μl) was added to 100μl of competent cells, which were left on ice or 30 minutes for adsorption. Cells were heat shocked for 45 seconds at 42 °C for DNA uptake and were allowed to recover on ice for 2 minutes. 0.9ml of LB medium was added and the tubes were incubated at 37 °C for 30 minutes with gentle agitation. 200μl of the transformation reaction was spread on ampicillin (50μl/ml) LB plates using a

sterile spreader. The plates were incubated at 37°C overnight. For blue/white selection, 100µl 100mM IPTG and 100µl 2% X-gal were spread on the agar plates prior to plating the transformations. The plates were incubated overnight at 37 °C. Single colonies were picked using a sterile loop and grown up at 37°C overnight in 5ml cultures of ampicillin (50µl/ml) treated LB broth.

2.11 Bacterial culture growth

The medium used for culture of E.coli was autoclaved Luria-Bertani (LB). LB Media was treated with ampicillin (50µl/ml). Liquid colonies were grown by incubation at 37°C in an orbital shaker. The liquid colonies were then plated out on ampicillan treated LB agarose medium and grown at 37°C overnight.

2.12 Mini preparations of subcloned plasmid DNA

Mini preparations of plasmid DNA were obtained using commercial spin columns from Qiagen according to the manufacturer's instructions. For DNA injection of embryos to generate transformants, the plasmid bulk prep procedure was used.

2.13 Plasmid bulk preparations

Liquid bacterial cultures were transferred to 50ml Falcon tubes and centrifuged at 1000 rcf for 20 minutes at 4°C. The pellets were drained thoroughly and resuspended carefully using a pastette in 2ml of solution I (50mM Glucose, 25mM Tris pH 8, 10mM EDTA, 5mg/ml lysozyme, prepared just before use), per 50ml of culture and left at room temperature for 10 minutes. 4ml of Solution II (0.2 M NaOH, 1% SDS - prepared just before use) was added and mixed thoroughly but not vigorously. The viscous mixture was incubated on ice for 10 minutes with regular gentle agitation. 3ml of Solution III (3M KOAc / 1.3M HCOOH) was added with immediate, thorough mixing and placed on ice for 15 minutes. The mixture was centrifuged at 4500 rcf for 15 minutes.

The clear supernatant was transferred to a clean tube avoiding transfer of any precipitate. 0.6 (v/v) of 100% isopropanol was added and the solution was mixed and incubated at RT for 5 minutes. The tube was then centrifuged at 4,500 rcf for 10 minutes. The supernatant was discarded and the pellet was rinsed with ~ 2ml of 70% ethanol. The inner walls of the tube were wiped clean and the still wet pellet dissolved in 1ml of TE. The DNA solution was transferred to eppendorfs and placed on ice for 5-10 minutes. An equal volume of cold 5M LiCl (stored at –20°C) was added and the tubes were incubated on ice for 5 minutes, followed by centrifugation at 20817 rcf for 5 minutes. The supernatant was transferred to clean eppendorf tubes (on ice) and an equal volume of isopropanol was added. The tubes were incubated on ice for 10 minutes and then centrifuged at 20817 rcf for 5 minutes. The supernatant was discarded and the pellets air-dried at RT. The pellets were then resuspended in a total of 300 µl TE.

To remove RNA, 1µl DNAse-free RNAse (10mg/ml stock) was added and the mixture incubated at 37 °C for 30 minutes. The mixture was then transferred to ice and an equal volume of PEG/NaCl (15% PEG, 1.6M NaCl) was added. This mixture was then incubated on ice for 5 minutes before centrifugation at 20817 rcf for 5 minutes. The supernatant was discarded and the pellet was resuspended in 300 µl TE. The plasmid DNA was then purified by PhOH/$CHCl_3$ extraction and a further chloroform extraction (described above). The DNA was precipitated by addition of 0.05 (v/v) 3M NaOAc (pH 5.2-5.6) and 2 (v/v) 100% Ethanol. This was thoroughly mixed and incubated at -20°C overnight. The tubes were then centrifuged at 20817 rcf for 5 minutes. The pellets were then washed with 70% Ethanol, air-dried and resuspended in 300 µl ddH_2O.

2.14 DNA sequencing

A BigDye Dye terminator kit (Perkin Elmer Applied Biosystems) was used according to the manufacturers instructions and in a reaction consisting of 4.0 µl reaction mix, between 250-

500 ng of template DNA, 1.6 μl pmol of primer (see appendix B) and sterile H_2O to a final volume of 10 μl. Cycle conditions were 31 cycles of melting at 92°C for 30 seconds, annealing at 55°C for 30 seconds and elongation at 72°C for two minutes. 10 μl of dH_20 were added and the reaction analysed on an ABI377 sequencer at ICMB, University of Edinburgh. The sequence was analysed using GeneJockey II (P.L. Taylor, Biosoft, UK).

2.15 Production of transformant fly lines by microinjection

Constructs were subcloned into GAL4 pUAST (P element vector) and injected into freshly laid *w; Δ2-3* embryos. *Δ2-3* is the source of transposase for the attenuated P element vector. DNA is introduced into precellular blastoderm embryos by injection and integrated into the genome by random transposition events. DNA for each construct was prepared using the bulk prep method.

Cages of flies were set up on grape juice agar plates with a globule of freshly prepared yeast paste as a nutrient source. The plates were changed at regular intervals to encourage egg-laying. For injection, plates were collected at 45 minute intervals. The injection procedure was carried out at 18 °C. Embryos were collected and dechorionated for 4 minutes in 50% bleach and then rinsed in water. Embryos were lined up under a microscope along the edge of a piece of agar with the posterior of the embryos facing the injection needle. The embryos were transferred to a coverslip coated with glue. The coverslip was attached to a microscope slide using a drop of oil and dehydrated with silica gel for approx 10 minutes at room temperature. Embryos were then covered with series 700 halocarbon oil and injected with pUAST subcloned with the construct of interest at a concentration of (800 ng/μl). Injected embryos were then covered in series 95 halocarbon oil and incubated in a humid chamber at 18 °C for 1.5 days then incubated at 21°C overnight. The embryos were then transferred to 25°C and hatched larvae were collected and transferred to standard cornmeal vials. The larvae were allowed to develop, pupate and eclose at 25°C.

2.16 Acquisition of stable transformant fly lines

DNA injected adult flies were crossed with *white* flies (w^{1118}) and screened for P element insertions on the basis of eye colour. This cross was repeated until mosaics were eliminated and even and stable eye colours were achieved.

The P element insertions where then mapped to chromosomes 2 or 3 by crossing with *Pin/CyO* or *Ly/TM3,Sb* flies. The F1 generation carrying the chromosome marker *Cy* or *Sb* with coloured eyes were re-crossed. If P elements are inserted on the second chromosome, the F2 generation will consist only of flies with coloured eyes with/without curly wings. If P elements are inserted on the third chromosome, the F2 generation will consist only of flies with coloured eyes with/without stubble bristles.

2.17 Dissection and fixation of adult flies

Flies were gassed with CO_2 and dissected in PBTx (PBS plus 0.3% Triton X-100, Sigma) under a standard dissecting light microscope (Zeiss Stemi 2000). The dissected organs were then fixed in 3.7% formaldehyde in PBS for 15 minutes on a rotating wheel. The dissected organs were then washed 4 times in PBTx followed by 3 x 15 minute washes in PBTx on a rotating wheel (standard wash procedure). The dissected organs were then mounted in 80% glycerol in PBS and sealed under a coverslip with nail varnish. For fly antenna, there was no need for fixation and they were mounted in Hoyer's medium (30g Gum Arabic in 50ml ddH_2O, stirring overnight, then 200g chloral hydrate and 20g glycerol gradually added with stirring and centrifuged at 25 000g for 30 minutes) and hardened on a slide dryer at 65°C overnight.

2.18 Fixation of embryos and imaginal discs for immunohistochemistry

Embryos were collected on grape juice plates with a globule of yeast paste (0.5% proprionic acid in ddH_2O) as a nutrient source. The grape juice plates were then aged for the appropriate length of time at appropriate temperatures. The embryos were removed using ddH_2O and a paintbrush, and pipetted into a fine sieve. Embryos were washed to remove yeast and dechorionated in 50% fresh bleach for 4 minutes, then thoroughly washed to remove bleach. The embryos were then transferred into a scintillation vial and fixed for 20 minutes with agitation in 1.25 ml formaldehyde (37%), 3.75ml PBS (8g NaCl, 0.2g KCl, 1.44g Na_2HPO_4, 0.24g KH_2PO_4 for 1 litre, adjusted to pH7.4) and 5 ml n-Heptane (Sigma). The bottom phase of formaldehyde was removed and 10ml of methanol was added. The scintillation vial was then shaken vigorously for 30 seconds to devitellinise the embryos. Embryos were allowed to settle to the bottom of the vial and then transferred to an eppendorf. The embryos were then washed with methanol to remove residual heptane, and then washed 4 times with PBTx. This was followed by the standard wash procedure.

Larval and pupal imaginal discs were dissected at room temperature in Grace's Insect medium (Sigma). The dissected discs were then fixed in 3.7% formaldehyde in PBS for 5 minutes. The embryos were then washed using the standard wash procedure.

2.19 Immunohistochemistry

Embryos and imaginal discs were blocked for at least two hours in 2% bovine serum albumin (BSA) solution (Sigma) in PBTx at room temperature on a rotating wheel. Primary antibody (appendix H), in PBTx at the appropriate concentration with 0.5% (v/v) BSA, 0.05% (v/v) Normal Goat Serum (NGS, Jackson labs) was added and samples were incubated at 4°C overnight. The primary antibodies were then rinsed with the standard wash procedure. The secondary antibody (fluorochrome conjugate) was added in PBTx to a concentration of

1:1000 for 2 hours at hour temperature. The samples were rinsed with the standard wash procedure, then mounted in Vectashield (Vector labs) on microscope slides sealed with a coverslip and nail varnish. Slides were stored in the dark at 4°C. Confocal images were taken on a Leica TCS-NT microscope, using Leica TCS-NT image capture software. Images were processed with Adobe Photoshop 6.0.

2.20 *Drosophila* strains

Fly stocks were maintained on standard cornmeal-agar medium ("Dundee Food" prepared by media kitchen staff) at 18°C or room temperature. Crosses for misexpression analysis were performed in incubators set at the appropriate temperatures. w^{1118} flies were used as the wildtype strain throughout (apart from preparation of genomic fly DNA).

2.21 Statistics

All statistical analyses were carried out using Microsoft Excel.

Bar charts are used to represent the arithmetic mean of data sets.

$$\overline{x} = \frac{\sum x}{n}$$

Error bars were used to represent the standard deviation of each data set.

$$\text{st.dev} = \sqrt{\frac{n\sum x^2 - (\sum x)^2}{n(n-1)}}$$

Heteroscedastic t-tests where used to determine similarities between means of distinct data sets (where $P \leq 0.05$).

$$\text{t-test} = \frac{\overline{x} - \overline{y} - \Delta 0}{\sqrt{\frac{s_1^2}{m} + \frac{s_2^2}{n}}}$$

Chapter 3

Comparison of the functional specificity of *atonal* and *amos*

3.1 Introduction

In this chapter I explore the function of two closely related Ato-like proneural proteins. In this thesis I am interested in establishing the nature and cause of their functional difference through misexpression. Developmental genetic studies of proneural gene mutations show that *amos* and *ato* have abundantly distinct functions in vivo. The basic question that I pose is: to what extent are these different functions merely due to differences in expression pattern, and to what extent are they due to differences in functional capabilities of the two proteins? These are questions of proneural protein specificity. Loss-of-function studies alone are unable to address this question. Instead several other approaches have been used. Firstly, the sequences can be examined to see what deductions may be made about function. Secondly, proneural specificity can be explored experimentally in several ways. One productive avenue has been to ask: do the proneural proteins behave identically or distinctly in misexpression studies. In the introductory sections of this chapter, I shall summarise what is deduced from sequence comparisons and then summarise what has been learned so far from misexpression analyses.

3.2 Structures of Amos and Ato

amos and *ato* encode bHLH proteins of the same subfamily. In fact their bHLH domains are so similar they share the highest identity of all proneural proteins. The structural similarities of the two proteins suggest that they are also functionally similar. That is to say they are likely to have diverged and specialised from a common ancestral protein.

3.2.1 Amos and Ato proteins share high bHLH identity

amos is the most recently isolated *Drosophila* proneural gene and was identified by degenerate PCR screens for Ato homologues (Goulding et al., 2000b). Not surprisingly therefore, this proneural gene is inherently very similar to *ato*. Sequence alignments of Amos and Ato reveal an 88% identity over the bHLH domain. This percentage identity therefore surpasses the 70% shared by the bHLH domains of the AS-C of proteins. Moreover, if

sequence alignments of all neural bHLH domains are examined, Amos is found to be closer to Ato than any other protein, including vertebrate orthologues. However, outwith the bHLH motif no apparent homology exists (Fig.3.1).

Presumably, the *ato* and *amos* genes derived from gene duplication of a common ancestor. This duplication must have been sufficiently ancient to explain the lack of homology in their non-bHLH regions. This in turn, implies a very strong functional constraint on the bHLH sequences.

3.2.2 The binding regions of Amos and Ato are almost identical

The high identity in the bHLH region of Amos and Ato is further demonstrated by their near identical DNA binding domain (b domain). Only one conservative change (Lys⇒ Arg) is found at residue 1 of the b domain, the rest of the residues are identical (Fig.3.2). This b domain was identified as being required for correct folding and interaction with DNA (Dang et al., 1992; Ellenberger et al., 1994; Ma et al., 1994). Thus the sequence similarities between Amos and Ato imply there may be similarities in the way the proteins bind to DNA. Again the suggestion is that there must be strong functional constraints maintaining the b domain sequence.

3.2.3 Amos and Ato are functionally similar but distinct

High sequence similarities suggest common functional constraints upon the bHLH regions of *ato* and *amos*. Firstly, both genes are required for SOP selection. Secondly, the translated proteins are only functionally active in the form of heterodimers with the gene product of *daughterless* (Da) (Goulding et al., 2000b; Huang et al., 2000; Jarman et al., 1993b). Furthermore *amos* and *ato* share the ability to inhibit the external sense organ lineage and determine subtype identity (Jarman and Ahmed, 1998; Jarman et al., 1993b; zur Lage et al., 2003). The functional similarity of *amos* and *ato* can be demonstrated in their requirement for the specification of olfactory sensilla, albeit of different subtypes (Goulding et al., 2000b;

Gupta and Rodrigues, 1997; zur Lage et al., 2003). However, misexpression experiments have also indicated that the functional capabilities of Ato and Amos proteins are distinct.

3.3 What has misexpression told us about the nature of the proneural genes?

3.3.1 Proneural gene expression is sufficient to drive SOP formation

Misexpression experiments have provided a cornerstone for proneural gene definition. A defining property of proneural genes is that misexpression in the developing ectoderm results in the appearance of ectopic SOPs. Thus proneural gene expression is both necessary and sufficient to promote SOP selection. Even in the earliest experiments, which used a *hs-sc* construct, it was obvious that this was only true in specific defined situations (Rodriguez et al., 1990). Heatshock induction of *sc* resulted in ectopic bristle formation only in restricted 'time windows' of larval and pupal development, which corresponded closely to the times of endogenous SOP formation.

3.3.2 Non-proneural genes can also induce ectopic neurogenesis

The capacity for inducing ectopic neurogenesis is not limited to misexpression of the proneural genes. Downstream target genes can bypass the requirement for proneural gene expression if they are misexpressed in a similar manner, as exemplified by *ase* and *cato*. *ase* is a common downstream target gene of all proneural genes (Brand et al., 1993). Although it is also part of the *AS-C*, it is not a proneural gene itself. *ase* is expressed in all neural precursors after they have been selected from their proneural domains (Brand et al., 1993). Thus *ase* is a neural precursor gene and its expression is required for development and survival of SOPs (Campuzano and Modolell, 1992; Jarman et al., 1993a). However if *ase* is ectopically expressed in proneural clusters it is able to produce ES organs bypassing the requirement of *ac* and *sc* (Brand et al., 1993). Thus misexpression of *ase* is sufficient to

drive neurogenesis. The ectopic sensory bristles that arise from *ase* misexpression are presumably an artefact of its neural function and close sequence relationship with *ac* and *sc*.

Similarly, *cato* is expressed in chordotonal precursors, but can apparently mimic aspects of *ato* function when misexpressed, even though it cannot be regarded as a proneural gene because it is not expressed in proneural domains (Goulding et al., 2000a). These observations illustrate one of the pitfalls of misexpression experiments: they define what a protein *can* do, rather than what it necessarily does *in vivo*. This is an important caveat to bear in mind.

3.3.3 Proneural genes also influence the subtype fate of SOPs

Misexpression evidence together with loss of function mutants, gives support to the idea that proneural genes encode sense organ subtype. Before the advent of misexpression studies in *Drosophila*, the proneural genes were only thought to be required for SOP selection. However misexpression studies have implied that *ato* is required for subtype specification in addition to SOP selection (Jarman and Ahmed, 1998; Jarman et al., 1993b).

Before the generation of *ato* mutants, misexpression was used to show the functional differences between *ato* and *sc* (Jarman et al., 1993b). This type of experiment became available in *Drosophila* after the development of the *Gal4/UAS* system (Brand and Perrimon, 1993). This system allows the expression of genes or constructs at specific sites under the control of the yeast transcriptional activator Gal4.

Misexpression of *UAS-sc* promotes ectopic external sense organ formation (Fig.3.3B). *UAS-amos* promotes ectopic olfactory-like sensilla (Fig.3.3C and D) and *UAS-ato* promotes ectopic chordotonal organs (Fig.3.3E). Misexpression of *ato* or *amos* can induce the formation of ectopic ES organs to a certain degree but misexpression of *scute* cannot specify ectopic sense organs of any type other than ES organs.

3.3.4 Misexpression of *sc* or *ato* result in different phenotypes

The misexpression phenotype of *ato* is different to that of *sc* (Chien et al., 1996; Jarman and Ahmed, 1998; Jarman et al., 1993b; Reddy et al., 1997). Misexpression of *ato* induces the formation of ectopic chordotonal organs and extra sensilla coeloconica, however misexpression of *sc* can only determine the formation of external sense organs (Chien et al., 1996; Gupta and Rodrigues, 1997; Jarman and Ahmed, 1998; Jarman et al., 1993b; Reddy et al., 1997). Misexpression of *ato* in larval discs or the embryo results in the formation of chordotonal organs (Jarman and Ahmed, 1998). When *ato* is misexpressed in proneural clusters of wing imaginal discs, chordotonal organs are formed at ectopic locations such as the scutellum and wing veins. Embryonic misexpression of *ato* increases the number of wild type chordotonal organs and misexpression in ato^{1} can rescue the mutant phenotype (Jarman et al., 1994). Thus misexpression of *ato* produces phenotypes in accordance with its wild type function.

3.3.5 Proneural specificity depends on context

One conclusion from these experiments is that proneural genes specify subtype identity. A parallel conclusion, however, is that this specificity strongly depends on the developmental context. In the eye *ato* misexpression results in extra R8 formation (White and Jarman, 2000). In the third antennal segment, *ato* misexpression results in extra numbers of sensilla coeloconica (Gupta and Rodrigues, 1997). Therefore, subtype determining functions work only in the background of cellular environment. Ultimately this has been taken to mean the presence or absence of other regionally expressed protein factors. This leads to the view that proneural subtype specificity relies heavily on the proneural proteins interacting with other specific cofactor proteins. The nature of such cofactors is unknown.

3.3.6 Misexpression of *ato* is able to suppress external sense organ fate

In addition to ectopic formation of *ato*-dependent sense organs, misexpression of *ato* also results in the formation of external sense organs, albeit less efficiently than *ac* or *sc* (Jarman

and Ahmed, 1998; Jarman et al., 1993b). The small number of external sense organs induced by *ato* (and by inference *amos*) are thought to be artefacts. It is thought that external sense organ fate is a default fate for SOPs, and that expression of *ato* must divert SOPs from this default to alternative pathways of neurogenesis. It is thought that this doesn't happen efficiently due to the inability of misexpressed *ato* to function appropriately in all parts of the ectoderm. Thus, SOP specification still occurs ectopically, but subtype determination is defective.

In particular, it is suggested that *ato* needs to suppress the neural selector gene, *cut* (Bodmer et al., 1989; Jarman and Ahmed, 1998). *cut* is expressed in all external sense organ SOPs and functions as a molecular switch that must be activated to allow SOPs to take on this fate (Blochlinger et al., 1990; Blochlinger et al., 1991; Bodmer et al., 1987). Under the conditions of misexpression, *ato* suppression of *cut* is sometimes not fully achieved (Fig.3.4). This illustrates that even apparent artefacts of misexpression can potentially be informative if interpreted carefully.

If this model of subtype determination is correct, then misexpression conditions should exist in which the opposite occurs: *ato* should be able to suppress bristle formation. This appears to be the case. When using a PNC-specific Gal4 driver, misexpression of *ato* appears able to supplant *AS-C* function and transform at least some wild type bristles on the thorax with chordotonal organs (Jarman and Ahmed, 1998). As might be expected from the model, the reverse is not true. Moreover, the ability of *ato* to do this is limited to a few areas of the ectoderm, notably the scutellum and third wing vein. These are also the areas most susceptible to the production of extra chordotonal organs by *ato* misexpression.

Again, non-proneural genes show interesting differences in the range of ectopic sense organs that they can induce when misexpression. For example *ase*, a panneural target gene can only induce ectopic ES organs whereas *cato*, the *ato* specific target gene, produces a phenotype more reminiscent of *ato* (Goulding et al., 2000b; Jarman et al., 1993a).

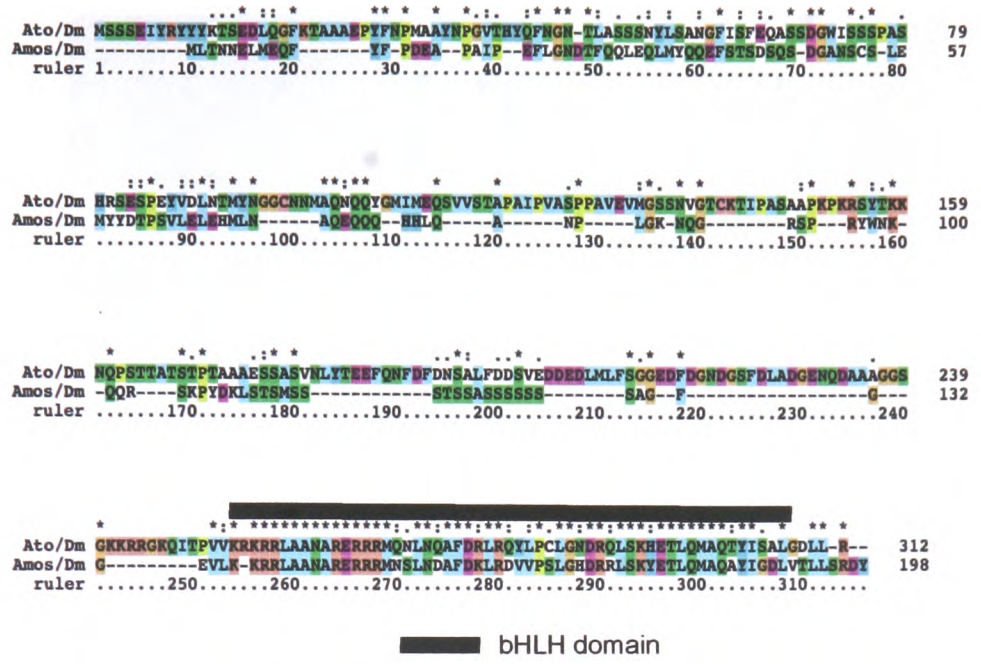

Figure 3.1 Sequence alignment of Ato and Amos orthologues

Conserved residues are indicated by *

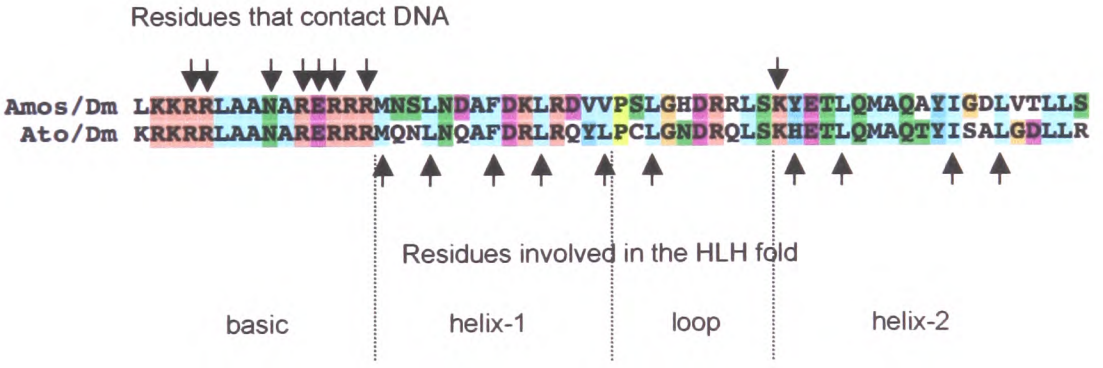

Figure 3.2 Line up of Amos and Ato bHLH domains. There is very high sequence conservation. Residues predicted to contact the DNA or to allow HLH folding are indicated (based on the MyoD crystal structure). All these are conserved between Amos and Ato, as they are between most neural bHLH proteins. The basic regions of the two proteins contain no divergent DNA contacting residues.

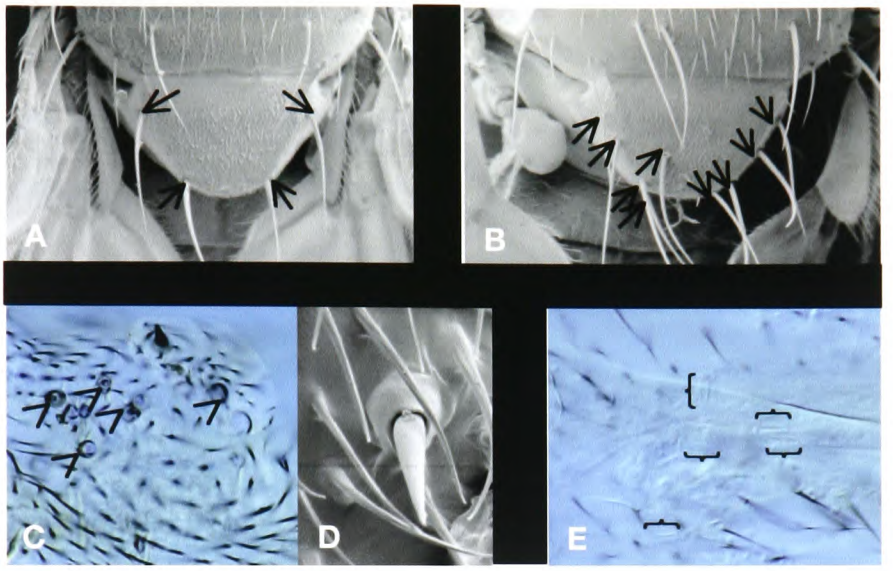

Figure 3.3 Misexpression of Scute, Ato and Amos induce the formation of protein-specific sense organs. **(A)** Wildtype scutellum showing stereotypical number and pattern of dorso-central macrochaetae (arrows). **(B)** Misexpression of *UAS-sc* produces ectopic bristle formation (arrows). Misexpression of *UAS-amos* produces ectopic olfactory sensilla on the wing (arrow heads-**C**) and scutellum (**D**). Misexpression of *UAS-ato* produces ectopic chordotonal organs in the wing veins (brackets-**E**). (Images adapted from Jarman and Ahmed, 1998 and Goulding et al., 2000b.)

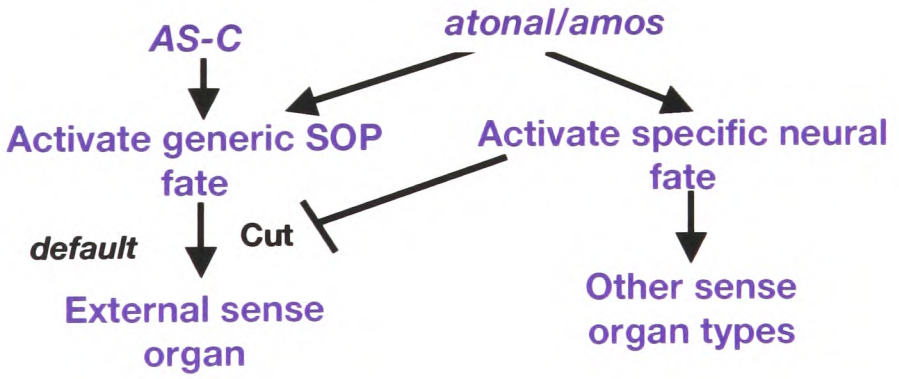

Figure 3.4 Model for subtype determination in SOPs. *AS-C* activates the generic SOP fate by activation of subtype selector proteins, in this case Cut. *ato* and *amos* activate proneural specific neural fate and inhibit generic ES fate by inhibition of cut. (From Jarman and Ahmed, 1998.)

3.4 Misexpression phenotype of *amos*

3.4.1 *amos* misexpression can promote and repress external sense organ formation

In general, *amos* shows interesting parallels to *ato*. Like *ato*, inappropriate *amos* misexpression results in artefactual external sensory organ formation (Goulding et al., 2000b). An extreme illustration of this is shown by the recent characterisation of a gain-of-function allele of *amos*. Studies aiming to characterise hairy bristle mutants have found that the dominant mutation known as *Tufted* (*Tft*) is actually a gain of function allele of *amos* (Lai, 2003; Villa-Cuesta et al., 2003). *Tft* flies exhibit large tufts of sensory bristles on their scutella. The *Tft* phenotype is due to the misexpression of *amos* in the wing disc, and furthermore does not rely upon the cross activation of the *AS-C* genes to produce ectopic bristles (Lai, 2003).

Despite the dramatic nature of *Tft*, *amos* is able (like *ato*) to suppress external sense organs when misexpressed in a limited range of tissue contexts. This suggests that such bristle suppression is an important feature of Ato-like proneural proteins, and that both proneural genes function in subtype determination in a similar way. Indeed, this has subsequently been supported by the fact that $amos^{1}$ mutants show not only olfactory sensillum loss but also the appearance of ectopic sensory bristles on the antenna (zur Lage et al., 2003). This function should result in some conserved features in the protein sequences.

3.4.2 *amos* misexpression produces ectopic olfactory sensilla

When *amos* is misexpressed in proneural clusters of imaginal discs, olfactory sensilla are formed at a limited range of locations, including the wing veins and scutellum (Goulding et al., 2000b; zur Lage et al., 2003). Interestingly, these are the same locations that are most susceptible to *ato* function. Despite their close similarity, however, it is thought that Ato misexpression cannot form *amos*-dependent olfactory organs. One problem with these

experiments is that they rely on recognising olfactory sensilla by morphology alone, however this approach is fallible because ectopic olfactory sensilla can often resemble stunted external sense organs. Therefore the question of olfactory organ formation by *amos* and *ato* has not been fully explored.

In the embryo, *amos* misexpression is reported to result in the formation of ectopic dbd and dda neurons (Huang et al., 2000). Thus, these Amos phenotypes are in line with its requirement for specification of olfactory sensilla, dbd and dda neurons.

3.4.3 *amos* has ectopic functions when misexpressed

Misexpression of *amos* also produces other phenotypes not ordinarily associated with *amos* function. When misexpressed, *amos* seems to mimic *ato* in the formation of chordotonal organs in the embryo and imaginal discs (Goulding et al., 2000b; Huang et al., 2000). Misexpression of either *amos* or *ato* in wing discs under the control of the same Gal4 driver, will produce ectopic chordotonal organs at similar locations i.e. the scutellum and wing veins (Goulding et al., 2000b; Huang et al., 2000; zur Lage et al., 2003). It is therefore suggested that chordotonal specification is an ancestral Ato-like protein function that has been retained by Amos after gene duplication.

Evidence that *amos* might be able to mimic *ato* in eye development comes from another dominant mutation that has recently been found to be a gain-of-function allele of *amos*. *Rough eye* (*Roi*) causes a roughening of the compound eye and was characterised as a chromosomal inversion that results in *amos* misexpression in the eye disc (Chanut et al., 2002). This seems to interfere with *ato* expression. This alone does not imply that *amos* may function as *ato*. However when *Roi* is placed in an ato^{1} mutant background, it is able to rescue the specification of some R8 photoreceptors and partially rescue the adult eye phenotype (Chanut et al., 2002). This finding has remained unconfirmed by more directed misexpression experiments.

3.5 Experimental aim of this chapter

Although *amos* shares a high sequence identity within its bHLH domain to *ato*, it is clear that it has at least some different proneural properties. Other properties seem to be shared. However, no research has addressed this specificity in detail. This chapter aims to characterise further the misexpression phenotypes of *amos* in order to understand what makes it different from *ato* and why it mimics *ato* when misexpressed.

3.6 Characterising the effect of *ato* and *amos* misexpression in imaginal discs

The enhancer trap line $Gal4^{109\text{-}68}$ is an insertion of the panneural downstream target gene *scabrous* (Mlodzik et al., 1990). This enhancer trap expresses Gal4 in the proneural clusters and SOPs of larval imaginal discs. This makes it an ideal line to ectopically express *amos* and *ato* at the appropriate developmental time and place to affect neurogenesis. For *ato*, it was shown to give the most informative misexpression phenotypes (Jarman and Ahmed, 1998).

3.6.1 Effect of misexpression on external sense organs

Although bristle phenotypes associated with the misexpression of *amos* and *ato* have been documented, there have been no quantitative comparisons. Using $Gal4^{109\text{-}68}$ I quantified the loss of bristles associated with misexpression of fly lines *UAS-ato#1*, *UAS-amos#9* and *UAS-amos#3*. *UAS-ato#1* is the strongest *ato* expressing UAS insertion available (Jarman and Ahmed, 1998), *UAS-amos#3* is a strong *amos*-expressing line, whilst *UAS-amos#9* is a weakly expressing line. I used this range of lines in order to determine whether any apparent *amos*-specific functions were not just a result of strength of misexpression. Moreover, I misexpressed these lines at various temperatures (18°, 25°and 29°C) to assay a range of misexpression strengths. $Gal4^{109\text{-}(2)68}$ like other Gal4 lines is temperature sensitive. Increases in temperature, are accompanied by increases in Gal4 protein activity. This in turn activates the transcription of the UAS lines.

External sense organs were scored on the scutellum (the scutellar macrochaetae) (Fig.3.3A). and the central notum (the dorsocentral macrochaetae). Both *amos* and *ato* inhibited scutellar and dorsocentral bristles efficiently. There is a positive trend associated with the level of Gal4 expression and the inhibition of external sense organ fate. I found that increases in temperature resulted in stronger phenotypes (Fig.3.5 A c.f. B).

UAS-amos#3 can achieve complete inhibition of bristles at a lower temperature than *UAS-ato#1* (Fig.3.6). At 25°C and above, *UAS-amos#3* can inhibit the formation of all macrochaetae on the scutellum (Fig.3.5D), *UAS-ato#1* is only able to do this efficiently at 29°C (Fig.3.6B). However it would be unwise to speculate from this result that *amos* can suppress the external sense organ lineage more efficiently than *ato*. It is more feasible to assume that this difference is due to the relative strength of the *amos* line rather than an intrinsic ability of *amos*. In support of this, *UAS-amos#9* is not as effective at inhibiting the macrochaetae, even at the highest temperature (*UAS-amos#9* Fig.3.5C c.f. *UAS-amos#3* Fig.3.5D at 29°). The strength of *UAS-amos#3* is further implied by the suppression of microchaetae, although this was not quantified (Fig.3.5D)

I have found no evidence to suggest any difference in the ability of *ato* or *amos* to inhibit external sense organ formation. Both *amos* and *ato* are capable of completely suppressing all the bristles on the scutellum, providing their expression levels are sufficiently high (the notum was found to be less affected in this assay Fig.3.6A).

Taken together, these results show that the ability to suppress the external sensory fate is an intrinsic ability of both *amos* and *ato* but the extent to which this takes place is dependent upon the level of *Gal4/UAS* expression and also the strength of the individual UAS-lines.

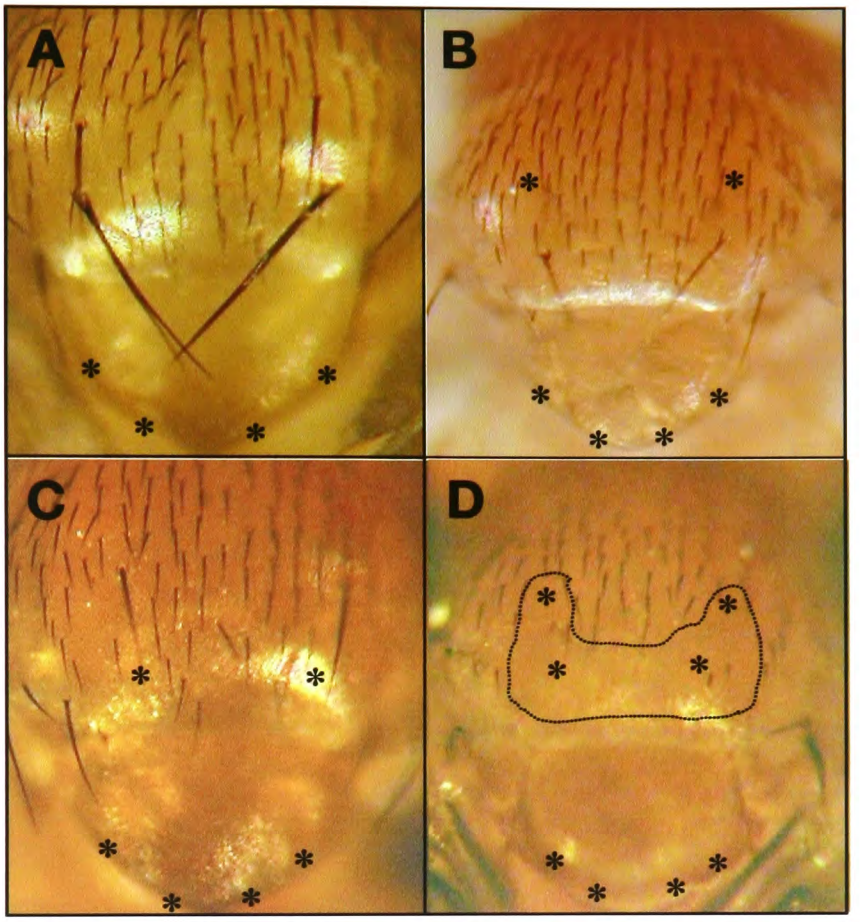

Figure 3.5 Misexpression of *amos* and *ato* inhibit the formation of thoracic macrochaetae. Locations where macrochaetae are suppressed are indicated by asterix. *UAS-ato#1* (**A**, 25°C; **B**, 29°C). *UAS-amos#9* at 29°C (**C**). *UAS-amos#3* at 29°C (**D**). The degree of macrochaetae suppression increases with temperature (**A** c.f **B**). *UAS-amos#3* is stronger than *UAS-amos#9* at comparable temperatures (**D** c.f. **C**). This suggests that the strength of the phenotype is dependent upon firstly the temperature and secondly, the relative strength of the individual lines. Strong expression of *UAS-amos#3* can also suppress microchaetae (area enclosed by dotted lines **D**).

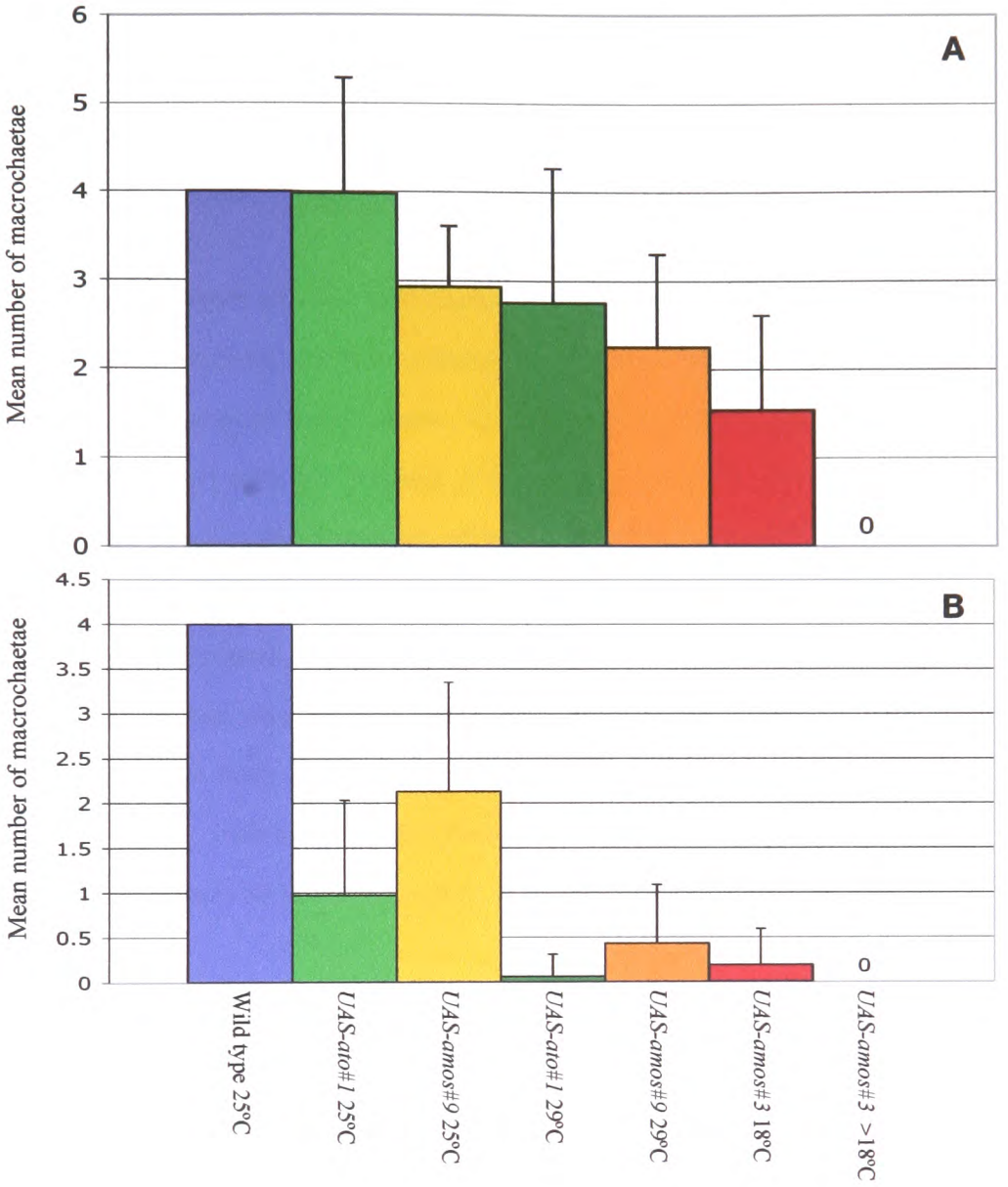

Fig 3.6. The external sense organ lineage is inhibited in the thorax by the misexpression of *amos* and *ato*. Misexpression of *amos* and *ato* reduce the number of external sense organs (macrochaetae) on the notum **(A)** and scutellum **(B)** compared to wild type. The inhibition increases with temperature. *UAS-amos#3* can achieve this inhibition at a lower temperature than *UAS-amos#9 or UAS-ato#1*. This indicates that *UAS-amos#3* is the strongest line in this assay. However *UAS-amos#9* is weaker than *UAS-ato#1* on the scutellum **(B)**. This suggests that the degree of inhibition is dependent upon the relative strengths of the lines assayed.

3.6.2 Both genes promote ectopic chordotonal organs

The literature acknowledges that *amos* is able to produce chordotonal organs (Goulding et al., 2000b). However the relative ability of Amos at Atonal to specify chordotonal organs has not been previously investigated.

3.6.2.1 Scoring chordotonal organs – GFP-nompA

Chordotonal organs are located internally, underneath the cuticle of the fly. This makes them harder to assay than external sense organs. The chordotonal organ is made up of one neuron and three support cells; the ligament, scolopale and cap cells. The scolopale cell secretes a refractile structure (the scolopale), which can be observed subcutaneously with a high magnification light microscope and DIC optics (see Fig.3.3.E). However, this requires much expertise and experience, especially to score accurately large arrays of chordotonal organs. Previous studies have scored the ectopic chordotonal organs produced by morphology alone. Flies have been dissected, fixed and then thoracic or wing cuticles mounted for microscopy. Initially I performed the same assay procedure. However, I found that this method was vulnerable to subjective error, therefore alternatives were explored.

Recently, a gene has been identified for a protein secreted by the chordotonal cap cell. This protein is required for the proper transduction of mechanical energy across the chordotonal organ and without it no mechanoreceptor potential can be produced, hence the gene has been termed *nompA* (Chung et al., 2001). The protein is confined to the dendritic cap, which is attached to the scolopale. These authors created flies that express a GFP-NompA fusion protein. This fusion protein localises correctly to the chordotonal cap and is readily visible by fluorescence microscopy. Thus flies containing this fusion have GFP as a marker for chordotonal organs. It must be noted that *nompA* is also expressed in other sensilla types, however the chordotonal organs are distinct because of cell morphology.

I obtained the GFP-nompA fusion line (gift from M. Kernan) and tested its efficacy by scoring wildtype chordotonal organs. Using confocal microscopy I was able to count unambiguously the wildtype chordotonal organs in the femur (62.8±3.45) and wing hinges (10.5±1.12) (Fig.3.7). This method has advantages over traditional light microscopy as the GFP allows the position of all chordotonal organs to be visible even in deep locations. I used the GFP-nompA fusion in most of my subsequent studies.

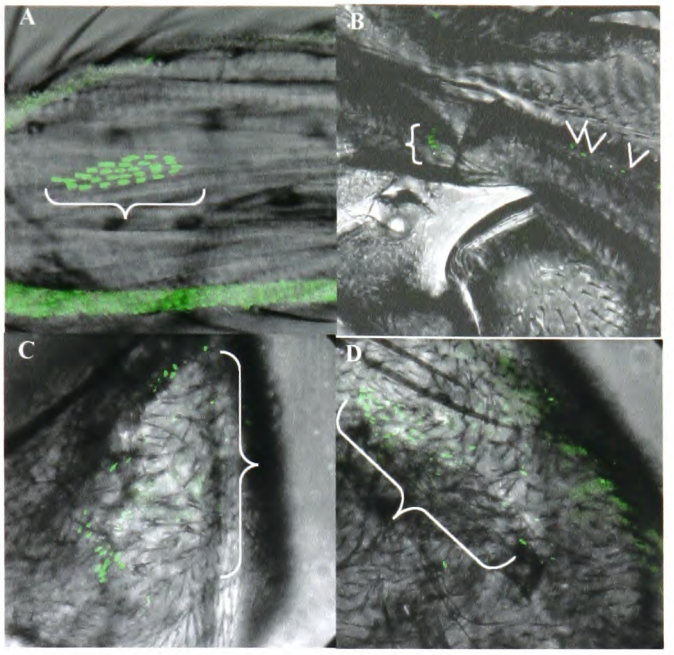

Figure 3.7 GFP-nompA labels chordotonal organs and ES organs. **(A)** wildtype femoral chordotonal organs. **(B)** wildtype wing chordotonal organs indicated by bracket and wing sensilla campaniformia (arrowheads) can be visualised and discriminated by the shape of GFP expression. GFP expression in ES organs is round whilst expression in chordotonal organs is oblong. Ectopic chordotonal organs are induced in the scutellum by misexpression of *UAS-ato#1* **(C)** and *UAS-amos#3* **(D)**.

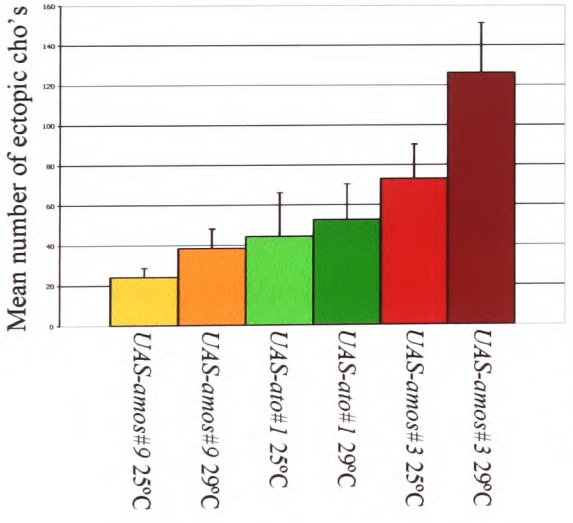

Figure 3.8 Misexpression of *amos* and *ato* produce ectopic chordotonal organs in the scutellum. The number of ectopic chordotonal organs produced increases with temperature. *UAS-amos#9* is not significantly different from *UAS-ato#1* at 29°C (t-test P=0.223). However *UAS-amos#3* does produce significantly more chordotonal organs than *UAS-ato#1* at 29°C (t-test P=0.004).

3.6.2.2 *amos* misexpression results in massive chordotonal organ formation

The *GFP-nompA* control assays have established the use of this marker as a reliable and accurate method for assaying wild type chordotonal organs. I inserted this GFP marker into the genetic backgrounds of *UAS-ato#1*, *UAS-amos#9 and UAS-amos#3* driven by $Gal4^{109-(2)68}$ and assayed for ectopic chordotonal organs in the scutellum. Flies were dissected, fixed, and examined by epifluorescence or confocal microscopy.

In these experiments (Fig.3.8), the mean number of ectopic chordotonal organs specified by *UAS-ato#1* was higher than that for *UAS-amos#9*, however this was not significant due to a large variation in the former number (52.8±17.8; 38.5±9.68, t-test P=0.223). Surprisingly *UAS-amos#3* induced the highest number of ectopic scutellar chordotonal organs (*UAS-amos#3* 126.3±25 c.f. *UAS-ato#1* 52.8±17.8 t-test P=0.004). This was more than two times the number induced by *ato*. Thus, it seems that *amos* is actually more efficient than *ato* at promoting chordotonal fate.

Previous studies have not indicated any differences in efficacy to produce chordotonal organs between *ato* or *amos* (*UAS-ato*, 70.3±10.3, Jarman and Ahmed, 1998; *UAS–amos*, 69±13, Goulding et al., 2000). The disparate findings can be explained by a number of possibilities. The experimental conditions between this study and other studies are not the same. Firstly there may be differences in temperature and in some cases different Gal4 drivers have been used (Jarman and Ahmed, 1998; Goulding et al., 2000). Secondly one cannot ignore the time that sets the misexpression studies apart. It is common for fly lines to pick up various background mutations over time. This in conjunction with a different genetic background (GFP-nompA), could be sufficient to alter the numbers. Furthermore, this study uses GFP as a marker for chordotonal organs, thus the problems associated with identifying and scoring chordotonal organs by light microscopy are resolved. Therefore the results are likely to be more accurate due to the improved methodology.

3.6.3 Misexpression of *amos* produces ectopic olfactory sensilla on the second antennal segment

Misexpression of *amos* has been reported to produce *amos*-specific sense organs (Goulding et al., 2000b). Heatshock Gal4 produces a number of phenotypes. Besides from the formation of ectopic chordotonal organs, misexpression of *amos* increases the number of all subtypes of olfactory sensilla in the funiculus by 24-44%, as a consequence, this antennal segment becomes bulbous and malformed. In addition, ectopic olfactory like sensilla are formed along the third wing vein (19.4±2.8) and scutellum (16±3.3) (Goulding et al., 2000b).

Initially, I tried to reproduce these results in the wing and scutellum, However I found it difficult to obtain accurate numbers for this study. This is because the presumed olfactory sensilla formed are often of mixed morphology, sometimes resembling small external sense organs. They are therefore difficult to score unambiguously. Therefore I decided to look for a location where the olfactory like sensilla more closely resembled the wild type sensilla of the third antennal segment (the funiculus). In preliminary work, I noted that the second antennal segment proved promising. Normally this segment has external sense organs and contains the large chordotonal array of Johnston's Organ, but no olfactory sensilla. However its proximity to the funiculus seems to make the second antennal segment more able to generate bona fide ectopic olfactory sensilla than the thorax (Fig.3.9B c.f. E). I therefore scored for the presence of ectopic olfactory sensilla on the second antennal segment after misexpression.

Gal4$^{(109\text{-}(2)68)}$ driven misexpression of *UAS-amos#9* and *UAS-amos#3* produces ectopic olfactory sensilla on the second antennal segment (Fig.3.10). However *UAS-amos#3* was much stronger than *UAS-amos#9* at 29°C (12.3±4.33 c.f. 1.25±1.42). But, *UAS-amos#3* at 18°C was not significantly different from *UAS-amos#9* at 29°C (1.44±1.15 c.f. 1.25±1.42). This suggests that differences in efficacy are quantitative rather than qualitative, both lines in this assay behave in the same way.

Morphological inspections of the olfactory sensilla formed by *UAS-amos#3* suggest variations in subtype dependent upon the site of misexpression. Olfactory sensilla formed on the scutellum and wing veins more closely resemble the coeloconica type but the sensilla of the second antennal segment more closely resemble trichodea (Fig.3.9). This suggests that there may be tissue specific factors, which limit the subtype of sensilla, which can be formed by misexpression.

3.6.4 *ato* cannot promote ectopic olfactory organ formation

I have confirmed the ability of *amos* to produce *ato*-specific chordotonal organs in misexpression assays. I showed that in some cases *amos* is quantitatively stronger than misexpression of *ato* itself. It has been proposed that this apparent overlap in specificity may be due to the structural closeness of their bHLH domains. However if this is true, it opens up the possibility that *ato* may be able to mimic *amos* in the formation of olfactory organs.

I misexpressed *ato* using $Gal4^{109(2)68}$ and assayed for the presence of olfactory-like sensilla on the third wing vein, scutellum and second antennal segment. In an extensive screen of 40 $Gal4^{109(2)68}$, *UAS-ato#1* flies at 25°C and 29°C, I found no ectopic olfactory organs on the scutellum or third wing vein. However I found the occasional olfactory-like sensilla on the second antennal segment (Fig.3.9C). Even at 29°C, the number of ectopic olfactory organs on the second antennal segment of *UAS-ato#1* flies was much lower than *UAS-amos#3* or even the weak *UAS-amos#9* line (Fig.3.10) (0.075±0.267 c.f. 12.3±4.33 and 1.25±1.42 t-test=9.62×10^{-5}).

Thus, *ato* and *amos* behave quite distinctively in this regard. It seems that *ato* is incapable of specifying olfactory sensilla outside the funiculus. But *amos* can produce ectopic olfactory sensilla outside their normal developmental context. This does not appear to be a quantitative difference due to strength of misexpression, since the weak *amos#9* line is able to promote olfactory organs better than *ato* even though it performs poorly in the external

sense organ and chordotonal organ assays. Thus, there is strong evidence to suggest these results reflect a real difference in the misexpression specificities of *amos* and *ato*. However, misexpression of *ato* is represented by a single line in all assays (the strongest available). I confirmed my original findings in this assay by combining two copies of *UAS-ato#1*. *UAS-ato#1 Gal4*$^{109\text{-}68}$*/UAS-ato#1* flies at 29°C still produced no ectopic sensilla in the second antennal segment, scutellum or wing veins (n=4). These flies however showed reduced viability and very strong chordotonal and bristle phenotypes implying high levels of misexpression. This confirms the qualitative difference between the abilities of *amos* and *ato* to produce olfactory sensilla in ectopic locations.

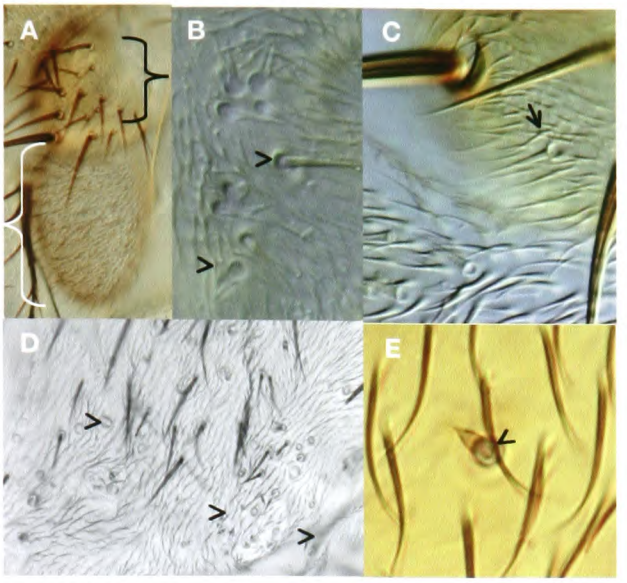

Figure 3.9 Ectopic olfactory sensilla are formed by *amos* misexpression. (A) Wild type antenna house olfactory sensilla in the 3rd segment (white bracket), there are no olfactory organs on the second antennal segment (black bracket). Misexpression of *UAS-amos#3* produces ectopic olfactory sensilla on the 2nd antennal segment **(B)**, notum **(D)** and scutellum **(E)** (arrowheads). *UAS-ato#1* rarely produces olfactory sensilla outside the funiculus, occasional single sensilla (arrows) are sometimes found on the 2nd antennal segment **(C)**.

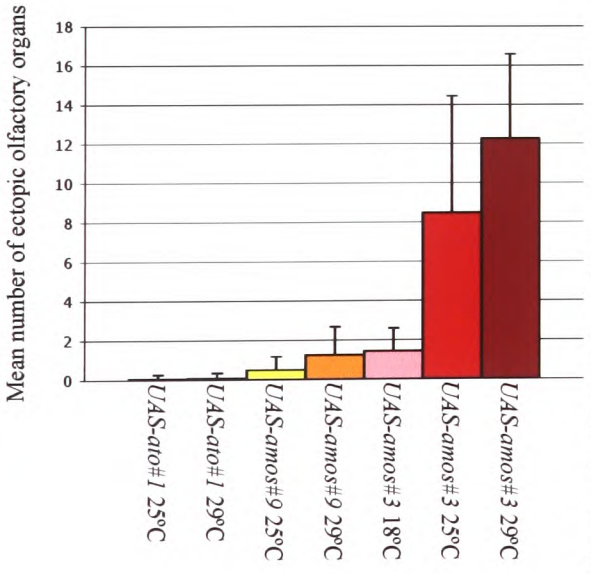

Figure 3.10 Ectopic olfactory organs are formed by the misexpression of *amos* on the second antennal segment. Only misexpression of *amos* can specify ectopic olfactory sensilla. The number of ectopic olfactory organs increase with temperature (*UAS-amos#3* at 18°C; 1.44±1.15 c.f. 29°C; 12.3±4.33). *UAS-amos#9* also specifies ectopic olfactory sensilla, but at a much lower level than *UAS-amos#3*. *UAS-ato#1* does not produce significant numbers of ectopic olfactory organs, and is unaffected by increases in temperature (25°C, 0.05±0.674 and 29°C, 0.075±0.267).

3.7 Assaying misexpression of *amos* and *ato* in the embryo

Relatively little work has been done to investigate the effects of proneural gene misexpression in embryos. In theory, this may produce clearer results since there are more molecular markers available for the embryonic PNS.

Gal4$^{109\text{-}(2)68}$ is not expressed well in embryos (A. Jarman, pers. comm.). Therefore I used a *sca-Gal4* driver line to drive misexpression. I misexpressed *UAS-ato#1*, *UAS-amos#9* and *UAS-amos#3* and assayed the sensory neurons by morphology in late embryos (stage 15) using the antibody 22C10 which marks all sensory neurons (Zipursky et al., 1984).

3.7.1 Misexpression of *ato* and *amos* produces supernumerary chordotonal organs in the embryonic lateral cluster

Unlike misexpression in the adult, misexpression in the embryo did not induce ectopic formation of chordotonal organs, as judged by morphology after staining with MAb 22C10. However, both *amos* and *ato* could induce the formation of extra chordotonal neurons within the existing lateral chordotonal cluster (Fig.3.11). Furthermore there was no significant difference between *UAS amos#9* and *UAS ato#1* at 25°C (Fig.3.12 6.14±0.378 ; 6.71±0.951, t-test P=0.179). *UAS amos#3* can produce comparable numbers of lateral chordotonal organs as *UAS amos#9* and *UAS ato#1* (7± 0.816). However, this is achieved at a lower temperature (18°C). This suggests that *UAS amos#3* is the strongest line in this assay. But this could not be confirmed because I was unable to assay the phenotype above 18°C due to the severe disruption of the entire PNS.

Misexpression of *amos* and *ato* induce comparable numbers of chordotonal organs in the embryo. However, the chordotonal phenotype was less severe in the embryo than in the adult. This could be a consequence of different *Gal4* drivers. However, it has also been reported that misexpression of proneural genes does not affect the embryonic PNS as strongly as it does the adult PNS (Giebel et al., 1997).

3.7.2 Assaying *amos*-specific neurons in the embryo

Misexpression of *ato* in the adult PNS is unable to specify ectopic olfactory sensilla (outside the funiculus). Therefore I wanted to know whether the functional constraints imposed on *ato* are also apparent in the embryo. *amos* is responsible for the specification of two types of MD neuron (dbd and dda) in each hemi-segment of the *Drosophila* embryo (Huang et al., 2000). However identification of these neurons is difficult under misexpression conditions. This is because misexpression of both *amos* and *ato* can disrupt the embryonic PNS in such a way that neurons may be mislocalised, which may hamper the identification of *amos*-specific neurons. To resolve these experimental difficulties I used a histological marker for *amos*-specific neurons. The POU-domain transcription factor, PDM, is expressed in wildtype dbd and dda neurons and also the ligament cells of chordotonal organs, which are distinguishable by their cell morphology (Fig.3.13A) (Brewster et al., 2001).

Misexpression of *amos* in the embryo produces significantly higher numbers of PDM-positive cells compared to wildtype (per hemisegment Fig.3.14: *UAS-amos#9* at 25°C; 4.45±1.26 and *UAS-amos#3* at 18°C; 6.31±2.59 c.f. w^{1118}; 2). Misexpression of *UAS-ato#1* at 25°C also produces more PDM+ cells than wild type (2.86±1.46), however this was still significantly less than *UAS-amos#9* (t-test=4.4×10^{-4}).

Thus, I found that misexpression of *amos* was better at specifying *amos*-specific neurons in the embryo than *ato* (Fig.3.14). This difference in specificity was not dependent upon the strength of the lines; *UAS-ato#1* is stronger in the external sense organ assay and the chordotonal organ assay than *UAS-amos#9*. However, *UAS-ato#1* did specify some extra *amos*-specific neurons indicating some leakage in specificity of *ato* under misexpression conditions in the embryo.

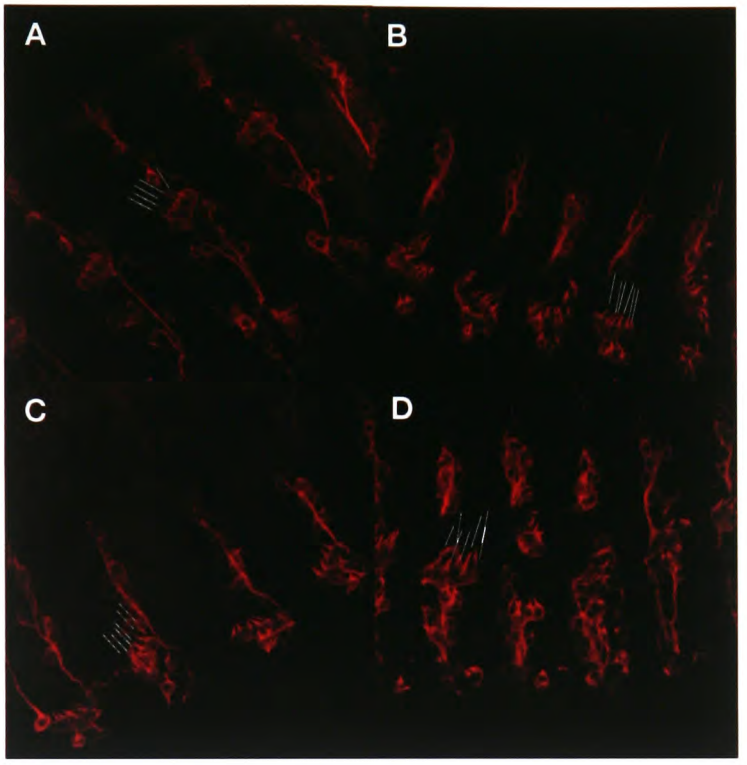

Figure 3.11 Misexpression of *amos* and *ato* induce the formation of extra chordotonal organs in the embryonic lateral clusters. Neurons are stained with mAB22C10. **(A)** Wildtype embryos display 5 chordotonal organs in each lateral cluster (white lines). Misexpression of *UAS-ato#1* **(B)**, *UAS-amos#9* **(C)** and *UAS-amos#3* **(D)** induce the formation of extra chordotonal organs in the lateral cluster compared to wild type **(A).**

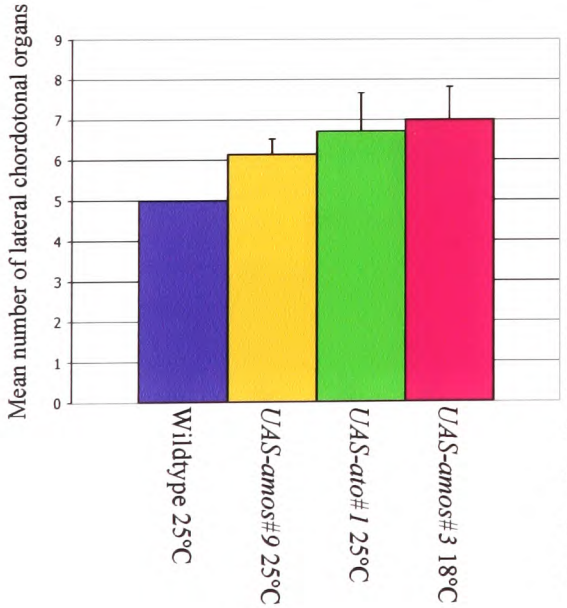

Figure 3.12 Misexpression of *amos* and *ato* produce extra lateral chordotonal organs in the embryo. The number of chordotonal organs produced by *UAS-amos#9* and *UAS-ato#1* are not significantly different at 25°C (6.14±0.378 ; 6.71±0.951, t-test P=0.179). *UAS-amos#3* however can produce comparable numbers of chordotonal organs at the lower temperature of 18°C (7±0.816). This suggest that *amos* and *ato* are qualitatively similar in this assay, however *UAS-amos#3* is the strongest line.

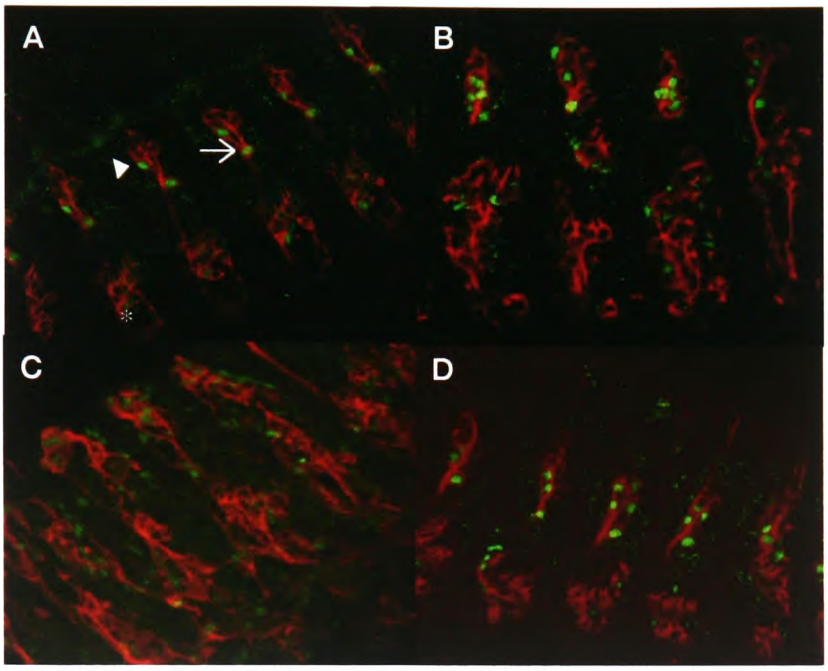

Figure 3.13 PDM labels the dorsal bipolar md neurons and chordotonal ligament cells of the embryonic PNS. **(A)** Wildtype dda (arrowhead), dbd (arrow) and ligament cells (asterix) are labeled with anti-PDM (green). **(B)** *UAS-amos#9* (25°C) induces expression of ectopic PDM+ cells in the dorsal cluster. **(C)** *UAS-amos#3* (18°C) has a stronger affect upon the number of ectopic PDM+ cells c.f. **(B)**. **(D)** *UAS-ato#1* (25°C) also induced formation of ectopic PDM+ cells, however to a lesser extent than *amos* **(B, C)**.

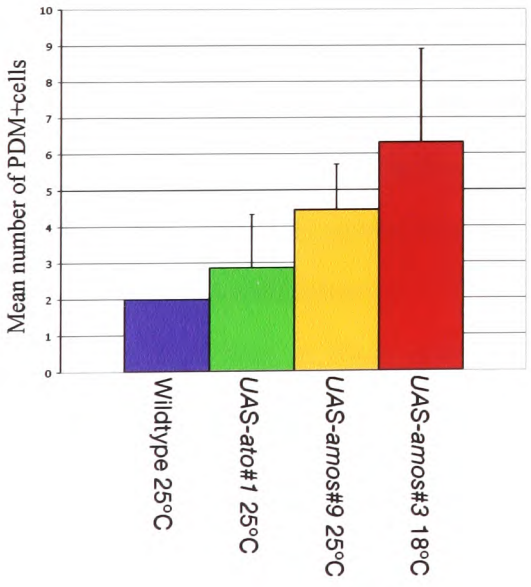

Figure 3.14 Misexpression of *amos* in the embryo produces extra dorsal md neurons. *Gal4^{Sca}* misexpression of *amos* and *ato*. *UAS-amos#9* at 25°C and *UAS-amos#3* at 18°C, produce significantly more dorsal md neurons than wildtype. *UAS-ato#1* at 25°C also produces extra dorsal md neurons compared to wild type, however this was not significant.

3.8 Investigating the basis for inappropriate chordotonal formation by *amos*

Misexpression of *amos* can mimic *ato* in the specification of adult and embryonic chordotonal organs (Figs. 311; 3.12 and Goulding et al., 2000b). The reciprocal however is not true. Misexpression of *ato* does not mimic *amos* in the specification of ectopic olfactory like sensilla. Here, I explore how and why there is a loss of specificity under some circumstances. Two possibilities can be considered:

1. *amos* may activate chordotonal target genes when expressed in the wrong context i.e. outside the antenna.
2. *amos* may inappropriately cross-activate *ato* when expressed in the wrong context. The formation of ectopic chordotonal organs may be a secondary result from this cross-activation, i.e. *amos* may be able to cross-activate *ato* directly via the latter's autoregulatory enhancers.

3.8.1 Misexpression of *amos* cross-activates endogenous *ato*

I dissected imaginal discs from 3rd instar larvae misexpressing *amos* and stained for the expression of *ato*. For *UAS-amos#3,* ectopic expression of *ato* could be readily detected in the presumptive thorax (Fig.3.16F c.f. A). However the reciprocal was not shown to be true; misexpression of *ato* did not result in ectopic *amos* expression (Fig.3.16C).

Similar experiments were performed in embryos (stage 10). I misexpressed *amos* in the embryo using *scaGal4* then stained the embryos for Amos or Ato and Senseless (Fig.3.15). I identified embryos misexpressing *UAS-amos#3* by their increased Senseless expression (as a marker of SOPs). In these embryos, I found that Ato was ectopically expressed compared with wild type (Fig.3.15B c.f. C). Similarly embryos misexpressing *ato* were identified by increased Senseless expression. *amos* expression in these embryos was not found to be different from wild type (Fig.3.15E c.f. F). This suggests that *ato* does not cross-activate *amos* even though its misexpression results in a few extra PDM-expressing cells.

In summary, inappropriate expression of *amos* can up-regulate endogenous *ato*. This activation of *ato* by *amos* could be responsible for ectopic chordotonal organ formation by *amos*. This experiment, however, does not indicate whether *ato* is required for the specification of chordotonal organs. I address this next.

3.8.2 *amos* production of ectopic chordotonal organs requires the presence of endogenous *ato*

The experiments in 3.8.1 show that *amos* can cross-activate *ato*, but do not indicate whether this cross activation is required for the specification of ectopic chordotonal organs. Therefore I asked whether *amos* misexpression can promote chordotonal organ formation even in the absence of endogenous *ato* function. Specifically, I repeated the misexpression experiments in an ato^1 mutant background. I scored for rescue of wild type chordotonal organs and assayed for ectopic chordotonal organs in the scutellum. Flies of the correct genotype were readily identified by their bristle suppression (*UAS-amos/ato*) and disrupted eye (*ato* mutant). I found that *UAS-ato#1* could rescue the chordotonal organ phenotype of ato^1 but *UAS-amos#3* could not (Fig.3.17).

The number of ectopic chordotonal organs produced by misexpression of *UAS-ato#1* and misexpression in the mutant background was not significantly different (fig. 3.17 t-test=0.734). However the reverse was not true, misexpression of *UAS-amos#3* in the mutant background produced significantly fewer ectopic chordotonal organs than in the non mutant background (73±17.2 ; 16.6±14.4, t-test=0.004). When I examined the wing discs of *UAS-amos#3* flies in an ato^1 background, the ectopic *ato* expression seen in the non mutant background was lost (Fig.3.16G). This suggest that *amos* must cross-activate *ato* in imaginal discs in order to specify chordotonal organs.

Previous experiments have shown that *amos* can cross-activate endogenous *ato* in the embryo (Fig.3.15). This may have an impact on the ability of *amos* to specify chordotonal

organs. However it has been reported that *amos* can rescue chordotonal organs in *ato* mutant embryos (Huang et al., 2000). This suggests that misexpression of *amos* is sufficient to specify chordotonal organs in the embryo. It is my supposition that the functional constraints that set *amos* and *ato* apart may be stronger in the adult than the embryo.

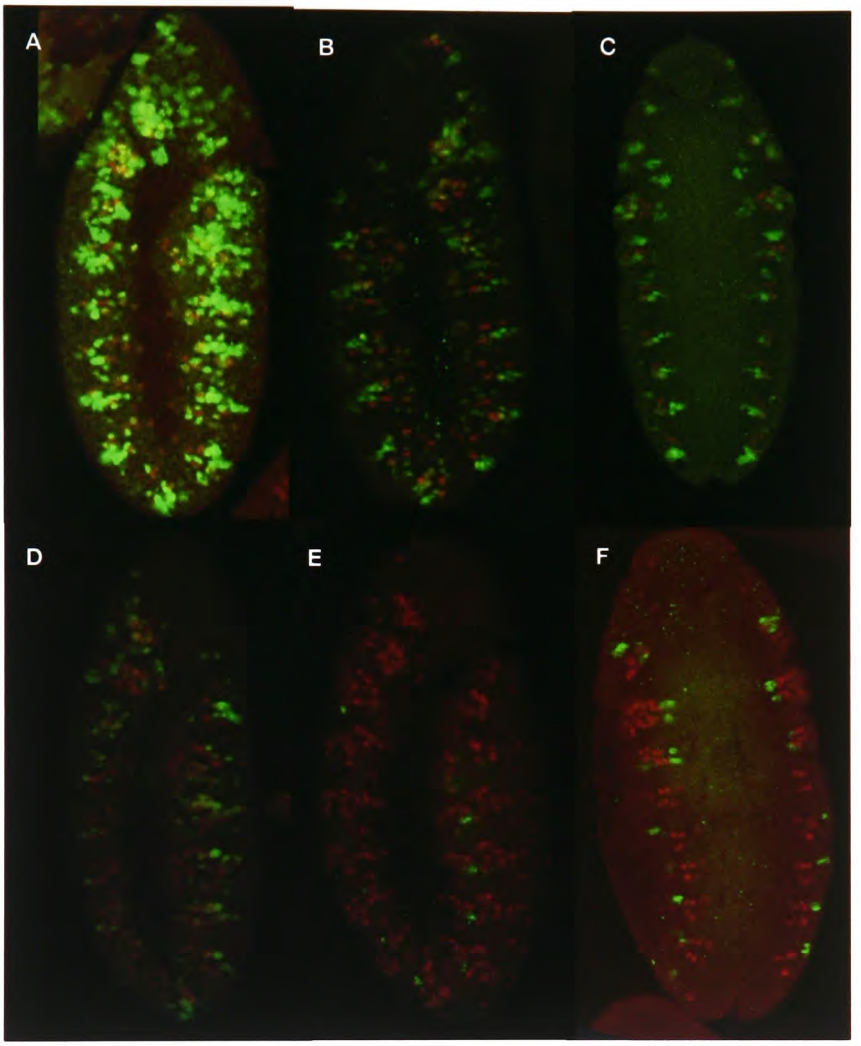

Figure 3.15 Misexpression of *amos* cross activates endogenous *ato* in the embryo.

(A) anti-Amos and **(B)** anti-Ato *Gal4^{Sca}* driven misexpression of *UAS-amos#3*.

(C) Wild type expression of Ato (green) and Senseless (red).

(D) anti-Ato and **(E)** anti-Amos *Gal4^{Sca}* driven misexpression of *UAS-ato#1*.

(F) Wild type expression of Amos (green) and Senseless (red).

Misexpression of *UAS-amos#3* upregulates endogenous Ato (green) **(B)** compared to wild type **(C)**. However, endogenous Amos (green) **(E)** is not upregulated by *UAS-ato#1* compared to wild type **(F)**.

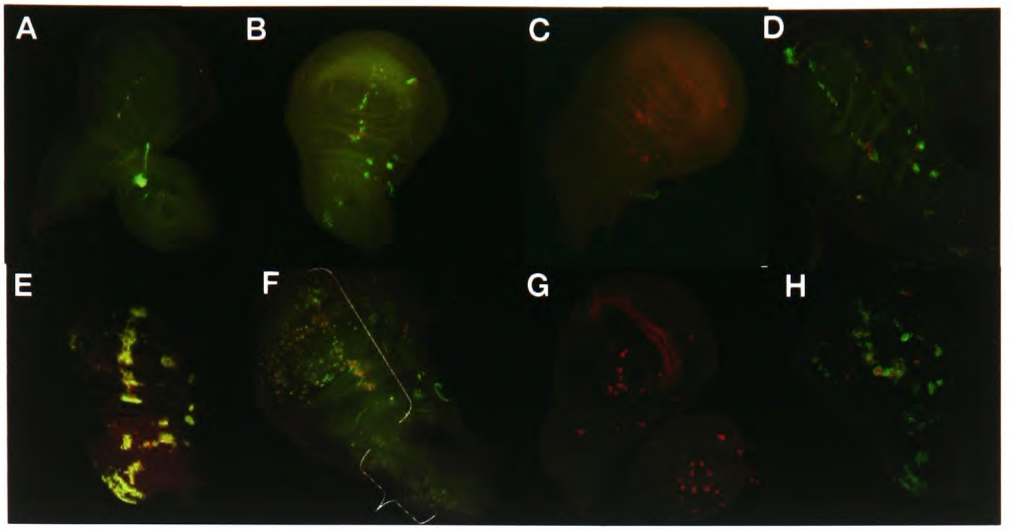

Figure 3.16 Misexpression of *amos* in wing imaginal discs cross-activates endogenous *ato*. **(A)** W^{1118} anti-Ato green, anti-Senseless red. **(B)** *UAS-ato#1* 29°C anti-Ato green, anti-Senseless red. **(C)** *UAS-ato#1* 29°C anti-Amos green, anti-Senseless red. **(D)** *UAS-ato#1; ato^1*/ato^1 29°C anti-Ato green, anti-Senseless red. **(E)** *UAS-amos#3* 29°C anti-Amos green, anti-Senseless red. **(F)** *UAS-amos#3* 29°C anti-Ato green, anti-Senseless red. **(G)** *ato^1, UAS-amos#3* / ato^1 29°C anti-Ato green, anti-Senseless red. **(H)** *ato^1, UAS-amos#3* / ato^1 29°C anti-Amos green, anti-Senseless red. Misexpression of *ato* does not cross activate *amos* **(C)**, however misexpression in *ato^1* rescues and produces ectopic *ato* expression **(D)**. Misexpression of *amos* however does cross activate *ato* particularly at the presumptive scutellum (curly bracket) and 3rd wing vein (bracket) **(F)**. However this is abolished in *ato^1* **(G)**, although strong ectopic expression of *amos* persists **(H)**.

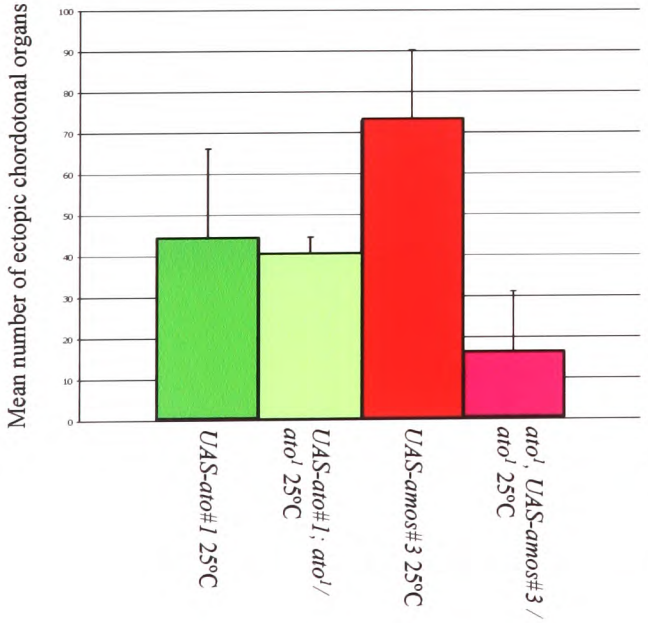

Figure 3.17 The formation of ectopic chordotonal organs on the scutellum requires *ato*. Removal of endogenous *ato* does not significantly affect the number of ectopic chordotonal organs produced by misexpression of *UAS-ato#1* (44.5±21.7; 40.4±4.16, t-test=0.734). However, ectopic chordotonal organs induced by *UAS-amos#3* are significantly reduced by removal of *ato* (73±17.3; 16.6±14.5, t-test=0.004).

3.8.3 Removing both copies of *ato* exacerbates the ectopic olfactory phenotype of *amos* misexpression

A further novel phenotype of *amos* is seen in the second antennal segment by misexpression in the ato^1 mutant. Removing one and both copies of *ato* produced significantly more ectopic olfactory organs compared to the non-mutant background (Fig.3.19 t-test=0.002 and 0.001 respectively). Furthermore, the ectopic olfactory organs formed in the wildtype background consisted mainly of trichoid-like sensilla, however removing both copies of *ato* resulted in formation of coeloconica and basiconica-type sensilla also (Fig.3.18).

It seems that removal of *ato*-function enforces the misexpression specificity of *amos.* In the ato^1 homozygote, *amos* no longer mimics *ato* in the specification of ectopic chordotonal organs, however its ability to induce *amos*-specific phenotypes is strengthened. It is possible that the strength of the Amos misexpression phenotype in the wildtype background is limited by the availability of Da. The truncated Ato^1 protein may be unable to dimerise with Da, in which case more Da will be available for interaction, thus potentiating the misexpression phenotype of Amos.

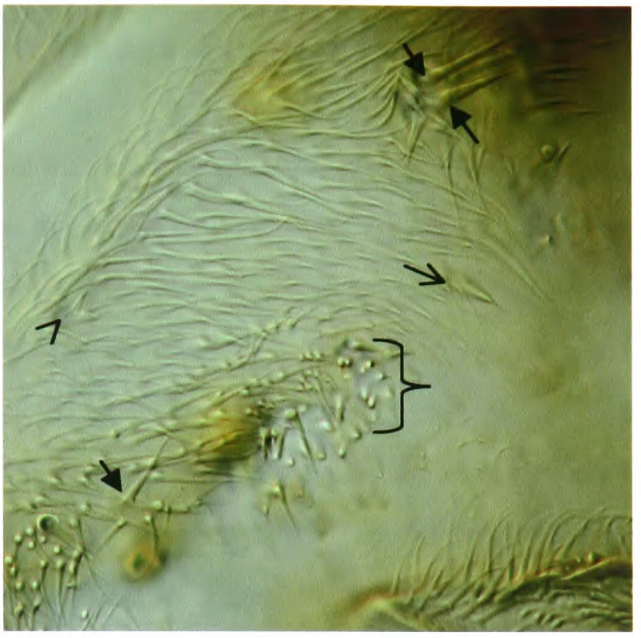

Figure 3.18 Removing both copies of *ato* exacerbates the ectopic olfactory organs on the second antennal segment of *UAS-amos-#3*. The ectopic olfactory organs are usually found in clusters, and all three subtypes are produced. In addition to trichoid-like sensilla (arrows), groups of coeloconica-type sensilla (bracket) and basiconic-like sensilla (open arrow) are ectopically formed. Furthermore occasional forked sensilla are produced (arrowhead).

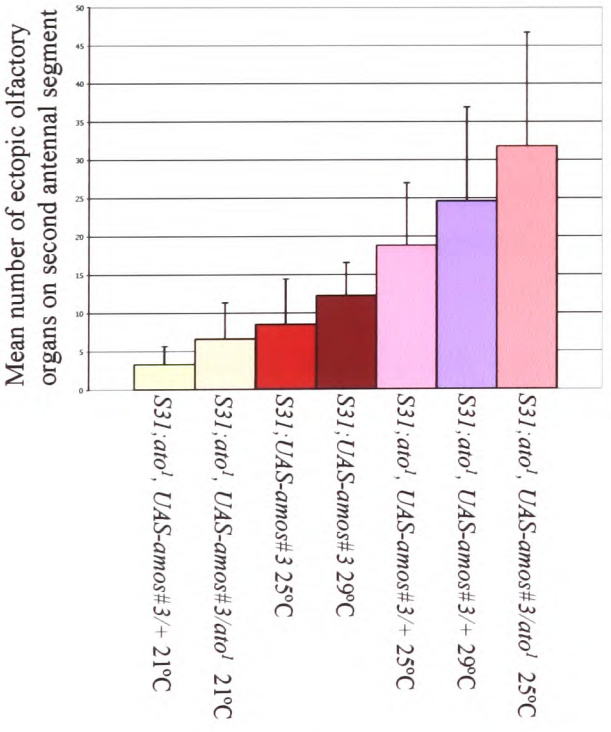

Figure 3.19 More ectopic olfactory organs are formed on the second antennal segment by *amos* misexpression in *ato*^{1}. Removing one or two copies of *ato* increases the ectopic olfactory phenotype of *UAS-amos#3* misexpressing flies. This is significant at 25°C, *S31;UAS-amos#3* c.f *S31;ato*^{1}, *UAS-amos#3/+* (t-test=0,002) and *S31;ato*^{1}, *UAS-amos#3/ato*^{1} (t-test=0.001).

3.8.4 *ato* can rescue Pdm-positive cells in *amos* mutant embryos

I previously showed that *ato* misexpression results in a very modest increase in PDM-positive cells. Given the apparent rescue of the *ato* mutant embryonic phenotype by *amos* (Huang et al., 2000), I explored whether *ato* can specify MD neurons in the absence of *amos*. Due to genetic restrictions an alternative Gal4 driver was used *hGal4*. As a pair-rule segmentation gene *hairy* has been used to express Gal4 in pairs of segments of the embryo (Jimenez 1996). I expected this Gal4 driver to have the advantage of misexpressing the UAS lines in some segments but not others. It has been reported that *hGal4* drives expression in abdominal segments A1, A3, A5, and A7 (Chien et al., 1996; Huang et al., 2000). I had hoped to identify segments which were misexpressing the UAS lines and compare them to unaffected segments in the same embryo.

In this experiment, however, it was not possible to determine embryo genotypes unambiguously. In the $amos^1$ mutant embryo, the *amos* dependent md neurons are lost, as indicated by the loss of dorsal PDM staining (Fig.3.20B c.f. wildtype A). Thus $amos^1$ homozygotes are easily identified. Identification and discrimination of other genotypes by phenotypic examination, however is not possible, for example; misexpressing embryos heterozygous for $amos^1$ and those in a non mutant background are expected to have the same phenotypes. However, the remaining observed phenotypes were unexpected.

I could not identify misexpression embryos with the $amos^1$ homozygote genotype (*$amos^1$UAS-ato#1/$amos^1$;hGal4* and *$amos^1$/$amos^1$; UAS-amos#3/hGal4*). Due to the pair-rule driver, I expected misexpression in $amos^1$ homozygotes to display phenotypes consisting of absent PDM-positive cells in some segments and possible rescue of PDM-positive cells in adjacent segments. However, I could only observe three phenotypes: wild type embryos; mutant embryos lacking PDM+ md neurons ($amos^1$ homozygote) and embryos with extra PDM+ cells in all segments (*UAS-ato#1*; *hGal4* or *UAS-amos#3/ hGal4*).

I suggest that the absence of the expected phenotype of misexpression embryos with the *amos*^{1} homozygote genotype is due to overspill of *hGal4* into all segments, leading to widespread rescue. To find support for this idea, I stained the embryos with anti-Amos (in the case of *amos* misexpression) and anti-Ato (in the case of *ato* misexpression). I found that *hGal4* drives strong Amos expression in wide indistinct bands (Fig.3.21B). This suggests that Amos is expressed sufficiently in all segments to rescue the *amos*^{1} phenotype. A similar result was found for the expression pattern of Ato, however at a much lower expression level (data not shown).

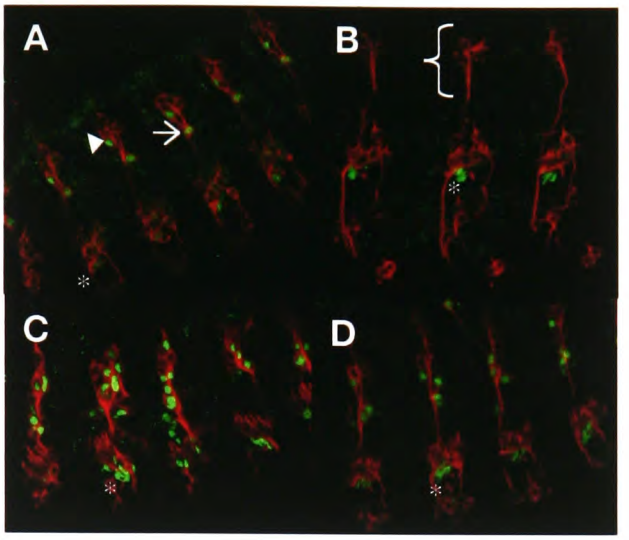

Figure 3.20 Misexpression of *amos* and *ato* can rescue the *amos*^{1} phenotype. **(A)** wildtype dda (arrowhead), dbd (arrow) and ligament cells (asterix) are labeled with anti-PDM (green). **(B)** *amos*^{1}*/S6* embryos lose this *amos*-dependent dorsal staining (bracket), however retain PDM expression in the ato-dependent ligament cells. **(C)** *UAS-amos#3* (18°C) can rescue dda and dbd neurons and induce neurogenesis of ectopic PDM+ neurons. **(D)** *UAS-ato#1*(25°C) restores PDM expression in the dorsal cluster and induces ectopic PDM+ neurons in *amos*^{1} homozygotes.

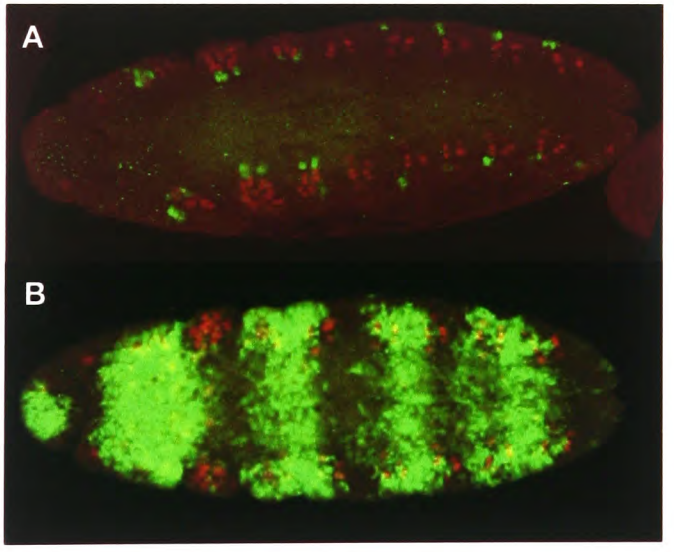

Figure 3.21 *hGal4* produces misexpression in all embryonic segments. **(A)** Wild type expression of Amos (green) and senseless (red). **(B)** *hGal4* drives *UAS amos#3* misexpression (green) in large bands which overlap two or more abdominal segments. (Leaky *hGal4* makes it impossible to differentiate between misexpression in *amos*^{1} homozygotes and misexpression in other genetic backgrounds.)

A further indication that the rescued embryos are merged with the population of misexpressing embryos comes from comparisons of expected and observed phenotypes. Provided that this indeed occurs, I found that the proportion of embryos displaying a misexpression phenotype is close to expected values. For rescue by *amos*, out of a population of 200 embryos, 25% displayed a misexpression phenotype, compared to the expected value of 24% (Fig.3.22C). For rescue by *ato*, out of a population of 200 embryos, 35% displayed a misexpression phenotype, compared to the expected value of 37.5% (Fig.3.23C).

Given this reasoning, it seems likely that misexpression of both *amos* and *ato* in the embryo can rescue the *amos*^{1} phenotype. This is opposed to the published finding of Huang et al. (2000), who state that misexpression of *amos* alone leads to the production of MD neurons. There are significant caveats with both sets of data, however. Firstly, the embryonic genotypes were not clear in either study. Secondly, PDM may not be an infallible marker of amos-specific MD neurons. For instance, its expression in *ato*-dependent chordotonal ligament cells may mean that extra PDM-positive cells resulting after *ato*-misexpression are more chordotonal-related.

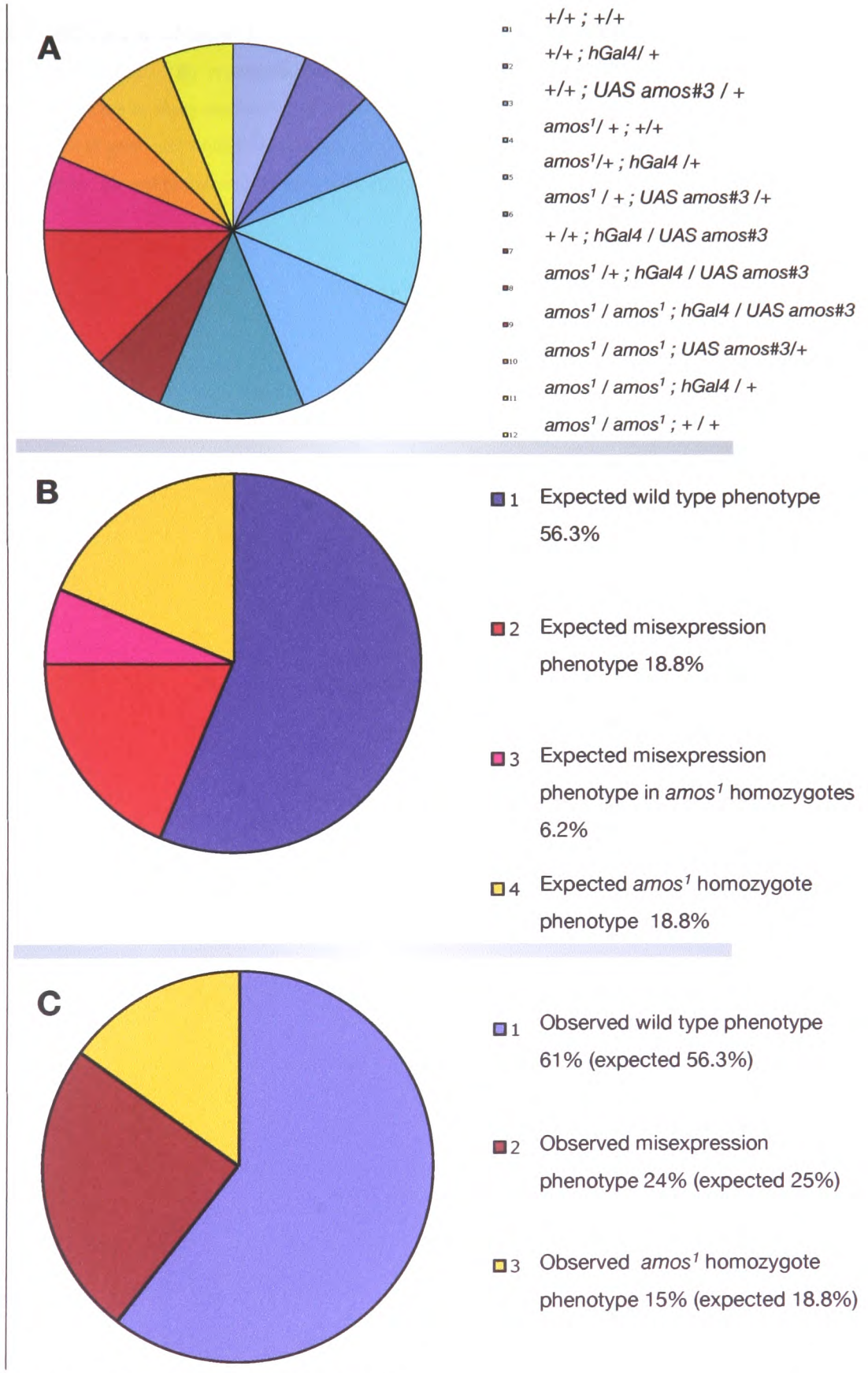

Figure 3.22 Rescue of *amos*^{1} by *UAS-amos#3*

Figure 3.22 Rescue of *amos*^{1} by *UAS-amos#3*. (**A**) represents the expected genotypes from experimental cross. (**B**) represents the expected phenotypes. (**C**) represents the observed phenotypes. Due to leaky expression of *hGal4*, the observed phenotypes of misexpression in the *amos*^{1} homozygote could not be distinguished from misexpression phenotypes in other genetic backgrounds. However the percentages of the observed phenotypes were close to expected (c.f.**B** and **C**).

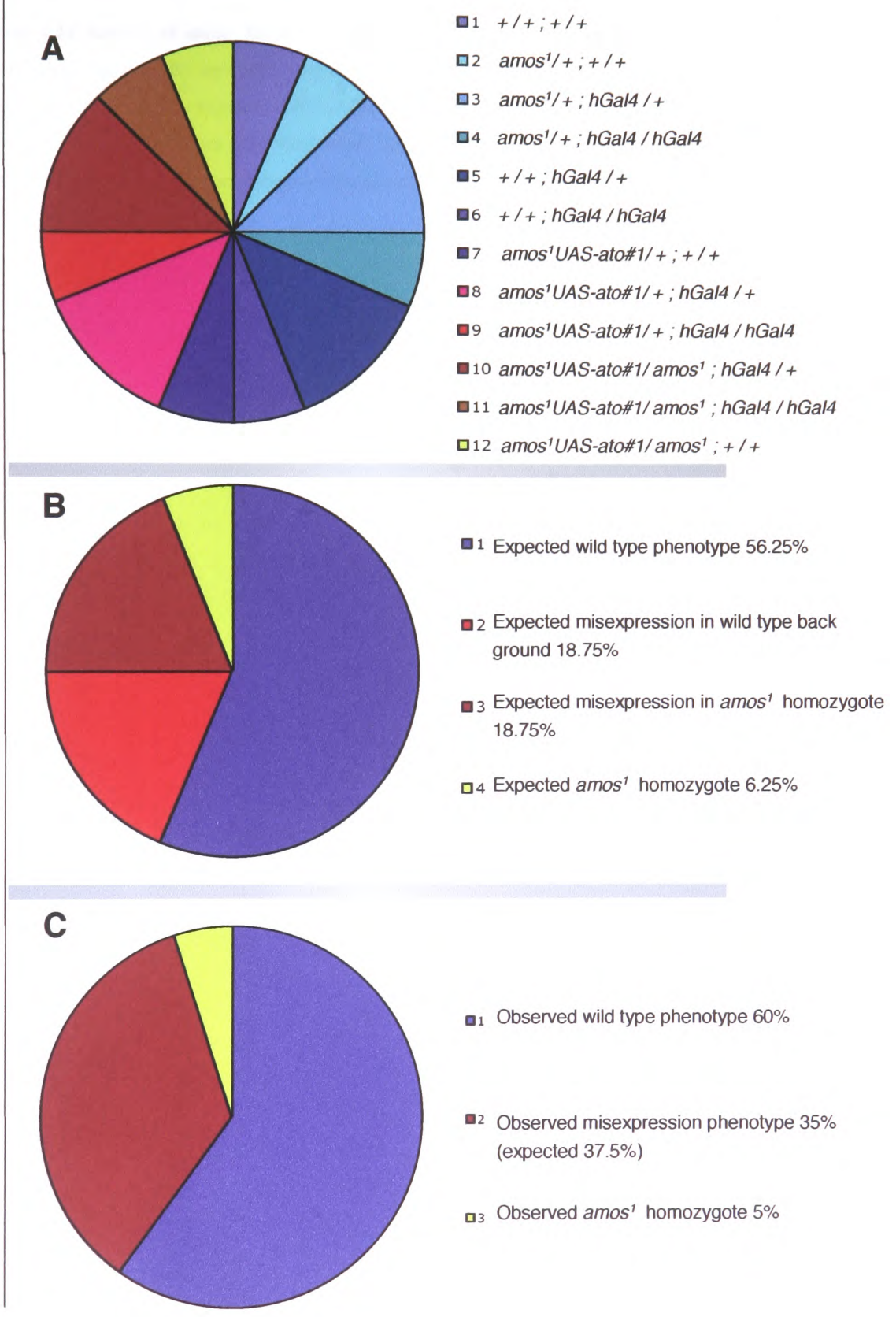

Figure 3.23 Rescue of *amos¹* by *UAS-ato#1*

Figure 3.23 Rescue of *amos*^{1} by *UAS-ato#1*. (**A**) represents the expected genotypes from experimental cross. (**B**) represents the expected phenotypes. (**C**) represents the observed phenotypes. Due to leaky expression of *hGal4*, the observed phenotypes of misexpression in the *amos*^{1} homozygote could not be distinguished from misexpression phenotypes in other genetic backgrounds. However the percentages of the observed phenotypes were close to expected (c.f.**B** and **C**).

3.8.5 Both *ato*-like genes can rescue R8 specification

I have found that misexpression of both *ato*-like genes can specify the formation of ectopic chordotonal organs. However in the case of *amos*, it can only do this by upregulation of *ato.* In ato^1, *amos* cannot functionally substitute for *ato* in the formation of adult chordotonal organs. Here I investigate if this is universal for other *ato*-functions such as R8 specification. No R8 cells are specified in ato^1 flies and as a result they have an eyeless phenotype (Fig.3.24B). Misexpression of *UAS*-ato*#1* can partially rescue this phenotype (Fig.3.24C). However, I found that misexpression of *UAS-amos#3* rescued the eye phenotype considerably better than *ato* (Fig.3.24D).

To investigate the nature of this rescue, I dissected eye imaginal discs of late 3rd instar larvae and looked for R8 formation by anti-Boss. Boss (bride of sevenless) is expressed on the R8 cell and is involved in recruitment of R7. I found that misexpression of *UAS-amos#3* in ato^1 by $Gal4^{109\text{-}(2)68}$ results in mass ectopic expression of Amos in a broad band across the eye disc (Fig.3.25B). This ectopic Amos co-localises with senseless, which endures longer than wildtype (Fig.3.25A). Furthermore, I could detect punctate Boss staining throughout the eye disc (Fig.3.25E). This suggests that *amos* can substitute for *ato* in R8 specification, but this is prohibited in wildtype by spatial and temporal restrictions on *amos* expression.

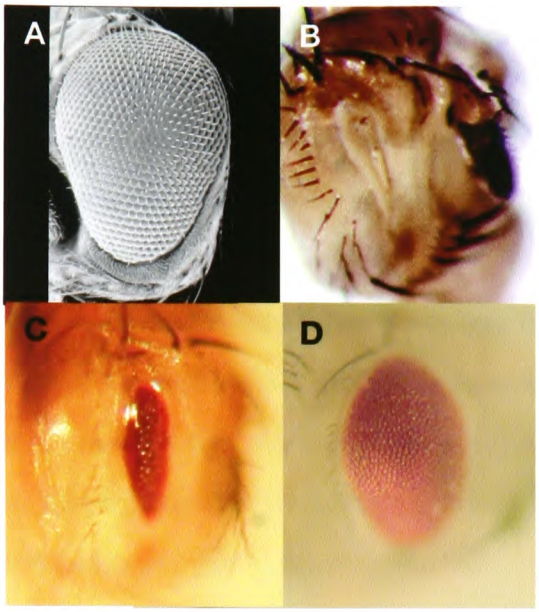

Figure 3.24 Misexpression of *ato*-like genes partially rescue the eye-less *ato*^{1} phenotype. **(B)** *ato*^{1} homozygous flies have no eye (Chanut et al., 2002). **(C)** *Gal4*$^{109\text{-}(2)68}$ misexpression of *UAS*-ato#1 at 29° can partially rescue the eye phenotype of *ato*^{1}. However, misexpression of *UAS-amos#3* **(D)** under the same conditions results in rescue approaching wild type (*N. White*) **(A).**

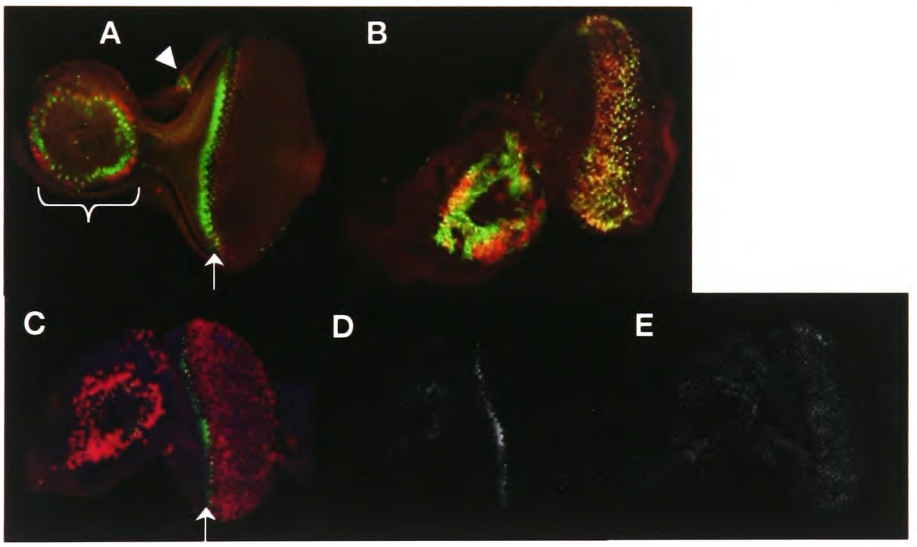

Figure 3.25 Misexpression of *UAS-amos#3* rescues R8 formation in *ato*^{1} eye disc.

(A) Wildtype eye-antennal disc, antennal disc indicated by bracket, presumptive ocelli (arrowhead), morphogenetic furrow (arrow) stained with anti-Ato (green), anti-Senseless (red). **(B-E)** Misexpression of *UAS-amos#3* in *ato*^{1}. Anti-Amos (green) detects a broad band of ectopic Amos expression spanning the eye disc **(B)**. This Amos expression co-localises with increased Senseless expression (red, also in **C**) compared to wildtype **(A)**. Antibodies to full length Ato protein can detect the truncated form translated by *ato*^{1}**(C**-green and **D)**. R8 photoreceptors are rescued by misexpression of *amos* as indicated by boss staining (**E** and **C**-blue).

3.9 Preliminary study of the capabilities of Math1 in *Drosophila*

The proneural genes *amos* and *ato* have two joint orthologues in vertebrates; *Math1* and *Math5*. The bHLH domain is the same size in all Ato homologues, furthermore the b-region is identical between Math1, Math5, Ato and Amos (Ben-Arie et al., 1996). What is interesting about these vertebrate orthologues is that they have analogous functions to both *amos* and *ato*. Math1 is expressed in cerebella granule cells and hair cells which are required for geotaxis, hearing, limb and eye movements (Ben-Arie et al., 1997; Bermingham et al., 1999). Math5 is required for the differentiation of retinal-ganglion cells (Bermingham et al., 1999; Brown et al., 1998b; Brown et al., 2001). Thus it seems that the functions of a single fly proneural protein (Ato) are shared between different vertebrate Ato-homologues.

Due to the multiplicity of the vertebrate *ato* homologues, many labs have carried out cross-species studies to determine their roles and phylogenetic position in the Ato superfamily of bHLH transcription factors. The most likely candidates for this kind of study are the *ath5* genes, which have functions in eye development. *Xath5* and *Math5* are both involved in RGC (retinal ganglion cell) determination in their respective animal models (Brown et al., 1998a; Brown et al., 2001; Kanekar et al., 1997; Wang et al., 2001; Wang et al., 2002). However, interspecies studies showed that they do not have interchangeable functions (Brown et al., 1998a; Brown et al., 2001; Kanekar et al., 1997; Wang et al., 2001; Wang et al., 2002). It is thought that the Ath5's diverged after the species split and it may be that further diversification continued in vertebrates so much so that the frog and mouse interspecies gap became too great to retain cross-species functionality.

Even if this is the case, it does not rule out the possibility that either one or both Xath5 and Math5 may be functionally interchangeable with Ato. This very question has been investigated. Sun et al. (2003) found that Xath5 and Ato are functionally interchangeable. Misexpression of *ato* in *Xenopus* resulted in an increased number of retinal ganglion cells

compared to wildtype, and misexpression of *Xath5* in *ato*^{1} could rescue the R8 defect as well as *UAS-ato*. *Math5* was shown to partially rescue the *ato*^{1} eye phenotype. However, very few R8 photoreceptors were rescued, and so the effect was quite similar to the rescue of *ato*^{1} by *UAS-sc* (Sun et al., 2003). The failure of *Math5* to complement *ato* in eye development may be due to the relative neural complexity in mammals and it is quite possible that *ato* function in higher animals may have been subdivided amongst many similar *Ath* genes.

Along with *Math5, Math1* is *ato*'s closest murine homologue and has functions in the CNS, PNS and also in non-neural tissue such as the gut epithelia (Akazawa et al., 1995; Ben-Arie et al., 2000; Chen et al., 2002). There is an 83% amino acid identity between the bHLH domains of Math1 and Ato, but more importantly the DNA binding domains are identical. Misexpression of *UAS-Math1* by *hs-Gal4* promotes the formation of ectopic chordotonal organs in the wing hinge, third wing vein and scutellum (Ben-Arie et al., 2000). Misexpression of *UAS-Math1* in *ato*^{1} embryos resulted in some apparent rescue of lateral chordotonal organs, suggesting that the Math1 protein retains some Ato-like functions (Ben-Arie et al., 2000). These results were confirmed by converse experiments where misexpression of *ato* in *Math1* deficient mice could rescue the deficiencies in gut development, hearing and balance (Wang et al., 2002).

3.9.1 Is *Math1* a functional homologue of *amos* as well as *ato*?

Presumably the *ato/amos* duplication occurred after the invertebrate-vertebrate split. If so did *ato* diverge from *amos* or did *amos* diverge from *ato* in insects? If *amos* diverged from *ato* after the species split, then it seems likely that the vertebrate *ato* homologues may retain some functional similarity to *ato* but not *amos*.

I decided to repeat the misexpression of *Math1* in flies but instead of assaying for *ato*-specific sense organs, look for evidence that *Math1* may function like *amos*. *UAS-Math1* flies

were crossed to *Gal4*$^{109\text{-}68}$ and the F1 progeny were assayed for the formation of ectopic olfactory sensilla. To verify that the misexpression system was working, the wings of the F1 generation were assayed for ectopic ES organ formation, that is excess campaniformia and ectopic bristles along the third wing vein. I found that *UAS-Math1* increased the mean number of campaniformia along the third wing vein and this was comparable to *UAS-ato#1* (Fig.3.26A). Furthermore *UAS-Math1* induced the formation of many ectopic bristles along the third wing vein (Fig.3.26B). These phenotypes are indicative of misexpression, and these flies were then assayed for ectopic olfactory organs. No olfactory like sensilla were formed on the 3rd wing vein, scutellum or second antennal segment (N=8,4,8 respectively).

These preliminary results show that Math1 does not have a single functional characteristic of Amos, although both proteins share common Ato-like functions such as the ability to specify chordotonal organs (Ben-Arie et al., 2000). It would be interesting to see if Math1 can still specify adult chordotonal organs in *ato*^{1} homozygotes. But so far the evidence suggests that *amos* diverged from *ato* after the species split.

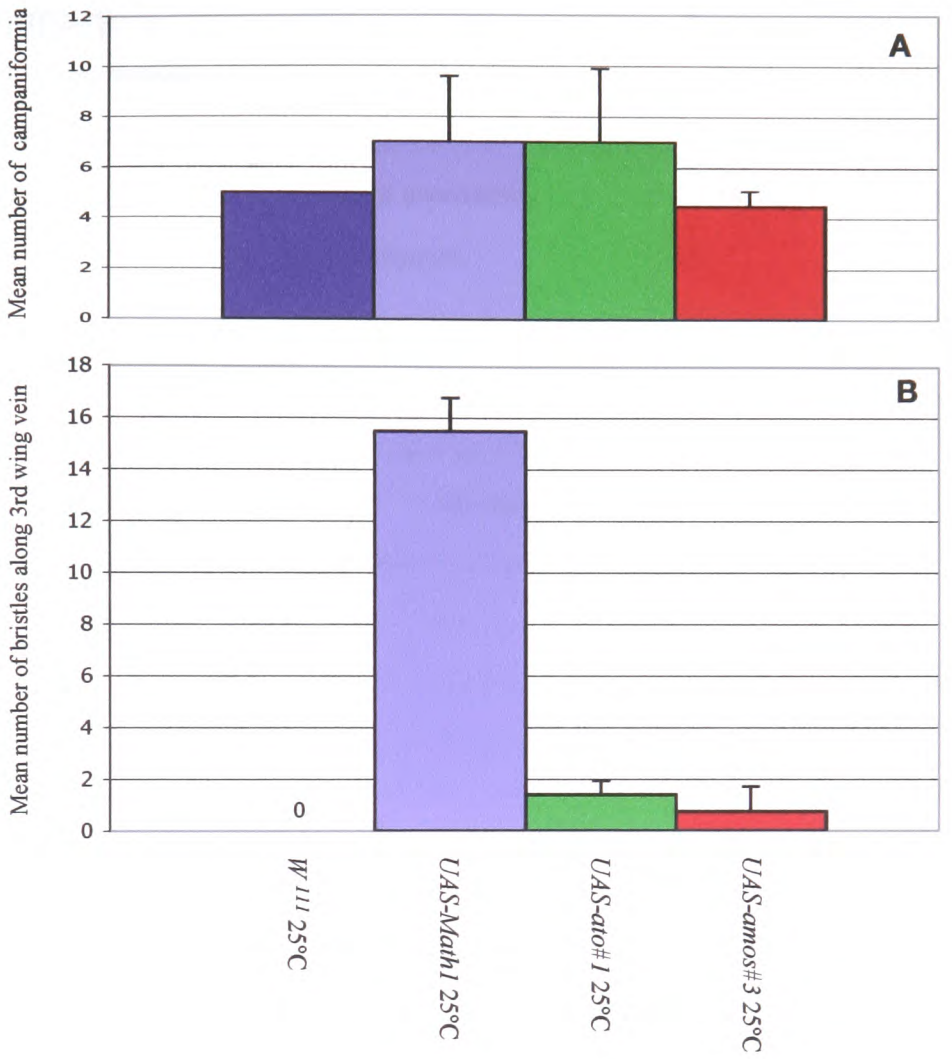

Figure 3.26 Misexpression of *Math1* produces excess ES organ formation along the third wing vein. Misexpression of *UAS-Math1* produces excess sensilla campaniformia **(A)** and ectopic bristles **(B)**. This suggests that misexpression of the vertebrate orthologue Math1 can promote neurogenesis when misexpressed in the fly.

3.10 Summary

The functional specificities of the Ato-like proneural proteins examined in this chapter are summarised in Table 3.1. It would be interesting to see if Math1 can behave more like Ato than Amos. To determine this, the rescue of chordotonal organs and R8 photoreceptors by misexpression of Math1 will have to be investigated.

Table 3.1. Summary of sense organs resulting from *ato*-like proneural gene misexpression

Proneural gene	ES suppr	Ch	Ch (ato-)	Ectopic Olf	R8 rescue
Ato	+++	+++	++	–	++
Amos	+++	+++	–	++	++
Math1	–	+	nd	–	nd

nd = not determined

3.11 Discussion

3.11.1 Specificity of the *ato*-like proneural genes

amos and *ato* have different functions as demonstrated by their mutant phenotypes (Jarman et al., 1995; zur Lage et al., 2003). But how much of this is due to different expression patterns and how much is due to intrinsic protein capability to activate different sense organ pathways? The method chosen here to address this question is to ask: do the proteins show identical or different abilities to drive ectopic neural development when identically misexpressed? I show that the answer depends on the neural fate choice being examined.

For chordotonal versus olfactory choice, Ato and Amos proteins have distinct abilities. This confirms and extends published ideas on proneural specificity. I also report, however, that both proteins seem capable of directing the R8 photoreceptor fate choice. These conclusions are expanded on below (and summarised in Fig.3.27).

Published reports suggest that both *ato*-like genes can specify ectopic chordotonal organs, but only *amos* can make ectopic olfactory organs (Goulding et al., 2000b; Jarman and Ahmed, 1998). The impression from these reports is that *amos* has the same capability as *ato* with an added unique capability to direct olfactory organ formation. This might suggest that a generalised *ato* function is ancestral and that a more specialised *amos* function evolved from a gene duplication of *ato*. But these previous studies were very superficial. I have carried out a thorough investigation of these phenotypes to put them on a firmer quantitative basis. I have also explored more deeply the basis of their misexpression phenotypes. My findings reveal that both *ato* and *amos* are specialised to perform unique functions. This calls for a reassessment of the relationship between *amos* and *ato*.

3.11.2 The complexities of olfactory sensilla specification

I show that only *amos* can direct the formation of ectopic olfactory organs. At one level this is counter-intuitive, since *ato* specifies one class of olfactory sense organ. *ato* makes coeloconica, but cannot make ectopic olfactory sensilla. In other words *ato* is only capable of specifying olfactory sensilla in the context of the developing third antennal segment. This suggests that this particular fate choice (chordotonal versus sensilla coeloconica) is dependent on the location in which *ato* is expressed. Outside the third antennal segment, *ato* drives chordotonal fate choice in preference to olfactory fate. In the third antennal segment some factor must divert this choice to a coeloconica fate. I suggest that olfactory specification requires Ato to interact with a specific cofactor that is only expressed in the third antennal segment. This criterion should give clues as to what kinds of genes might be involved. For instance the genes *distal antenna* and *distal antenna related* (*dan* and *danr*)

are candidates for encoding *ato*-modifying cofactors (Emerald et al., 2003). These genes encode novel nuclear proteins that are expressed only in the distal antenna.

It shouldn't be surprising that *ato* cannot specify olfactory organs on the second antennal segment (or elsewhere) since *ato* is already strongly expressed in this segment, where its function is to form the precursors of a large chordotonal array — the Johnston's Organ.

It is therefore even more interesting that *amos can* make olfactory sensilla on the second antennal segment despite the fact that it is closely related to *ato*. The Amos protein must contain specificity information not present in Ato. Also rather paradoxical is that this occurs despite the fact that Amos readily mimics Ato in making chordotonal organs outside the antenna. I think we're seeing a mixture of mechanisms here. Even Amos has a very limited ability to specify ectopic olfactory organs, which I think points again to the importance of cofactor interactions within the antenna. Lack of such interactions outside the antenna causes Amos aberrantly to mimic Ato.

An overall conclusion is that olfactory sensillum formation is very highly dependent on region specific cofactors; and it is challenging for a proneural gene to specify olfactory sensilla in their absence, although Amos is able to do this to some extent.

3.11.3 Only *ato* can independently specify chordotonal organs

It has been assumed that Amos can completely mimic Ato. The conclusion would be that chordotonal-specifying property is shared between the two proteins. This would lead to the search for structural features shared by the two proteins that might be responsible for this function. However, I discovered that such a conclusion would largely be a mistake. I found no evidence for functional redundancy to produce chordotonal organs by the Amos and Ato proteins. I found that Amos absolutely requires intact endogenous *ato* function in order to specify chordotonal organs. This further suggests that Amos does not cross-activate *ato*

target genes to produce chordotonal organs. Therefore, Amos does not have the ability to specify chordotonal organs intrinsically.

Amos misexpression however does result in inappropriate cross-activation of *ato*. This is inappropriate because there is no overlap in the expression of these two proteins normally – so cross-activation is not a reflection of a wildtype Amos function. Another way of putting this is that Amos can mimic Ato only in that it can activate its expression. This possibly means that Amos can mimic an Ato autoregulatory circuit (Sun and Artavanistsakonas, 1996).

Therefore, we must revise our conclusion. On the whole, the ability to activate chordotonal target genes is confined to Ato. Therefore, the structural requirements for chordotonal specification must be found among the differences between the two proteins.

3.11.4 Both *ato*-like genes can specify R8 cells

From the chordotonal rescue results one might expect R8 formation to also be an *ato*-specific property, particularly as *sc* is unable to specify R8 fate (Sun et al., 2000; Sun et al., 2003). However, in rescue experiments I found that the ability to drive the R8 fate choice is shared by both *ato* and *amos*. Unlike chordotonal specification, Ato and Amos may share true functional redundancy to specify R8 photoreceptors, however this is not apparent in the wildtype situation where *amos* expression is spatially and temporally different from *ato*. The mechanism by which Amos rescues R8 formation remains unclear. In addition to true protein interchangeabilty between Ato and Amos, misexpression of Amos may trigger cross-activation of *ato* eye-specific target genes, though these target genes are unknown.

Thus, there is no single basis for specificity of Amos and Ato functions: it depends on the level of specificity that is being examined. The differences in chordotonal and R8 specificity are relatively easy to rationalise for several reasons. Firstly, it is obvious that *ato* function must be modified in the eye so that R8s are formed rather than chordotonal organs: there

must be eye-specific cofactors that divert *ato*-dependent neurogenesis down the R8 pathway. Secondly, chordotonal organs and olfactory sensilla (and sensory bristles) are all thought to be evolutionarily homologous structures (i.e. sensilla) whereas ommatidia/photoreceptors are not likely to be derived from an ancestral sensillum. As such, R8s are not generally regarded as SOPs.

One can therefore envisage a hierarchy of fate choices that have to be made. In the eye, neurogenesis goes down the R8 pathway rather than the SOP/sensillum pathway. The key to this choice is provided by eye-specific cofactors interacting with an *ato*-like proneural gene. Therefore in the eye, *ato* (normally) or *amos* (when misexpressed) drive R8 formation. Outside the eye, *ato* and *amos* specify sensilla. In this case they drive sensillum differentiation down alternative pathways (e.g. chordotonal or olfactory), which may be due to differential interaction with different 'specificity cofactors'. One would predict that the eye cofactors must be able to interact with shared structural features of the Ato and Amos proteins.

As the aim of this chapter, I posed the following question: how much of the apparent functional difference between *amos* and *ato* is due to different expression patterns and how much is due to intrinsic protein capability to activate different neural pathways? I have shown that both mechanisms apply. For chordotonal/olfactory formation, there are clear intrinsic differences in protein capability. For R8 formation, however, the difference in wildtype function of the two genes is due to differences in expression pattern (i.e. only *ato* is normally expressed in the eye) rather than intrinsic protein capability. The latter reinforces the danger in inferring transcription factor specificities from loss-of-function mutant phenotypes alone.

A further shared property of Amos and Ato is the ability to suppress external sense organ fate. This has been proposed to fit a model of sensillum fate determination in which the *ato*-like proneural genes must suppress a default Ac/Sc-directed SOP pathway and divert neurogenesis down alternative pathways (Jarman and Ahmed, 1998) (Fig.3.4). More

recently, based on the *amos* mutant phenotype it was proposed that these two functions may have different mechanistic bases. While the latter may be due to direct target gene activation, the former was proposed to occur by protein-protein interaction (zur Lage et al., 2003). At least two possible mechanisms can be envisaged for this process (Fig.3.27). It is interesting to note that this ability of the *ato*-like proneural genes appears very depend on the timing and nature of their expression (Jarman and Ahmed, 1998). The *Tufted* (*Tft*) mutation was recently shown to result from ectopic *amos* expression in wing imaginal discs (Lai, 2003). However, misexpression in this case results in ectopic external sense organ formation rather than suppression.

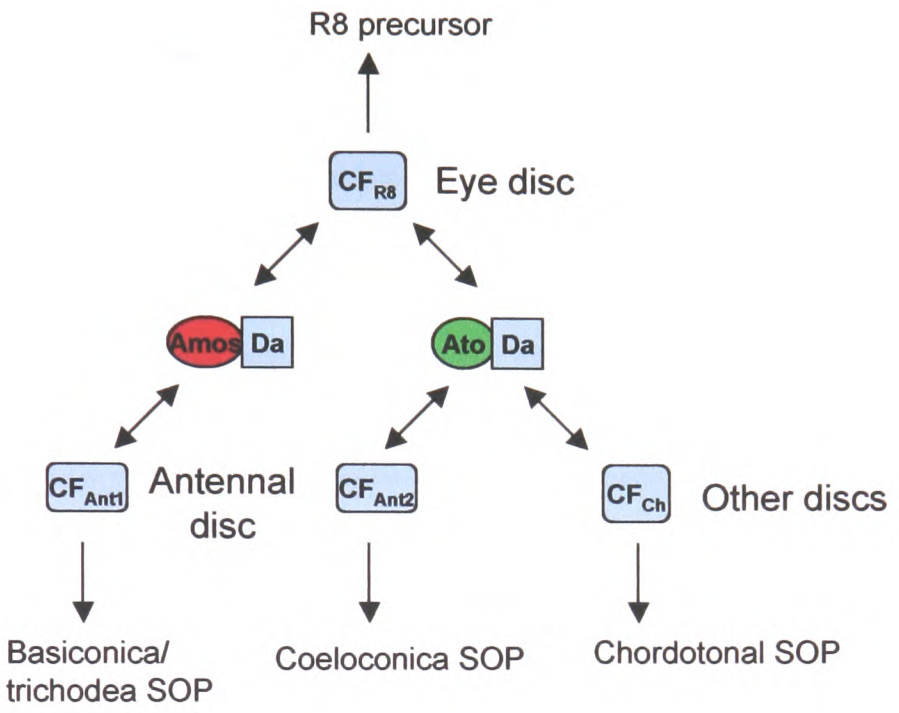

Fig. 3.27 Summary of putative cofactor interactions that lead to specificity of the Ato-like proneural proteins. The function of *ato* and *amos* are context dependent, i.e. dependent upon the proposed tissue-specific cofactor interactions. In the eye, both Ato and Amos are capable of interacting with eye-specific cofactor(s) that lead to R8 formation. Clearly only Ato actually does this in vivo because Amos is not expressed in the eye. Elsewhere, the two proneural proteins interact differentially with cofactors, leading to different neural fate outcomes. Because of the spatial and temporal expression of *ato* and *amos*, it is possible that CF_{Ant1} and CF_{Ant2} are the same protein.

3.11.5 Functional abilities of Math1 – how much is conserved?

In the literature, it has been reported that *Math1* conserves *ato* functional capability (and vice versa) (Ben-Arie et al., 2000; Wang et al., 2002). However, the question of whether the structure of *Math1* also allows it to replace *amos* functions has not been addressed. I have only carried out limited studies on *Math1* here, but there are two general conclusions so far. *Math1* does not have one property of *amos* (production of ectopic olfactory organs) although it can produce chordotonal organs. The latter property was not tested in an *ato* mutant background, so I cannot determine whether *Math1* behaves completely like *ato* or must function via the activation of the endogenous *ato* gene. However, the former is more likely since it was reported that *Math1* can at least partially rescue the chordotonal phenotype of *ato* mutant embryos (Ben-Arie et al., 2000). This would suggest that *ato* function is a more ancestral state for *ato*-like genes and has been conserved. Conversely, *amos* function is a new, derived feature that has evolved since the *Math1-ato/amos* split.

However, it also seems that *Math1* is a rather weak *ato*-like proneural gene in *Drosophila*. Chordotonal formation is not high compared with *ato* or *amos*, and *Math1* tends to produce more external sense organs instead. Since this is thought to be a default sensillum fate (Jarman and Ahmed, 1998), this may be a sign that *Math1* is unable to activate even *ato*-specific pathways very well. It would be interesting to see if *Math1* can rescue R8 formation in the *ato* mutant eye.

3.11.6 Differences between Ato and Amos proteins

There are clear differences between what the two Ato-like proteins can do. Only Amos can specify ectopic olfactory organs; only Ato has the intrinsic ability to specify chordotonal organs. This must translate at some point to differences in target genes – at least a subset even if most overlap. It is important to understand how such differences in regulatory ability arise. This could be by differences in DNA binding properties or by differences in cofactor interactions, or a combination of both. A prerequisite for understanding this further is to know

where specificity maps within the proteins' primary sequences. Do the structural features underlying functional specificity reside in amino acids that contact the DNA? Do they reside in residues that might form a protein interaction interface? It is impossible to address these questions at this point. Many studies show the prime importance of the bHLH domain in DNA-binding and protein interaction (see next chapter). But in the case of Ato and Amos, the major sequence differences between these proteins lie overwhelmingly outside their bHLH domains. Mapping specificity within these proneural proteins would be a major help in proposing mechanisms. Initial structure-function analysis is the subject of the next chapter.

3.11.7 Limitation of misexpression studies

There are clear limitations of testing proneural protein specificity by misexpression studies. In a number of cases, proneural specificity is strongly dependent on other region-specific factors. Therefore, the genes do not always behave appropriately when ectopically expressed. Moreover, it is difficult to extricate the effect of misexpression strength. Clearly misexpression experiments are not ideal for complete definition of the true activities and functions of proneural proteins. An alternative approach is to ask whether one protein can substitute for a related protein – can a protein rescue its homologue's mutant. In this case, the appropriate cofactors should be available for interaction. However, rescue experiments aren't always easy to perform. It assumes that conditions can be obtained in which a given mutant phenotype can be rescued by experimental expression of the protein itself. I have not carried out rescue studies exhaustively in this work, except in the case the *ato* mutant. This illustrates very well the value of rescue experiments: it is not possible to assess R8 specificity outside the eye because such specificity entirely depends on eye-specific factors. Rescue experiments for *amos* mutants would constitute useful future directions to help dissect the specificity of other aspects of *ato* function. Rescue of $amos^{1}$ phenotypes has been carried out as part of the continuing studies in the next chapter.

Chapter 4

Structural analysis of the functional specificity of Amos and Atonal

4.1 Introduction

In the previous chapter, I showed that Amos and Ato have different functional capabilities, despite their closely related bHLH domains. To build molecular models of how bHLH transcription factors achieve functional specificity, at the protein-target gene level, it is important to dissect the protein sequences important for the functional differences of these factors. In this chapter I begin the determination of the elements of Amos and Atonal required for their differing functional specificity.

4.2 Studies on the structural determinants of bHLH transcription factor specificity

An increasing number of studies have been directed at the question: what makes one bHLH protein function differently from another? This question can be asked at various levels. For instance, what makes a neurogenic protein (say, Sc) different from a myogenic one (MyoD)? Or, of more interest to me, what makes one proneural protein (Sc) different from another (Ato)? A common experimental approach to this question has been to alter part of one protein to resemble the sequence of another, and then to assay the functional capability of this engineered protein. This alteration can be on the scale of swapping whole regions or domains (to produce so-called 'chimeric' proteins). Or at a finer level of detail, it can involve substituting one or a few amino acids.

A general key finding of the above types of studies has been that specificity resides in the bHLH domain itself rather than in accessory sequences in the rest of the protein (see below). That is, the sequence of the bHLH domain is sufficient to determine specificity of a protein. What is not so clear is *how* this specificity is encoded in the bHLH domain or the functional consequence. It needs to be clearly understood, moreover, that this does not mean that non-bHLH parts of these

proteins are non-functional. On the contrary, the bHLH domain alone can only rarely make a functional protein (e.g. Chien et al., 1996). Therefore accessory functions must be provided by other parts of the protein (such as interaction with the general transcriptional machinery) – but they are not determinants of specificity. In the following, I review studies of bHLH function and their conclusions.

4.2.1 Class I versus Class II of Group A bHLH proteins

Dimerisation properties constitute a major difference between class I and class II proteins. Class I proteins (i.e. E proteins) can exist as stable homodimers but generaly cannot bind to DNA; however class II proteins can only form stable dimers with their partner E-proteins in the presence of DNA (Kunne and Allemann, 1997; Wendt et al., 1998).

There is some evidence to suggest that the stability and dimerisation of E-proteins are facilitated by a conserved region just carboxy terminal to helix 2 (Goldfarb et al., 1998). This conserved region is not found in class II proteins, thus the extension of the second helix of E-proteins could constitute a structural distinction between class I and class II proteins. Furthermore there are structural differences between class I proteins that function as heterodimers and those that function as stable homodimers. There is evidence to suggest that the DNA interaction of some class I homodimers is dependent upon residues present in helix 2 (Shao et al., 1998). There is evidence that structural differences between class II proteins and their partner E-proteins also determine their functional differences. It could be inferred that elements present in class II proteins but not class I proteins enable the bHLH heterodimer to bind to DNA. If this is true, what aspects of class II bHLH proteins distinguish them from class I proteins and determine DNA binding?

This type of question was addressed by a study which investigated the myogenic specificity of class II bHLH protein MyoD in relation to its dimerisation partner class I protein, E12 (homologue of Daughterless). MyoD is one of the primary bHLH transcription factors required for the determination of skeletal myoblasts (Davis et al., 1987; Tapscott et al., 1988). MyoD, but not E12, is able to induce myogenic differentiation in a cell culture system and myogenic potential resides in the basic region of MyoD (Davis and Weintraub, 1992). Substitution of three residues in the basic region of E12 with those of MyoD, allows this E-protein to gain myogenic potential. Thus residues in the DNA binding domain determine the transcriptional activities of a class II bHLH factor relative to class I, suggesting that DNA binding differences are the key to specificity between class I and II proteins. However, the important residues do not seem to contact the DNA directly, therefore it is unclear how specificity is achieved.

4.2.2 Specificity within class II: Myogenic versus Neural specification

A number of studies have addressed specificity within class II. How do different class II bHLH transcription factors initiate divergent developmental processes such as myogenesis and neurogenesis? A recent study compares MyoD with Mash1 and Math1 (Nakada et al., 2004). It seems that, compared to MyoD, the neural differentiation properties of Mash1 and Math1 map not to their DNA binding regions but to their HLH regions (Fig.4.1). Substituting the HLH domain of MyoD with that of Mash1 or Math1 allows MyoD to gain neural potential (Nakada et al., 2004). The HLH domain of Mash1 and Math1 can thus impart neural differentiation properties to a myogenic transcription factor. The implication is that DNA binding differences may not be involved in specificity here.

Given that the HLH domain is involved in dimerisation, one possibility is that interaction with different E-proteins can be sufficient to determine the specificities of these class II bHLH proteins. However, all are thought to function as heterodimers with E12/47.

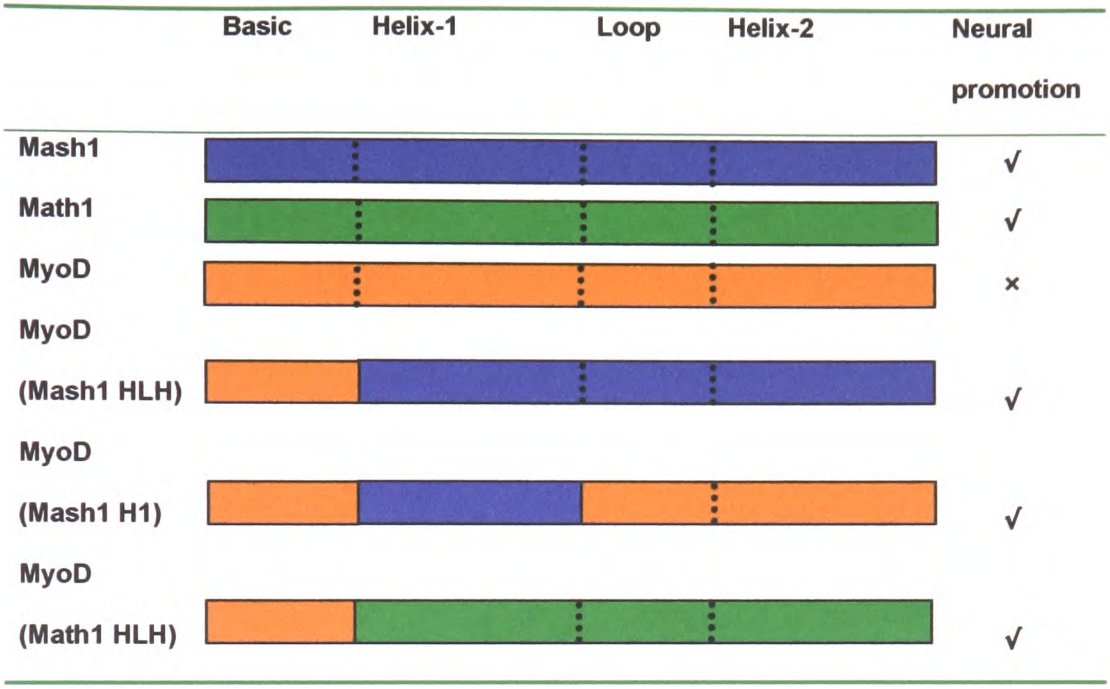

Figure 4.1 Neural promoting properties are specified by the Helix-Loop-Helix of Mash1 and Math1 (adapted from Nakada et al., 2004). Mash1 sequences are shown in blue, MyoD sequences are shown in orange and Math1 sequences are shown in green. Electroporation of Mash1 and Math1 promote neuronal differentiation in the chick neural tube, however MyoD has no effect on neural proliferation. The HLH domains of Mash1 and Math1 are required for neuronal differentiation as shown by the neural activities of the MyoD (Mash1 HLH) and MyoD (Math1 HLH) chimeras. Further more helix1 of Mash1 is able to promote neural differentiation as shown by the neural activity of the MyoD (Mash1 helix1) chimera. Thus the HLH of Math1 and helix-1 of Mash1 are sufficient to confer neural specificity to MyoD.

4.2.3 Subtype specificity of neural bHLH proteins: Math1 versus Mash1

Neural subtype specification between the mouse proteins, Math1 (Ato homologue) and Mash1 (Sc homologue), has been investigated. Both are expressed in progenitor cells of the mammalian neural tube, where they are required for neuronal differentiation (Anderson, 1994; Ben-Arie et al., 1996; Guillemot et al., 1993; Helms and Johnson, 1998; Hirsch et al., 1998). The temporal expression of Math1 and Mash1 overlap; nevertheless they have cell-type specification properties. Math1 is required for the specification of dI1 interneurons and Mash 1 is required for the specification of dI3 interneurons (Gowan et al., 2001; Parras et al., 2002).

As discussed above, the neuronal differentiating properties of both Mash1 and Math1 were shown to reside in their HLH domains with respect to MyoD (Nakada et al., 2004). But which domains determine the subtype specification between neural bHLH proteins? It seems that neuronal specification of Mash1 versus Math1 also resides in the HLH domain (Nakada et al., 2004). Electroporation of Mash1/Math1 chimeric proteins into the developing chick neural tube show that helix 2 of Math1 is required for the specification of dI1 interneurons whilst both helices 1 and 2 of Mash1 are required for the specification of dI3 interneurons (Fig.4.2).

The interesting conclusion is that distinct regions of Mash1 and Math1 are required for neuronal specification and sub-type specification. Therefore, the basis of specificity crucially depends on the level of specificity being investigated.

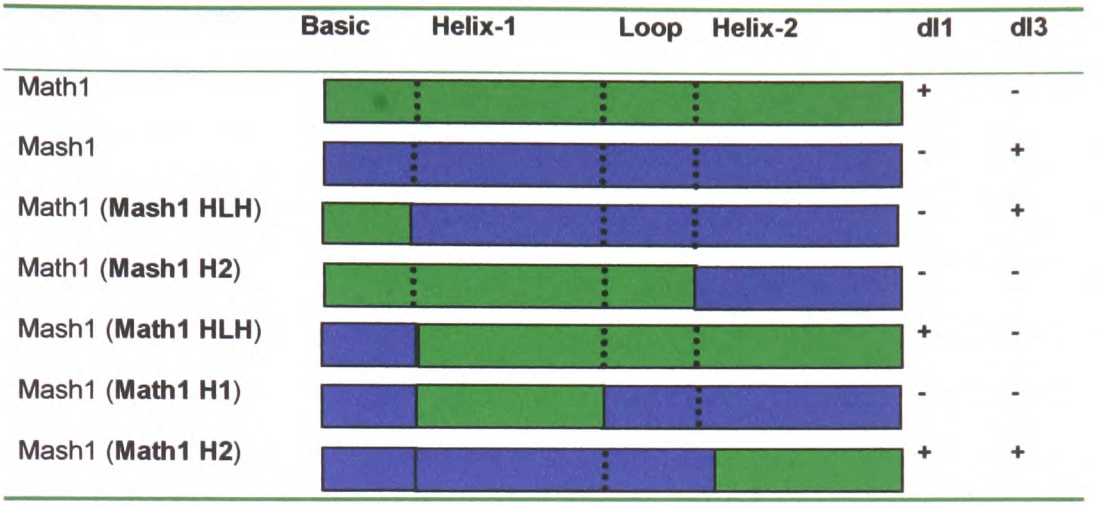

Figure 4.2 Essential structural components of Math1 and Mash1 required for their neuronal specification properties (adapted from Nakada et al., 2004). Schematic of the Math1 and Mash1 chimeric bHLH constructs. Mash1 sequences are shown in blue and Math1 sequences are shown in green. Electroporation of Math1 into the chick neural tube promotes the formation of dI1 interneurons but electroporation of Mash1 promotes the formation of dI3 interneurons. The HLH of Math1 and in particular its helix-2 is required for the specification of dI1 interneurons as indicated by the neural promoting activity of the Mash1 (**Math1 HLH**) and Mash1 (**Math1 H2**) chimeras. The HLH region, particularly helix1 of Mash1 are required for the specification of dI3 interneurons as indicated by the specification properties of Math1 (**Mash1 HLH**) and Mash1 (**Math1 H2**) c.f. Mash1 (**Math1 H1**).

4.2.4 Neuronal specificity of Ato-related proteins: Ato versus Neurogenin

The issue of specificity has also been addressed for proteins *within* the Ato superfamily. Neurogenin (Ngn) and Ato both belong to the Ato superfamily. Although they share a high bHLH identity, they have species-specific proneural activities. Ato is proneural in *Drosophila*. In vertebrates, its place appears to be taken by the Ngns, which appear to be proneural in specifying neural versus glial cell fate (Ma et al., 1996; Nieto et al., 2001; Sun et al., 2001). Ngns

are expressed in the vertebrate neural plate in domains reminiscent of proneural clusters (Sommer et al., 1996). Furthermore there is evidence that the Ngns are also subject to Notch/Delta signalling for specification of single neural precursor cells (Fode et al., 1998; Ma et al., 1998). Therefore, different Ato-related proteins control early neural determination in flies and vertebrates, although the mechanism remains similar. Interestingly, the *Drosophila* Ngn homologue (called Tap) is not expressed in neural precursor cells and does not appear to have proneural activity when misexpressed (Gautier et al., 1997). Similarly, misexpression of Ngn in proneural clusters of *Drosophila* is insufficient for neural promotion (Quan et al., 2004). Conversely, Ato is a strong neural inducer in *Drosophila*, but it has very weak neural promoting capability in *Xenopus* (Quan et al., 2004). Hence, different Ato subfamilies seem to have taken on the proneural function in the invertebrate and vertebrate lineages. What permits Ngn to be neural promoting in vertebrates, but not in *Drosophila*?

Alignments of the basic regions show that eight of twelve residues in fly Ato are identical to equivalent residues in vertebrate Ngn1. Notably, these common residues are predicted to contact DNA. Thus, it is suggested that specific activities of Ato and Ngn1 are unlikely to depend upon differential DNA binding as both proteins have identical DNA binding residues (Hassan and Bellen, 2000). Of the remaining four residues, three show group specificity within Ato and Ngn class proteins (residues 4, 7 and 11 of b region, Table 4.1). These residues are consequently good candidates for defining the different proneural specificities of Ato and Ngn1. Substitutions of the group-specific residues between Ato and Ngn1 have confirmed this (Quan et al., 2004).

The group specific residues of Ato and Ngn1 are orientated away from the DNA interface and are available for protein-protein interactions. Therefore it is assumed that the species-specific neural promoting activities of *Drosophila* Ato versus vertebrate Ngn1 is determined by their

ability to differentially interact with specific protein cofactors. However, as in all these studies, there is no direct evidence for this.

Construct	B domain sequence 1 2 3 4 5 6 7 8 9 10 11 12	Neural Promotion	
		Fly	Xenopus
Ato	R R L A A N A R E R R R	+++	+
Ngn	R R V K A N D R E R N R	+	+++
Ngn^{bATO}	R R V A A N A R E R R R	+++	N/A
Ato^{bNGN}	R R L K A N D R E R N R	N/A	+++

Table 4.1 Basic residues involved in species-specific neuronal differentiation are identified (adapted from Quan et al., 2004). Basic domain sequence alignment of Ato and Ngn1. Conserved residues Between Ato and Ngn1 are shown in blue. Ato group specific-residues are shown in green and Ngn group-specific residues in purple. Substituted residues are shown in red. Ato can promote strong neuronal differentiation in flies but has weak activity in *Xenopus*. Exchanging the species-specific residues of Ato with those of Ngn (ATO^{bNGN}) allows Ato to gain neural promoting properties in *Xenopus*. Conversely, Ngn is a strong neural promoter in *Xenopus* but weak in flies. Again substitution of the Ngn group-specific residues with those of Ato (Ngn^{bATO}) allows Ngn to induce neural differentiation in flies.

4.3 Proneural protein specificity in *Drosophila*

In one of the first studies of its kind, chimeric constructs were used to test the proneural specificity of Ato versus Sc in *in vivo* misexpression assays (Chien et al., 1996). Chimeras of Ato were made containing the bHLH and HLH of Sc (Ato-$bHLH^{(SC)}$ and Ato-$HLH^{(SC)}$ respectively). Conversely, chimeras of Sc were made containing the bHLH, b and HLH of Ato (Sc-$bHLH^{(ATO)}$,

Sc-b$^{(ATO)}$ and Sc-HLH$^{(ATO)}$ respectively) (summarised in Fig.4.3). The misexpression phenotypes of these chimeras were investigated in the wing and compared against the misexpression phenotypes of intact Ato and Sc. The proximal quarter of the wing was assayed for ectopic chordotonal and external sense organs. It was found that the functional specificity of the hybrid proteins correlated well with the bHLH domains they contained. For example only misexpression of constructs containing the bHLH domain of Ato (Ato itself and Sc-bHLH$^{(ATO)}$) were able to specify ectopic chordotonal organs. The conclusion here is that the bHLH domain of Ato contains the important residues required to promote chordotonal organ formation.

	Structure	Ectopic external sense organs	Ectopic chordotonal organs	Ato-like phenotype?
Ato		+++	+++	*yes*
Sc		+++++	-	*no*
Ato-bHLH$^{(SC)}$		+++	-	*no*
Sc-bHLH$^{(ATO)}$		+++	+++	*yes*
Sc-b$^{(ATO)}$		+++++	+	**Partial**
Sc-HLH$^{(ATO)}$		++	-	*no*

Figure 4.3. Summary of findings of Chien et al. (1996).

Further swap experiments suggested that the basic region is the dominant factor for determining Ato specificity, although it was less effective than the bHLH domain as a whole. The DNA binding regions of Sc and Ato differ in 7 (of 15) residues, 4 of which are amino acid substitutions at homologous positions and the other 3 are residues present in Ato which correspond to a gap in the Sc basic region (Table 4.2). Mutagenesis analyses of the seven divergent residues in the b region were unable to definitively locate the specificity further, although substitution of the

Arg14 in Ato with Asn of Sc did significantly decrease its specificity. Likewise deletions of the three residues present in Ato but not in Sc also significantly decreased the number of ectopic chordotonal organs induced. It appears that Ato's specificity depends on all 7 residues of the Ato b domain that differ from their counterparts in Sc.

Computer modelling of the Ato/Da heterodimer predicts that all the DNA contacting residues of the b region are conserved with Sc (Chien et al., 1996). This suggests that the residues involved directly in DNA binding do not determine functional specificity. Seven of the non-conserved residues and one conserved residue point away from the DNA interface suggesting that these residues are available for contact with other proteins. This raises the possibility that the functional specificity between Ato and Sc is dependent upon their interaction with currently unknown cofactors. Again, there is no direct evidence for this assertion. Notably, the specificity residues could indirectly affect DNA binding specificity. Alternatively, interaction with cofactors could allow conformational changes that induce differential DNA binding. It is curious that these findings appear different from those for Mash1 and Math1, where the HLH is important.

	B domain sequence															Ectopic chordotonal induction
	1	2	3	4	5	6	7	8	9	10	11	12	13	14	15	
Ato (WT)	K	R	K	R	R	L	A	A	N	A	R	E	R	R	R	+++
Scute (WT)	S	V	Q	R	R	-	-	-	N	A	R	E	R	N	R	-
Ato-deletion	K	R	K	R	R	-	-	-	N	A	R	E	R	R	R	++
Ato-(R-N)	K	R	K	R	R	L	A	A	N	A	R	E	R	N	R	++
Scute-in	S	V	Q	R	R	L	A	A	N	A	R	E	R	N	R	-
Scute-m	K	R	K	R	R	-	-	-	N	A	R	E	R	R	R	+
Scute-m	S	R	Q	R	R	-	-	-	N	A	R	E	R	R	R	+
Scute-m	S	V	Q	R	R	-	-	-	N	A	R	E	R	R	R	+

Table 4.2 Summary findings of Ato and Scute b domain mutations (Chien et al 1996).

4.4 Summary of published chimeric studies

So far, all these studies have agreed that the functional differences of bHLH transcription factors are governed by features within the bHLH domain rather than in the rest of the protein. Concerning the basis of differences in bHLH domain function that are relevant to specificity, a number of possible mechanisms could apply.

Specificity may depend upon differences in the b region. Perhaps due to the ability to interact with specific E-boxes, although in most cases the crucial residues do not seem to contact the DNA directly. Alternatively, specificity may depend upon differences in the HLH region. Residues in the HLH are proposed to interact with putative tissue specific protein cofactors.

Astonishingly to date, there is no direct evidence of a role for differential binding either to DNA sites or to cofactors.

4.5 Aim and strategy: what determines the functional specificity of Amos with respect to Ato?

Sc and Ato, functional differences can be attributed to differences in the bHLH domain (Chien et al., 1996). This raises an interesting question. The bHLH domains of Ato and Amos are much more similar than in any of the previous chimeric studies (88% identity). Strikingly, the b regions are practically identical. The specificity of Ato relative to Sc mapped to the b region, but clearly this cannot distinguish Amos from Ato. Are the small sequence differences in the HLH region sufficient to underlie the functional differences between Ato and Amos?

I aim to investigate whether the bHLH domain determines the functional specificity of Amos with respect to Ato. I aim to achieve this by constructing chimeric proteins; to swap the bHLH

domains of Amos and Ato and compare their functional specificities. In Chapter 3, I characterised the functional specificity of Amos and Ato in misexpression experiments. Here I use this as the basis for testing the specificity of chimeric Amos/Ato proteins (see Fig.4.4 for the nomenclature of the chimeric proteins tested).

In particular, I aim to answer the following questions: firstly, is the bHLH domain of Amos sufficient to confer functional specificity to Atonal, that is to say can Ato-bHLH$^{(AMOS)}$ behave like Amos? Secondly, is the bHLH domain of Amos necessary for its functional specificity, explicitly can Amos-bHLH$^{(ATO)}$ behave like Amos?

4.6 Construction of Proneural Chimeras

Four proneural chimeras were constructed for this thesis. They were designed and constructed in order to determine the regions required for the specificity of Amos with respect to Ato and Scute. Amos-bHLH$^{(ATO)}$ and Ato-bHLH$^{(AMOS)}$ (Fig.4.4) were made to investigate the regions required for Amos functional specificity compared with Ato. Experiments using these lines will be described in this chapter. Amos-bHLH$^{(SCUTE)}$ and Scute-bHLH$^{(AMOS)}$(Scute) (Fig.4.4) were made to investigate the regions required for Amos functional specificity compared with Scute. Although, construction of these two chimeras is described here, the experiments using these constructs will be described in Chapter 5.

My strategy was to create the chimeric genes by crossover PCR, clone them into a P-element transformation vector, and make transformant fly lines by microinjection. The cDNA sequences of Amos, Ato and Scute were obtained from Flybase and used to design the DNA fragments, which would eventually make up the final chimeras (Fig.4.4). Primers were designed with residues overlapping the non-bHLH and bHLH regions of different proneural genes. Each pair of primers was used initially to amplify the bHLH or non-bHLH portions of the genes from genomic

DNA (there being no introns in the proneural genes). The fragments were then used as templates in crossover PCR. By designing primers to hybrid sequences, fragments from different PCR reactions could be annealed together to create a chimeric template for the crossover PCR. For this reaction, the extreme 5' and 3' end primers of each fragment were used. Finally, outer primers were designed to include an *Eco*RI restriction site (see appendix B) for subcloning into bacterial vectors. The 3' end primers also included a stop codon prior to the EcoR1 site. See Fig.4.5 for example of experimental procedure to make chimeras.

4.6.1 Construction of Amos-bHLH$^{(ATO)}$ chimera

The Amos-bHLH$^{(ATO)}$ chimera is made up of two fragments, the 5' Amos region (excluding the bHLH domain) and the bHLH region of Ato, these two fragments were designated product 1 and product 2 respectively. Product 1 (450bp) was obtained by PCR from genomic DNA using primers JF1 and SM1. Product 2 (200bp) was obtained by PCR from genomic DNA using primers SM2 and SM3. The final chimeric sequence Amos-bHLH$^{(ATO)}$ (650bp) was amplified using annealed products 1 and 2 as templates and primers JF1 and SM3 (see Fig.4.5).

4.6.2 Construction of Ato-bHLH$^{(AMOS)}$ chimera

The Ato-bHLH$^{(AMOS)}$ chimera is made up of two fragments, the 5' Ato region (excluding the bHLH domain) and the bHLH region of Amos, these two fragments were designated product 4 and product 5 respectively. Product 4 (800bp) was obtained by PCR from genomic DNA using primers SM4 and SM5. Product 5 (200bp) was obtained by PCR from genomic DNA using primers SM6 and JF2. The final chimeric sequence Ato-bHLH$^{(AMOS)}$ (1000bp) was amplified using annealed products 4 and 5 as templates and primers SM4 and JF2.

4.6.3 Construction of Sc-bHLH$^{(AMOS)}$(-Sc) chimera

The Sc-bHLH$^{(AMOS)}$(-Sc) chimera is made up of three fragments, the 5' Sc region (excluding the bHLH domain), the bHLH region of Amos and the 3' Sc region (excluding the bHLH domain). These three fragments were designated product 7, product 8 and product 9 respectively. Two further PCR reactions were performed using these fragments to obtain the final chimera Sc-bHLH$^{(AMOS)}$-Sc. Product 7 (300bp) was obtained by PCR from genomic DNA using primers SM7 and SM8. Product 8 (200bp) was obtained by PCR from genomic DNA using primers SM9 and SM10. Product 9 (540bp) was obtained by PCR from genomic DNA using primers SM11 and SM12. Products 8 and 9 were used as the templates to create the chimeric fragment product 10, bHLH$^{(AMOS)}$-3'Sc (740bp) using primers SM9 and SM12 The final chimeric sequence product 11, Sc-bHLH$^{(AMOS)}$-Sc (1040bp) was amplified using annealed products 7 and 10 as templates and primers SM7 and SM12.

4.6.4 Construction of Amos-bHLH$^{(SC)}$ chimera

The Amos-bHLH$^{(SCUTE)}$ chimera is made up of two fragments, the 5' Amos region (excluding bHLH domain) and the bHLH region of Sc, these two fragments were assigned product 12 and product 13 respectively. Product 12 (450bp) was obtained by PCR from genomic DNA using primers JF1 and SM13. Product 13 (200bp) was obtained by PCR from genomic DNA using primers SM14 and SM15. The final chimeric sequence product 14 Amos-bHLH$^{(SC)}$ (650bp) was amplified using annealed products 12 and 13 as templates and primers JF1 and SM15.

The PCR conditions and buffers used to amplify the individual fragments and chimeric fragments were varied for each PCR to achieve the highest specific yield and reduce non-specific by products (see appendix D). In addition each PCR product was separated on an agarose gel and the required size of product was cut out and column purified before use in further PCR reactions.

4.6.5 Cloning the chimeric genes

The final chimeric products were cloned into the *Eco*RI site of the plasmid pBluescript (pBS). The constructs were sequenced to check for the fidelity of amplification. No point mutations were found in the bHLH regions of any of the chimeric constructs. The constructs were then subcloned into pUAST for transformation. pUAST has been routinely used to insert constructs into the fly genome for misexpression analysis (Brand and Perrimon, 1993).The pUAST vector is 9050 bp and contains 5 GAL4 binding sites followed by the *hsp70* TATA box and transcriptional start site and a polylinker containing the *Eco*RI site for subcloning. The orientation of the inserts was then assessed using restriction endonucleases (see appendix F).

4.6.6 Transformant fly lines

Each chimera in pUAST was microinjected to produce transformant fly lines. These were mapped by segregation analysis (appendix G).

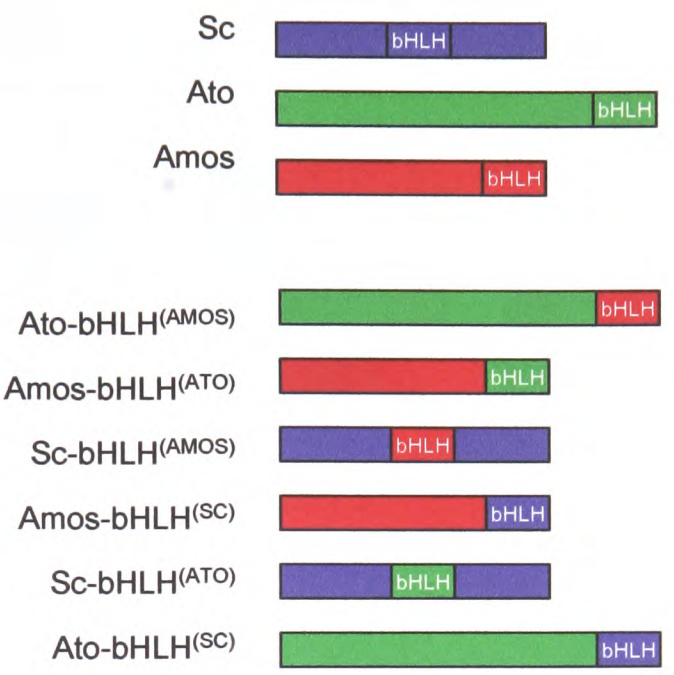

Figure 4.4 Shorthand notation used for chimeras in this thesis. The construction and analysis of the first two chimeras is described in this chapter. The next two chimeras are the subject of Chapter 5. The last two were constructed and described by Chien et al. (1996).

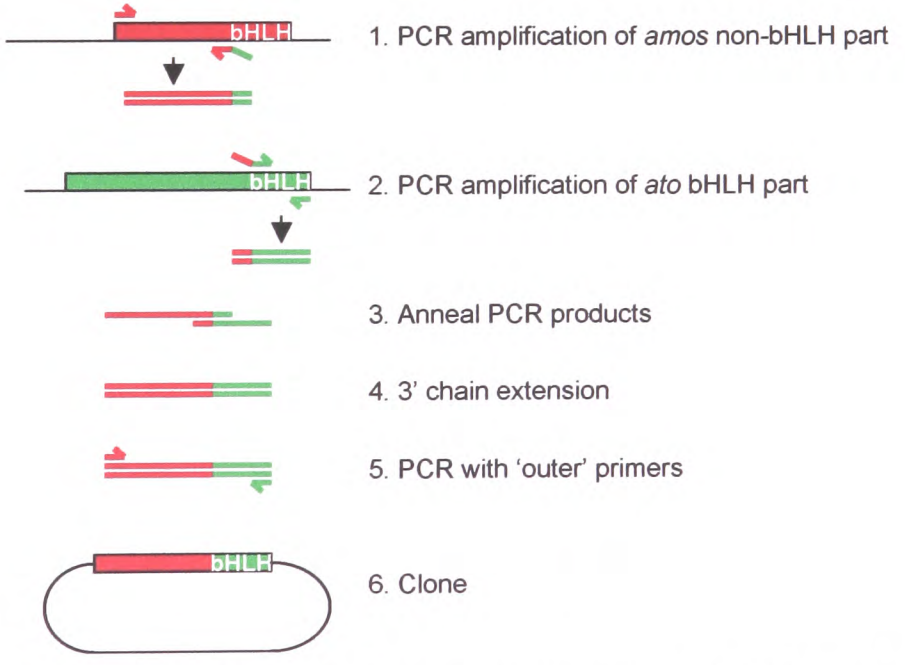

Figure 4.5 Strategy for construction of chimeric genes. *ato* and *amos* are used in this example.

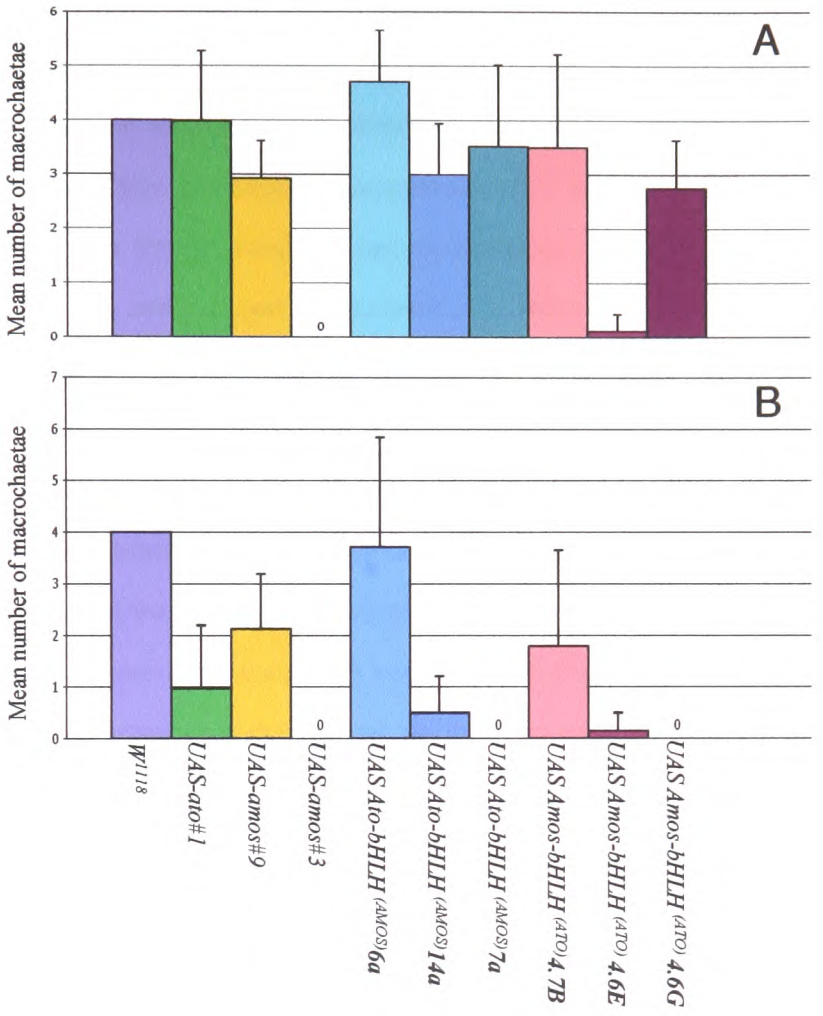

Fig 4.6 Inhibition of thoracic macrochaetae by misexpression of the Amos-bHLH$^{(ATO)}$ and Ato-bHLH$^{(AMOS)}$ chimeric proteins. The macrochaetae on the notum **(A)** and scutellum **(B)** of misexpressed, control and chimeric lines are quantified at 25°C. The results indicate that selected lines of both chimeras are able to mimic misexpression of Amos and Atonal under the same conditions. These charts show that *UAS-Amos-bHLH$^{(ATO)}$* and *UAS-Ato-bHLH$^{(AMOS)}$*are able to inhibit the external sense organ lineage. I found that the standard deviations of the chimeras is large, indicating a wide range within individual lines to suppress bristle formation.

4.7 Initial characterisation and selection of transformant UAS-Ato-bHLH$^{(AMOS)}$ and UAS-Amos-bHLH$^{(ATO)}$ lines

Microinjection of P-elements into embryonic pole cells, produce various strengths of transformant lines. This is because the amount of protein produced is dependent upon the site of P-element insertion. Protein translation can be influenced by insertion near to genomic elements such as promoters and silencers. To accommodate this variation in strength, it was important that I characterised a number of lines for each chimera.

In order to select suitable lines for my study I had to determine which of the transformant lines were producing a functional protein and furthermore determine the relative strengths of these lines. I decided that the initial assay must be applicable to both my chimeras and independent of specificity. In Chapter 3, I showed that misexpression of both Amos and Ato could inhibit the formation of macrochaetae. I showed that this inhibition was positively correlated to the general efficacy of the line (c.f. *UAS-amos#9* and *UAS-amos#3*). Furthermore, I found no evidence to suggest that this inhibition was different between Amos and Ato. Thus, I decided that inhibition of thoracic macrochaetae would be a viable initial assay for characterisation of transformant line strength. The caveat of this approach is that misexpression of the chimeras must be able to mimic Amos and Ato in inhibiting the external sense organ lineage.

4.7.1 Amos-bHLH$^{(ATO)}$ and Ato-bHLH$^{(AMOS)}$ form functional proteins that mimic Amos and Ato to inhibit thoracic macrochaetae

I misexpressed the *UAS Ato-bHLH $^{(AMOS)}$* and *UAS Amos-bHLH $^{(ATO)}$* lines using *Gal4$^{109\text{-}(2)68}$* and scored the number of macrochaetae on the notum and scutellum at 25°C (Fig.4.6). I found that a number of chimeric lines could mimic Amos and Ato in their ability to inhibit thoracic

macrochaetae. This suggests that a functional proneural-like chimeric protein is formed in these lines. The lines with the most significant loss of macrochaetae were selected for further study.
I chose three Ato-bHLH$^{(AMOS)}$ lines for further analysis: 6a, 14a and 7a (Fig.4.8A, B and C). All three of these lines displayed a general loss of thoracic macrochaetae. However I found the variation was high within individual lines (see Fig.4.6 error bars). Thus, 7a showed the strongest and 6a showed the weakest inhibition of macrochaetae. Together with an intermediate strength line 14a, I inferred that the three lines represented the function of Ato-bHLH$^{(AMOS)}$ at various levels of misexpression. Amos-bHLH$^{(ATO)}$ lines 4.7B, 4.6E and 4.6G were also selected for their ability to inhibit thoracic macrochaetae (Fig.4.6 and Fig.4.8D, E and F). Again these lines were selected to represent a range of strengths for characterisation of this chimera.

However, I observed that two Amos-bHLH$^{(ATO)}$ lines exhibited a different phenotype (Fig.4.8G and H). Amos-bHLH$^{(ATO)}$ 4.6B and 4.6C showed no inhibition of thoracic macrochaetae. Instead their misexpression phenotype showed an overall increase in the numbers of thoracic macrochaetae compared to wild type (Fig.4.7). This unexpected result suggests that in some circumstances the Amos-bHLH$^{(ATO)}$ chimeric protein shows a new functionality that is not present in either parent protein. In fact this new function resembles Sc in this assay (Jarman and Ahmed, 1998, and Chapter 5).

The loss of external sense organs is taken as a good indicator of line strength. However, this is not independently proven in this study. Future experiments could be aimed at rectifying this. Western blot analyses are not possible for testing protein production levels because the antibodies to Amos or Ato will cross react with endogenous proteins (and may not detect the chimeric proteins well). A possible alternative is to carry out real time RT-PCR using primers that span the chimera breakpoints. This would allow the specific quantification of chimeric mRNAs in each of the lines. A caveat however, is that protein stability may affect expression levels.

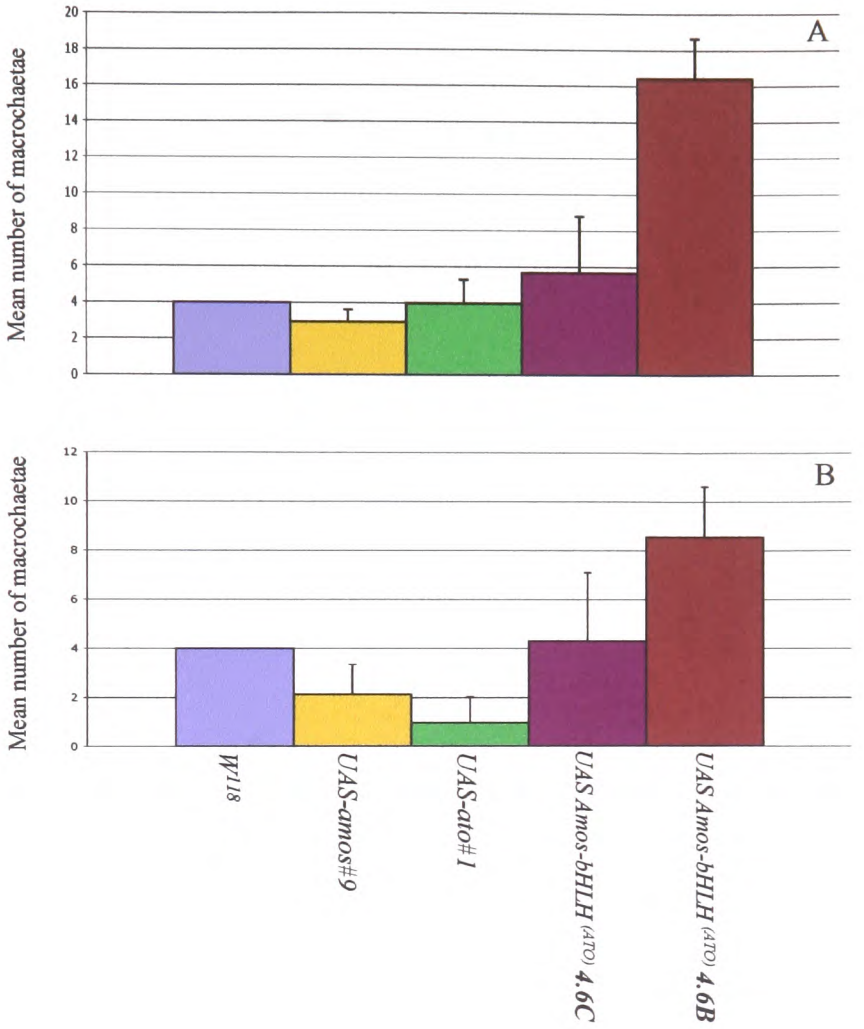

Fig 4.7 Misexpression of some Amos-bHLH$^{(ATO)}$ chimeric lines fail to repress external sense organs. The macrochaetae on the notum **(A)** and scutellum **(B)** of control, Amos-bHLH$^{(ATO)}$4.6C and 4.6B lines are quantified at 25°C. The results indicate that Amos-bHLH$^{(ATO)}$ chimeras 4.6C and 4.6B cannot inhibit the external sense organ lineage, unlike either parent protein. The mean number of thoracic macrochaetae of Amos-bHLH$^{(ATO)}$4.6C is comparable to wild type. However Amos-bHLH$^{(ATO)}$ 4.6B displays a significant increase in thoracic macrochaetae.

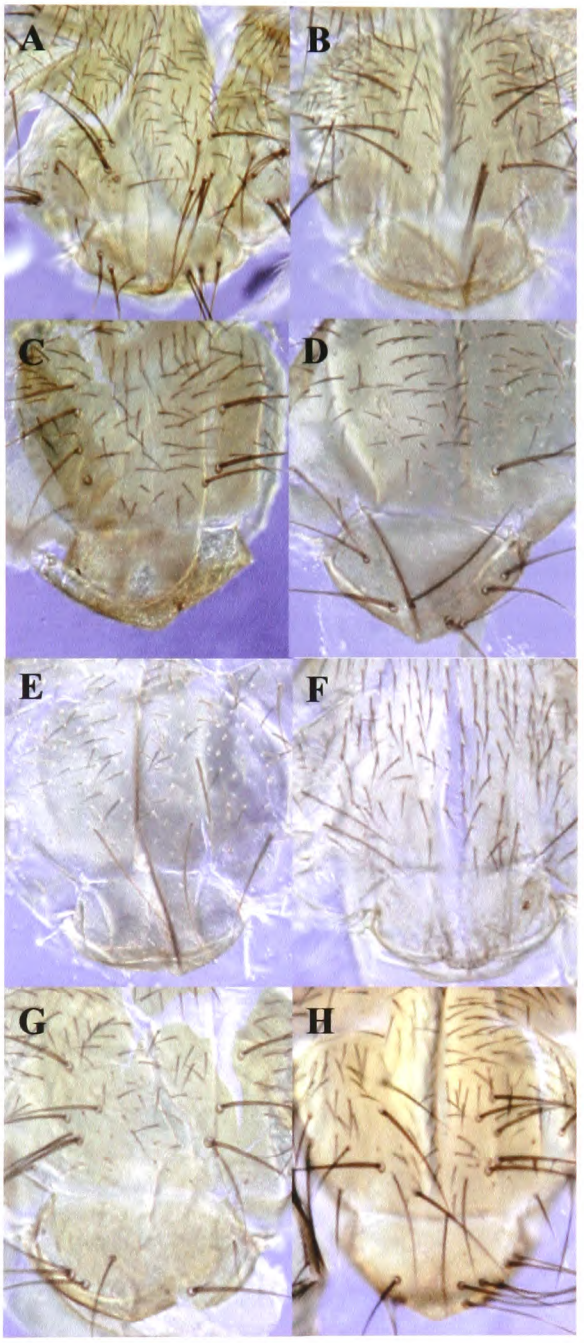

Figure 4.8 Mesothoracic macrochaetae phenotype of Ato-bHLH$^{(AMOS)}$ and Amos-bHLH$^{(ATO)}$ chimeras misexpressed with *Gal4$^{109-(2)-68}$* at 25°C. **(A)** 6a Ato-bHLH$^{(AMOS)}$. **(B)** 14a Ato-bHLH$^{(AMOS)}$. **(C)** 7a Ato-bHLH$^{(AMOS)}$. **(D)** 4.6E Amos-bHLH$^{(ATO)}$. **(E)** 4.7B Amos-bHLH$^{(ATO)}$. **(F)** 4.6G Amos-bHLH$^{(ATO)}$. **(G)** 4.6C Amos-bHLH$^{(ATO)}$. **(H)** 4.6B Amos-bHLH$^{(ATO)}$.

4.8 Exploring the aberrant bristles phenotypes of Amos-bHLH$^{(ATO)}$ lines

Before proceeding to investigate Amos/Ato specificity, I initially examined the aberrant phenotypes of the Amos-bHLH$^{(ATO)}$ lines 4.6C and 4.6B. As explained in Chapter 3, when misexpressed Amos and Ato both inhibit the formation of thoracic macrochaetae and also specify olfactory and chordotonal organs respectively. This supports a model in which both proteins must inhibit the default bristle fate as an intrinsic part of their determination functions (Chapter 3; Jarman and Ahmed, 1998). To the greater extent, I found that misexpression of both chimeras can inhibit the external sense organ lineage. However two Amos-bHLH$^{(ATO)}$ lines appeared to promote bristle formation rather than inhibiting it. I wanted to explore why *UAS Amos-bHLH $^{(ATO)}$ 4.6B* and *UAS Amos-bHLH $^{(ATO)}$ 4.6C* exhibit aberrant bristle phenotypes.

With regard to the neural fate determination model of *amos* and *ato* proposed by Jarman and Ahmed (1998), there are a number of explanations for the behaviour of these two particular chimeric proteins. The chimeric proteins may be unable to suppress the external sense organ lineage. Alternatively, the chimeric proteins may be unable to impose an alternate sense organ fate. In such an event, the external sense organ lineage becomes the default neural fate.

Both scenarios need not be mutually exclusive and in both cases the aberrant bristle phenotype may share a common mechanism. The observed increase in thoracic macrochaetae compared to misexpression of either parent protein, suggests that the *AS-C* may be upregulated. I decided to investigate this by assessing levels of *achaete* expression in *UAS Amos-bHLH $^{(ATO)}$4.6B* and *4.6C* lines. *UAS Amos-bHLH $^{(ATO)}$4.6B* and *4.6C* were misexpressed at 29°C with *Gal4$^{109\text{-}(2)68}$*. The wing imaginal discs were then stained with Ac antibody to detect any changes in Ac expression compared to wild type. I found that Amos-bHLH $^{(ATO)}$4.6B and 4.6C both showed increased levels of Ac expression (Figure 4.9 B and C c.f wild type A). This suggests that these

particular chimeric proteins have lost the property of their parent proteins to inhibit the external sense organ lineage.

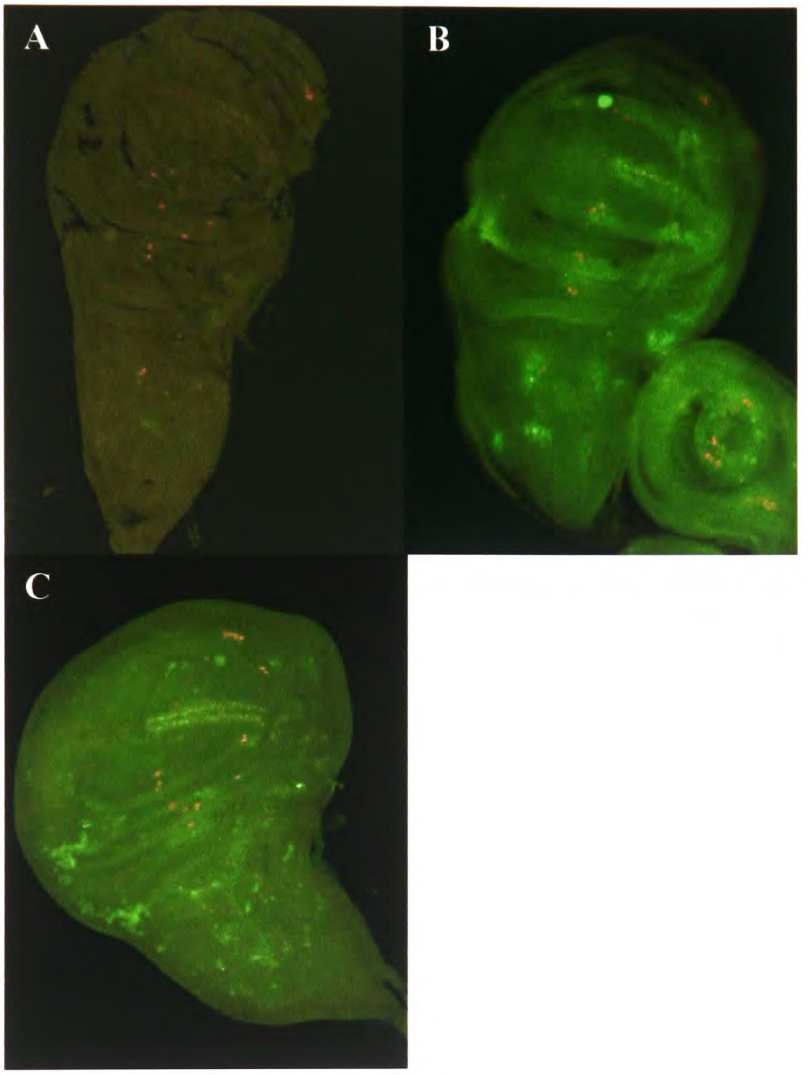

Figure 4.9 *achaete* expression is up-regulated in third instar larval wing discs of 4.6C and 4.6B Amos-bHLH$^{(ATO)}$ lines misexpressed by *Gal4$^{109-(2)68}$* at 29°C

(A) *W^{1118}* wildtype shows low level of *achaete* staining (green, senseless-red) compared to the hairy bristle phenotype lines 4.6C Amos-bHLH$^{(ATO)}$ **(B)** and 4.6B Amos-bHLH$^{(ATO)}$ **(C)**. This suggests that these lines are unable to inhibit *ac* and subsequently the external sense organ lineage which is regarded as the default pathway of neurogenesis.

4.9 Ectopic chordotonal organ induction by the chimeric proteins

In this section I assess the ability of the chimeric proteins to impose an alternative sense organ fate, specifically the chordotonal fate. I quantify ectopic chordotonal organ formation by misexpression of Ato-bHLH$^{(AMOS)}$ and Amos-bHLH$^{(ATO)}$ chimeras driven by *Gal4$^{109\text{-}(2)68}$* at 25°C. I used GFP-nompA to label chordotonal organs and assayed for their ectopic formation at the scutellum. Since misexpression of both Amos and Ato can induce ectopic chordotonal organs, one might expect the chimeras to behave qualitatively identical in this assay. However the primary aim of this assay is to determine whether functional Ato-like proteins are formed.

4.9.1 Ato-bHLH$^{(AMOS)}$ and Amos-bHLH$^{(ATO)}$ chimeras form functional Ato-like proteins

I found that misexpression of both chimeras could induce the formation of ectopic chordotonal organs in the scutellum (Fig.4.10). All the chimeric lines tested could produce equal numbers or more ectopic chordotonal organs than Ato. This shows that the chimeras can mimic both parent proteins in this assay to form functional Ato-like proteins and can impose a sense organ fate on SOPs. Interestingly the line which displayed the strongest inhibition of scutellar macrochaetae (Amos-bHLH$^{(ATO)}$ 4.6G) shows the lowest induction of ectopic chordotonal organs. This suggests that inhibition of thoracic macrochaetae is indicative but not directly correlated with the strength of the line in all aspects.

4.9.2 Behaviour of the aberrant Amos-bHLH$^{(ATO)}$ lines

For the aberrant Amos-bHLH$^{(ATO)}$ lines 4.6C and 4.6B, loss of inhibition of bristles could be due to a defect in the chimeric protein function. Alternatively, this phenotype may represent weakly

expressing lines (as seen for *UAS-Ato* Jarman and Ahmed, 1998). The second possibility would predict that misexpression of a weak line would result in reduced or absent induction of ectopic chordotonal or olfactory organs compared to other *UAS Amos-bHLH* $^{(ATO)}$ lines. This is not the case. Amos-bHLH$^{(ATO)}$ 4.6C, which showed no inhibition of thoracic macrochaetae, induces the highest number of ectopic chordotonal organs (Fig.4.10). This further suggests that inhibition of the external sense organ lineage is independent of the function to impose an alternate sense organ fate.

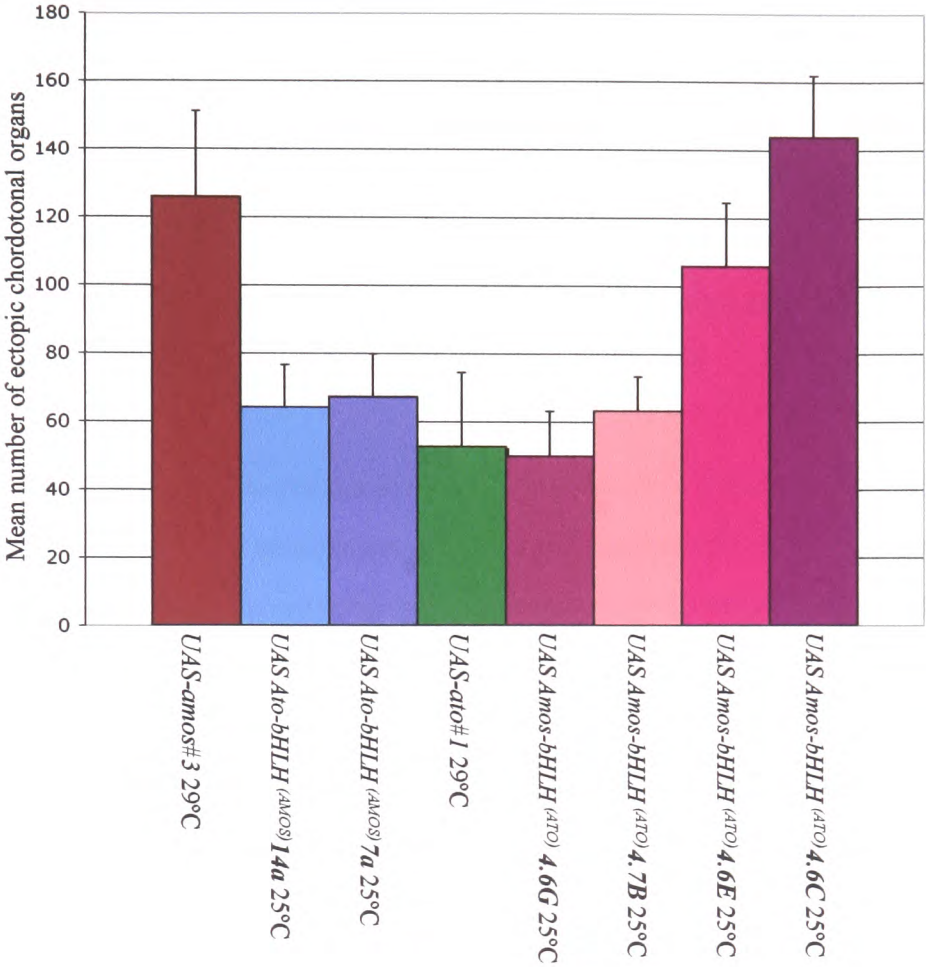

Figure 4.10 Ato-bHLH$^{(AMOS)}$ and Amos-bHLH$^{(ATO)}$ chimeras are able to form functional Ato-like proteins. The ectopic chordotonal organs formed on the scutellum of Ato-bHLH$^{(AMOS)}$ and Amos-bHLH$^{(ATO)}$ lines are quantified. Lines of both chimeras selected showed the induction of ectopic chordotonal organs. This suggests that the chimeras form a functional Ato-like protein and also impose an alternate sense organ fate. Although Amos-bHLH$^{(ATO)}$4.6C does not completely inhibit the external sense organ lineage, this chimera is able to impose an alternate sense organ fate.

4.9.3 Is endogenous *ato* required for ectopic chordotonal organ specification by Amos-bHLH$^{(ATO)}$ and Ato-bHLH$^{(AMOS)}$?

The ability to promote chordotonal SOP formation does not differentiate functional differences between Ato-bHLH$^{(AMOS)}$ and Amos-bHLH$^{(ATO)}$. In Chapter 3, I showed that cross-activation of endogenous *ato* is responsible for most of the ectopic chordotonal organs induced by Amos misexpression. Therefore it is important to investigate whether the chimeric proteins specify chordotonal organs directly, like Ato, or indirectly via *ato,* like Amos?

To address this question, I tested the ability of the chimeric lines to promote chordotonal organ formation in the absence of endogenous ato (in the *ato*^{1} background). The results are striking. I found that the numbers of chordotonal organs induced by Amos-bHLH$^{(ATO)}$ is greatly reduced (Fig.4.11). Thus, Amos-bHLH$^{(ATO)}$ requires endogenous *ato* to specify ectopic chordotonal organs. This chimera therefore behaves more like Amos than Ato.

In striking contrast, Ato-bHLH$^{(AMOS)}$ is still able to specify chordotonal organs in the absence of *ato*. Although the average number of ectopic chordotonal organs was lower in the *ato*^{1} background compared to the wild type background, the difference was not statistically significant (t-test=0.0121). Thus, the Ato-bHLH$^{(AMOS)}$ chimera behaves more like Ato than Amos in this assay.

4.9.4 Ato-like behaviour maps outside its bHLH domain

These findings are very striking because they suggest that it is the non-bHLH portion of Ato that allows it to specify chordotonal organs directly. This contradicts all other published bHLH chimeric studies. Thus the bHLH domain is not the key factor in determining specificity between Amos and Ato.

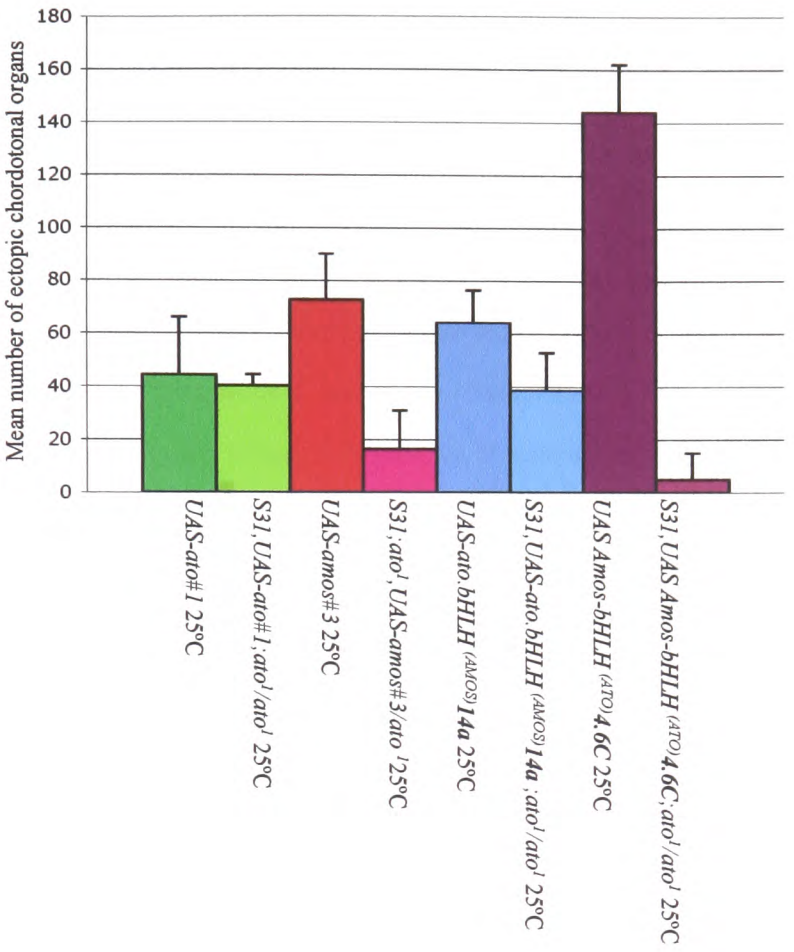

Figure 4.11 *UAS-ato#1* and *UAS-Ato-bHLH (AMOS)* can specify ectopic scutellar chordotonal organs in the absence of endogenous *ato*. Misexpression of *ato* can specify ectopic chordotonal organs in ato^1 homozygote, however the ectopic chordotonal organs specified by *amos* are significantly reduced. The Ato-bHLH(AMOS) chimera continues to specify substantial numbers of ectopic chordotonal organs in ato^1 mutant, however Amos-bHLH(ATO) shows a significant reduction under the same conditions (t-test=6.44×10^{-5}) . This suggests that both Amos and Amos-bHLH(ATO) require the cross activation of endogenous *ato* to specify ectopic chordotonal organs. In contrast Ato-bHLH(AMOS) behaves like Atonal, and doesn't require *ato* to specify chordotonal organs.

4.9.5 Ato-bHLH$^{(AMOS)}$ and Amos-bHLH$^{(ATO)}$ promote ectopic chordotonal organ formation in the embryonic PNS

I corroborated the adult results in the embryo. Ato-bHLH$^{(AMOS)}$ and Amos-bHLH$^{(ATO)}$ misexpression was driven in the embryo by *scaGal4* and the chordotonal organs formed were assayed after staining with the antibody, 22C10. In Chapter 3 I showed that misexpression of *amos* in the embryo was more efficient at specifying extra lateral chordotonal organs than *ato*. This assay was carried out at 18°C due to the pronounced disruption of the PNS. The results show that both chimeras can induce the formation of ectopic chordotonal organs (Fig. 4.12). This is consistent with the findings of the adult assay. However Amos-bHLH$^{(ATO)}$ is better than Ato-bHLH$^{(AMOS)}$ in this assay. Thus, to some extent, Amos-bHLH$^{(ATO)}$ behaves more like Amos than Ato. However, further experiments would need to be performed in the future to test the requirement for endogenous *ato* for these phenotypes.

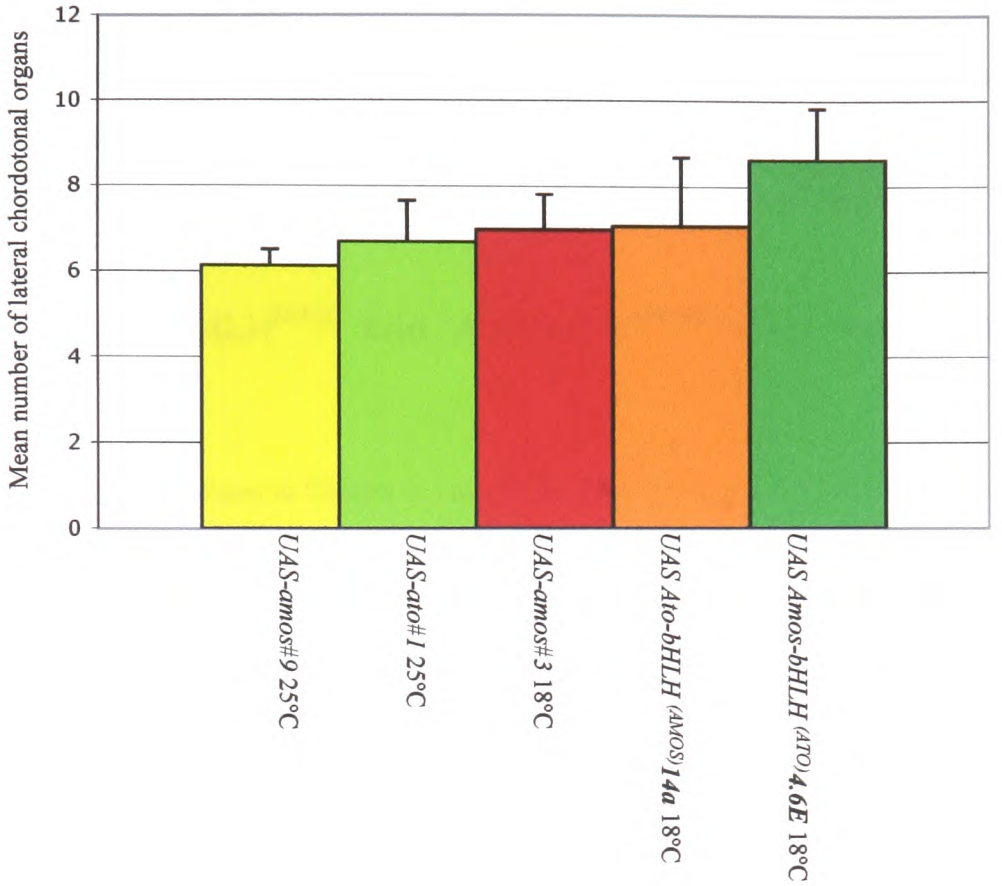

Figure 4.12 Amos-bHLH $^{(ATO)}$ and Ato-bHLH$^{(AMOS)}$ can specify extra lateral chordotonal organs in the embryo. Misexpression of *UAS Ato-bHLH$^{(AMOS)}$14a* and *UAS Amos-bHLH$^{(ATO)}$4.6C* by *Gal4^{sca}*, promote the formation of embryonic lateral chordotonal organs. These results are in line with observations in the adult.

4.10 Ectopic olfactory organ production by the chimeras

The previous section has shown that the specificity of Ato for chordotonal precursor selection lies outside the bHLH domain. What about the converse specificity of Amos for olfactory specification? In Chapter 3, I showed that Amos but not Ato can induce ectopic olfactory organs on the second antennal segment. This assay was used to assess the chimeric proteins.

4.10.1 Amos-bHLH$^{(ATO)}$ and Ato-bHLH$^{(AMOS)}$ can both mimic Amos

Using the assay I developed in Chapter 3, I tested two *UAS Ato-bHLH $^{(AMOS)}$* lines (6a and 14a) and two *UAS Amos-bHLH $^{(ATO)}$* lines (4.6C and 4.7B) for their ability to produce ectopic olfactory sensilla on the second antennal segment (Fig.4.13 and 4.14). In contrast to Ato, misexpression of Ato-bHLH$^{(AMOS)}$ results in ectopic olfactory sensilla. I found that line 14a was stronger than 6a (13.7±9.89 c.f. 10.7±5.12) (Fig.4.13). Importantly, both lines produced numbers of ectopic sensilla comparable to *UAS-amos#3* at 29°C (12.3±4.33). Thus, Ato-bHLH$^{(AMOS)}$ behaves like Amos rather than Ato in this assay.

Remarkably, the Amos-bHLH$^{(ATO)}$ lines tested could also promote ectopic olfactory sensilla formation. Amos-bHLH$^{(ATO)}$ 4.6C produced similar numbers of ectopic olfactory organs to *UAS-amos#3* (13.2±3.87 c.f. 12.3±4.33). Amos-bHLH$^{(ATO)}$ 4.7B however induced even more ectopic olfactory sensilla than Amos (24.1±10.4 c.f. 12.3±4.33).

I conclude that both the bHLH and non-bHLH portions of Amos can confer olfactory specificity independently. No similar situation has been reported in any other chimera study.

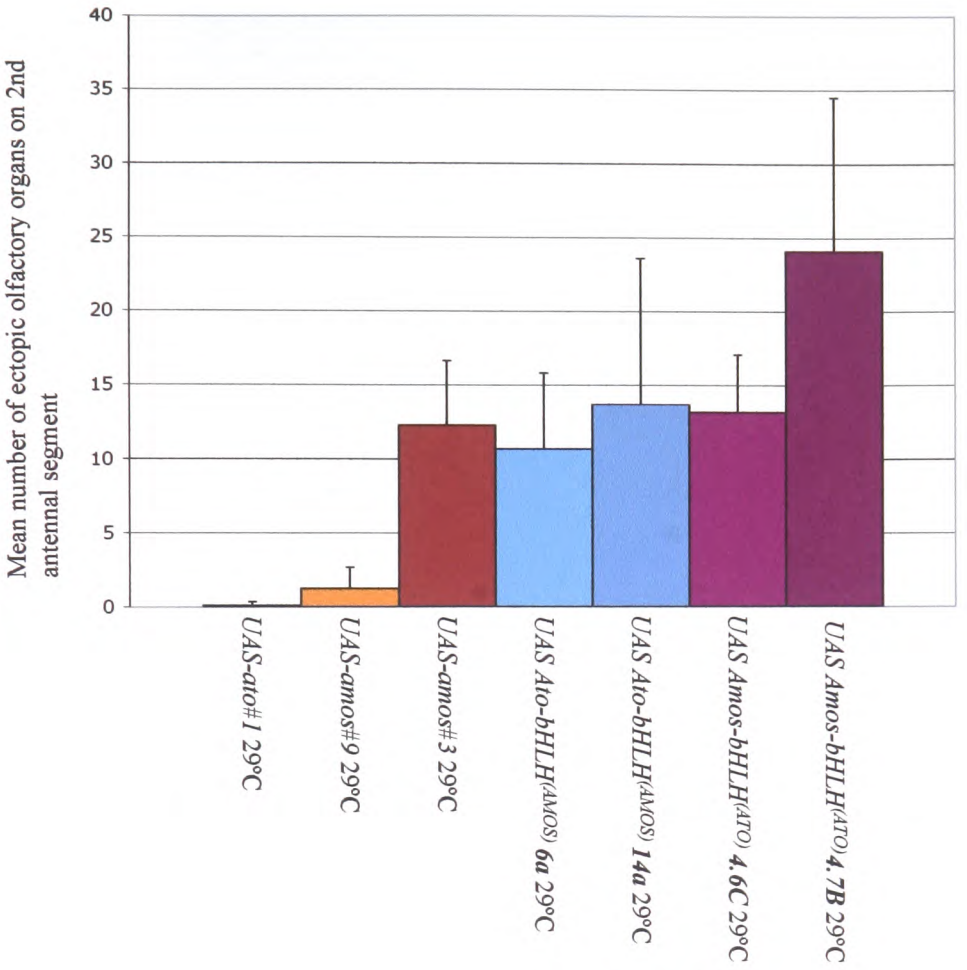

Figure 4.13 Ato-bHLH$^{(AMOS)}$ and Amos-bHLH$^{(ATO)}$ chimeras can induce the formation of ectopic olfactory organs on the second antennal segment. Ectopic olfactory organs on the second antennal segment are specified by *UAS-amos#3* but not *UAS-ato#1*. *UAS Ato-bHLH$^{(AMOS)}$* can also specify olfactory organs suggesting that the bHLH of Amos is sufficient to confer specificity to the Ato-bHLH$^{(AMOS)}$ chimera. Surprisingly *UAS Amos-bHLH$^{(ATO)}$* also specifies ectopic olfactory formation suggesting that the bHLH of Ato is able to substitute for this function in the context of Amos.

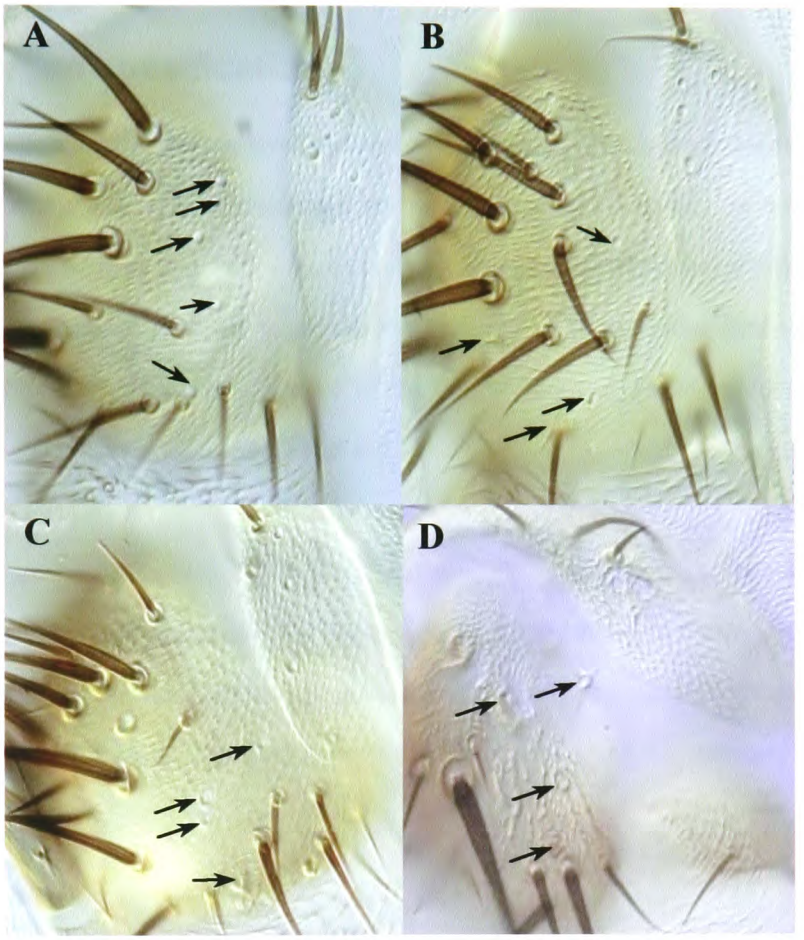

Figure 4.14 Ectopic olfactory sensilla are formed on the second antennal segment by misexpression of Ato-bHLH$^{(AMOS)}$ and Amos-bHLH$^{(ATO)}$ chimeras driven by *Gal4$^{109-(2)68}$* at 29°C. 6a Ato-bHLH$^{(AMOS)}$ **(A)** and 14a Ato-bHLH$^{(AMOS)}$ **(B)** are able to specify ectopic olfactory sensilla (arrows), this suggests that the bHLH domain of Amos is sufficient to enable Ato to behave like *amos*. Interestingly, the Amos-bHLH$^{(ATO)}$ chimeras also specify ectopic olfactory sensilla. 4.6C Amos-bHLH$^{(ATO)}$ **(C)** is unable to inhibit *ac* (Fig.4.9B) but can initiate alternative fate pathways such as chordotonal organ formation (Fig.4.10) and here I show its is also able to mimic *amos* in the promotion of ectopic olfactory sensilla. This does not appear to be an artifact of this line alone, all lines of this chimera are able to do this as exemplified by 4.7B Amos-bHLH$^{(ATO)}$ **(D)**. This suggests that the Ato bHLH domain is able to substitute and mimic Amos misexpression in this context.

4.10.2 The requirement for endogenous *amos* for ectopic olfactory organ specification

To further investigate the mechanisms behind specification of olfactory organs by Amos-bHLH$^{(ATO)}$ and Ato-bHLH$^{(AMOS)}$, I repeated the olfactory sensilla assay in an *amos*^{1} null background. The results of this assay in an *amos*^{1} background show that *UAS-amos#3* can continue to specify ectopic olfactory organs in the absence of endogenous *amos*. Surprisingly more ectopic olfactory organs are formed in the *amos*^{1} background than in the wild type background (20.7±7.94 c.f. 12.3±4.33) (Fig.4.15).

In contrast, neither the Amos-bHLH$^{(ATO)}$ nor the Ato-bHLH$^{(AMOS)}$ chimeras can efficiently promote ectopic olfactory sensilla in the absence of endogenous *amos*. There is a dramatic reduction in ectopic olfactory organ formation when the chimeras are misexpressed in an *amos*^{1} background compared to the wild type background (Ato-bHLH$^{(AMOS)}$ 14a 1.5± 1.41; Amos-bHLH$^{(ATO)}$ 4.6C 1.44±1.65) .

Thus the chimeras behave distinctly differently from both Ato and Amos in the specification of ectopic olfactory organs. They are both able to specify ectopic olfactory sensilla, unlike Ato. However, they both rely on cross-activating endogenous *amos* in order to achieve this, unlike misexpressed Amos.

This assay is based on an ectopic ability of Amos when misexpressed. To clarify the nature of the chimera capabilities, it would be better to investigate their ability to rescue the loss of wildtype olfactory sensilla in the *amos* mutant. This is done next.

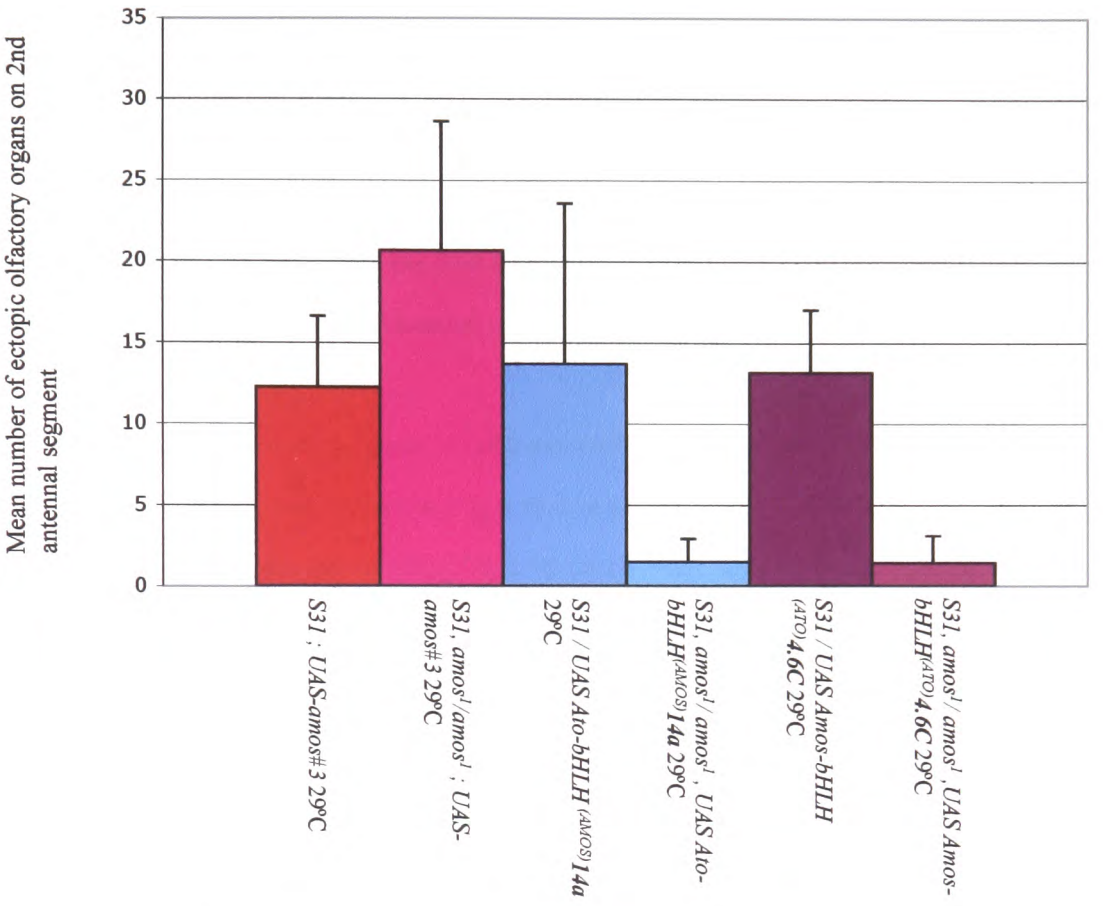

Figure 4.15 *UAS-Ato-bHLH (AMOS)* and *UAS-Amos-bHLH (ATO)* require endogenous *amos* to specify ectopic olfactory organs on the second antennal segment. Endogenous *amos* is required for the specification of ectopic olfactory organs by the Ato-bHLH(AMOS) and Amos-bHLH(ATO) chimeric proteins. The results show that true rescue of the ectopic olfactory phenotype in an *amos*^{1} background can only be achieved by the intact Amos protein. In fact the number of ectopic olfactory organs produced by misexpression of *UAS-amos#3* increases in the *amos*^{1} mutant (*S31, amos*^{1}*/amos*^{1} *; UAS-amos#3*) . In contrast the number of ectopic olfactory organs produced by misexpression of Ato-bHLH(AMOS) and Amos-bHLH(ATO) is dramatically reduced in *amos*^{1} homozygote. Although both chimeric proteins are able to mimic Amos, in the *amos*^{1}mutant neither protein can rescue the olfactory phenotype. This suggest that both chimeric proteins must cross-activate endogenous Amos to achieve an Amos-like olfactory phenotype.

4.11 Rescue of endogenous olfactory sensilla on the third antennal segment

I misexpressed proneural gene constructs in *amos*^{1} flies using $^{109\text{-}(2)68}$Gal4 and assayed for rescue of the mutant phenotypes. To reiterate this, mutation of *amos* results in the loss of all sensilla basiconica and trichodea, but has no effect on sensilla coeloconica (which are *ato*-dependent) (zur Lage et al., 2003). Moreover, a number of ectopic sensory bristles appear.

Interestingly, I found that misexpression of *UAS-amos#3* could completely inhibit the emergence of bristles on the *amos* mutant funiculus (Fig.4.16 and 4.19C). However misexpression of *UAS-ato#1* did not inhibit the ectopic bristles (Fig.4.16 and 4.19D). Likewise misexpression of the chimeras did not inhibit the ectopic bristles (Fig.4.19E and F). Instead the chimeric proteins increased the formation of ectopic bristles (Fig.4.16). This suggests that the chimeric proteins are able to promote neural precursor selection, however they are unable to transform the external sense organ lineage as efficiently as Amos.

4.11.1 Amos, but not Ato, can rescue olfactory sensilla in *amos*^{1} mutant flies

In the absence of endogenous *amos* sensilla basiconica are no longer specified (*amos*^{1} 0 c.f. wild type 177.5±8.6). I found that misexpression of *UAS-amos#3* rescues a significant proportion of the sensilla basiconica (Fig.4.17). This rescue is not complete (25°C 44.8±21.3), perhaps because the expression pattern of the Gal4 driver is not ideal. Moreover, rescue is less efficient at a higher temperature (29°C 30.8±14), perhaps due to an apparent toxicity of strong Amos expression.

Sensilla trichodea are also completely absent in *amos* mutant flies (*amos*^{1} 0 c.f. wild type 114.5±3.5). I found that misexpression of *UAS-amos#3* can rescue significant numbers of sensilla trichodea (Fig.4.18). Moreover, like the sensilla basiconica, rescue decreases with increased temperature (*UAS-amos#3* 25°C 51.8±22.1 c.f. 29° 27.5±12.3).

As might be expected, misexpression of *UAS-ato#1* does not significantly rescue sensilla basiconica (Fig.4.17 25°C 3.9±2.47 and 29°C 4.69±4.08). No sensilla trichodea are rescued by *UAS-ato#1* at 25°C (0) and at 29°C the numbers of trichodea remain insignificant (0.188±0.544) (Fig.4.18). Thus Amos and Ato behave quite distinctly in this assay: only Amos can rescue sensilla basiconica and trichodea. In contrast, it had been shown that Ato could rescue the loss of sensilla coeloconica in *ato* mutant flies (Gupta and Rodrigues, 1997).

4.11.2 Rescue of olfactory sensilla by the chimeras

UAS-Amos-bHLH$^{(ATO)}$ 4.6C can rescue sensilla basiconica (Fig.4.17). It therefore differs from Ato. However the level of rescue is lower than *UAS-amos#3* (*UAS Amos-bHLH* $^{(ATO)}$ 4.6C 29°C 17.4±6.23 c.f. *UAS-amos#3* 29°C 30.8±14). Unlike *UAS-amos#3*, temperature shifts do not affect the level of rescue by *UAS Amos-bHLH* $^{(ATO)}$ 4.6C (25°C 15.3±12.8 c.f. 29°C 17.4±6.23).

UAS-Ato-bHLH$^{(AMOS)}$ is able to rescue basiconica to the same degree as *UAS-amos#3* (Fig.4.17 *UAS-ato-bHLH*$^{(AMOS)}$ 25°C 42.5±6.45 c.f. *UAS-amos#3* 25°C 44.8±21.3). Interestingly the level of rescue by this chimera decreases with increasing temperature showing the same trend as *UAS-amos#3* (*UAS-Ato-bHLH*$^{(AMOS)}$ 25°C 42.5±6.45 c.f. 29°C 27.4±8.16).

It seems that both chimeras are less able to rescue sensilla trichodea (Fig.4.18). *UAS Amos-bHLH* $^{(ATO)}$ does not rescue trichodea at 25°C, but shows some rescue at 29° (3.3±1.97). *UAS*

Ato-bHLH $^{(AMOS)}$ shows a more convincing rescue (*UAS Ato-bHLH $^{(AMOS)}$* 25°C 6.25±5.85 and 29°C 9.13±17.5). However this rescue is clearly much lower than that achieved by *UAS-amos#3*.

Overall (particularly with respect to sensilla basiconica), Ato-bHLH$^{(AMOS)}$ behaves very much like Amos; Amos-bHLH$^{(ATO)}$ is less efficient than Amos, but still shows much better rescue ability than Ato. These results convincingly suggest that Amos's unique olfactory specifying ability is somewhat dispersed between both the bHLH and non-bHLH portions of the protein.

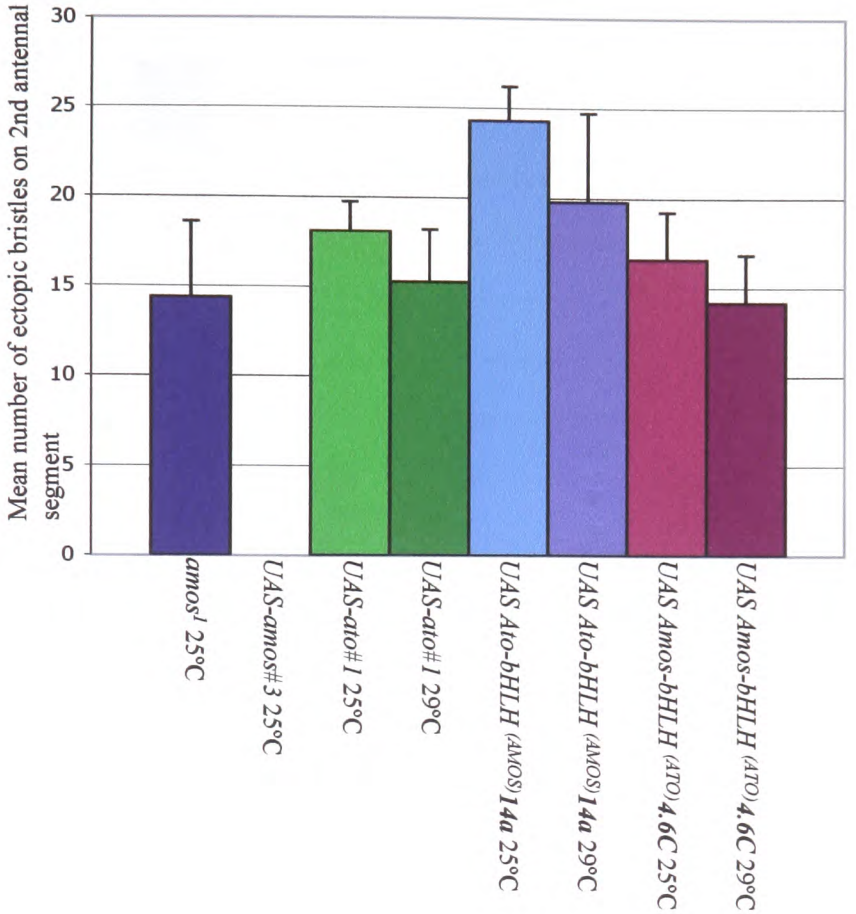

Figure 4.16 The emergence of ectopic external sense organs in *amos*^{1} can only be inhibited by Amos. In the absence of endogenous *amos*, ectopic external sense organs emerge on the funiculus. The formation of these ectopic bristles can only be inhibited by the misexpression of Amos. Misexpression of Ato does not have a significant effect upon the number of ectopic bristles compared to *amos*^{1} control. Misexpression of Ato-bHLH$^{(AMOS)}$ or Amos-bHLH$^{(ATO)}$ chimeras cannot inhibit the ectopic bristles. On the contrary, there seems to be a small increase in ectopic bristle formation. This increase is significant in the case of Ato-bHLH$^{(AMOS)}$.

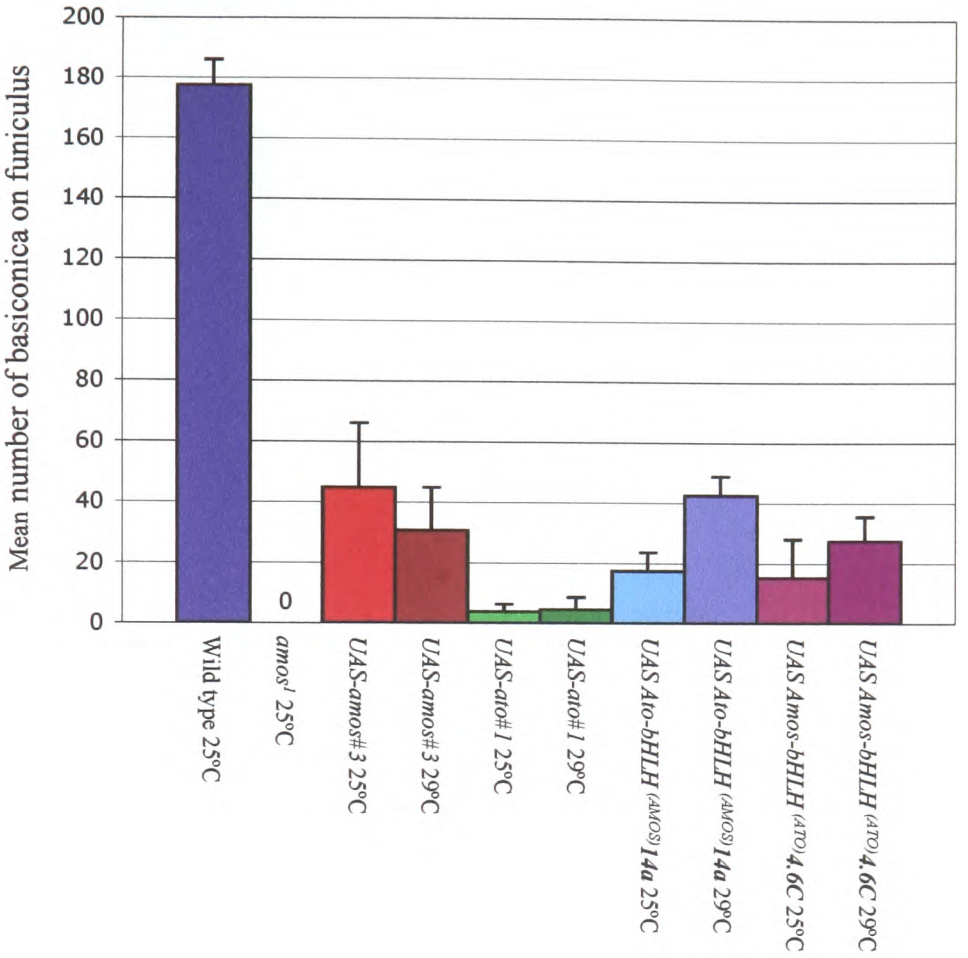

Figure 4.17 Rescue of sensilla basiconica by misexpression in *amos*^{1}. *amos* dependent sensilla basiconica are not specified in *amos*^{1} mutant. Misexpression of Amos can rescue some of the basiconica, however at higher temperatures, this rescue is reduced (*UAS-amos#3* at 25°C compared with 29°). This may be due to toxicity of the Amos protein at high expression levels. Misexpression of Ato shows the lowest rescue of basiconica. This suggests that Ato lacks the domains required for the specification of basiconica. However, the Ato-bHLH$^{(AMOS)}$ chimera can rescue basiconica to levels comparable to rescue by Amos. Thus, the Ato-bHLH$^{(AMOS)}$ chimera behaves more like Amos than Ato in this assay. Interestingly the Amos-bHLH$^{(ATO)}$ chimera also rescues basiconica, however this rescue is lower than either Amos or Ato-bHLH$^{(AMOS)}$. This result supports previous findings which indicate some Amos function to structural elements out with the Amos bHLH domain.

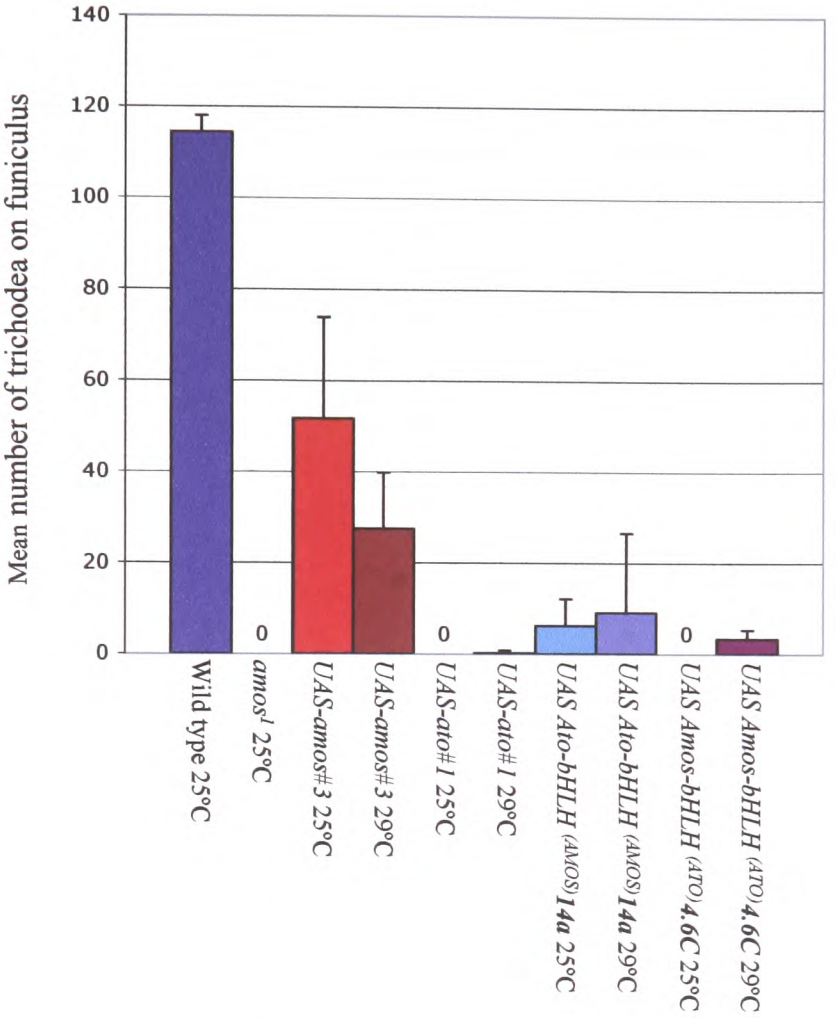

Figure 4.18 Rescue of sensilla trichodea by misexpression in *amos*^{1}. *amos* dependent sensilla trichodea are not specified in an *amos* null background (*amos*^{1} compared to wild type). Misexpression of Amos can rescue some of the trichodea, however at higher temperatures, this rescue is reduced (*UAS-amos#3* at 25°C compared 29°). This suggests an upper limit of rescue at which protein levels become toxic. Misexpression of Ato shows no rescue at 25°C and negligible rescue at 29°C. This suggests that Ato lacks the structural elements required for the specification of sensilla trichodea. The Ato-bHLH$^{(AMOS)}$ and Amos-bHLH$^{(ATO)}$ (at 29°C) chimeras can rescue trichodea. The Ato-bHLH$^{(AMOS)}$ chimera does not rescue trichodea to the same extent as Amos, however it can rescue better than Amos-bHLH$^{(ATO)}$. The partial rescue of trichodea by the two chimeras suggest that they are functionally more similar to Amos than Ato in this assay.

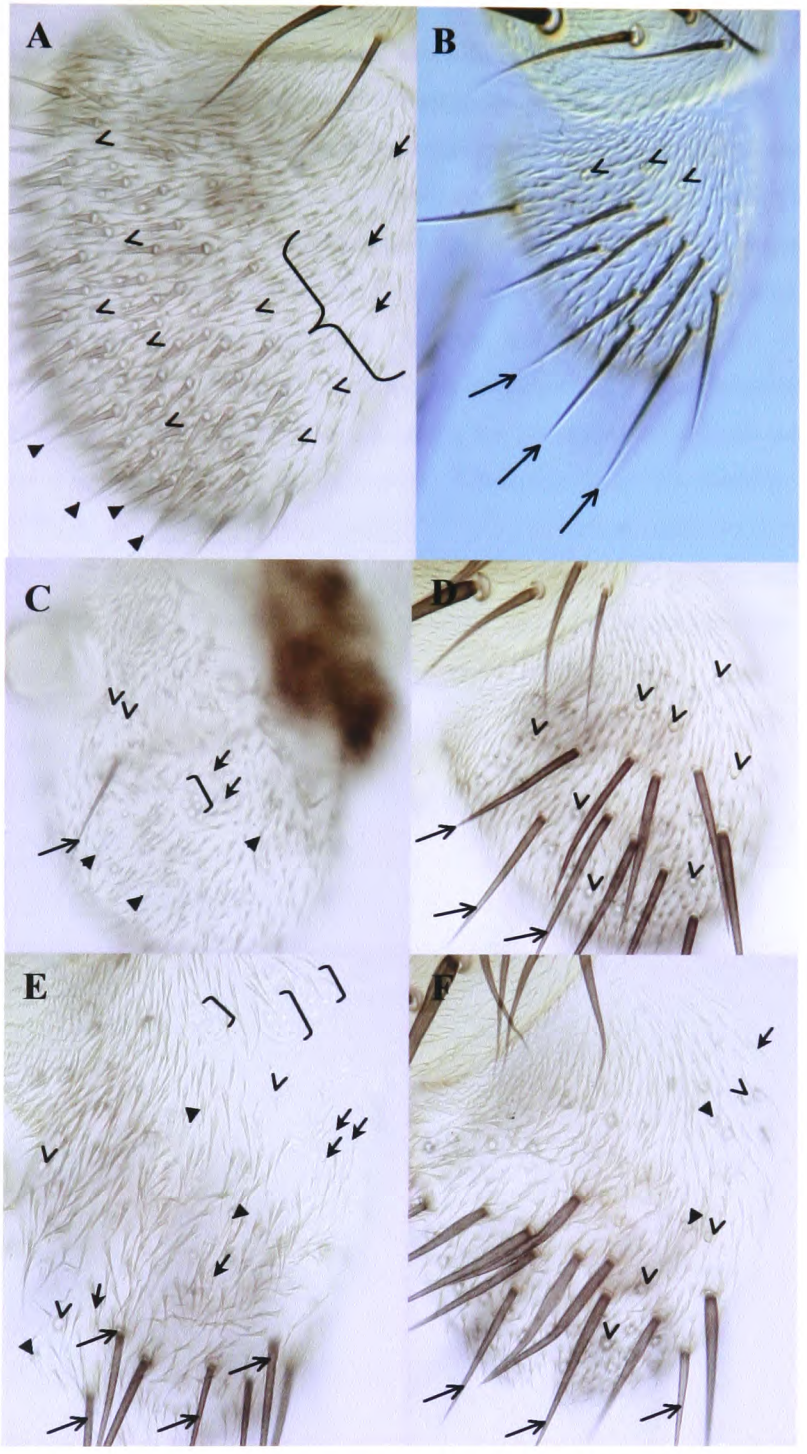

Figure 4.19 Misexpression of Amos, Ato, Ato-bHLH$^{(AMOS)}$ and Amos-bHLH$^{(ATO)}$ chimeras in the third antennal segment of *amos^{1}* mutants

(A) Wild type third antennal segment (funiculus). **(B)** *amos^{1}* homozygote (from zur Lage et al., 2003). **(C)** *UAS-amos#3*. **(D)** *UAS-ato#1*. **(E)** 14a Ato-bHLH$^{(AMOS)}$. **(F)** 4.6C 14a Amos-bHLH$^{(ATO)}$.

Figure 4.19 Misexpression of Amos, Ato, Ato-bHLH$^{(AMOS)}$ and Amos-bHLH$^{(ATO)}$ chimeras in the third antennal segment of *amos^{1}* homozygotes at 29° by *Gal4$^{109-(2)68}$*. Wild type third antennal segment (funiculus) (**A**) houses three subtypes of olfactory sensilla; coeloconica (open arrowheads), trichodea (arrowheads) and basiconica (arrows, normal site of formation indicated by curly bracket). In the *amos^{1}* homozygote (**B**), sensilla trichodea and basiconica are lost, however coeloconica remain unaffected. In addition there is emergence of large external sense organs (open arrows). The emergence of these external sense organs in inhibited by misexpression of *UAS-amos#3* (**C**), furthermore, some trichodea and basiconica are rescued. Misexpression of *UAS-ato#1* (**D**) does not inhibit the emergence of external sense organs and there is no rescue of trichodea and basiconica. Misexpression of the chimeric lines 14a Ato-bHLH$^{(AMOS)}$ (**E**) and 4.6C 14a Amos-bHLH$^{(ATO)}$ (**F**) also fail to inhibit external sense organs suggesting that inhibition requires the intact Amos protein (alternatively this Amos line may be unique in some way). Nonetheless, both chimeras are able to rescue some trichodea and basiconica, suggesting they retain functional features of Amos.

4.12 Effect of misexpression on numbers of sensilla coeloconica

I took advantage of the *amos* rescue experiments to score the effects of proneural protein misexpression on sensilla coeloconica numbers in *amos*^{1} mutant flies. Although the *amos*^{1} mutation has no effect on these sensilla (Fig.4.20) (therefore this is not a rescue experiment), the absence of other olfactory sensilla made it far easier to count sensilla coeloconica accurately.

4.12.1 Ato, but not Amos, promotes increased numbers of sensilla coeloconica

As mentioned above, misexpression of Ato has been shown to increase the number of sensilla coeloconica on the third antennal segment, consistent with these sensilla requiring *ato* function (Gupta and Rodrigues, 1997). Here I show that this increase is also observed in *amos*^{1} flies as anticipated (*amos*^{1}*;UAS-ato#1* 25°C 83.1±13.2 and 29°C 106±18.5 c.f. *amos*^{1} 70.3±1.5) (Fig.4.20). Misexpression of *UAS-amos#3* shows the opposite phenotype. There is a sharp reduction in coeloconica numbers (*amos*^{1}*;UAS-amos#3* 25°C 46±12.9 and 29°C 45.5±11.3 c.f. *amos*^{1} 70.3±1.5). This suggests that either Amos is inhibiting sensilla coeloconica formation or transforming coeloconica precursors into *amos* dependent olfactory sensilla.

4.12.2 Ato-bHLH$^{(AMOS)}$, but not Amos-bHLH$^{(ATO)}$, can promote sensilla coeloconica formation

Misexpression of Amos-bHLH$^{(ATO)}$ does not significantly affect the numbers of coeloconica compared to *amos*^{1} (Fig.4.20 *amos*^{1}*;UAS Amos-bHLH* $^{(ATO)}$ 25°C 60.3±20.5 and 29°C 64.6±14.1 c.f. *amos*^{1} 70.3±1.5). In contrast, Ato-bHLH$^{(AMOS)}$ behaves differently in this assay. At 25°C Ato-

bHLH$^{(AMOS)}$ behaves like Ato, increasing the mean number of coeloconica (*amos^{1};UAS Ato-bHLH $^{(AMOS)}$* 87.5±24.4 c.f. *amos^{1};UAS-ato#1* 83.1±13.2). However at 29°C this increase in coeloconica is no longer seen, returning to non-mutant numbers (61±17.1 c.f. *amos^{1}* 70.3±1.5).

In general these results are strikingly consistent with those for chordotonal specification. Ato-bHLH$^{(AMOS)}$ behaves more like Ato than does Amos-bHLH$^{(ATO)}$. This suggests that for two very different Ato-specific functions, Ato specificity relative to Amos lies outside the bHLH domain.

4.13 Ato-bHLH$^{(AMOS)}$ and Amos-bHLH$^{(ATO)}$ promote the formation of extra PDM+ cells in the embryo

I found that both chimeras could rescue some *amos*-specific olfactory sensilla in the adult. This suggests that both chimeras have some *amos*-like functions. I decided to corroborate this result in the embryo. Ato-bHLH$^{(AMOS)}$ and Amos-bHLH$^{(ATO)}$ misexpression was driven in the embryo by *scaGal4* and the dorsal md neurons were assayed after staining with the antibody, PDM. In Chapter 3 I showed that misexpression of *amos* in the embryo was more efficient at specifying extra PDM+ cells than *ato*. The results show that both chimeras can induce the formation of extra PDM+ cells (Fig.4.21). This is consistent with findings in the adult. The bHLH domain of Amos is sufficient to allow Ato-bHLH$^{(AMOS)}$ to produce significantly more PDM+ cells than the intact Ato protein (Fig.4.22) (*UAS Ato-bHLH $^{(AMOS)}$* 14a 6.86±1.59, 6a 7.14±1.21 c.f. *UAS-ato#1* 2.86±1.26). However Amos-bHLH$^{(ATO)}$ is better than Ato-bHLH$^{(AMOS)}$ in this assay (*UAS Amos-bHLH$^{(ATO)}$4.6G* 10.6±2.66 c.f. *UAS Ato-bHLH $^{(AMOS)}$6a* 7.14±1.21) Thus, to some extent, Amos-bHLH$^{(ATO)}$ behaves more like Amos than Ato. However, further experiments would need to be performed in the future to test the requirement for endogenous *amos* for these phenotypes.

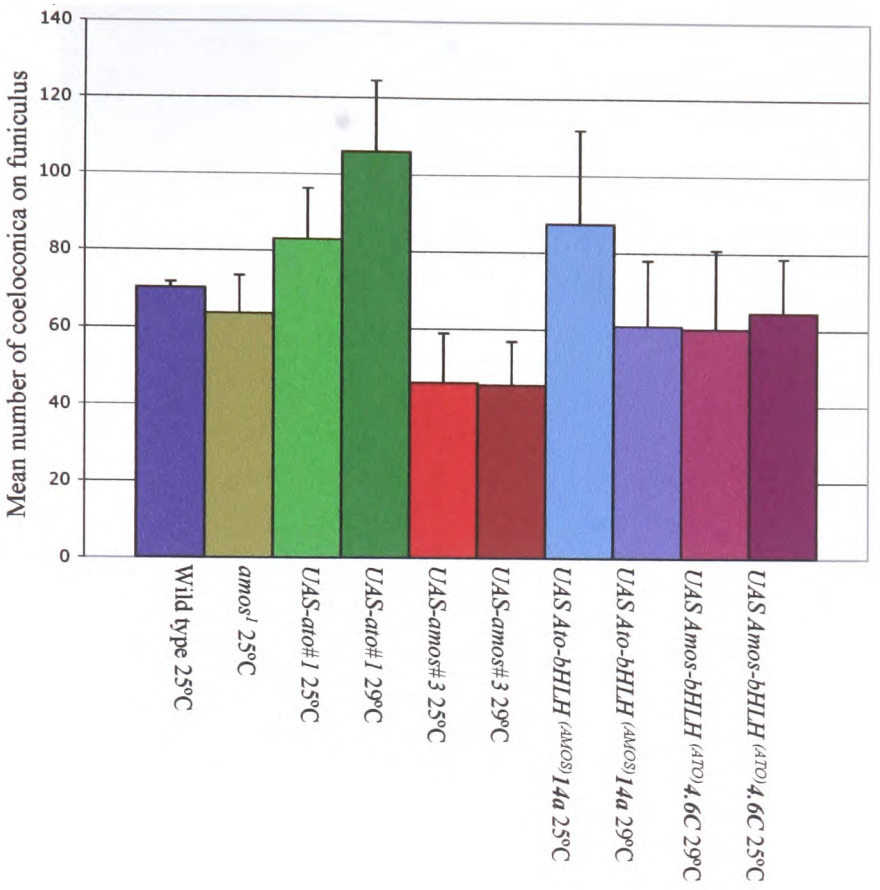

Figure 4.20 Mean number of sensilla coeloconica in *amos*^{1} Sensilla coeloconica are *ato* dependent. Misexpression of Ato results in increased numbers of coeloconica (compared to wild type and *amos*^{1}*).* The number of coeloconica are unaffected in *amos*^{1} (compared to wild type). This suggests that *amos* is not required for the formation of sensilla coeloconica. Accordingly, the misexpression of Amos does not increase the numbers of coeloconica formed. In fact the results show a small decrease, a possible explanation for this is fate transformation of *ato*-dependent precursors to *amos* dependent sensilla. In the mutant background, misexpression of Amos-bHLH$^{(ATO)}$ leads to slight reductions in the numbers of coeloconica formed. Thus Amos-bHLH$^{(ATO)}$ does not behave like Ato. Interestingly, Ato-bHLH$^{(AMOS)}$ at 25°C does make comparable numbers of coeloconica to Ato.

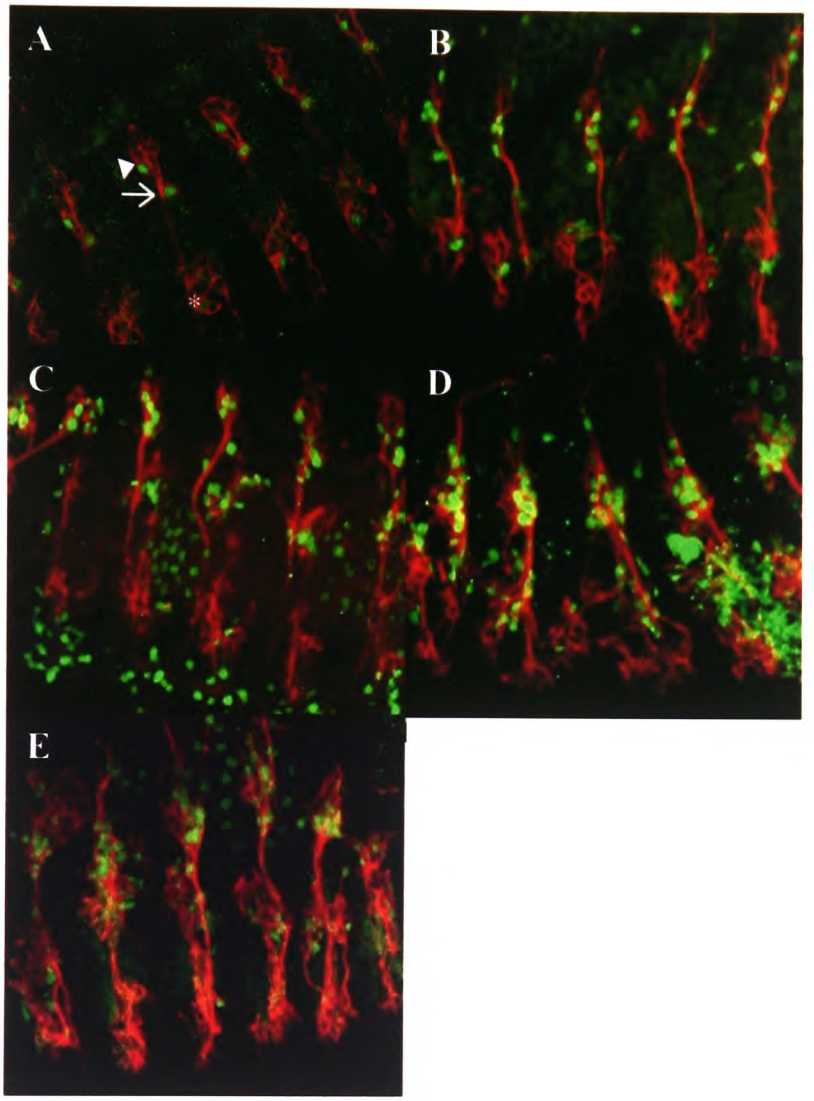

Figure 4.21 Misexpression of Ato-bHLH$^{(AMOS)}$ and Amos-bHLH$^{(ATO)}$ chimeras by *Gal4^{sca}* at 25°C promote the formation of extra PDM+ cells in the embryo. (A) Wildtype *W^{1118}* embryo stained with anti-22C10 (red) and anti-PDM (green), there is PDM staining in the *amos*-dependent dda (arrowhead) and dbd (arrow) md neurons and the ligament cells of the lateral chordotonal organs (asterix). Misexpression of Ato-bHLH$^{(AMOS)}$ chimeric lines 14a (**B**) and 6a (**C**) have increased PDM+ cells compared to wildtype. Misexpression of the Amos-bHLH$^{(ATO)}$ chimeras 4.6E (**D**) and 4.6G (**E**) also promote the formation of extra PDM+ cells compared to wildtype.

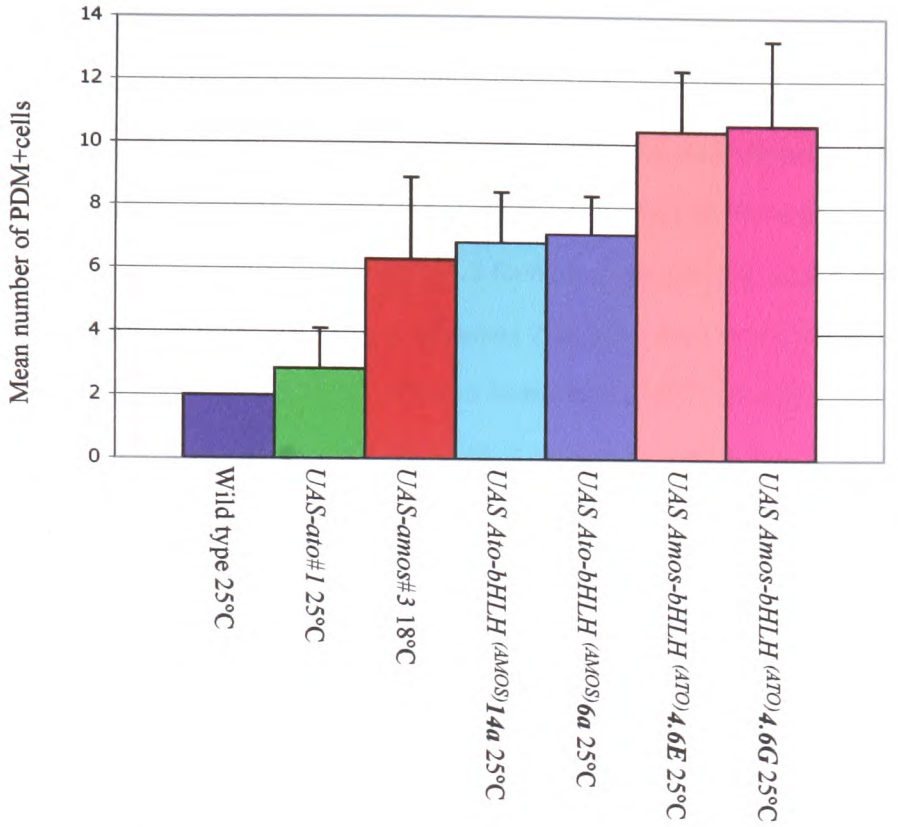

Figure 4.22 Both Ato-bHLH$^{(AMOS)}$ and Amos-bHLH$^{(ATO)}$ can promote the formation of extra *amos*-specific md neurons in the embryo. Misexpression of *UAS-amos#3* produces a significant increase in PDM+ cells compared to wildtype. The bHLH domain of Amos is able to specify extra PDM+ cells in the context of the Ato protein (*UAS-Amos-bHLH$^{(ATO)}$ 14a* and *6a*) . However the bHLH domain of Ato can substitute for Amos-like function in the context of Amos. Interestingly the Amos-bHLH$^{(ATO)}$ chimera is better than the Ato-bHLH$^{(AMOS)}$ chimera at specifying extra PDM+ cells.

4.14 Confirming the chimera lines by genomic PCR

The results of the mutant chordotonal and olfactory assays are different from expected. Therefore it was important to exclude any errors in the identity of the chimeric transgenic lines. I confirmed the identity of the chimeric lines by PCR across the chimeric breakpoints (Fig.4.23b). I designed primers to bridge the 5' non-bHLH and bHLH regions of Amos and Ato. Firstly I tested the primers by PCR of W^{1118} genomic DNA. I found that the primers worked well and amplified products around 200bp in length (Fig.4.23a lanes 2 and 3). I then used selected combinations of the primers to amplify genomic DNA obtained from Ato-bHLH$^{(AMOS)}$14a and Amos-bHLH$^{(ATO)}$4.6C chimeric lines (Fig.4.23a lanes 4 and 5). Using the selected combination of primers (depicted in Fig.4.23b), I could verify that the correct chimeric constructs had been produced, otherwise no product would be amplified (Fig.4.23a lanes 6 and 7).

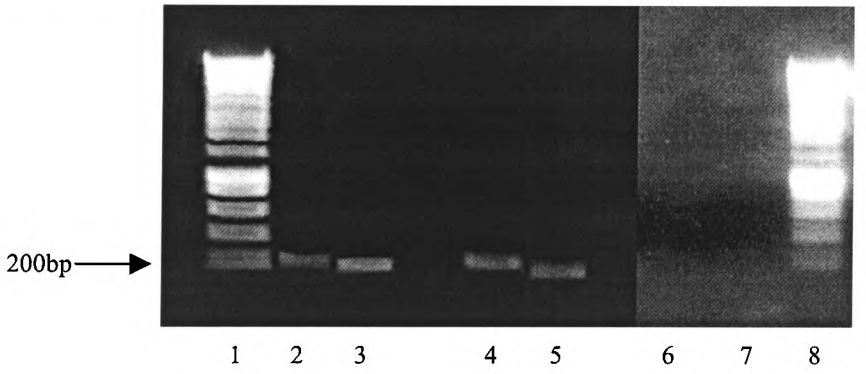

Figure 4.23a Verification of Amos-bHLH$^{(ATO)}$ and Ato-bHLH$^{(AMOS)}$ chimeric constructs. Lanes 1 and 8: Hyperladder I. Lane 2: w^{1118} genomic DNA with primers Atotest1 and Atotest2. Lane 3: w^{1118} genomic DNA with primers Amostest3 and Amostes4. Lane 4: Amos-bHLH$^{(ATO)}$ 14a genomic DNA with primers Amostest3 and Atotest2. Lane 5: Ato-bHLH$^{(AMOS)}$ 4.6C genomic DNA with primers Atotest1 and. Amostest4. Lane 6: w^{1118} genomic DNA with primers Amostest3 and Atotest2. Lane 7: w^{1118} genomic DNA with primers Atotest1 and. Amostest4. These PCR products verify that the correct chimeric constructs are correct.

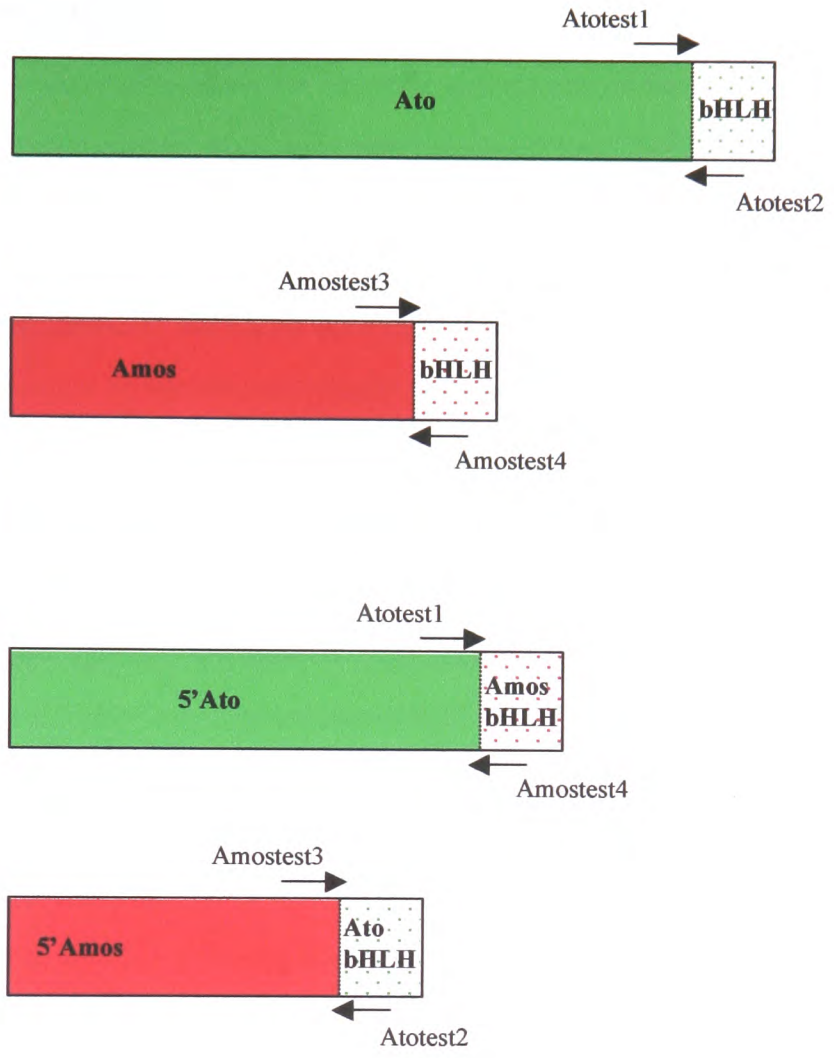

Figure 4.23b Design of primers for testing chimeric constructs:

The 5'-3' primers were designed to sequences ~33 amino acid residues before the bHLH region and the reverse 3'-5' primers were designed to sequences ~ 33 amino acid residues inside the bHLH region. These primers would thus give PCR products ~200bp in length. These primers were then used to test the chimeric constructs to verify that they contained the desired bHLH domains.

4.15 Discussion

This chapter attempts to define the structural requirements of the Ato-like proteins (Ato and Amos) that determine their different functional abilities in vivo. Such information is an important prerequisite for understanding the mechanistic basis of how different functions are performed. I have attempted to assign functional abilities to the bHLH and the non-bHLH portions of the proteins using chimeras. The results show many interesting features, but are quite complex. The message seems to be that structural requirements are different for different aspects of functional specificity.

4.15.1 Bristle suppression

In general, both chimeras can suppress thoracic bristles when misexpressed, thus preserving a function that is present in both parent proteins (Jarman and Ahmed, 1998; Goulding et al., 2000; zur Lage et al., 2003). This shows that on the whole, the chimeric genes produce functional proteins. It is consistent with one model proposed for how bristle suppression is achieved – that is that Ato and Amos can complex with Ac/Sc proteins to suppress their activity if co-expressed (zur Lage et al., 2003). At odds with this, however, is the finding that neither Ato nor either of the chimeras can suppress the ectopic bristles that appear on the *amos* mutant antenna. This is surprising both for the chimeras and particularly for Ato itself. There is no straightforward explanation, but a possibility is that Amos is much better at complexing with (and inhibiting) Ac/Sc than is Ato, but that this is only apparent in the antennal assay. Perhaps only a low degree of inhibitory ability is required in the thorax, and Ato and the chimeras can perform well enough there.

Another finding complicates this picture. Two Ato-bHLH$^{(AMOS)}$ lines showed a lack of bristle inhibition ability. In fact, they were able to produce more bristles on misexpression. I showed that this correlated with an increased expression of endogenous Ac. It is not clear why these lines

should behave oppositely from the others. One possibility is that they are simply very weak expressers, since it was shown that only strong Ato misexpression results in bristle suppression, whereas weak misexpression resulted in a modest increase in bristles (Jarman and Ahmed, 1998). However, this is does not appear to be the explanation, since one of the lines (4.6C) is able to promote very strong chordotonal organ specification. Another possibility is that this is a position effect. It could be that the UAS P-element insert is causing misexpression of an adjacent endogenous gene that promotes bristle formation. However, the two lines are independent inserts (on separate chromosomes), which makes this less likely.

I used the loss of thoracic bristles as an indicator of strength of misexpression for the various lines. However, I also showed that this must be at best a crude measure, since strength of bristle suppression does not necessarily correlate with strength of other phenotypes (such as chordotonal organ specification).

In retrospect, the problems associated with identifying the expression pattern of the chimeric constructs could have been resolved by incorporating one of a wide range of protein tags such as GFP, Myc or FLAG tags. Furthermore incorporating an HA or GST tag would also allow for the quantification of protein levels. Since no such tags are fused to the chimeric constructs, the only method available to measure protein levels is indirect, by RT PCR.

4.15.2 Chordotonal organ specification

Both chimeras have a strong ability to specify ectopic chordotonal organs. This, of course, does not distinguish Amos and Ato since I showed in Chapter 3 that both were capable of this behaviour. That is, this is an ability of both Ato-like proteins. However, the result is useful since it demonstrates that both chimeric genes are producing functional Ato-like proteins. It confirms not

only that the genes are transcribed and translated, but also that the hybrid proteins can fold appropriately to form a functional proneural protein.

For chordotonal organs, the real test of specificity is whether the chimeras can specify these organs in the absence of endogenous *ato* function. I showed in Chapter 3 that Amos and Ato were distinguishable on this score. Here, I found a clear difference between the chimeras: only Ato-bHLH$^{(AMOS)}$ was able to specify chordotonal organs in the *ato* mutant. Thus, by this criterion, the ability to specify chordotonal organs maps not to the bHLH domain, but to the rest of the Ato protein. This conclusion is different from most other bHLH protein specificity studies. It shows that one cannot assume that a bHLH domain contains the important information without performing the necessary structure-function studies. There are two inferences from this.

Firstly, the Amos bHLH domain can substitute perfectly well for the Ato bHLH domain in chordotonal organ specification (the Ato-bHLH$^{(AMOS)}$ chimera). However, the bHLH domain clearly does not drive chordotonal specification, since the Ato bHLH domain cannot impose chordotonal specification in the Amos-bHLH$^{(ATO)}$ chimera. Nevertheless we know that the bHLH domain is not irrelevant, since an Ato-bHLH$^{(SC)}$ chimera cannot specify chordotonal organs at all, even in a wildtype background (Chien et al., 1996). In other words, the bHLH domain must be Ato-like — the structural features required appear to be conserved between the Amos and Ato bHLH domains.

Secondly, there must be structural determinants within the rest of the Ato protein that, in combination with an Ato-like bHLH domain, drive the specification of chordotonal organs. What are these determinants? It is impossible to say at present. There is no similarity between Amos and Ato outside their bHLH domains (Fig.3.1 in Chapter 3), and so no clue that would help narrow down what might be unique to Ato. On the other hand, some indication can be obtained

from phylogenetic sequence comparisons between different Ato orthologues (Fig.4.24). These show large regions of high conservation that are therefore candidates for chordotonal determining regions. How might they function? They could modify the DNA binding properties of the bHLH domain. More plausibly, they might interact directly with protein cofactors that are important for chordotonal specification (Fig.4.25). Future experiments could be aimed at pin-pointing the important regions and identifying proteins that bind to them.

4.15.3 Olfactory organ specification

The neat conclusion for chordotonal specification does not readily apply to olfactory specification functions. Moreover, the findings of these studies are varied, depending on the assay used. In the following I try to make sense of these data and glean what can be deduced of specificity.

I show for the first time that *UAS-amos* can rescue the loss of sensilla basiconica and trichodea of *amos*^{1}. However, rescue is not complete. This may be because the Gal4 line does not correctly reproduce the normal Amos expression pattern in the antenna. Better rescue would require the use of other Gal4 drivers. In particular, a line in which the enhancer region of the amos gene itself drives Gal4 has now been constructed (E. Holohan, pers. comm.) and is more likely to result in correct expression of a UAS line.

In contrast to *amos*, *ato* was unable to rescue more than a small number of sensilla basiconica and trichodea. This result parallels the inability of *amos* to promote chordotonal organ specification in the absence of *ato* (Chapter 3). In contrast, *ato*, but not *amos*, could promote extra sensilla coeloconica on the third antennal segment. These three observations strongly underline the conclusion that Amos and Ato are abundantly different in their capabilities, if the right assay is used. In this case, the correct assay is to observe the effects of misexpression in the third antennal segment, which is the appropriate place for olfactory sensillum specification.

Interestingly, for sensilla coeloconica, Ato's unique ability maps to its non-bHLH portion just as it did for chordotonal specification. This suggests that there may be a common structural and functional component to these two different Ato functions in different contexts.

For sensilla basiconica and trichodea a different result is observed. Both chimeras clearly behave like Amos rather than Ato in this assay. The major conclusion is therefore that there are important structural features for basiconica/trichodea specification both within and outside the bHLH domain. This is different from chordotonal specification. Most notably, the Amos bHLH domain can determine the olfactory specificity of a proneural protein in the absence of the rest of the Amos protein: it does not need the rest of the Amos protein for specificity. The Ato bHLH domain could not do this in chordotonal specification. Moreover, at least for sensilla basiconica rescue, the Ato-bHLH$^{(AMOS)}$ chimera can perform as well as the whole protein. Therefore, based on the difference in functionality between Ato and the Ato-bHLH$^{(AMOS)}$ chimera, the Ato bHLH domain lacks some important feature that is present in the Amos bHLH domain, which can drive olfactory specification.

However, this is not the end of the story. There also appear to be determinants in the rest of the Amos protein too. In the Amos-bHLH$^{(ATO)}$ structural elements in the non-bHLH portion of Amos can collaborate with either Ato-like bHLH domain in olfactory specification. Thus, to some extent the Amos bHLH domain can be substituted by that of Ato. In other words, for olfactory specificity, the Amos bHLH domain is sufficient (in the context of a protein), but not totally necessary. In this case, we cannot say whether it is important to have an Ato-like bHLH domain, since no Amos-bHLH(^{SC}) chimera has been tested. In conclusion, important determinants of basiconica/trichodea specificity appear to be dispersed somewhat redundantly over both parts of the Amos protein.

4.15.4 What are the Amos specificity determinants?

Since the basic regions are virtually identical, this means that one or more of the few amino acids that are unique to the Amos HLH region are important for olfactory specification (fig. 4.26). Although DNA binding is mostly achieved through the basic region residues, it is possible that HLH region residues could modulate the DNA-binding properties of Amos relative to Ato. However it seems more likely that the unique HLH residues of Amos function to contact other cofactor proteins that are important in olfactory specificity. To rationalise the somewhat dispersed nature of olfactory specificity, one could speculate that an olfactory cofactor may bind to Amos at a contact site that is spread across both the bHLH and non-bHLH parts of the protein (Fig. 4.27). Interestingly, an alignment of Amos orthologues reveals rather little conservation outside the bHLH domain, unlike that seen for Ato (Fig. 4.28). This may therefore be consistent with the less important requirement for the non-bHLH region of Amos.

4.15.5 A difference between sensilla basiconica and trichodea

Another interesting observation is that there is a difference in the rescue of the two classes of Amos-dependent olfactory sensillum. For instance, the Ato-bHLH$^{(AMOS)}$ chimera works as well as Amos in rescuing sensilla basiconica, but not as well in rescuing sensilla trichodea. One relatively trivial explanation for this might be that the chimeric proteins are less stable than Amos itself. It is thought that sensilla trichodea are normally specified late compared with basiconica (zur Lage et al., 2003). It may be that by the time olfactory cells are competent to become trichodea rather than basiconica, the burst of protein produced by misexpression may have decayed.

Another possibility has to do with the mechanism by which this fate decision is made. Clearly, Amos alone does not decide basiconica versus trichodea fate. Instead, this decision seems to be at least partly under the control of the Runt-domain transcription factor encoded by *lozenge*

(Jhaveri and Rodrigues, 2002; Stocker et al., 1993). Indeed, it has been speculated that Lozenge and Amos proteins may collaborate as a protein complex in this fate decision (Goulding et al., 2000). Therefore, a lower ability for the chimeric proteins to specify sensilla trichodea might represent a lesser ability to interact with the Lozenge protein.

4.15.6 Significance of ability to make ectopic olfactory organs

Other aspects of my data are apparently in contradiction to the general conclusion that olfactory specificity is dispersed through the Amos protein. In a different assay, I tested the production of ectopic olfactory sensilla in a wildtype background. Both chimeras could perform this function well, and so resembled Amos rather than Ato. This appears completely consistent with the rescue results. However, I went on to show that for both chimeras, the ability to promote ectopic olfactory sensilla was largely dependent on the function of the endogenous Amos gene. This, clearly is not consistent with the rescue experiments, in which the chimeras could bypass the need for endogenous Amos. A potential explanation comes from my suggestion (Chapter 3) that it is more 'challenging' for any proneural protein to force the production of ectopic olfactory sensilla than it is to direct formation of these sensilla on the third antennal segment. I suggested that this is because of the apparent strong need for cofactors that are restricted largely to the third antennal segment.

I think the key to this is that it is important not to confuse the ability to promote ectopic olfactory sensilla with the ability to rescue olfactory sensillum formation in the proneural mutants. *A priori*, my inclination would be that the most informative results are those obtained from rescue of the *amos* mutant phenotype, since this is a measure of replacement of wild type function rather than of an ectopic (and potentially artefactual) capability. Therefore, I would put less weight on the latter findings as it is not clear how ectopic olfactory sensillum formation is related to the wildtype

function of these proteins. Overall, this reinforces the usefulness of rescue experiments in preference to misexpression assays.

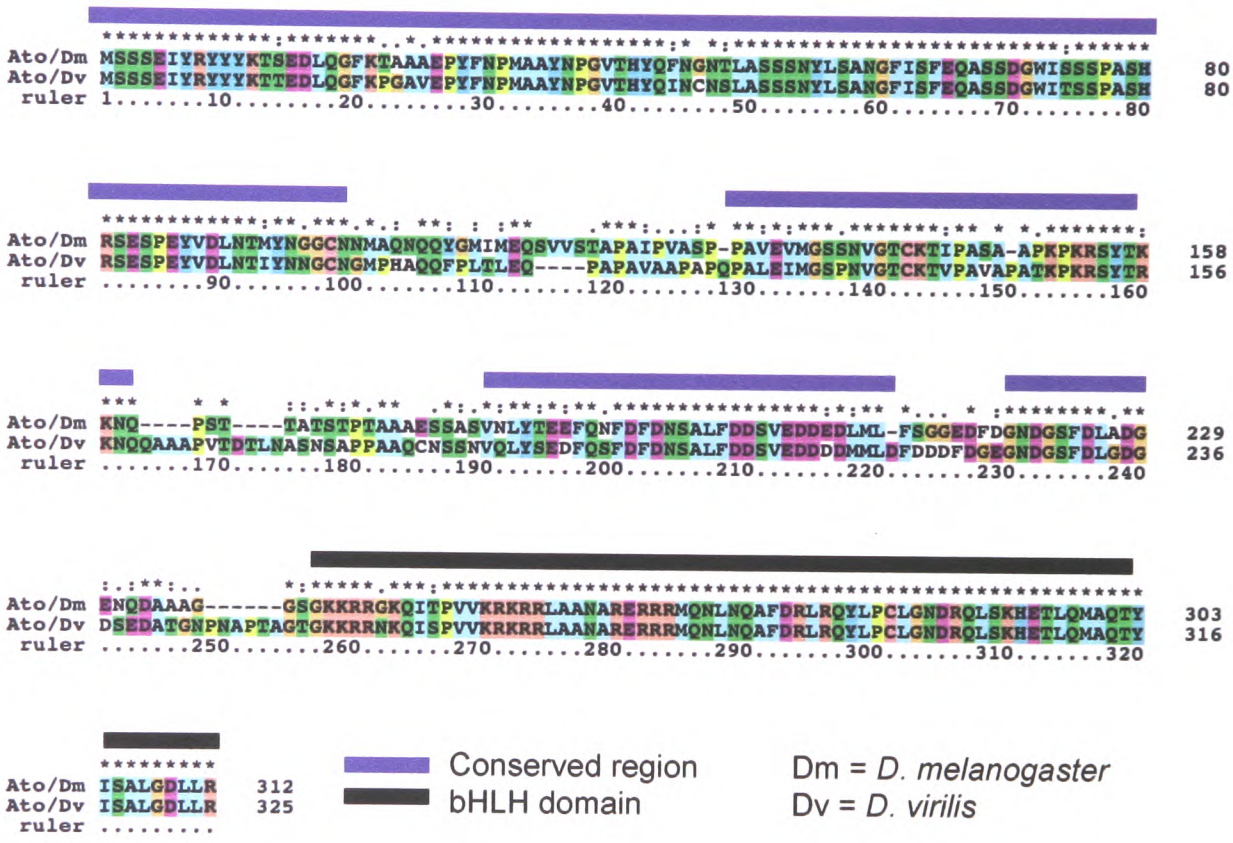

Figure 4.24 Sequence alignment of Ato orthologues

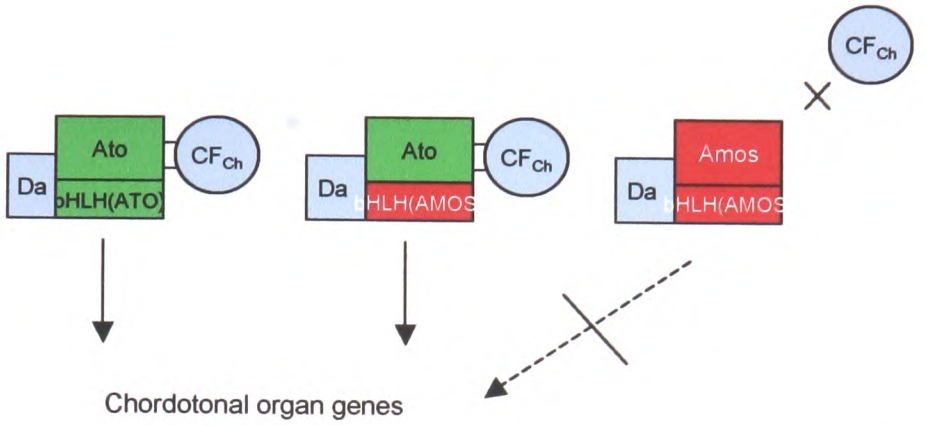

Figure. 4.25 Possible mechanisms to explain the chordotonal specificity of chimeric proneural proteins. The non-bHLH portion of Ato but not Amos is able to bind an essential chordotonal cofactor protein (CF_{Ch}). This works in combination with any Ato-like bHLH domain to activate chordotonal organ target genes.

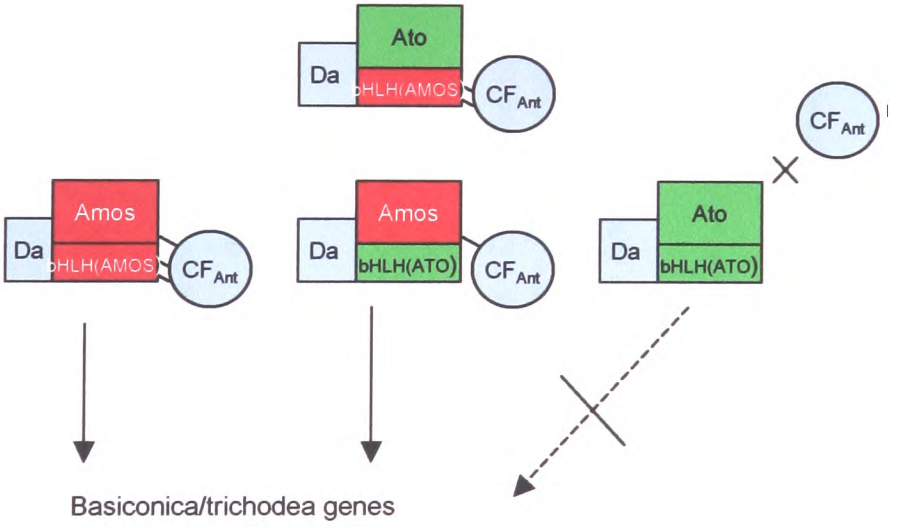

Figure. 4.27 Possible mechanisms to explain the basiconica/trichodea specificity of chimeric proneural proteins. The both portions of Amos but not Ato are able to bind an essential antennal cofactor protein (CF_{Ant}).

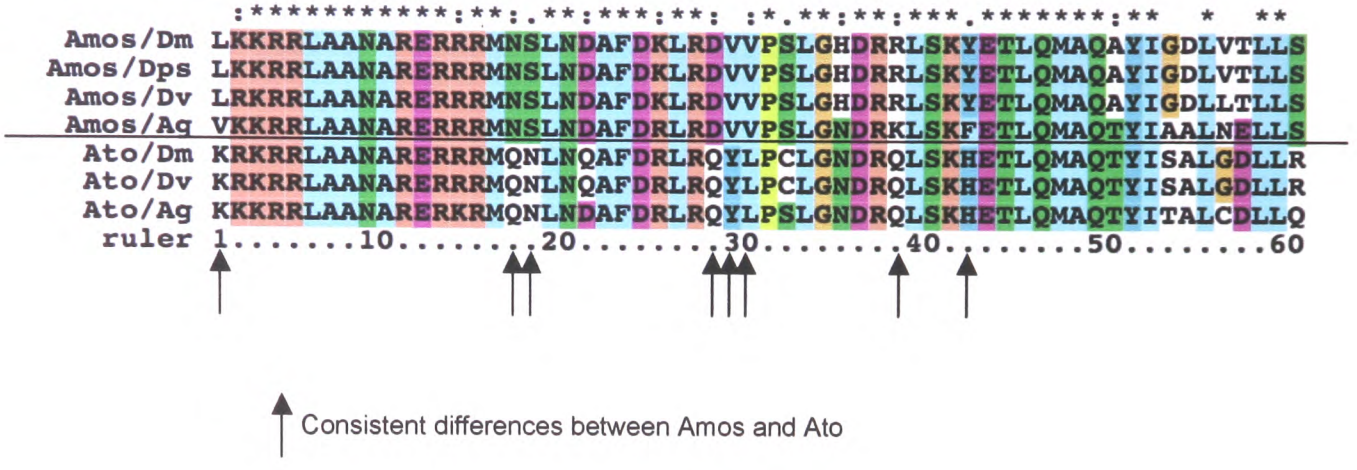

Dm = *D. melanogaster*
Dps = *D. pseudoobscura*
Dv = *D. virilis*
Ag = *Anopheles gambiae*

Figure 4.26 Sequence alignment of Ato and Amos bHLH domains. Arrows indicate significant and consistent differences between Ato and Amos. These differences are therefore implicated in the functional differences between the bHLH domains.

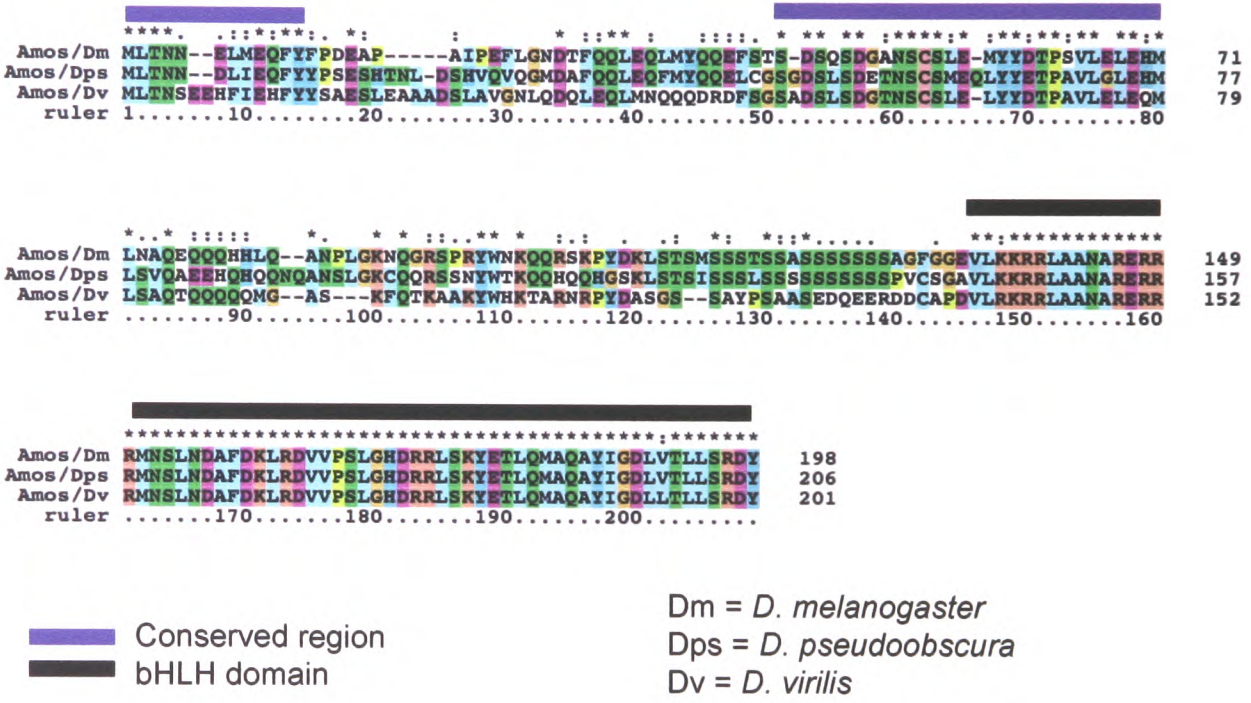

Figure 4.28 Sequence alignment of Amos orthologues

Chapter 5

Structural analysis of the functional specificity of Amos and Scute

5.1 Introduction

In all published chimeric studies of bHLH proteins, the bHLH domain itself has been found to be the determinant of functional specificity. This includes a report concerning the specificity of Ato with respect to Sc (Chien et al., 1996). In particular, the basic region of Ato was found to contain much of the information needed for functional specificity of Ato with respect to Sc. In the previous chapter I showed that the non-bHLH regions of Ato and Amos may be involved in the specification of *ato*-specific chordotonal/coeloconica and *amos*-specific olfactory organs respectively. How do these findings fit together? I suggested that bHLH domains of Amos and Ato may be close enough to be able to substitute for each other in the Ato-Amos chimeras, thereby allowing the non-bHLH portions to function correctly. The Sc bHLH domain may therefore be too divergent to allow this. If so, then I would predict that Sc-Amos chimeras would reveal the importance of an Ato-like bHLH domain for Amos function. In other words, like Ato, the specificity of Amos relative to Sc will appear to map to its bHLH domain. Therefore, in this chapter I investigate the functional specificity of Amos with respect to Sc. Does Amos' functional specificity reside in its bHLH domain (as would be inferred from (Chien et al., 1996) or can its non-bHLH region function in collaboration with the Sc bHLH domain (as I showed it can with the Ato bHLH domain)?

5.2 Construction of Sc-Amos chimeras and transformant lines

The construction of the Sc-bHLH$^{(AMOS)}$ and Amos-bHLH$^{(SCUTE)}$ chimeras are described in section 4.6 of Chapter 4.

5.3 External sense organ phenotypes

5.3.1 Misexpression of Amos-bHLH$^{(SCUTE)}$ leads to the induction of extra macrochaetae on the mesothorax

Sc and Amos proteins are abundantly distinguishable by the effects of their misexpression on thoracic macrochaetae. As in previous studies (Chien et al., 1996; Jarman and Ahmed, 1998), *UAS-Sc* misexpression at 29°C results in the formation of extra macrochaetae on the notum and scutellum (9.63±1.68 and 16.5±5.37 respectively). In contrast, as I reported in Chapter 3, both *UAS-amos#9* and *UAS-amos#3* inhibit macrochaetae on the notum and scutellum (Fig.5.1). Therefore this is a clear assay for examining the Sc-Amos chimeras.

I assayed the number of macrochaetae formed on the notum and scutellum by misexpression of the transformant lines with *Gal4$^{109\text{-}(2)68}$* at 29°C. I found that misexpression of the Amos-bHLH$^{(SCUTE)}$ chimera also resulted in increased numbers of macrochataetae on the notum and scutellum. I selected 6 lines of this chimera for detailed study: *4.11*, *4.21*, *4.16*, *3.8*, *3.11* and *4.8*. Although all of these lines produced extra macrochaetae, the quantity was different for each line, representing a range from the weakest line *UAS Amos-bHLH $^{(SCUTE)}$ 4.11* (notum, 4.33±0.5; scutellum, 6.5±1.94) to the strongest line *UAS Amos-bHLH $^{(SCUTE)}$ 4.8* (notum, 5.84±1.86; scutellum, 12.6±1.89) (Fig.5.1). Thus the bHLH of Sc in context of Amos is sufficient to make this chimera behave like Sc rather than Amos in the thoracic bristle assay. The efficiency of bristle formation, however, appears somewhat lower.

5.3.2 Misexpression of Sc-bHLH$^{(AMOS)}$ does not inhibit the macrochaetae of the mesothorax

Given that the bHLH domain of Scute in the context of Amos [Amos-bHLH$^{(SCUTE)}$] induces extra macrochaete on the scutellum, one might expect the converse to be true; the inhibition of thoracic macrochaetae by Sc-bHLH$^{(AMOS)}$ (like misexpression of Amos). However, I found that none of the *UAS Sc-bHLH$^{(AMOS)}$* lines could inhibit the wildtype number of thoracic

macrochaetae (although they could produce other phenotypes as shown below). In fact, I found that the numbers of thoracic macrochaetae were slightly increased compared to wildtype (Fig.5.1). The 6 lines I chose for further investigation also displayed mislocalised macrochaetae (Fig.5.3); *UAS Sc-bHLH$^{(AMOS)}$ 18.1.1*, *18.1.2*, *18.1.3*, *18.1.4*, *18.1.5* and *18.1.6*. Thus the bHLH domain of Amos in context of Scute is insufficient to inhibit macrochaetae.

Although the Sc-bHLH$^{(AMOS)}$ chimera contains an Ato-like bHLH domain, the position of this domain with respect to the rest of the protein is quite different from both Amos and Ato. For both Amos and Ato, the bHLH domain is located towards the carboxy terminus of the protein, whereas in the Sc-bHLH$^{(AMOS)}$ chimera the bHLH domain is located in the centre of the protein. It is possible that regions surrounding the bHLH domain in the Sc-bHLH$^{(AMOS)}$ chimera alter the folding of the protein, thus masking putative contact sites in the Amos bHLH domain required for inhibiting macrochaetae.

5.3.3 Misexpression of Scute and Amos-bHLH$^{(SCUTE)}$ lead to the induction of ectopic microchaetae on the scutellum

In addition to macrochaetae formation, I noted that misexpression of *UAS-Sc* produced 7.5±4.95 microchaetae on the scutellum. I found that all six *UAS Amos-bHLH $^{(SCUTE)}$* lines also produced ectopic microchaetae, ranging from the weakest line *UAS Amos-bHLH $^{(SCUTE)}$ 4.11* (7.5±4.95) to the strongest line *UAS Amos-bHLH$^{(SCUTE)}$ 4.8* (25.8±5.17) (Fig.5.2). Interestingly the latter line and *UAS Amos-bHLH$^{(SCUTE)}$ 3.11* (20.3±7.59) induced more microchaetae than *UAS-scute*, even though these lines failed to produce as many extra macrochaetae as *UAS-scute*. This suggests that the Amos-bHLH$^{(SCUTE)}$ chimera is biased towards producing microchaetae rather than macrochaetae. There are two possible explanations for this. Firstly the chimeric proteins may not be as efficient at inducing macrochaetae as Scute, subsequently inducing microchaetae as a default ES organ, or there may be a real preference for this chimera to produce microchaetae over macrochaetae.

Misexpression of *UAS-amos#9* and *UAS-amos#3* do not induce microchaetae on the scutellum. Similarly, none of the *UAS Sc-bHLH* $^{(AMOS)}$ lines could do so. In summary, the information required to produce ES organs of the microchaetae type is contained within the bHLH domain of Scute.

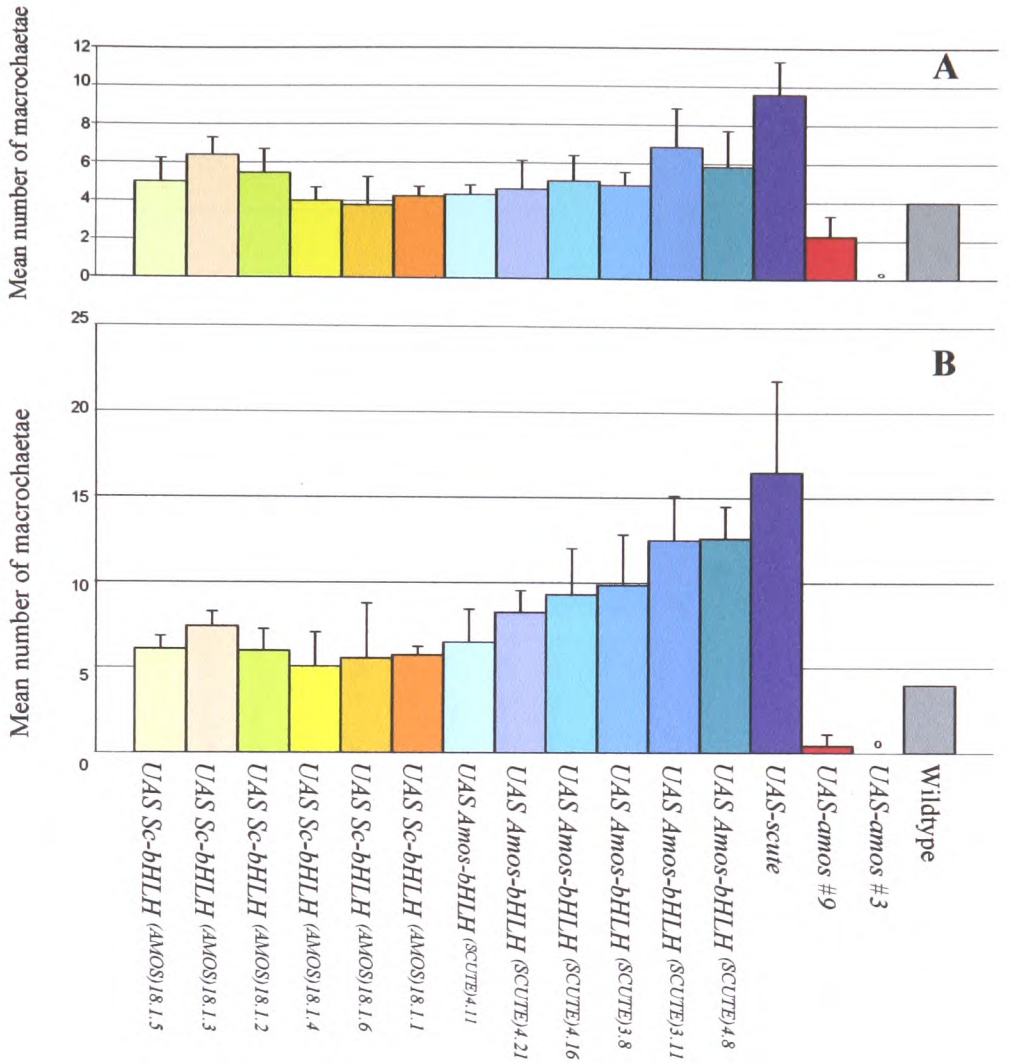

Figure 5.1 Number of macrochaetae on the mesothorax. Macrochaetae on notum **(A)** and scutellum **(B)** at 29°C. Misexpression of *UAS-amos#9* and *UAS-amos#3* inhibit the wildtype macrochaetae on the notum and scutellum. Misexpression of *UAS-scute* has the opposite phenotype leading to the induction of extra macrochaetae on the notum and scutellum. The ability of Scute to induce extra macrochaetae is impaired by replacement of its bHLH domain with that of Amos [Sc-bHLH$^{(AMOS)}$]. However the bHLH domain of Amos is not sufficient to inhibit macrochaetae in the context of the Scute protein [Sc-bHLH$^{(AMOS)}$]. Replacement of the Amos bHLH with that of Scute [Amos-bHLH$^{(SCUTE)}$], abolishes the ability of the Amos protein to inhibit macrochaetae, instead this chimera behaves more like Scute inducing the formation of extra macrochaetae.

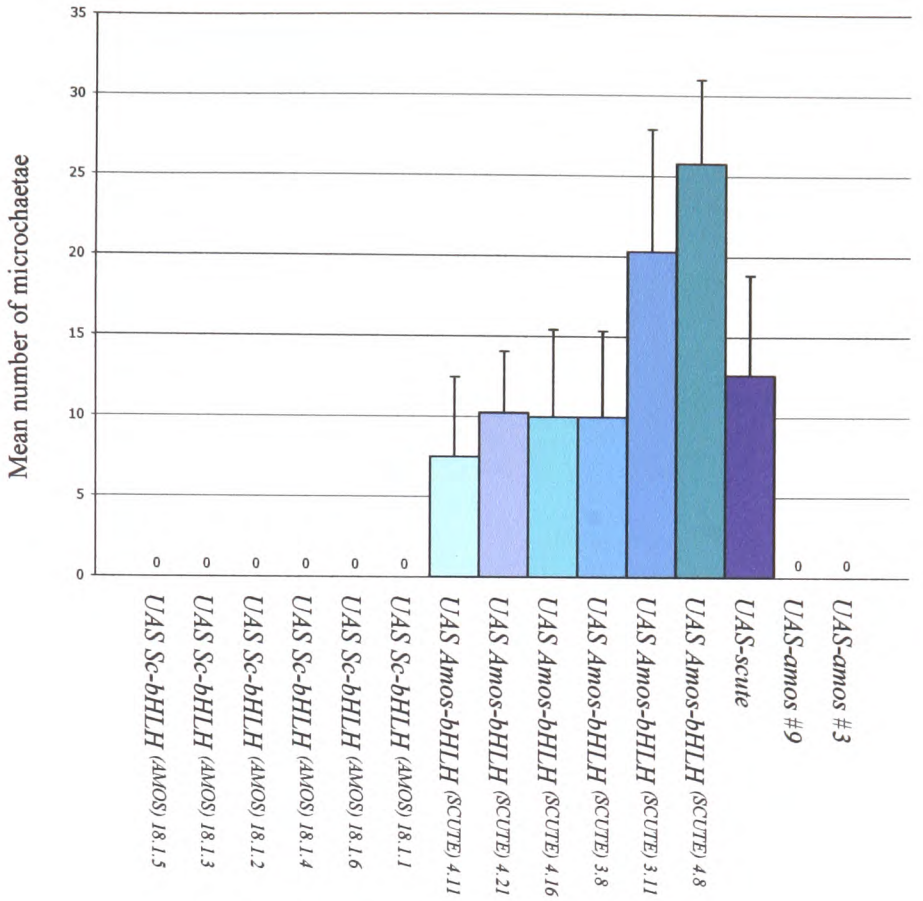

Figure 5.2 Ectopic microchaetae on scutellum at 29°C. Misexpression of *UAS-scute* leads to the induction of ectopic microchaetae on the scutellum. Misexpression of *UAS-amos* cannot induce ectopic microchaetae. Misexpression of the *UAS Amos-bHLH*$^{(SCUTE)}$ lines can induce the formation of ectopic microchaetae, like Scute. The *UAS Sc-bHLH*$^{(AMOS)}$ lines however cannot induce microchaetae. This suggests that the ability to induce ectopic microchaetae is contained within the bHLH region of Scute.

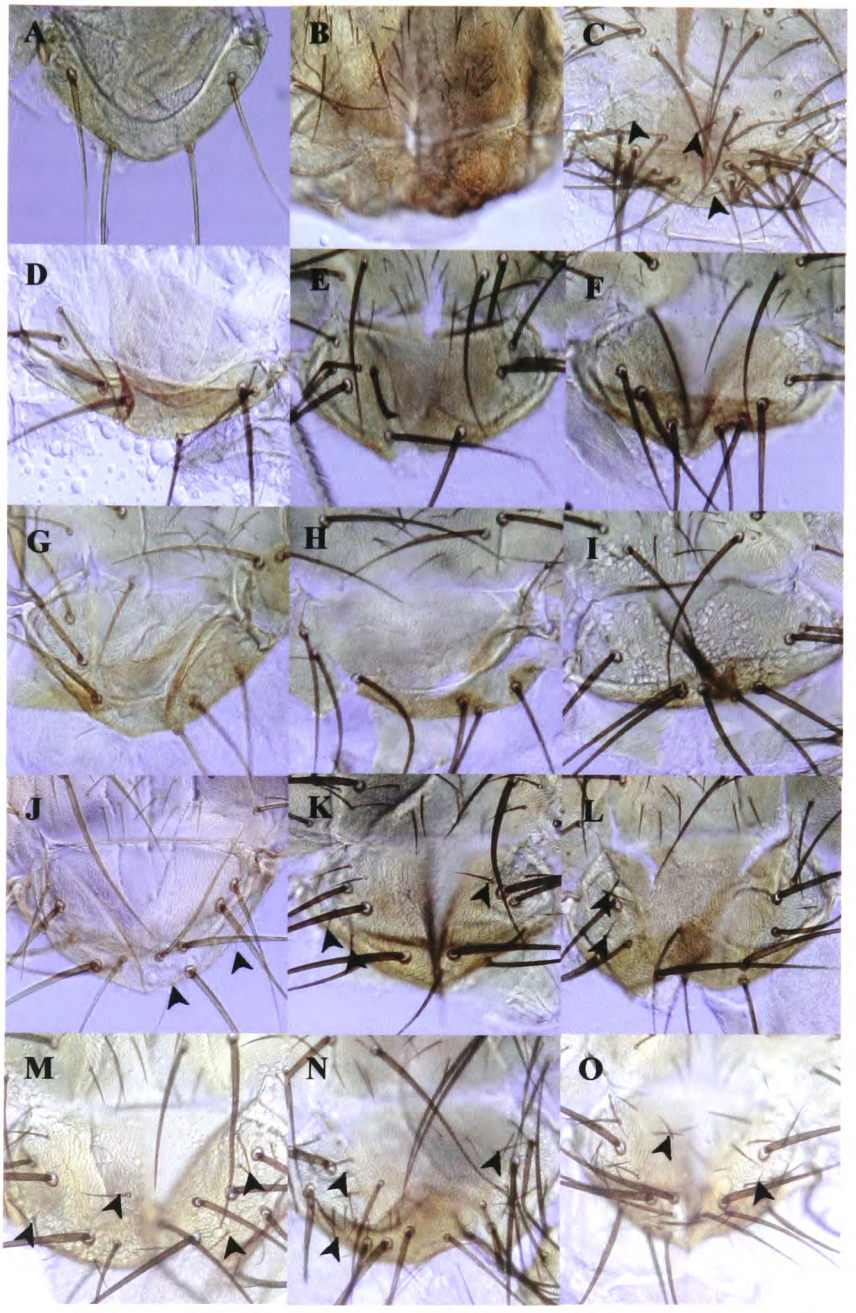

Figure 5.3 External sense organ phenotype on scutellum produced by misexpression at 29°C. Ectopic microchaetae (arrows) are induced by *UAS-scute* and *UAS Amos-bHLH*$^{(SCUTE)}$ chimeric lines with *Gal4*$^{109\text{-}(2)68}$.

Figure 5.3 External sense organ phenotype on scutellum produced by misexpression at 29°C

(A) Wildtype. **(B)** *UAS-amos#3*. **(C)** *UAS-scute*. **(D)** *UAS Sc-bHLH$^{(AMOS)\ 18.1.5}$*. **(E)** *UAS Sc-bHLH$^{(AMOS)\ 18.1.3}$*. **(F)** *UAS Sc-bHLH$^{(AMOS)\ 18.1.2}$*. **(G)** *UAS Sc-bHLH$^{(AMOS)\ 18.1.4}$*. **(H)** *UAS Sc-bHLH$^{(AMOS)\ 18.1.6}$*. **(I)** *UAS Sc-bHLH$^{(AMOS)\ 18.1.1}$*. **(J)** *UAS Amos-bHLH$^{(SCUTE)\ 4.11}$*. **(K)** *UAS Amos-bHLH$^{(SCUTE)\ 4.21}$*. **(L)** *UAS Amos-bHLH$^{(SCUTE)\ 4.16}$*. **(M)** *UAS Amos-bHLH$^{(SCUTE)\ 3.8}$*. **(N)** *UAS Amos-bHLH$^{(SCUTE)\ 3.11}$*. **(O)** *UAS Amos-bHLH$^{(SCUTE)\ 4.8}$*.

5.4 External sense organs on the wing

The wing is another location where misexpression phenotypes of Sc can be observed. Heatshock induction of *UAS-Sc* produces ectopic external sense organs all over the wing (Chien et al., 1996). I chose this location to assess the misexpression phenotype of my chimeras. I misexpressed *UAS-scute*, *UAS-amos* and the selected lines of the Sc-bHLH$^{(AMOS)}$ and Amos-bHLH$^{(SCUTE)}$ chimeras with *Gal4$^{109\text{-}(2)68}$* at 29°C and assayed for ectopic ES organs along the 3rd wing vein. This is the region most affected by the Gal4 driver used. I assayed ectopic bristles and sensilla campaniformia. Misexpression of *UAS-amos#3* induces very strong protein expression, which interferes with the full inflation of the wings after eclosure. Therefore it was not possible to assay the wings of *UAS-amos#3* flies at 29°C. Thus the misexpression of *amos* in the wing assays is represented by *UAS-amos#9* at 29°C and *UAS-amos#3* at 18°C.

5.4.1 induction of bristles on the wing

Misexpression of *UAS-scute* produces significant numbers of ectopic bristles along the third wing vein (14.1±4.61). *UAS-amos#9* and *UAS-amos#3* could also induce ectopic bristles but to a lesser degree (3.0±1.73 and 2.83±1.6 respectively) (Fig.5.4). Thus there seems to be a quantitative difference between Scute and Amos in this assay. This assay however could not distinguish between the two chimeras Sc-bHLH$^{(AMOS)}$ and Amos-bHLH$^{(SCUTE)}$. All lines of the two chimeras could produce more ectopic bristles than *UAS-amos#9* and *UAS-amos#3* but less than *UAS-scute*. The strongest chimeric lines in this assay are *UAS Sc-bHLH $^{(AMOS)}$ 18.1.2* (10.4±2.96) and *UAS Amos-bHLH $^{(SCUTE)}$ 3.11* (12.4±3.06) but there was no statistical difference between them (t-test P=0.046).

Although this assay could not differentiate between the two chimeras, there appeared to be differences if the whole wing is considered (Fig.5.9). *UAS-amos#9*, *UAS-amos#3* and *UAS Sc-bHLH$^{(AMOS)}$* lines can only induce ectopic bristles along the wing veins but not elsewhere. In contrast the Amos-bHLH$^{(SCUTE)}$ chimera. like Scute. can induce ectopic bristles all over the

wing. This suggests that Amos and the Sc-bHLH$^{(AMOS)}$ chimera can only induce ectopic bristles (aberrantly) in the context of the wing veins. Thus if the whole wing is examined, the Sc-bHLH$^{(AMOS)}$ chimera behaves like Amos rather than Scute, but the Amos-bHLH$^{(SCUTE)}$ chimera behaves like Scute. Therefore, again the bHLH domain of Scute contains the information required for the specification of ectopic bristles.

5.4.2 Misexpression of Scute and Amos-bHLH$^{(SCUTE)}$ induce excess sensilla campaniformia along the third wing vein

There are five wildtype sensilla campaniformia distributed along the distal third wing vein. These modified external sense organs detect cuticular strain during flight. Sensilla campaniformia arise from external sense organ SOPs, which are initiated by *scute* expression. Misexpression of *UAS-scute* produces excess sensilla campaniformia along the third wing vein (17±3.85) (Fig.5.5). Misexpression of *UAS-amos#9* produced a small but insignificant decrease in sensilla campaniformia compared to wildtype (3.83±1.38) (Fig.5.5). However misexpression of *UAS-amos#3*, even at 18°C lead to a small but significant reduction in campaniformia number compared to wildtype (2.5±0.548) (Fig.5.5). It could be that the campaniformia of *amos* misexpressing flies may be diverted to other sense organ subtypes such as chordotonal organs or olfactory like sensilla.

I found that all the *UAS Amos-bHLH $^{(SCUTE)}$* lines could induce equivalent or more campaniformia than *UAS-scute*. The weakest *UAS Amos-bHLH $^{(SCUTE)}$* line *4.11* (16.3±7.63) produced significantly more sensilla campaniformia than *UAS-amos#9* (t-test 2.1×10^{-3}), in numbers that were not significantly different to *UAS-scute* (t-test 0.637) (Fig.5.5). This suggests that the Amos-bHLH$^{(SCUTE)}$ chimera behaves more like Scute than Amos in this assay.

The *UAS Sc-bHLH $^{(AMOS)}$* lines produced slightly higher numbers of sensilla campaniformia to wildtype, however this was much less than *UAS-scute*. The *UAS Sc-bHLH $^{(AMOS)}$* line that

induced the highest number of campaniformia was *18.1.1* (8.75±3.06) (Fig.5.5). However, this was significantly less than *UAS-scute* (t-test $3.6x10^{-4}$). This suggests that this chimera cannot behave like Scute in this assay.

5.5 External sense organs on the antenna

The third antennal segment (funiculus) houses olfactory sensilla. No wildtype external sense organs are formed in this area. *scute* expression is not normally seen in the funiculus. However there is some evidence to suggest that *achaete/scute* must be inhibited by *amos* for the specification of olfactory sensilla (zur Lage et al., 2003), as ectopic bristles are observed in an *amos* null mutant.

Misexpression of *UAS-scute* produces ectopic bristles on the funiculus (26.4±7.29) (Fig.5.6 and 5.7). Ectopic bristles are not formed by the misexpression of *UAS-amos#9* or *UAS-amos#3* (Fig.5.6). Misexpression of all *UAS Amos-bHLH* $^{(SCUTE)}$ lines also produced ectopic bristles on the funiculus (Fig.5.7). Thus the Amos-bHLH$^{(SCUTE)}$ chimera behaves like Scute but not Amos in this assay. The strongest *UAS Amos-bHLH* $^{(SCUTE)}$ line was *4.8* and the weakest line was *4.11*. These lines produced 21±3.71 and 10.4±1.38 ectopic bristles respectively (Fig.5.6). Therefore they appeared to be slightly weaker than Scute itself.

In contrast none of the *UAS Sc-bHLH* $^{(AMOS)}$ lines could produce ectopic bristles. This suggests that the information required to produce ectopic bristles on the funiculus is contained within the bHLH domain of Scute.

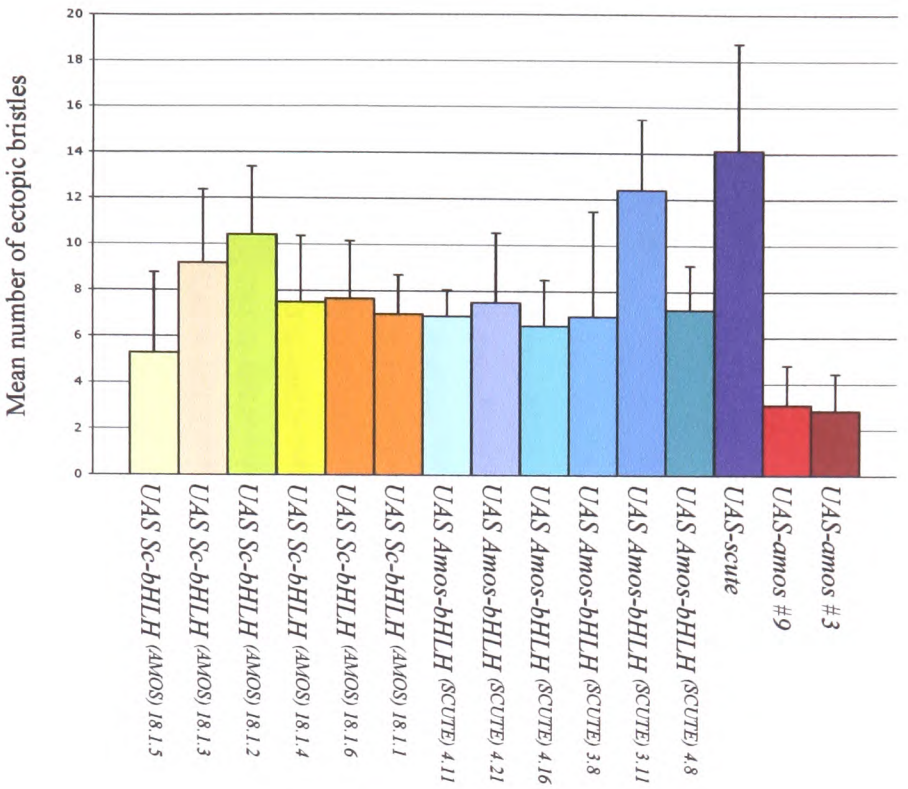

Figure 5.4 Ectopic bristles along the third wing vein at 29°C. Misexpression of *UAS-amos* or *UAS-scute* leads to the induction of ectopic bristles along the third wing vein. However there is a quantitative difference between the *amos* lines and *scute*, the latter being abundantly more efficient at producing bristles. Both *UAS Amos-bHLH* $^{(SCUTE)}$ and *UAS Sc-bHLH* $^{(AMOS)}$ chimeric lines also induce ectopic bristles, however there seems to be little difference between the chimeras. But Amos-bHLH$^{(SCUTE)}$ produces ectopic bristle in the intervein regions, but the bristles formed by Sc-bHLH$^{(AMOS)}$ are confined to the wing veins (see Fig.5.9).

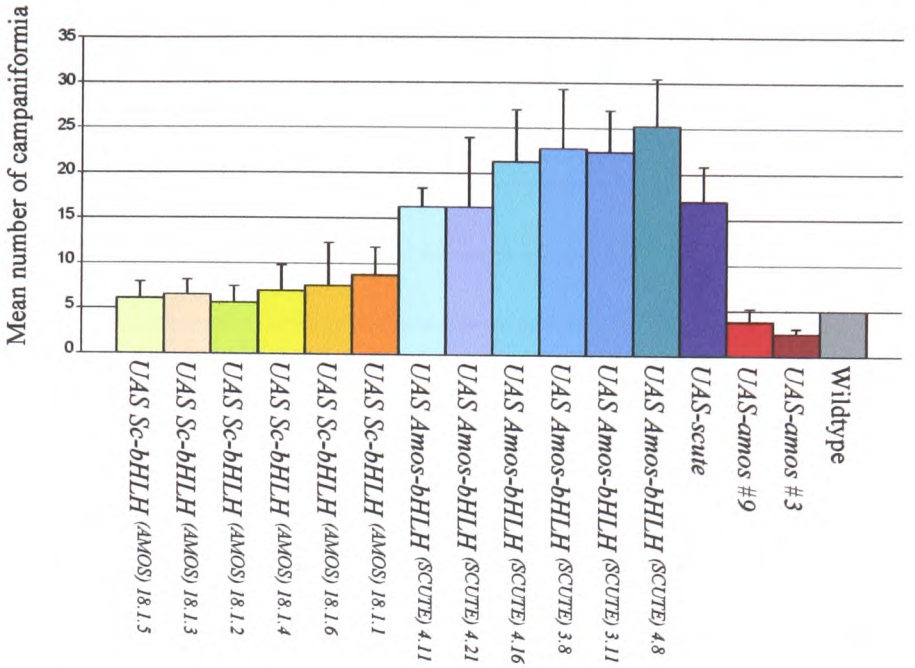

Figure 5.5 Number of Sensilla Campaniformia along third wing vein at 29°C. There are 5 wildtype sensilla campaniformia distributed along the third wing vein. These organs arise from the external sense organ lineage. Misexpression of *UAS-scute* leads to a significant increase in the number of campaniformia (17±3.85). Misexpression of *UAS-amos#9* results in a small decrease in the number of campaniformia compared to wildtype (3.83±1.38 c.f. 5). However misexpression of *UAS-amos#3* at 18°C produces a more significant reduction in the numbers of campaniformia (2.5±0.548). Misexpression of the Sc-bHLH$^{(AMOS)}$ chimera showed a small increase in the number of campaniformia. But misexpression of the Amos-bHLH$^{(SCUTE)}$ chimera increased the number of campaniformia to the same degree as *UAS-scute*.

The Amos-bHLH$^{(SCUTE)}$ chimera which induced the lowest number of campaniformia 4.21 (16.3±7.63) is significantly different from *UAS-amos#9* (t-tests 2.1×10^{-3}) but is not significantly different from *UAS-scute* (t-test 0.637). This suggests that the Amos-bHLH$^{(SCUTE)}$ chimera behaves more like Scute than Amos in this assay. The Sc-bHLH$^{(AMOS)}$ chimera which induced the highest number of campaniformia (18.1.1 8.75±3.06) was still significantly different from *UAS-scute* (t-test 3.6×10^{-4}) suggesting that this chimera cannot behave like Scute in this assay.

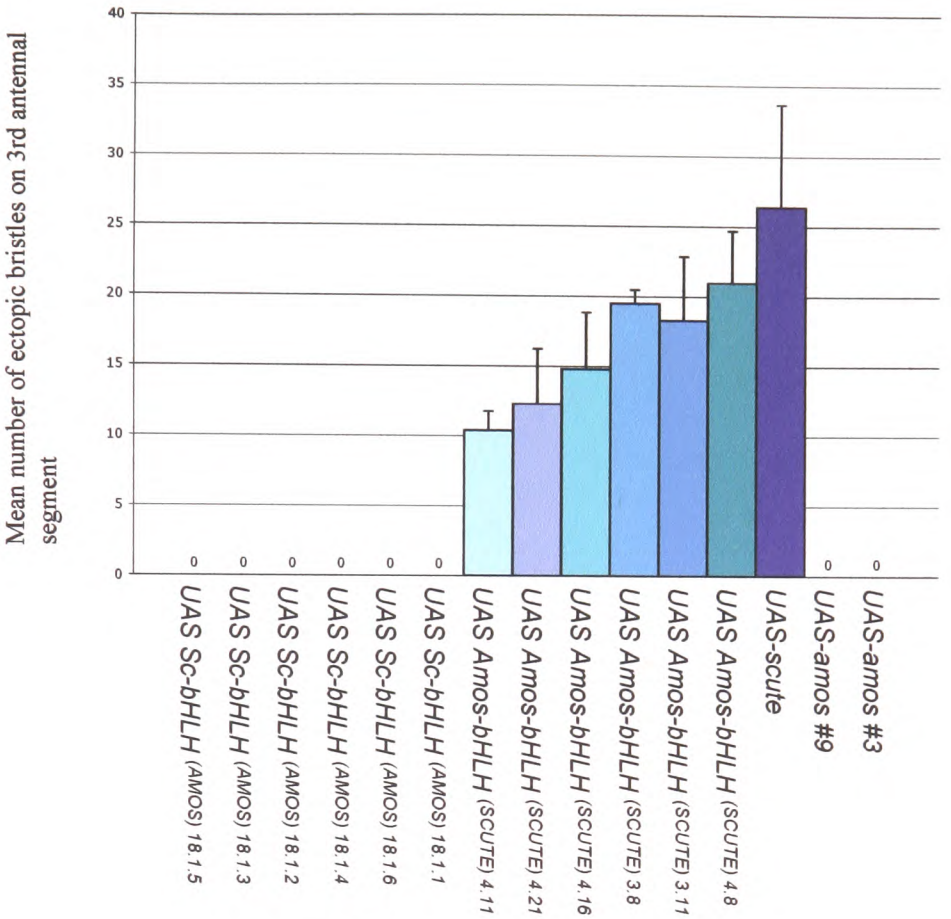

Figure 5.6 Misexpression induces ectopic bristles on the third antennal segment at 29°C. Misexpression of neither *UAS-amos* nor the Sc-bHLH$^{(AMOS)}$ chimera can induce ectopic bristles on the funiculus. However *UAS-scute* and all the *UAS Amos-bHLH$^{(SCUTE)}$* lines induced high numbers of bristles on the funiculus. Thus Amos-bHLH$^{(SCUTE)}$ has functional characteristics of Scute in this assay. This suggests that the bHLH domain of Scute is required and sufficient to induce the formation of ectopic bristles on the funiculus.

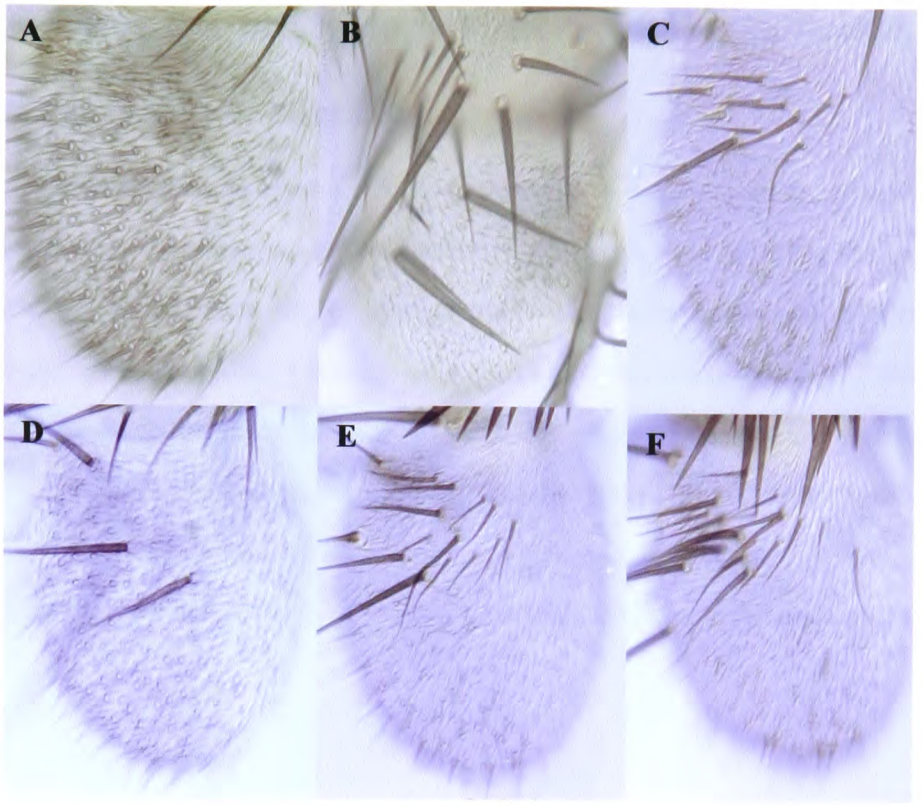

Figure 5.7 Ectopic bristles are induced on the funiculus by misexpression of *UAS-scute* and Amos-bHLH$^{(SCUTE)}$ chimeras at 29°C

(A) Wildtype. **(B)** *UAS-scute*. **(C)** *UAS Amos-bHLH$^{(SCUTE)\ 4.11}$*. **(D)** *UAS Amos-bHLH$^{(SCUTE)\ 4.16}$*. **(E)** *UAS Amos-bHLH$^{(SCUTE)\ 3.11}$*. **(F)** *UAS Amos-bHLH$^{(SCUTE)\ 4.8}$*.

5.6 Summary: the bHLH domain of Scute is sufficient for external sense organ specification

In all assays of external sense organ production, the ability to induce external sense organs correlated well with the presence of the Scute bHLH domain. This was true for ectopic microchaetae on the scutellum, ectopic bristles and excess sensilla campaniformia on the wing, and ectopic bristles on the funiculus. Misexpression of the Amos-bHLH$^{(SCUTE)}$ chimera can produce all of these phenotypes but the Scute-bHLH$^{(AMOS)}$ chimera cannot (see summary figure 5.13). This suggests that the external sense organ determinants are contained within the bHLH region of Scute and but not Amos. Conversely, without its bHLH domain, Scute loses the ability to induce Scute-specific external sense organ phenotypes.

5.7 Assaying Amos-like misexpression phenotypes

Misexpression of Amos produces a number of phenotypes that are distinguishable from Scute. Ectopic olfactory organs are formed on the second antennal segment and wing veins (Chapter 3). Moreover, misexpression of Amos also cross-activates endogenous *ato* to produce ectopic chordotonal organs (Chapter 3). In this section I assess the ability of Amos-bHLH$^{(SCUTE)}$ and Scute-bHLH$^{(AMOS)}$ chimeras to mimic these aspects of Amos misexpression.

5.7.1 Ectopic olfactory organs are formed along the third wing vein

Misexpression of *UAS-amos#9* at 29°C and *UAS-amos#3* at 18°C induces the formation of small numbers of olfactory-like sensilla along the third wing vein (1.67±0.98 and 3.6±0.816 respectively) (Fig.5.8). In contrast, *UAS-scute* did not produce any olfactory-like sensilla. Therefore there is a small but clear difference between Amos and Sc. All *UAS Sc-bHLH$^{(AMOS)}$* lines produced olfactory-like sensilla. Interestingly they were able to induce higher numbers of ectopic sensilla than UAS-*amos#9* itself. The weakest *UAS Sc-bHLH$^{(AMOS)}$* line (*18.1.5*) produced 1.76±1.39 olfactory like sensilla and the strongest *UAS Sc-bHLH $^{(AMOS)}$* line (*18.1.2*) produced 7.85±3.56 olfactory-like sensilla at 29°C (Fig.5.8).

Three out of the six *UAS Amos-bHLH$^{(SCUTE)}$* lines also induced the formation of olfactory-like sensilla (Fig.5.8). However the numbers induced were much lower than the *UAS Sc-bHLH$^{(AMOS)}$* lines. Furthermore the strongest *UAS Amos-bHLH$^{(SCUTE)}$* line (*4.8*) could only produce olfactory sensilla to the same degree as *UAS amos#9* (1.53±3.07 c.f. 1.67±0.98). This suggests that there is a quantitative difference between the two chimeras to induce olfactory-like sensilla. The bHLH domain of Amos is the foremost region required for this Amos-like function; however, the region of Amos outside the bHLH domain could also carry some residual Amos-specific function.

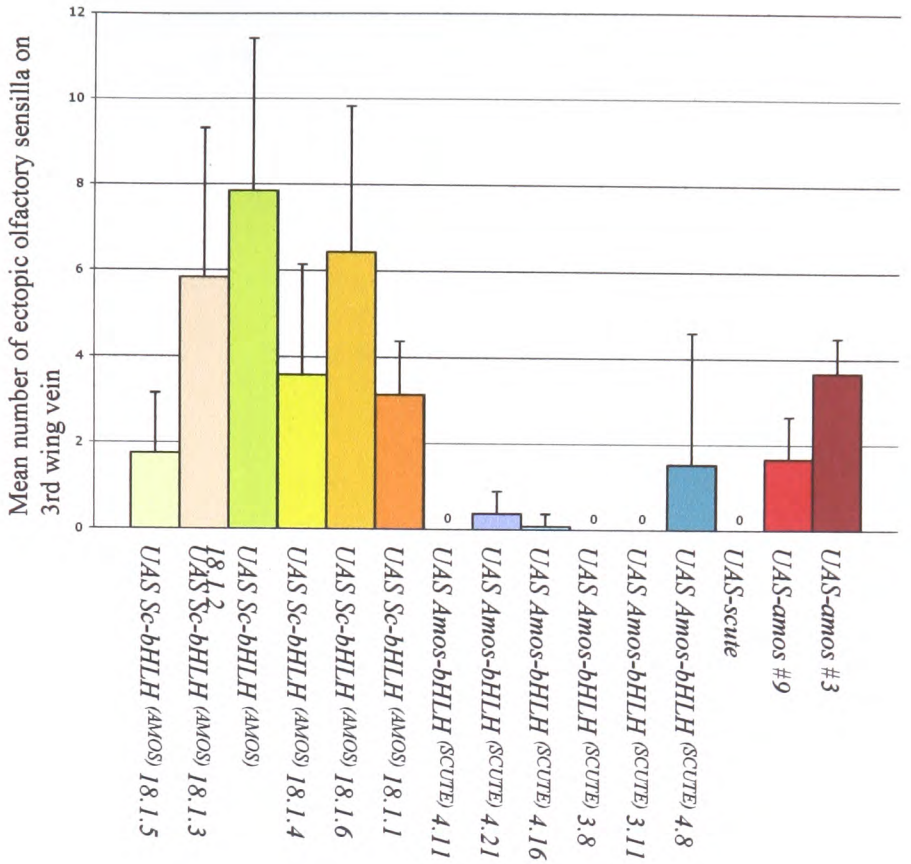

Figure 5.8 Ectopic olfactory-like sensilla along the third wing vein at 29°C. Misexpression of *UAS-amos#9 and UAS-amos#3* (18°C) causes the induction of ectopic olfactory-like sensilla along the third wing vein. Misexpression of *UAS-scute* cannot induce substantial numbers of ectopic olfactory sensilla. Both Amos-bHLH$^{(SCUTE)}$ and Sc-bHLH$^{(AMOS)}$ chimeras, to varying degrees, can behave like Amos in this assay. This figure suggests a quantitative difference between Amos-bHLH$^{(SCUTE)}$ and Sc-bHLH$^{(AMOS)}$ to induce ectopic olfactory sensilla. All of the Sc-bHLH$^{(AMOS)}$ lines tested could do this, however only 3/6 Amos-bHLH$^{(SCUTE)}$ lines were able induce olfactory-like sensilla, notably this was at a lower level than the Sc-bHLH$^{(AMOS)}$ lines. This suggests that the Amos bHLH domain is sufficient to confer Amos-like specificity to Scute, but as was suggested in chapter 4, the other parts of Amos also seem to carry minimal Amos-like functions.

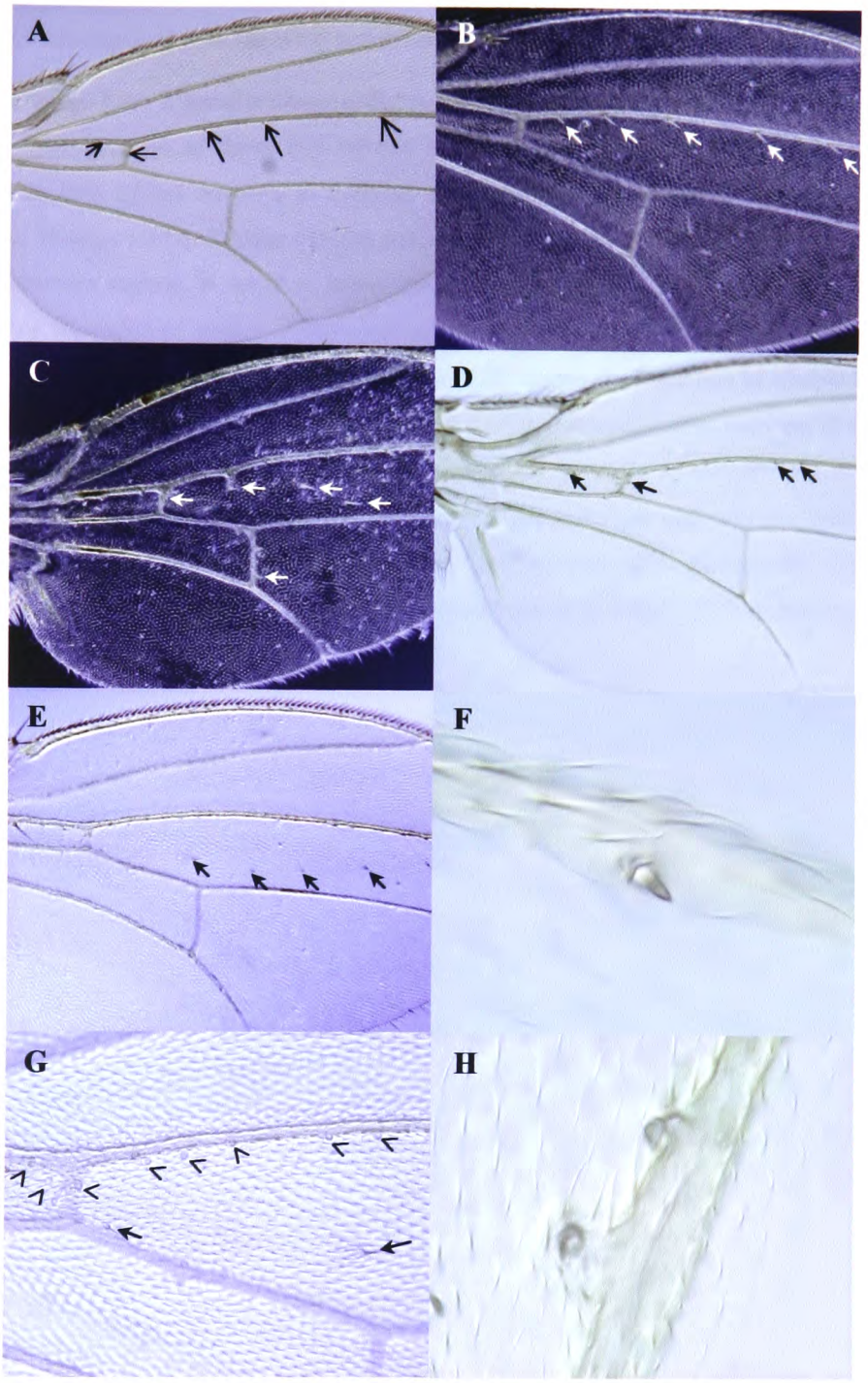

Figure 5.9 Misexpression in the wing produces sub-type specific sense organs at 29°C

(A) Wildtype. **(B)** *UAS-amos#9*. **(C)** *UAS-scute*. **(D, F and H)** *UAS SC-bHLH*$^{(AMOS)\ 18.1.1}$. **(E and G)** *UAS Amos-bHLH*$^{(SCUTE)\ 4.16}$.

Figure 5.9 Misexpression in the wing produces sub-type specific sense organs at 29°C

Wildtype wings have 5 sensilla campaniformia distributed along the third wing vein (**A**-open arrows). Misexpression of Scute (**C**) induces ectopic bristles along the third wing vein and intervein regions (filled arrows), in addition extra sensilla campaniformia are formed (not indicated). Misexpression of Amos (**B**) also induces ectopic bristles along the third wing vein but not the intervein regions, in addition Amos reduces the number of sensilla campaniformia and induces the formation of ectopic chordotonal organs and olfactory-like sensilla (not indicated). Misexpression of *UAS Amos-bHLH$^{(SCUTE)\ 4.16}$* (**E** and **G**) induce the formation of ectopic bristles along the wing veins but also the intervein regions, further more substantial numbers of sensilla campaniformia are induced (arrowheads). Misexpression of *UAS SC-bHLH$^{(AMOS)\ 18.1.1}$* (**D**) induces ectopic bristles only at the wing veins, but can induce ectopic olfactory like sensilla (**F**) and chordotonal organs (**G**) in the wing veins. Thus misexpression phenotypes of Amos-bHLH$^{(SCUTE)}$ resemble Scute and misexpression phenotypes of Sc-bHLH$^{(AMOS)}$ resemble Amos.

5.7.2 Ectopic olfactory organs are formed on the second antennal segment

Misexpression of *UAS-amos* produces ectopic olfactory organs on the second antennal segment. However there is a quantitative difference between the two *amos* lines. Misexpression of *UAS-amos#3* produced 12.3±4.33 olfactory organs, whilst misexpression of *UAS-amos#9* could only produce 1.25±1.42 olfactory organs. Unexpectedly, misexpression of *UAS-scute* could also induce olfactory organs (3.1±2.81) (Fig.5.10). Therefore this assay does not readily distinguish Amos from Scute (unlike Amos and Ato, Chapter 3).

Given this lack of distinguishing ability, it is not surprising that both chimeras can also induce ectopic olfactory organs (Fig.5.10 and 5.11). However, there was a quantitative difference between them. For the *UAS Amos-bHLH $^{(SCUTE)}$* lines, the highest number induced was by *4.8* (2±1.55). In contrast, the *UAS Sc-bHLH $^{(AMOS)}$* lines produced olfactory organs to a much higher degree than *UAS-scute* or the *UAS Amos-bHLH $^{(SCUTE)}$* lines. Two *UAS Sc-bHLH$^{(AMOS)}$* lines produced particularly high numbers of olfactory organs (*18.1.2*, 7.3±2.89; *18.1.6*, 8.29±5.04).

Thus both chimeras are capable of producing olfactory organs. However in the case of Amos-bHLH$^{(SCUTE)}$, this is only to minimal degree (like Scute), whilst the Sc-bHLH$^{(AMOS)}$ chimera could produce substantial numbers of olfactory organs (even more than *UAS-amos#9*).

5.7.3 Sc-bHLH$^{(AMOS)}$ produces ectopic chordotonal organs

Misexpression of *UAS-scute* cannot induce the formation of ectopic chordotonal organs (Jarman and Ahmed, 1998). Misexpression of *UAS-amos#9* and *UAS-amos#3* can induce the formation of ectopic chordotonal organs on the scutellum, due to the ability of Amos to cross-activate endogenous *ato* (Chapter 3). I investigated whether this ability was observed for either of the chimeras. Interestingly, the misexpression of Sc-bHLH$^{(AMOS)}$ but not Amos-

bHLH$^{(SCUTE)}$ can induce ectopic chordotonal organs (Fig.5.12). Two of the six Scute-bHLH$^{(AMOS)}$ lines produced slightly less numbers of chordotonal organs than *UAS-amos#9* (*18.1.5*, 23.4±6.99 and *18.1.3*, 28±9.27 c.f *amos#9*, 38.5±9.68). However the remaining four lines (*18.1.2*, 75.2±10.6; *18.1.4*, 83.8±4.19; *18.1.6*, 85.3±24.9; *18.1.1*, 93±15.6) produced more chordotonal organs than *UAS-amos#9* and even *UAS-ato#1* (52.7±17.8) (see chapter 3) This indicates that the bHLH region of Amos is sufficient to promote chordotonal organ formation, presumably due to its closeness to that of Ato.

5.8 Summary: the bHLH domain of Amos is sufficient for olfactory and chordotonal organ specification

In the olfactory organ assays, the ability to induce ectopic olfactory organs correlated well with the presence of the Amos bHLH domain. This was true for ectopic olfactory formation along the third wing vein, and to a large degree the ectopic olfactory organs on the second antennal segment. The latter was less clear than the assay in the wing. This is because Scute and some of the Amos-bHLH$^{(SCUTE)}$ chimeras did produce some olfactory like sensilla. However this was minimal, compared to the numbers induced by Amos and the Scute-bHLH$^{(AMOS)}$ chimera. The assay of ectopic chordotonal organs was even clearer, only Amos and the Scute-bHLH$^{(AMOS)}$ chimeras could specify chordotonal organs on the scutellum. This suggests that the Amos bHLH domain is important for the specification of chordotonal organs. In summary, these preliminary studies show that the bHLH domain of Amos is sufficient for Amos-like protein functions (see summary figure 5.13).

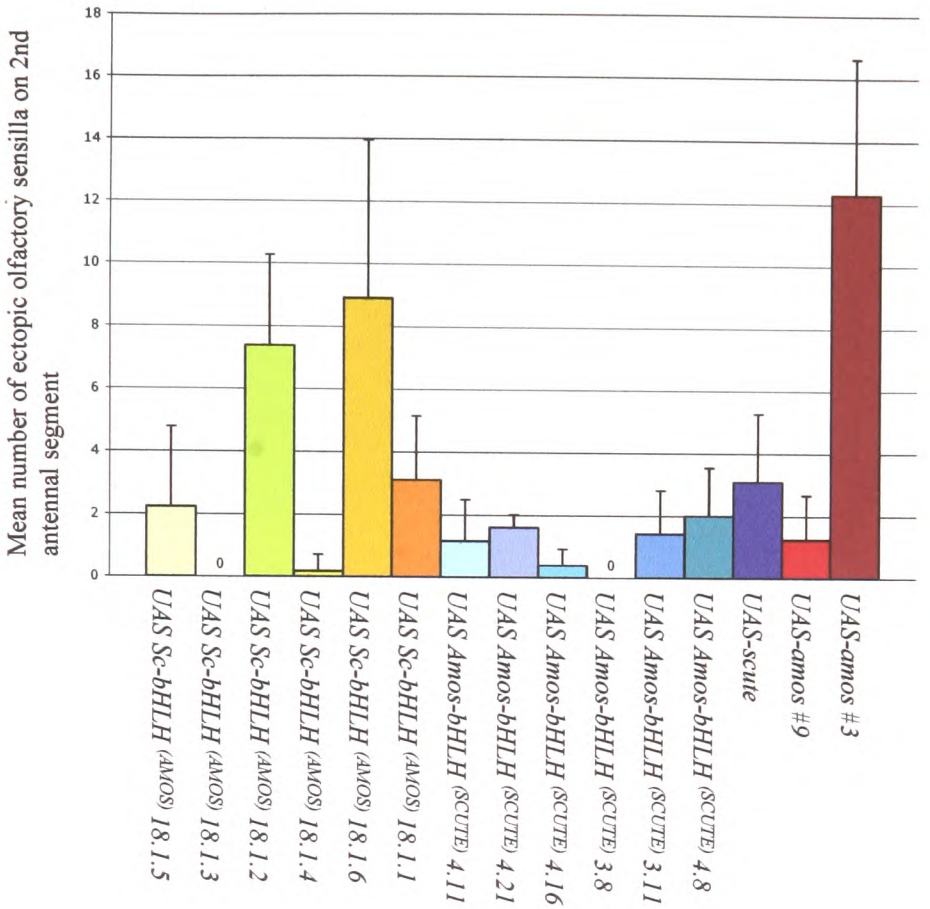

Figure 5.10 Ectopic olfactory-like sensilla on the second antennal segment at 29°C. Misexpression of *UAS-amos* and *UAS-scute* can induce the formation of ectopic olfactory-like sensilla on the second antennal segment. However *UAS-amos#3* is quantitatively much stronger than *UAS-scute* (12.3±4.33 c.f. 3.08±1.73). Misexpression of the Amos-bHLH$^{(SCUTE)}$ chimera also produces ectopic olfactory sensilla on the second antennal segment, however the olfactory sensilla produced are quantitatively similar or less than *UAS-scute*. The Sc-bHLH$^{(AMOS)}$ chimera can also produce ectopic olfactory sensilla. However the ability to do this was much stronger than *UAS-scute* and the Amos-bHLH$^{(SCUTE)}$ lines. This suggests that the bHLH domain of Amos allows this chimera to behave more like Amos than Scute.

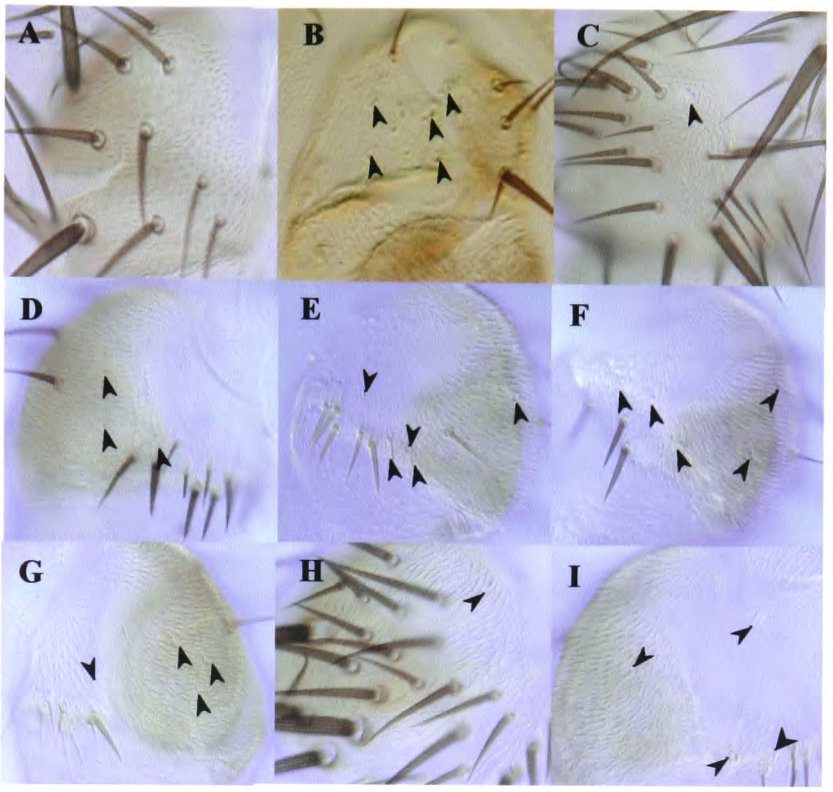

Figure 5.11 Ectopic olfactory organs are induced on second antennal segment by misexpression at 29°C

(A) Wildtype. **(B)** *UAS-amos#3*. **(C)** *UAS-scute*. **(D)** *UAS Sc-bHLH$^{(AMOS)\ 18.1.5}$*. **(E)** *UAS Sc-bHLH$^{(AMOS)\ 18.1.5}$*. **(F)** *UAS Sc-bHLH$^{(AMOS)\ 18.1.2}$*. **(G)** *UAS Sc-bHLH$^{(AMOS)\ 18.1.4}$*. **(H)** *UAS Sc-bHLH$^{(AMOS)\ 18.1.6}$*. **(I)** *UAS Sc-bHLH$^{(AMOS)\ 18.1.1}$*.

Substantial numbers of ectopic olfactory organs (arrowheads) are induced by misexpression of *amos* but not *scute*. The Sc-bHLH$^{(AMOS)}$ chimeric lines can also induce relatively high numbers of ectopic olfactory organs compared to *scute*.

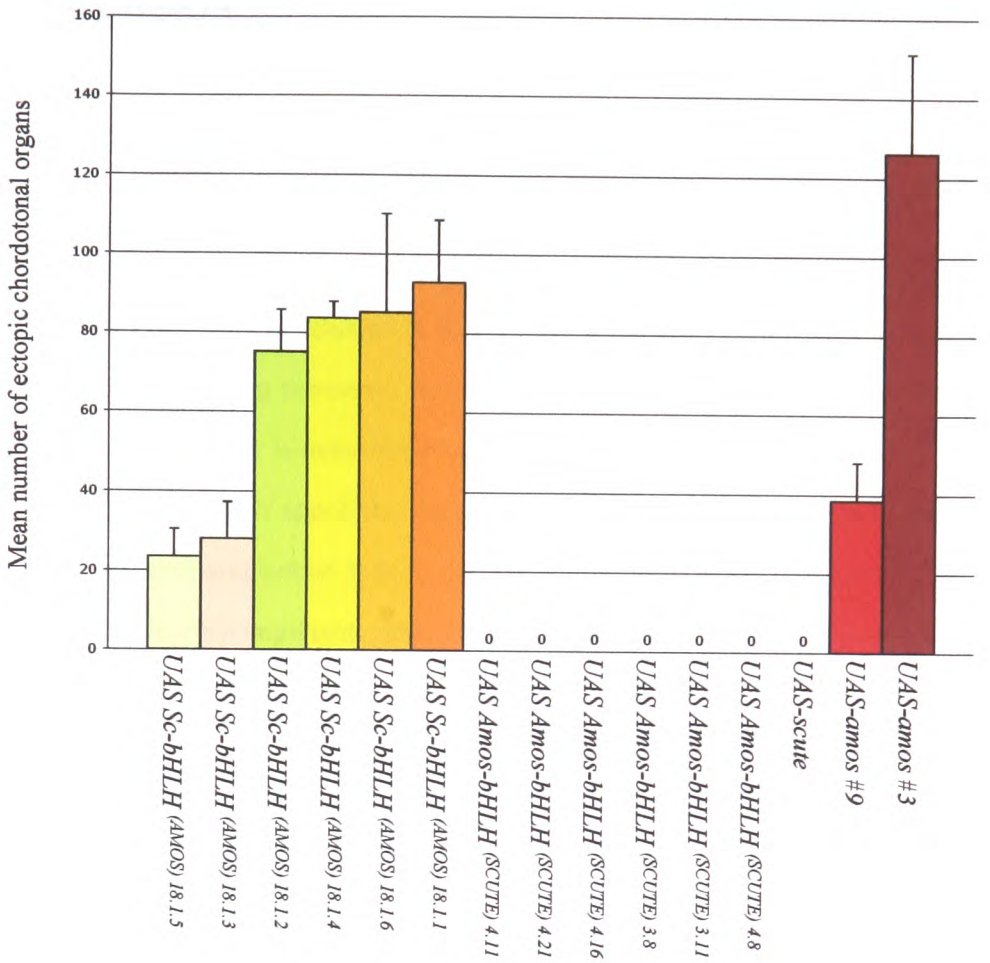

Figure 5.12 Ectopic chordotonal organs induced on the scutellum by misexpression at 29°C. Misexpression of *UAS-amos#9* and *UAS-amos#3* can induce the formation of ectopic chordotonal organs on the scutellum. *UAS-scute* cannot induce ectopic chordotonal organs, but replacement of its bHLH domain with that of Amos; Sc-bHLH$^{(AMOS)}$ chimera, allows this protein to behave like Amos to produce ectopic chordotonal organs. This suggest that the bHLH domain of amos is sufficient to specify chordotonal organs. The Amos-bHLH$^{(SCUTE)}$ chimera does not specify chordotonal organs. This suggests that the rest of the Amos protein cannot specify chordotonal organs without an Ato-like bHLH domain.

5.9 DISCUSSION

5.9.1 The sequence basis of specificity depends on the fate decisions being investigated

I show in this chapter that Sc versus Amos specificity maps to their bHLH domains. Therefore, the interesting conclusion is that where specificity resides depends on which proteins/functions are being compared. At one level, the distinction between Sc on one hand and Amos/Ato on the other is determined very strongly by the nature of their bHLH domains (Fig.5.13). At a finer level of specificity, the distinction between closely related Amos and Ato is dependent on uncharacterised features of their sequences out with their bHLH domains. This conclusion is very important: taking the evidence on Sc/Ato or Sc/Amos chimeras alone, it would be easy to conclude mistakenly that the non-bHLH sequences of these proteins provide nothing interesting with respect to target gene specificity. This was widely believed to be the case after the initial report of Chien et al. (1996).

In recent published literature concerning bHLH transcription factors state the bHLH region as the primary region required for functional specificity (Quan et al., 2004). This could have important consequences. For instance, a search for specificity cofactors might entail looking for proteins that interact with the proneural bHLH domains. Such a search might at best detect only some of the important cofactors; at worst it may not detect the important cofactors at all.

Is there a role for the non-bHLH portion of Sc? There is no positive evidence for this, but we must remain open minded. It is notable that the Amos-bHLH$^{(SCUTE)}$ chimera is rather less powerful in promoting external sense organs than Sc. This might suggest that the Sc bHLH domain must collaborate with the non-bHLH portions of Sc for full function.

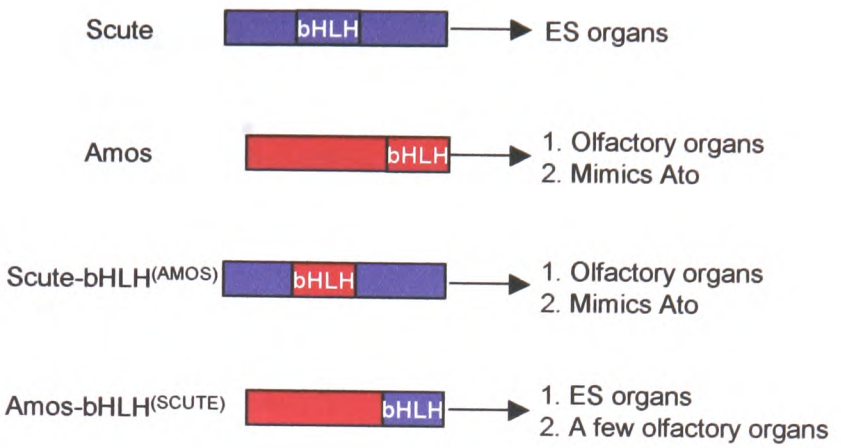

Figure 5.13. Summary of behaviour of Sc/Amos chimeric (proneural) proteins. I found that the functional specificity of the Scute-bHLH$^{(AMOS)}$ resembles the intact Amos protein. This suggest that the bHLH domain of Amos is sufficient for Amos-specificity with respect to Scute. The Amos-bHLH$^{(SCUTE)}$ has the same characteristics as the full Scute protein, suggesting the Scute bHLH domain is sufficient for Scute-specificity. However, additional Amos-like characteristics are also gained. This gives some weight to the idea that elements outside the Amos bHLH domain may be involved in Amos-specificity (Chapter 4).

5.9.2 Scute is more conducive to olfactory organ fate than is Ato

An unexpected phenotype of Scute is its ability to induce a small number of ectopic olfactory organs. In comparison, misexpression of Ato never produced olfactory organs. On the contrary, Ato appears to suppress ectopic olfactory organ formation by Amos. The reason behind this overlap in specificity between rather distantly related proteins is unknown. I suspect, however, that the answer has something do to with the interchangeability of the Ato/Amos bHLH domains. I would propose that the non-bHLH sequence of Ato must not only actively promote chordotonal specificity, but also suppress basiconica/trichodea specificity. Sc does not do this, and so one observes a mixture of sense organs, as is often the case in these misexpression experiments.

5.9.3 The need for rescue experiments

The experiments reported in this chapter are limited in an important respect. Future experiments should be aimed at examining mutant rescue in addition to the misexpression experiments reported here.

Without such experiments, the conclusions that I can draw are limited. This is especially true given the apparent interchangeability of the Ato and Amos bHLH domains. While it is clear that the Sc-bHLH$^{(AMOS)}$ chimera doesn't act like Sc, does it act like Amos, or Ato, or both? The results suggest like Amos – the chimera can make ectopic olfactory organs and chordotonal organs. The former is consistent with Amos behaviour, but the latter cannot be interpreted as Ato or Amos-like behaviour. I would need to test whether the chordotonal organs of the Sc-bHLH$^{(AMOS)}$ chimera are dependent on endogenous Ato. I concluded in Chapter 4 that this experiment would be required to test whether chordotonal production had Ato- or Amos-like characteristics. The obvious prediction might be that chordotonal specification by Sc-bHLH$^{(AMOS)}$ would be Ato-dependent. However, I think there is a possibility this chimera will behave unexpectedly like Ato in this assay. I suspect that the Ato/Amos bHLH domains have a generic ability to promote chordotonal/olfactory fate. This ability is then restricted by the non-bHLH sequences of the proteins. Such restriction may not

be observed in the Sc-bHLH$^{(AMOS)}$ chimera. Similarly, I suspect that a Sc-bHLH$^{(ATO)}$ chimera may be able to promote ectopic olfactory organs (unlike Ato). Unfortunately, the fly lines of this construct, as reported in Chien et al. (1996), are no longer extant. For olfactory specificity it will similarly be important to examine the phenotypes of the Sc-Amos chimeras in an *amos* mutant background to assess rescue of olfactory sensilla.

It is as though the Amos/Ato non-bHLH domains exert a decisive influence on a generic Amos/Ato bHLH domain. What is the molecular basis of this? Moreover, what is the molecular basis of the different kind of specificity shown by Sc? In the last chapter I present a molecular model that rationalises these conclusions.

Chapter 6

Conclusion

6.0 Conclusion

In this study I have obtained much informative, diverse, and sometimes apparently contradictory data on the question of the structural basis of functional differences between the proneural proteins. As is probably true in all biological research, it is difficult to incorporate every observation into a unifying model. However, I think the most important conclusions and inferences are relatively clear. In this final chapter, I shall attempt to integrate these into an overall molecular model.

The most important conclusion is that the external sense organ versus olfactory/chordotonal fate choice is distinct from the chordotonal/coeloconica versus basiconica/trichodea fate choice. The structural basis of each choice is therefore distinct and must to some extent be addressed separately.

The bHLH domain sequence has overriding importance in deciding the first fate choice. For the second fate choice, the bHLH domain must be Ato-like, but otherwise, it does not influence the fate choice (Fig.6.1). The Ato-like bHLH domain has the ability (competence) to specify both chordotonal and all three olfactory-type fates. This ability is restricted by non-bHLH sequences. This restriction involves promotion of one fate choice as well as direct inhibition of the alternative choice (Fig.6.1). These basic conclusions are expanded upon below.

6.1 Sc versus Ato/Amos

The highest level of fate choice is that between external sense organ versus olfactory/chordotonal fate, i.e. Sc versus Ato/Amos function. For this fate choice, the following observations are the most pertinent:

1. The general inability of the Sc bHLH domain to suffice for olfactory/chordotonal fate.
2. Overriding ability of the Sc bHLH domain for external sense organ function.

The evidence from misexpression of Sc-Amos (here) and Sc-Ato chimeras (Chien et al., 1996) clearly shows that this fate choice specificity resides in the bHLH domain. The basis of the fate choice must therefore be sought in the sequences of these domains.

3. Known ability of Sc and Ato (therefore probably also Amos) to function via different E boxes in vivo.

Work in the lab has recently proved that Ato and Sc function via different E box consensus sequences in vivo (Powell et al., 2004). Indeed distinct E_{Sc} and E_{Ato} consensus binding sites have been recognised (Amos target sites are not known). I suggest that the difference between Sc and Ato (and implicitly between Sc and Amos) is due to the difference in intrinsic abilities of their bHLH domains to recognise DNA sequences (Fig.6.2). This overrides any effect the non-bHLH portions might have. It should be made clear, however, that we do not know *how* Sc and Ato/Amos recognise different target sequences *in vivo*. Despite their specificity, the DNA-contacting residues of the bHLH domains are conserved in Sc, Ato, and Amos. This has led to the conclusion that DNA binding properties may not differ – all proneural proteins may have the ability to bind to the same target E boxes for target gene regulation (Chien et al., 1996). Indeed, there is no apparent difference in Sc and Ato DNA binding properties *in vitro* (Powell et al., 2004). It is quite feasible therefore that interaction with specific cofactors induces specificity in DNA binding *in vivo* (Powell et al., 2004).

6.2 Amos versus Ato

A separate level of choice is between chordotonal/coeloconica fates and basiconica/trichodea fates, i.e. Ato versus Amos. For this choice, the following findings are pertinent:

1. Apparent interchangeability of Ato/Amos bHLH domains for olfactory versus chordotonal fate.

2. Overriding importance of the non-bHLH portions in deciding olfactory versus chordotonal function.

Most persuasively, an Ato-bHLH$^{(AMOS)}$ chimera generally behaves like Ato, whereas an Amos-bHLH$^{(ATO)}$ chimera behaves like Amos.

3. Possible lack of DNA binding discrimination between Ato and Amos

This is speculative at the moment, since there is no direct evidence. However, given the virtually complete sequence identity of their basic regions, it seems highly likely that there is no instrinsic ability of the Ato and Amos bHLH domains to discriminate DNA binding sites. They may therefore have identical abilities to recognise target E boxes *in vivo.*

4. Apparent antagonism between Ato and Amos functions.

I showed in Chapter 3 that reducing *ato* gene dosage increased Amos' ability to produce ectopic olfactory organs.

I propose therefore that Amos and Ato can both bind to the same target sites, but target gene activation requires additional interaction with specific cofactors (Fig.6.2). The non-bHLH portions of Ato and Amos provide the major *specific* contacts for this protein interaction. However, the Ato/Amos bHLH domains also provide some 'generic' contact too with both types of specificity cofactor (Fig.6.2). Hence, they may be able to impose some 'generic' chordotonal/olfactory specificity on Sc-bHLH(Ato/Amos) chimeras.

In this model (Fig.6.2), a proneural protein must bind to the right E box and also interact with the right cofactor for specific target gene regulation. The Sc bHLH domain targets the proneural protein to external sense organ target gene E_{Sc} boxes. In contrast the Amos/Ato bHLH potentially targets the protein to <u>both</u> olfactory and chordotonal target gene $E_{Ato/Amos}$ boxes. Once targeted to these E boxes, interaction of the non-bHLH domains with specific cofactors produces either chordotonal/coeloconica or basiconica/trichodea target gene regulation. In this scenario, Ato and Amos may occupy the same sites *in vivo.* But they only

productively result in target gene expression if their specific cofactor is present. Hence antagonism between Ato and Amos can be explained: they may compete for binding to the same E box sites. An alternative scenario is that the cofactor interaction itself forces bHLH targeting to olfactory (Amos) or chordotonal target genes. Either way, the result is the same, the Amos/Ato bHLH domain has the potential to recognise both olfactory and chordotonal targets; cofactor interactions enforce more refined specificity. Both summary models Fig.6.1 and 6.2 are combined to form the final model (Fig. 6.3) of Amos/Ato chimeric protein specificity. Figure 6.3 illustrates how both Amos-bHLH$^{(ATO)}$ and Ato-bHLH$^{(AMOS)}$ proteins can switch on basiconica/trichodea target genes, but only the Ato-bHLH$^{(AMOS)}$ protein can switch on chordotonal/coeloconica target genes.

Chien et al (1996) showed that only the bHLH domain is important (between Sc and Ato). I can rationalise this by saying that this study explored only the DNA binding ability and generic cofactor contacts, which separate Sc from Ato/Amos. The crucial cofactor-specific contacts hypothesised for the non-bHLH portions could not be detected in the assays used. This shows, ultimately, that specificity must take into account the assay used and how easily one can come to premature/wrong conclusions. It also shows the power of *Drosophila* to tackle such questions in a fine level of detail and continues to make investigation of *Drosophila* proneural genes a crucial paradigm for control of neurogenesis and the function of bHLH proteins.

From an evolutionary perspective, my work suggests a reassessment of the view that Amos is a 'new' derived function in *Drosophila* neurogenesis, compared to an ancestral function provided by Ato. Instead, it may be hypothesised that the ancestral proto-Ato/Amos gene combined the function of Ato and Amos. Through its distinctive (non-Sc) bHLH domain, proto-Ato/Amos specified both chordotonal and olfactory sensilla (or at least the sense organs that were ancestral to these), as well as photoreceptor precursors. After gene duplication, the two daughter genes became specialised to perform different subsets of these functions. One can imagine that the bHLH domains were already highly constrained to

recognise specific target genes, so specialisation occurred through divergence of their non-bHLH sequences. Interestingly, this specialisation apparently did not include R8 photoreceptor specification, perhaps because non-overlapping expression made specialisation unnecessary. It is likely therefore, that vertebrate Ato-like homologues will be functionally equally similar to (or distinct from) both Ato and Amos.

6.4 Future work

An obvious avenue to explore further is the finer dissection of specificity, particularly for olfactory versus chordotonal fate choice. It would be interesting to map the important parts/residues of the non-bHLH domains that are required for this fate choice.

It would also be interesting to determine the *in vivo* site occupancy of Amos and Ato. Whether Amos and Ato bind only to E boxes of their own respective target genes or to E boxes for both sets of target genes. Determining the *in vivo* e-box site occupancy of Amos and Ato would prove useful in interpreting the effects of their misexpression. This can be addressed by chromatin immunoprecipitation (ChIP), and is currently being investigated by L. Powell in the lab.

Cofactor identification is another major direction for future investigation. Clearly my work continues all the other lines of evidence that suggest the importance of cofactors. It is essential that such proteins are identified in order to take this field further. Some possible methods include yeast 2-hybrid screening; co-IP and mass spectrometry detection; genetic modifier screens for interacting genes that affect the olfactory-chordotonal fate choice by proneural genes.

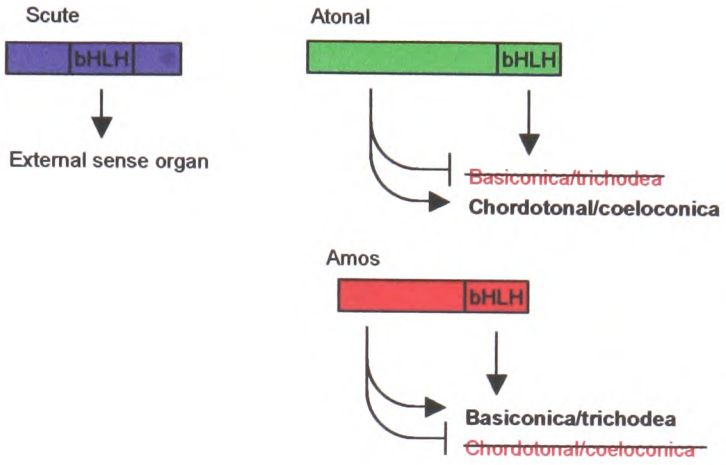

Figure 6.1. Summary of sense organ fate determination. This summarises the essential findings of this thesis. The bHLH domain of Scute drives the specification of external sense organ fate. The bHLH domains of Ato and Amos drive other fates, but otherwise appear to be largely interchangeable, and have the same potential for chordotonal or the three olfactory-type fates. The non-bHLH portions of Ato and Amos restrict this potential to chordotonal/coeloconica fate (for Atonal) or basiconica/trichodea fate (for Amos).

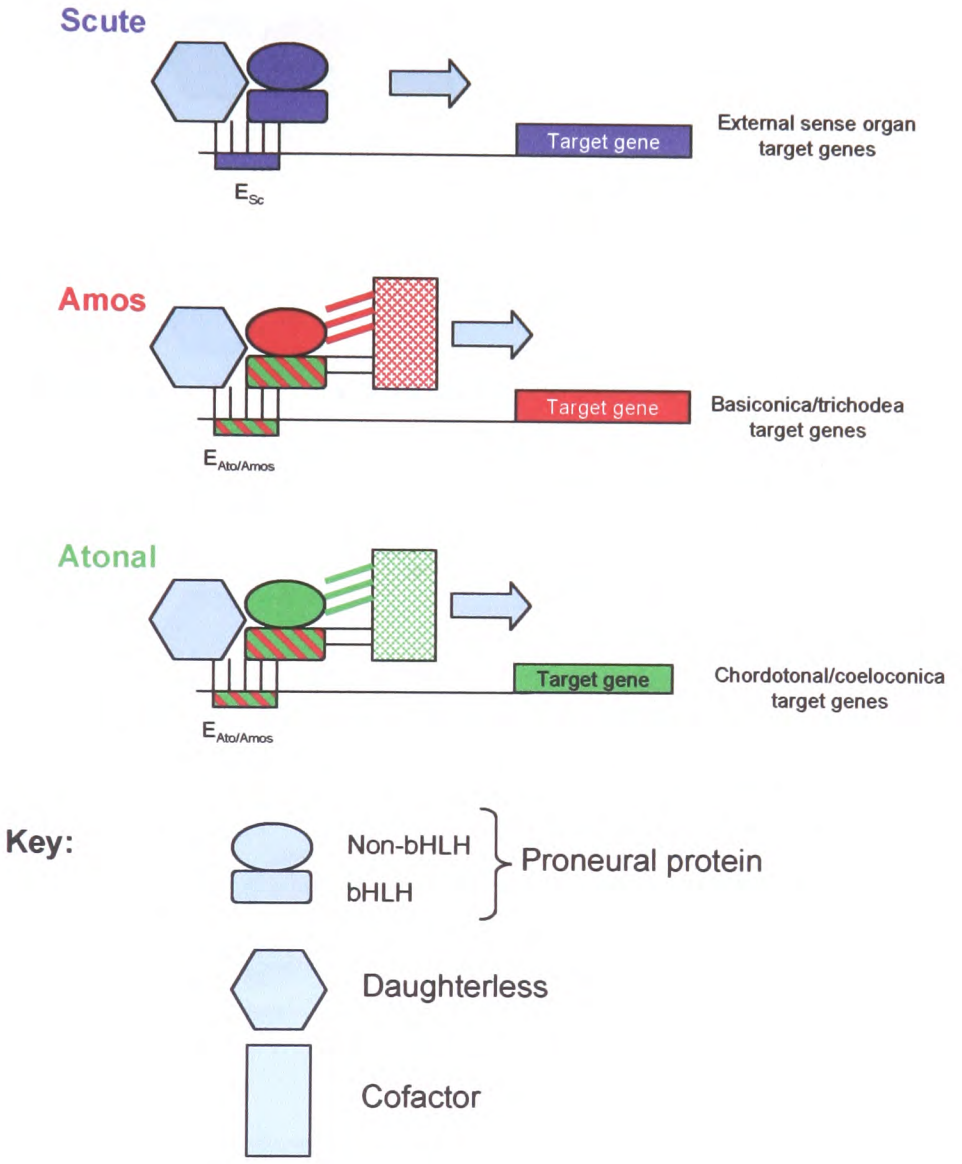

Figure 6.2. Summary model to explain the interrelationship of DNA specificity and cofactor specificity in deciding proneural protein specificity. Sense organ specification by proneural proteins utilise different mechanisms. For Scute DNA binding is sufficient to activate external target genes. DNA binding to differential E-boxes is sufficient to discriminate the functions of Scute and the Ato-like proteins. However, Ato-like proteins require an additional mechanism for finer specifications. DNA binding alone is insufficient to discriminate between the specific functions of closely related bHLH proteins such as Ato and Amos. This is because Amos and Ato are able to bind to the same E-box. Thus DNA binding is coupled to cofactor interactions. This requires elements out side the bHLH domain, in this way Ato and Amos can specify chordotonal/coeloconica and basiconica/trichodea fates respectively.

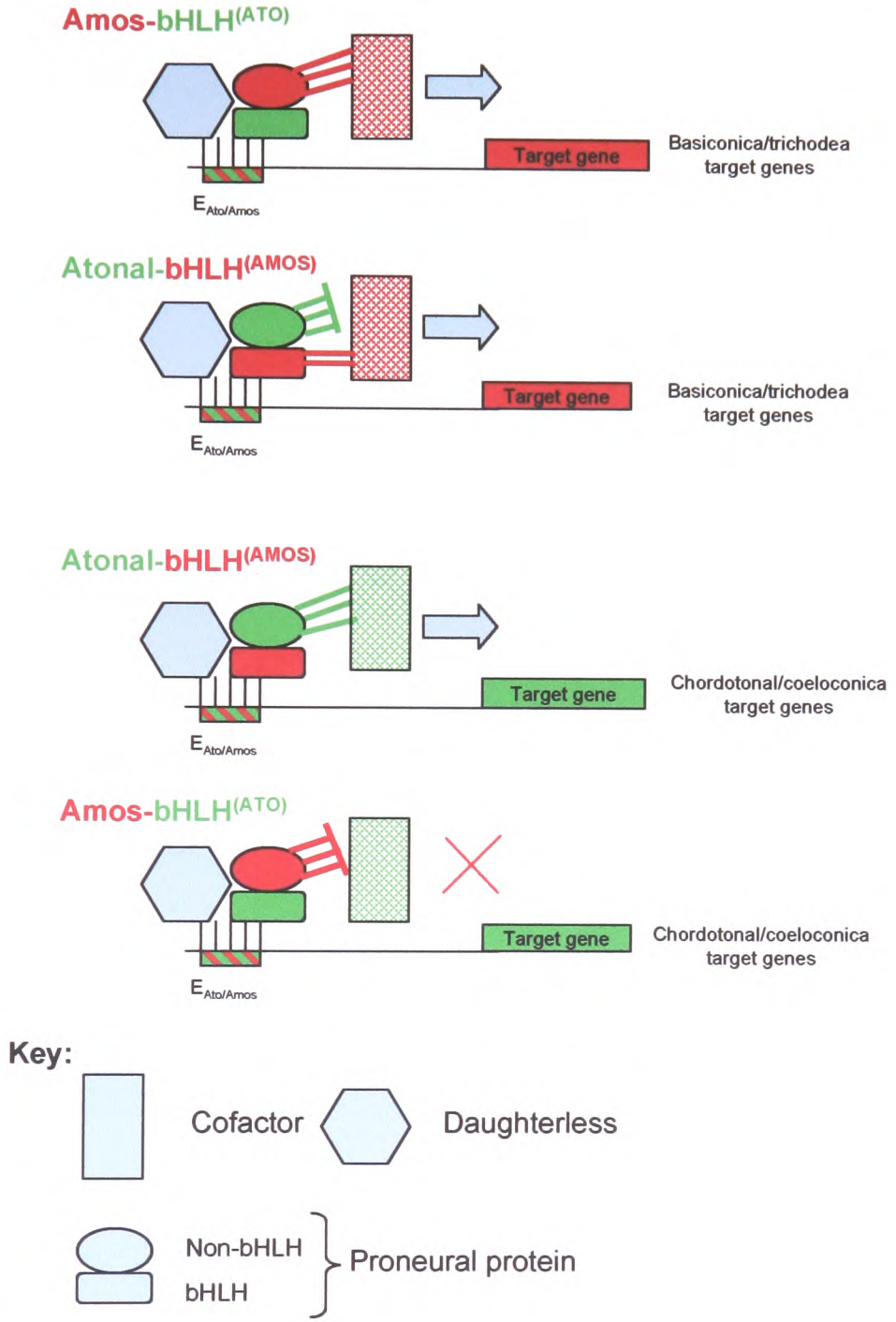

Figure 6.3. Summary model to explain the interaction of the Amos-Ato chimeras with specificity co-factors. The Amos protein has specific contacts both outside and within the bHLH domain for basiconica and trichodea cofactors. Thus both Amos-bHLH$^{(ATO)}$ and Ato-bHLH$^{(AMOS)}$ chimeras can specify basiconica and trichodea fates. Atonal contains specific contact sites outside the bHLH domain for chordotonal cofactors. Therefore, only the Ato-bHLH$^{(AMOS)}$ chimera but <u>not</u> the Amos-bHLH$^{(ATO)}$ chimera can specify the chordotonal fate.

Appendix

Appendix A

cDNA sequences used to design and construct chimeras

Amos cDNA

ORIGIN

```
1    gtcgacctgt agctgataca gtaaatacct gggagaaaga gggagagagt tgcagccaga
61   gacaattaaa cgtcttgacc gcaagccaat ttagggcacg ggctgtgctg ctgatcctca
121  agaggttggc aatcgggtac ctgagcggat cggatcagct tgaggcagcg aatcaggtaa
181  crgracatat gtagtgaacc aatcacgtga gagctgaatc ctcggcaggc agstatataa
```

Position of primer JF1

```
241  agacccatcc tcaagcagcc acttcagttg tcccttgagc ctgcaaacgt aaacatgttg
301  accaacaacg agctaatgga gcagttctac ttccccgacg aagccccagc gattcccgag
361  ttcctgggca acgacacctt ccagcagttg gagcagctca tgtaccagca ggagttcagc
421  accagcgaca gccagtcgga tggcgccaac agttgctcct tggagatgta ttacgatacg
481  ccgtctgtcc tggaattgga gcacatgctg aatgcccagg agcagcagca gcaccacctt
541  caagcgaatc ccttgggcaa gaatcagggc agaagtccaa ggtactggaa caagcagcag
601  aggagcaagc catacgacaa gctgtccact tccatgtcat catctacatc ctccgcctct
```

Position of primers SM1, SM2, SM6, SM8, SM9 SM13, SM14,

```
661  tcgagcagtt catcgtccgc gggattcggt ggcgaagtcc tcaaaaaacg gcgactggcc
721  gccaatgctc gggaacggag gcggatgaac agcctgaacg atgccttcga caagttgaga
781  gatgtggttc catcactcgg ccacgatcgg cgactctcca aatacgaaac tctgcaaatg
```

Position of primers JF2, SM10, SM11

```
841  gcgcaagcat acatcgggga tctggtcacg ttgctgtcca gagactacta gccagtgtgg
901  gcgatccttt atcctttctt cctcaaatgg aagttccttt tgcgggctgt gttgcagcaa
961  caccttccat atcctagtgg aaatcttata aaggctgtta gttttacgtt tattatcata
1021 nttgtacnca attcaagcaa tagttttata ataaaaatga atacaaaata tcaattatat
1081 tgttttaaat tcatatcgta tgaaatggtg gagtnggaat gaaaatnatg ttatgcgaac
1141 ttgggaaatt tatattt
```

Ato cDNA

ORIGIN

```
1    atcatcttgt tagcggcttt agagccgaat cgttttctag cgccatttta agctcgcaac
61   gaactgaggt ataaccgggc tctctgagac cgctgcaact caccaccaac tgccattggt
121  cgtgccactc gggcggcacg tgctgccttc tgtggcaact cgtttacctg ccccctacc
181  tgcctttcag gcccttctga ccgtcgtggt ggatttgtga gtataaatag ggccgaaagg
```

Position of primer SM4

```
241  acgagagacc agtcagaaac ccgccagcac tcgcagcgtt cgtatcgttt catccagcaa
301  cataacacca ccatacagca gcagcaacat gtcgtccagt gagatctatc gctactacta
361  caagacctcc gaggacttgc agggcttcaa gacagccgcc gccgagccgt acttcaatcc
421  catggcagcc tacaatcccg gcgtgaccca ctaccagttc aatggcaaca ccctggccag
481  cagcagcaac tacttgtcgg ccaatggctt catcagcttc gagcaggcca gttccgatgg
541  ctggatctcc tcctcgccgg ctagccaccg atctgagagt cccgagtatg tggatctcaa
601  taccatgtac aatggaggct gcaacaacat ggcccagaac caacaatacg gaatgattat
661  ggagcagtct gttgtttcca cagcgcctgc aattccagtg gcctctcctc cggcagtgga
721  ggtcatgggc tcctccaacg tgggcacttg caaaacgatt ccagcctcag cagctccgaa
781  accgaagcgt agctatacca agaagaacca gccaagcacc accgccacct ccacaccgac
841  tgcagctgcg gagtcatctg cctcagtgaa tctctacacg gaggagttcc agaactttga
901  ctttgacaac tccgccttgt tcgatgacag cgtcgaggat gacgaggacc tcatgctctt
961  cagtggcggt gaggacttcg atggcaatga tggatccttt gacttggccg atggtgagaa
```

Position of primers SM1, SM2, SM5 and SM6

```
1021 ccaagatgcc gctgccggag gctctggaaa gaagaggcgt ggcaagcaga tcacacccgt
1081 cgtgaagagg aagcgtcgcc tggccgccaa tgcacgtgag cgtcgtcgga tgcagaacct
1141 caaccaggcc ttcgatcgtc tccgccagta ccttccctgt ctgggaaacg atcgccagct
```

Position of primer SM3

```
1201 gtccaaacac gagaccctcc aaatggccca gacctacata tccgctctcg gggatctgct
1261 gcgctgaatt cccggatccc gatcccagtc ccaagtacta ttctcagtta ttgttggagc
1321 ttgccaaatg ttgtagctac tttgtatata ttgcctggag cccagtagtg aattaccgct
1381 taagtattat gctgtttatt gtttagttaa ttagcctaaa tggaagacaa tgattaagac
1441 taaggaagac aaaataaaag caccattaat aatttaa
```

Scute cDNA

ORIGIN

1 aaaaaatttt gatccttttg ataatttaat tggagaaata agtgaaattg tttgaacacc
61 tttagggagc gtactccgaa tgtctaataa ggaggatccc aggatcggct gtcgatccct
121 tggatccgtc cggcgctaat gaatagaagc gtgcgtgagc tgcacataaa attggcgatc
181 gcgacttttg ctaagttaat taacacagaa atcaaattcc tggcgtgccg tagcaaaaag
241 agccctcact cagatacctt gatcgttttt cgatatttcg agttgatatt ttgagtttaa
301 aatttgagtg tttcttttgg actgtcgagt gagaacagtt ttcctgtggg atactcgagt
361 acctgagaca gagaaagaga gagagactac ctgtggctca ctcacttcga gttccctacc
421 tgtgcaggca gctcttgccg tcactctctc tctctctttc tctccgattc tctcgcccgt
481 ttctctgcct gagtgttgtg cagagagttg cataaagggt acataacgcg agggtttagg
541 acgaagggac tcattcttgt gtaaggtgtc aaacgatcaa gttcaagtat tgtactctgt

Position of primer SM7

601 tcatttattt ttttct**gttg atcgttatcc ggaaagtg**aa agaaagctcc gagtgtgtta
661 atgaaaaaca ataataatac aacgaaaagc actaccatgt catcgagtgt gctgtccacc
721 aacgaaacgt ttccaacgac catcaattcg gcaacgaaga tctttcgtta tcagcacata
781 atgccagccc ctagtccatt aattcccggt ggcaatcaaa atcaacccgc tggcacaatg
841 ccaattaaga ctcgcaagta tacaccaagg ggtatggcac tgaccagatg ctctgaatca

Position of primers SM8 and SM9

901 gtatcatctc tatcgcctgg ttcctcgccg gctccatat**a atgtagacca atcccag**tcg
961 gtccaaaggc gcaatgctag agaacgaaat cgtgtaaagc aggtgaacaa cagcttcgcc
1021 aggttgcggc aacatatacc acaatccata atcacggatt tgacaaaggg tggtggtcga
1081 ggacctcaca aaaagatctc caaagtagac acactgcgca ttgccgtcga gtacatccgg

Position of primers SM10 and SM11

1141 agccttcagg atctggtg**ga tgacctaaat gggggc**agca atattggtgc caacaatgca
1201 gtcacccagc ttcaactttg tttggatgag tccagcagtc acagttcgag cagcagtact
1261 tgcagttcct cagggcataa tacctactat caaaacagga tctctgtcag tcctgtgcaa
1321 caacagcagc agctacagag gcagcagttc aatcaccaac cgctgacagc gctctcatta
1381 aataccaact tggtgggcac atccgtacca ggtggagatg caggatgcgt atccaccagc
1441 aaaaaccagc aaacctgcca ctcgccaaca tcatcattca actccagcat gtcctttgat
1501 tcaggcacct acgaaggagt tccccaacaa atatccaccc acctggatcg tctggatcat
1561 ctggacaacg aattacacac gcactcccaa cttcagctaa aatttgaacc gtacgaacat
1621 tttcaattag acgaggagga ctgcaccccc gacgacgagg agattttgga ctacatctct

Position of primer SM12

1681 **ctatggcagg agcagtga**ct taatccccaa aatttaccac cacgccctat tttcttctag
1741 tcaatgttga gttgaaccaa gtgcctcaaa ttgtaaataa cactaataca aaaacaacat
1801 acccccaatt ttttttttctt actttaagct attttttac attgttaaga accacgagac
1861 cagtttcaaa tttatatatt tatgaaataa ctatagcatg gaaacgaaaa catatttttt
1921 tggctaatac aattttatgt taattagttt tggtggaaaa ataaaatgaa aaaattaaac
1981 gaaaaataat atttaagttt ttttgtacaa aggggatcca tctattgcat caggtttgta
2041 aaacattcgg gtactacttg cattgccttg cagtgccgat gggaccatgt gcagccgtta
2101 tgtacattgg ttgctttgca ttggttttcc a

Appendix B

Primers used in PCR and verification of chimeric constructs

Primer list for construction of chimeric fragments

JF1: CAG GAA TTC GTT GTC CCT TGA GCC TGC

JF2: GCA GAA TTC ATC GCC CAC ACT GGC TAG

SM1: CTT CAC GAC TTC GCC ACC GAA TCC CGC

SM2: GGT GGC GAA GTC GTG AAG AGG AAG CGT

SM3: CGG GAA TTC AGC GCA GCA GAT CCC C

SM4: CGC GAA TTC GTA TCG TTT CAT CCA G

SM5: TTT GAG GAC CAC GAC GGG TGT GAT CTG

SM6: CCC GTC GTG GTC CTC AAA AAA CGG CGA

SM7: CAG GAA TTC GTT GAT CGT TAT CCG GAA AGT G

SM8: TTT GAG GAC CTG GGA TTG GTC TAC ATT

SM9: CAA TCC CAG GTC CTC AAA AAA CGG CGA

SM10: TAG GTC ATC GTA GTC TCT GGA CAG CAA

SM11: AGA GAC TAC GAT GAC CTA AAT GGG GGC

SM12: CCT GAA TTC TCA CTG CTC CTG CCA TAG

SM13: TTG GAC CGA TTC GCC ACC GAA TCC CGC

SM14: GGT GGC GAA TCG GTC CAA AGG CGC AAT

SM15: GGA GAA TTC CTA CAC CAG ATC CTG AAG GCT

EcoR1 restriction sites underlined

Primers used to sequence chimeric constructs

SM16: CAC AGG ACT GAC AGA GAT CCT

ID 12: ACC AGC CAA CCA AGT AAA TC

ID 13: TGT CCA ATT ATG TCA CAC C

Primers used to verify chimeric constructs

Atotest1: AAT GAT GGA TCC TTT GAC TTG

Atotest2: TTG GAG GGT CTC GTC TTT G

Amostest3: AGG AGC AAG CCA TAC GAC AAG

Amostest4: GAG TGA TGG AAC CAC ATC TCT

Scutetest5: TAT ACA CCA AGG GGT ATG GCA

Scutetest6: CGT GAT TAT GGA TTG TGG TAT

Appendix C

Summary table of PCR products amplified

PCR Product	Predicted size (bp)	Tempiate	Primers		Final Chimera
			5' to 3'	3' to 5'	
Product 1: 5'Amos	~450	Genomic DNA	JF1	SM1	Amos-bHLH$^{(ATO)}$
Product 2: bHLH of Ato	~200	Genomic DNA	SM2	SM3	Amos-bHLH$^{(ATO}$
Product 3: 5'Amos-bHLH of Ato	~650	Product 1 and 2	JF1	SM3	Amos-bHLH$^{(ATO}$
Product 4: 5'Ato	~800	Genomic DNA	SM4	SM5	Ato-bHLH$^{(AMOS)}$
Product 5: bHLH of Amos	~200	Genomic DNA	SM6	JF2	Ato-bHLH$^{(AMOS)}$
Product 6: 5'Ato-bHLH of Amos	~1000	Product 4 and 5	SM4	JF2	Ato-bHLH$^{(AMOS)}$
Product 7: 5' Scute	~300	Genomic DNA	SM7	SM8	Sc-bHLH$^{(AMOS)}$-Sc
Product 8: bHLH of Amos	~200	Genomic DNA	SM9	SM10	Sc-bHLH$^{(AMOS)}$-Sc
Product 9: 3' Scute	~540	Genomic DNA	SM11	SM12	Sc-bHLH$^{(AMOS)}$-Sc
Product 10: bHLH of Amos-3'Sc	~740	Product 8 and 9	SM9	SM12	Sc-bHLH$^{(AMOS)}$-Sc
Product 11: 5'Sc-bHLH of Amos-3'Sc	~1040	Product 7 and 10	SM7	SM12	Sc-bHLH$^{(AMOS)}$-Sc
Product 12: 5' Amos	~450	Genomic DNA	JF1	SM13	Amos-bHLH$^{(SCUTE)}$
Product 13: bHLH of Scute	~200	Genomic DNA	SM14	SM15	Amos-bHLH$^{(SCUTE)}$
Product 14: 5'Amos-bHLH of Scute	~650	Product 12 and 13	JF1	SM15	Amos-bHLH$^{(SCUTE)}$

Appendix D

PCR conditions used to construct chimeras

Standard PCR reaction

Lid temperature: 100°C

Initial denaturing step: 94°C for 2 minutes,

Denaturing step: 94°C for 30 seconds

Annealing step: 55°C for 30 seconds

Elongation step: 72°C for 2 minutes

Total of 30 cycles

Final elongation step: 72°C for 10 minutes

Hold: 4°C until purification and analysis

The standard PCR reaction was used to amplify the following fragments with a low salt buffer: Amos 5' (product 1, 450bp), Ato bHLH (product 2, 200bp), Ato 5' (product 4, 800bp), Amos bHLH (for Ato-bHLH$^{(AMOS)}$, product 5, 200bp), Sc3' (product 9, 540bp) and Amos 5' (for Amos-bHLH$^{(SCUTE)}$, product 12, 450bp).

The standard PCR reaction was used to amplify the following fragments with a high salt buffer: Sc 5' (product 7, 300bp), Amos bHLH (for Scute-bHLH$^{(AMOS)}$, product 8, 200bp) and Scute bHLH (product 13, 200bp).

Variations of standard PCR reaction used for annealing fragments

Variation 1

Lid temperature: 100°C

Initial denaturing step: 94°C for 2 minutes,

Denaturing step: 94°C for 30 seconds

Annealing step: 50°C for 30 seconds

Elongation step: 72°C for 2 minutes

Final elongation step: 72°C for 10 minutes

Hold: 4°C until purification and analysis

Total of 20 cycles

The above PCR reaction was used with a low salt buffer to anneal: Amos 5' and Ato bHLH (products 1 and 2) to construct the Amos-bHLH$^{(ATO)}$ chimera and Ato 5' and Amos bHLH (products 4 and 5) to construct the Ato-bHLH$^{(AMOS)}$ chimera.

Variation 2

Lid temperature: 100°C

Initial denaturing step: 94°C for 2 minutes,

Denaturing step: 94°C for 30 seconds

Annealing step: 58°C for 30 seconds

Elongation step: 72°C for 2 minutes

Final elongation step: 72°C for 10 minutes

Hold: 4°C until purification and analysis

Total of 25 cycles

The above PCR reaction was used with a low salt buffer to anneal Amos 5' and Scute bHLH (products 12 and 13) to construct the Amos-bHLH$^{(SCUTE)}$ chimera.

Variation 3

Lid temperature: 100°C

Initial denaturing step: 94°C for 2 minutes,

Denaturing step: 94°C for 30 seconds

Annealing step: 55°C for 30 seconds

Elongation step: 72°C for 2 minutes

Total of 20 cycles

Final elongation step: 72°C for 10 minutes

Hold: 4°C until purification and analysis

The above PCR reaction was used with a high salt buffer to anneal Amos bHLH and Scute 3' (products 8 and 9) to construct the $bHLH^{(AMOS)}$-Scute 3' fragment.

Variation 4

Lid temperature: 100°C

Initial denaturing step: 94°C for 2 minutes,

Denaturing step: 94°C for 30 seconds

Annealing step: 55°C for 30 seconds

Elongation step: 72°C for 2 minutes

Total of 20 cycles

Final elongation step: 72°C for 10 minutes

Hold: 4°C until purification and analysis

The above PCR reaction was used with a high salt buffer to anneal Scute5' and $bHLH^{(AMOS)}$-Scute3' (products 7 and 10) to construct the Scute-$bHLH^{(AMOS)}$ chimera.

Appendix E

Restriction Endonucleases and Vectors

Restriction endonucleases used for cloning and checking orientation of inserts

EcoR1 : G/AA TTC

BamH1 : G/GA TCC

Bgl II : A/GATCT

Map of pBluescript used for cloning (from www.stratagene.com)

f1 (+) origin 135–441
β-galactosidase α-fragment 460–816
multiple cloning site 653–760
***lac* promoter** 817–938
pUC origin 1158–1825
ampicillin resistance (*bla*) ORF 1976–2833

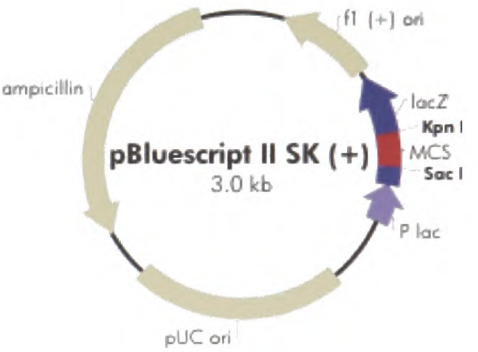

pBluescript II SK (+/–) Multiple Cloning Site Region (sequence shown 598–826)

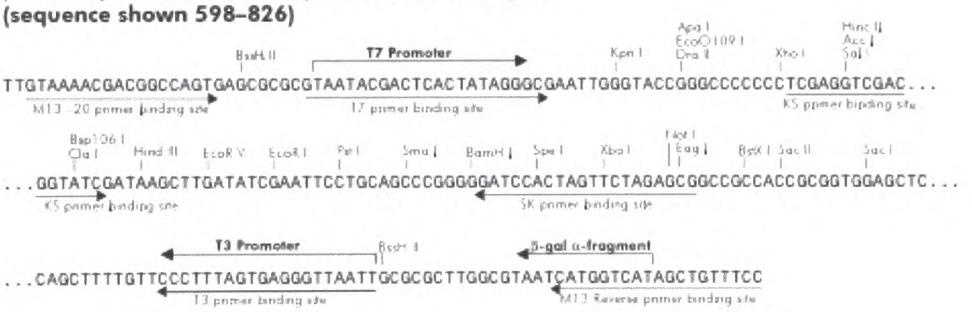

Map of pUAST used for subcloning (from www.gurdon.cam.ac.uk/~brandlab/)

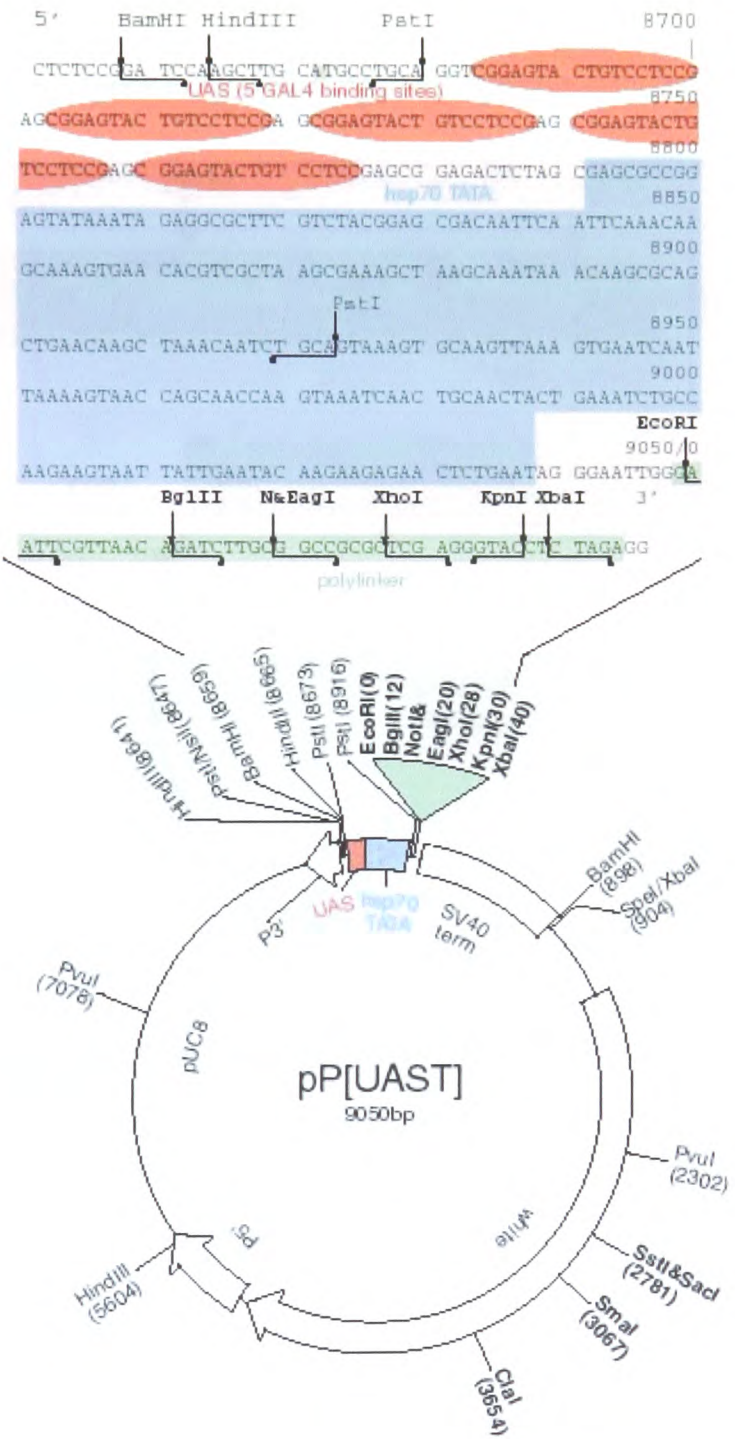

Appendix F

Methods used to determine orientation of constructs in pUAST

Determination of Ato-bHLH$^{(AMOS)}$ insert orientation in pUAST

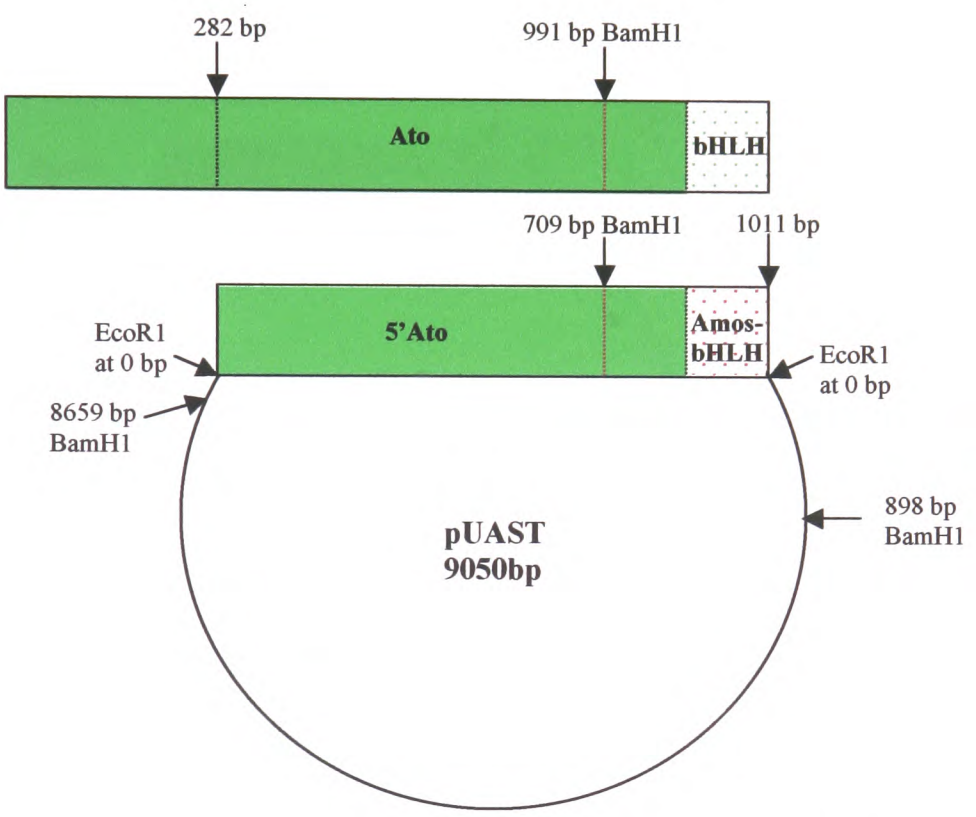

Ato-bHLH$^{(AMOS)}$ absolute size 1011bp. BamH1 restriction site in Ato-bHLH$^{(AMOS)}$ at 709bp and BamH1 restriction sites in pUAST at 8659bp and 898bp. If construct inserted in correct orientation, BamH1 restriction cutting will produce a 1100bp ([9050-8659]+709) band and 1200bp ([1011-709]+898) band, plus large (`~8kb) pUAST band on agarose gel.

Determination of Amos-bHLH$^{(SCUTE)}$ insert orientation in pUAST

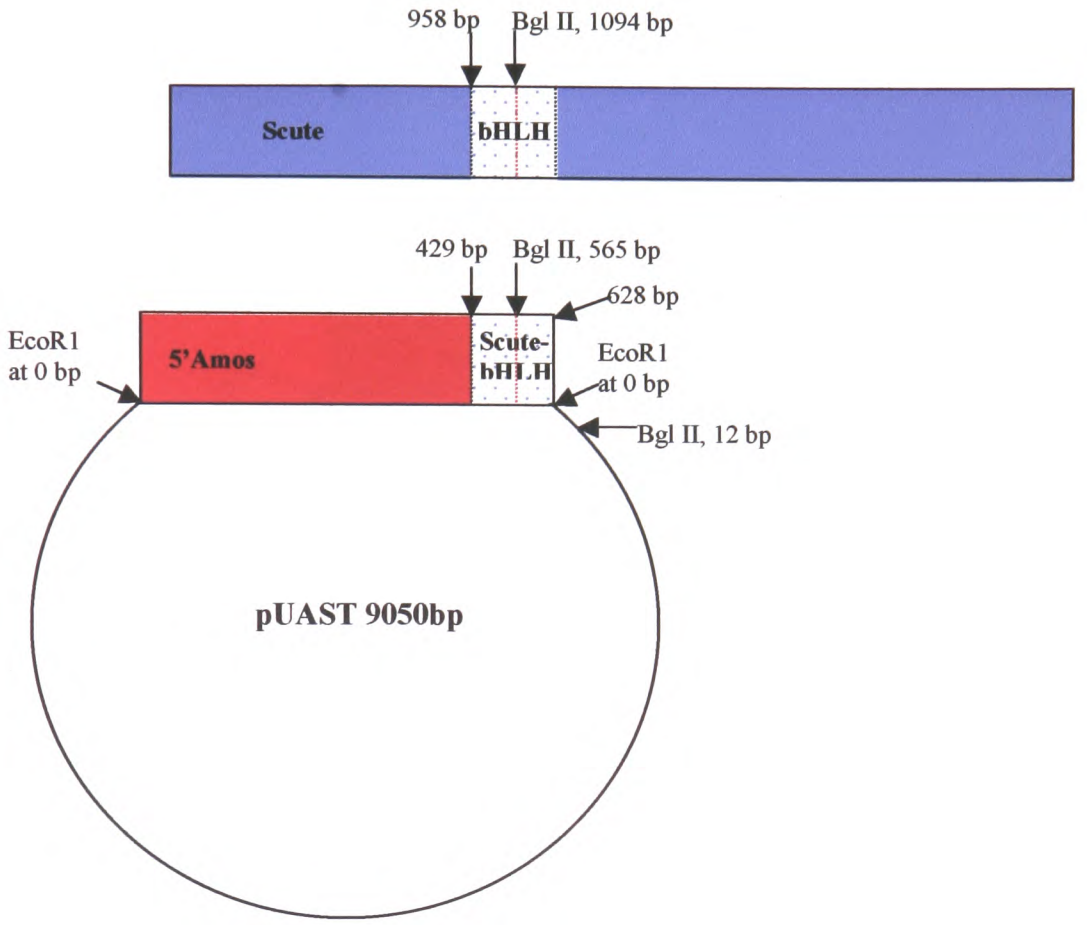

Amos-bHLH$^{(SCUTE)}$ absolute size 628bp. Bgl II restriction site in Amos-bHLH$^{(SCUTE)}$ at 565bp and Bgl II restriction site in pUAST polylinker at 12bp. If construct inserted in correct orientation, Bgl II restriction cutting will produce a 75bp ([628-565]+12) band, plus large (~9kb) pUAST band on agarose gel.

Determination of Sc-bHLH$^{(AMOS)}$ insert orientation in pUAST

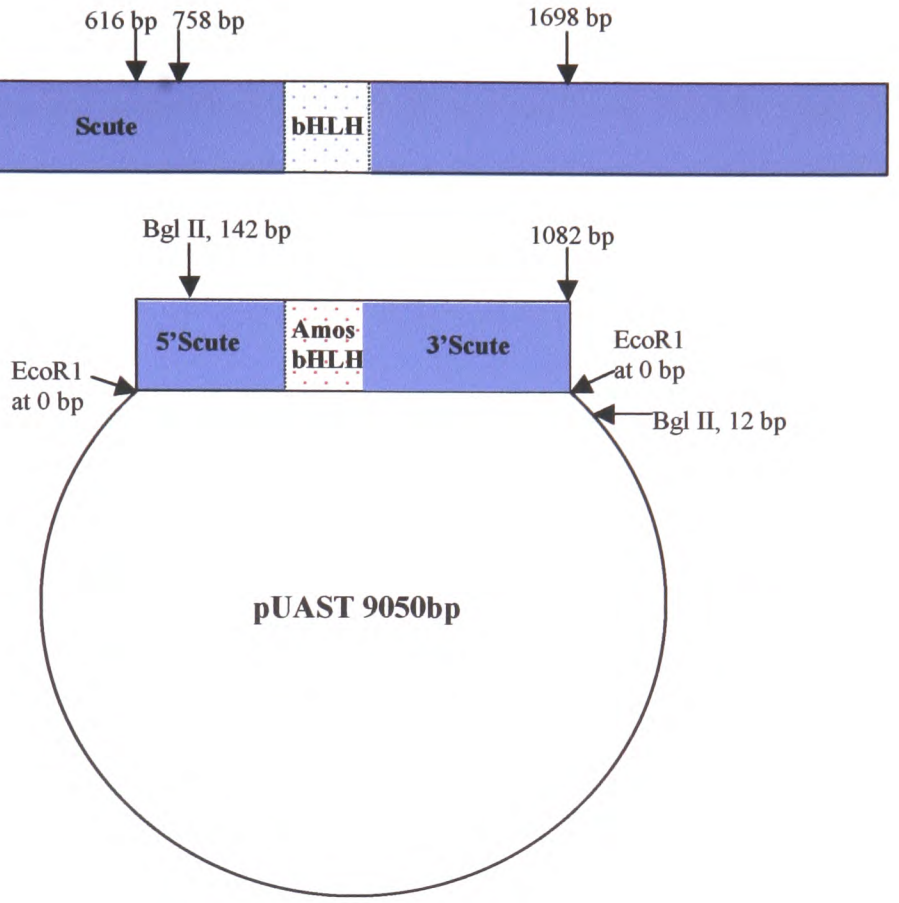

Sc-bHLH$^{(SCUTE)}$-Sc absolute size 1082bp. Bgl II restriction site in Sc-bHLH$^{(SCUTE)}$-Sc at 142bp and Bgl II restriction site in pUAST polylinker at 12bp. If construct inserted in correct orientation, Bgl II restriction cutting will produce a 952bp ([1082-142]+12) band, plus large (`~9kb) pUAST band on agarose gel.

Determination of Amos-bHLH$^{(ATO)}$ insert orientation in pUAST

No appropriate restriction sites were found in the Amos-bHLH$^{(ATO)}$ construct, therefore a different method was used to determine the orientation of this construct in pUAST. I decided to sequence into the pUAST vector with primer ID 12 and ID 13 (gift from Ilan Davis). The PCR sequencing reaction was carried out using the Big-Dye terminator kit and sequences were analysed as before.

Appendix G

Fly lines used in study

Summary table of *D. melanogaster* strains

Genotype	Nature of allele	Source/reference
Gal4$^{109\text{-}(2)68}$	Gal4 driver in PNC and SOP	(Jarman and Ahmed, 1998)
hairyGal4	Gal4 driver in pair-rule gene *hairy*	I Davis
scaGal4	Gal4 driver	(Egger et al., 2002)
ato$^{109\text{-}(2)68}$/CyO	*ato* misexpression	(White and Jarman 2000)
scute$^{109\text{-}(2)68}$/CyO	*scute* misexpression	(Jarman and Ahmed 1998)
Δ 2-3	P-transposase	Lab stock
yw; Pin/Cyo	Visible, dominant, balancer	Bloomington
w; Ly/TM3	Visible, dominant, balancer	Bloomington
UAS ato#1	Construct	Lab stock
UAS amos#9	Construct	Lab stock
UAS amos#3	Construct	Lab stock
UAS GFPnompA/TM3.sb	Construct	Lab stock
w^{1118}	Mutation of *white* gene	Lab stock
OreganR	Wildtype strain	Lab stock
Df(2L)M36F-S6/CyO	Deletion of 36F (spanning *amos*)	Bloomington
amos^{1}/CyO	Null	Lab stock
ato^{1}	Null	(Jarman et al., 1993)

Summary table of chimeric fly lines

Chimeric construct	Chromosome insertion	Homozygous viable?
Ato-bHLH$^{(AMOS)}$ 6a	2	√
Ato-bHLH$^{(AMOS)}$ 7a	2	√
Ato-bHLH$^{(AMOS)}$ 14a	2	√
Amos-bHLH$^{(ATO)}$ 4.6B	3	√
Amos-bHLH$^{(ATO)}$ 4.6C	2	×
Amos-bHLH$^{(ATO)}$ 4.6E	2	√
Amos-bHLH$^{(ATO)}$ 4.6G	2	√
Amos-bHLH$^{(ATO)}$ 4.7B	3	√
Scute-bHLH$^{(AMOS)}$ 18.1.1	2	×
Scute-bHLH$^{(AMOS)}$ 18.1.2	2	×
Scute-bHLH$^{(AMOS)}$ 18.1.3	3	×
Scute-bHLH$^{(AMOS)}$ 18.1.4	2	×
Scute-bHLH$^{(AMOS)}$ 18.1.5	2	×
Scute-bHLH$^{(AMOS)}$ 18.1.6	2	×
Amos-bHLH$^{(SCUTE)}$ 3.8	2	×
Amos-bHLH$^{(SCUTE)}$ 3.11	3	×
Amos-bHLH$^{(SCUTE)}$ 4.8	3	×
Amos-bHLH$^{(SCUTE)}$ 4.11	2	×
Amos-bHLH$^{(SCUTE)}$ 4.16	3	×
Amos-bHLH$^{(SCUTE)}$ 4.21	2	×

Appendix H

Summary of primary antibodies

Antibody	**Concentration**	**Staining pattern**	**Reference/Source**
Rabbit α Atonal	1: 2000	*ato*-dependent SOPs	(Jarman et al., 1993)
Rabbit α Amos	1: 1000	*amos*-dependent SOPs	(zur Lage et al., 2003)
Guinea pig α Senseless	1: 5000	All SOPs	(Nolo et al., 2000)
Mouse α 22C10	1: 200	Neuronal cell body and processes	(Zipursky et al., 1984)
Mouse α Boss	1:200	R8 precursors	(Hafen and Basler, 1991)

References

References

Ahmad, I., Dooley, C. M. and Afiat, S. (1998). Involvement of Mash1 in EGF-mediated regulation of differentiation in the vertebrate retina. *Developmental Biology* **194**, 86-98.

Akagi, T., Inoue, T., Miyoshi, G., Bessho, Y., Takahashi, M., Lee, J. E., Guillemot, F. and Kageyama, R. (2004). Requirement of multiple basic helix-loop-helix genes for retinal neuronal subtype specification. *J Biol Chem* **279**, 28492-8.

Akazawa, C., Ishibashi, M., Shimizu, C., Nakanishi, S. and Kageyama, R. (1995). A mammalian helix-loop-helix factor structurally related to the product of Drosophila proneural gene atonal is a positive transcriptional regulator expressed in the developing nervous system. *Journal of Biological Chemistry* **270**, 8730-8738.

Akazawa, C., Sasai, Y., Nakanishi, S. and Kageyama, R. (1992). Molecular characterization of a rat negative regulator with a basic helix-loop-helix structure predominantly expressed in the developing nervous system. *J Biol Chem* **267**, 21879-85.

Anderson, D. J. (1994). Stem cells and transcription factors in the development of the mammalian neural crest. *FASEB Journal* **8**, 707-713.

Anderson, D. J. (1995). Neural development. Spinning skin into neurons. *Curr Biol* **5**, 1235-8.
Atchley, W. R. and Fitch, W. M. (1997). A natural classification of the basic helix-loop-helix class of transcription factors. *Proc Natl Acad Sci U S A* **94**, 5172-6.

Badenhorst, P. (2001). Tramtrack controls glial number and identity in the Drosophila embryonic CNS. *Development* **128**, 4093-101.

Bailey, A. M. and Posakony, J. W. (1995). Suppressor of hairless directly activates transcription of enhancer of split complex genes in response to Notch receptor activity. *Genes Dev* **9**, 2609-22.

Bain, G., Maandag, E. C., Izon, D. J., Amsen, D., Kruisbeek, A. M., Weintraub, B. C., Krop, I., Schlissel, M. S., Feeney, A. J., van Roon, M. et al. (1994). E2A proteins are required for proper B cell development and initiation of immunoglobulin gene rearrangements. *Cell* **79**, 885-92.

Baker, N. E., Yu, S. and Han, D. (1996). Evolution of proneural atonal expression during distinct regulatory phases in the developing Drosophila eye. *Curr Biol* **6**, 1290-301.

Baker, N. E. and Yu, S. Y. (1998). The R8-photoreceptor equivalence group in Drosophila: fate choice precedes regulated Delta transcription and is independent of Notch gene dose. *Mech Dev* **74**, 3-14.

Bartholoma, A. and Nave, K. A. (1994). NEX-1: a novel brain-specific helix-loop-helix protein with autoregulation and sustained expression in mature cortical neurons. *Mech Dev* **48**, 217-28.

Ben-Arie, N., Bellen, H. J., Armstrong, D. L., McCall, A. E., Gordadze, P. R., Guo, Q., Matzuk, M. M. and Zoghbi, H. Y. (1997). Math1 is essential for genesis of cerebellar granule neurons. *Nature* **390**, 169-72.

Ben-Arie, N., Hassan, B. A., Bermingham, N. A., Malicki, D. M., Armstrong, D., Matzuk, M., Bellen, H. J. and Zoghbi, H. Y. (2000). Functional conservation of atonal and Math1 in the CNS and PNS. *Development* **127**, 1039-48.

Ben-Arie, N., McCall, A. E., Berkman, S., Eichele, G., Bellen, H. J. and Zoghbi, H. Y. (1996). Evolutionary conservation of sequence and expression of the bHLH protein Atonal suggests a conserved role in neurogenesis. *Hum Mol Genet* **5**, 1207-16.

Benezra, R., Davis, R. L., Lockshon, D., Turner, D. L. and Weintraub, H. (1990). The protein Id: a negative regulator of helix-loop-helix DNA binding proteins. *Cell* **61**, 49-59.

Bermingham, N. A., Hassan, B. A., Price, S. D., Vollrath, M. A., Ben-Arie, N., Eatock, R. A., Bellen, H. J., Lysakowski, A. and Zoghbi, H. Y. (1999). Math1: an essential gene for the generation of inner ear hair cells. *Science* **284**, 1837-41.

Bertrand, N., Castro, D. S. and Guillemot, F. (2002). Proneural genes and the specification of neural cell types. *Nat Rev Neurosci* **3**, 517-30.

Bier, E., Vaessin, H., Younger-Shepherd, S., Jan, L. Y. and Jan, Y. N. (1992). deadpan, an essential pan-neural gene in Drosophila, encodes a helix-loop-helix protein similar to the hairy gene product. *Genes Dev* **6**, 2137-51.

Blochlinger, K., Bodmer, R., Jan, L. Y. and Jan, Y. N. (1990). Patterns of expression of Cut, a protein required for external sensory organ development in wild-type and *cut* mutant *Drosophila* embryos. *Genes and Development* **4**, 1322-1331.

Blochlinger, K., Jan, L. Y. and Jan, Y. N. (1991). Transformation of sensory organ identity by ectopic expression of Cut in Drosophila. *Genes Dev* **5**, 1124-35.

Bodmer, R., Barbel, S., Sheperd, S., Jack, J. W., Jan, L. Y. and Jan, Y. N. (1987). Transformation of sensory organs by mutations of the cut locus of D. melanogaster. *Cell* **51**, 293-307.

Bodmer, R., Carretto, R. and Jan, Y. N. (1989). Neurogenesis of the peripheral nervous system in Drosophila embryos: DNA replication patterns and cell lineages. *Neuron* **3**, 21-32.

Bodmer, R. and Jan, Y. N. (1987). Morphological differentiation of the embryonic peripheral neurons in *Drosophila. Roux's Archives of Developmental Biology* **196**, 69-77.

Boulianne, G. L., Delaconcha, A., Camposortega, J. A., Jan, L. Y. and Jan, Y. N. (1991). The Drosophila Neurogenic Gene Neuralized Encodes a Novel Protein and Is Expressed In Precursors Of Larval and Adult Neurons. *Embo Journal* **10**, 2975-2983.

Brand, A. H. and Perrimon, N. (1993). Targeted gene expression as a means of altering cell fates and generating dominant phenotypes. *Development* **118**, 401-415.

Brand, M., Jarman, A. P., Jan, L. Y. and Jan, Y. N. (1993). asense is a Drosophila neural precursor gene and is capable of initiating sense organ formation. *Development* **119**, 1-17.

Brewster, R. and Bodmer, R. (1995). Origin and specification of type II sensory neurons in Drosophila. *Development* **121**, 2923-36.

Brewster, R. and Bodmer, R. (1996). Cell lineage analysis of the Drosophila peripheral nervous system. *Dev Genet* **18**, 50-63.

Brewster, R., Hardiman, K., Deo, M., Khan, S. and Bodmer, R. (2001). The selector gene cut represses a neural cell fate that is specified independently of the Achaete-Scute-Complex and atonal. *Mech Dev* **105**, 57-68.

Brown, N. L., Dagenais, S. L., Chen, C. M. and Glaser, T. (2002). Molecular characterization and mapping of ATOH7, a human atonal homolog with a predicted role in retinal ganglion cell development. *Mamm Genome* **13**, 95-101.

Brown, N. L., Kanekar, S., Vetter, M. L., Tucker, P. K., Gemza, D. L. and Glaser, T. (1998). Math5 encodes a murine basic helix-loop-helix transcription factor expressed during early stages of retinal neurogenesis. *Development* **125**, 4821-4833.

Brown, N. L., Patel, S., Brzezinski, J. and Glaser, T. (2001). Math5 is required for retinal ganglion cell and optic nerve formation. *Development* **128**, 2497-508.

Brunet, J. F. and Ghysen, A. (1999). Deconstructing cell determination: proneural genes and neuronal identity. *Bioessays* **21**, 313-8.

Bush, A., Hiromi, Y. and Cole, M. (1996). Biparous: a novel bHLH gene expressed in neuronal and glial precursors in Drosophila. *Dev Biol* **180**, 759-72.

Cabrera, C. V. and Alonso, M. C. (1991). Transcriptional activation by heterodimers of the achaete-scute and daughterless gene products of Drosophila. *Embo J* **10**, 2965-73.

Cagan, R. (1993). Cell fate specification in the developing *Drosophila* retina. *Development* **S1**, 19-28.

Campuzano, S., Balcells, L., Villares, R., Carramolino, L., Garciaalonso, L. and Modolell, J. (1986). Excess Function Hairy-Wing Mutations Caused By Gypsy and Copia Insertions Within Structural Genes Of the Achaete-Scute Locus Of Drosophila. *Cell* **44**, 303-312.

Campuzano, S. and Modolell, J. (1992). Patterning of the *Drosophila* nervous system: the *achaete-scute* gene complex. *Trends in Genetics* **8**, 202-208.

Carmena, A., Bate, M. and Jimenez, F. (1995). Lethal of scute, a proneural gene, participates in the specification of muscle progenitors during Drosophila embryogenesis. *Genes Dev* **9**, 2373-83.

Casarosa, S., Fode, C. and Guillemot, F. (1999). Mash1 regulates neurogenesis in the ventral telencephalon. *Development* **126**, 525-34.

Cau, E., Gradwohl, G., Fode, C. and Guillemot, F. (1997). Mash1 activates a cascade of bHLH regulators in olfactory neuron progenitors. *Development* **124**, 1611-1621.

Chan, S. K. and Mann, R. S. (1996). A structural model for a homeotic protein-extradenticle-DNA complex accounts for the choice of HOX protein in the heterodimer. *Proc Natl Acad Sci U S A* **93**, 5223-8.

Chan, Y. M. and Jan, Y. N. (1999). Conservation of neurogenic genes and mechanisms. *Curr Opin Neurobiol* **9**, 582-8.

Chanut, F., Woo, K., Pereira, S., Donohoe, T. J., Chang, S. Y., Laverty, T. R., Jarman, A. P. and Heberlein, U. (2002). Rough eye is a gain-of-function allele of amos that disrupts regulation of the proneural gene atonal during Drosophila retinal differentiation. *Genetics* **160**, 623-35.

Chen, P., Johnson, J. E., Zoghbi, H. Y. and Segil, N. (2002). The role of Math1 in inner ear development: Uncoupling the establishment of the sensory primordium from hair cell fate determination. *Development* **129**, 2495-505.

Chien, C.-T., Hsiao, C.-D., Jan, L. Y. and Jan, Y. N. (1996). Neuronal type information encoded in the basic-helix-loop-helix domain of proneural genes. *Proceedings of the National Academy of Sciences, USA* **93**, 13239-13244.

Choi, J. K., Shen, C. P., Radomska, H. S., Eckhardt, L. A. and Kadesch, T. (1996). E47 activates the Ig-heavy chain and TdT loci in non-B cells. *Embo J* **15**, 5014-21.

Chung, Y. D., Zhu, J., Han, Y. and Kernan, M. J. (2001). nompA encodes a PNS-specific, ZP domain protein required to connect mechanosensory dendrites to sensory structures. *Neuron* **29**, 415-28.

Clyne, P., Grant, A., O'Connell, R. and Carlson, J. R. (1997). Odorant response of individual sensilla on the Drosophila antenna. *Invert Neurosci* **3**, 127-35.

Crews, S. T. (1998). Control of cell lineage-specific development and transcription by bHLH-PAS proteins. *Genes Dev* **12**, 607-20.

Cubadda, Y., Heitzler, P., Ray, R. P., Bourouis, M., Ramain, P., Gelbart, W., Simpson, P. and Haenlin, M. (1997). u-shaped encodes a zinc finger protein that regulates the proneural genes achaete and scute during the formation of bristles in Drosophila. *Genes Dev* **11**, 3083-95.

Cubas, P., de Celis, J. F., Campuzano, S. and Modolell, J. (1991). Proneural clusters of achaete-scute expression and the generation of sensory organs in the Drosophila imaginal wing disc. *Genes Dev* **5**, 996-1008.

Culi, J., Martin-Blanco, E. and Modolell, J. (2001). The EGF receptor and N signalling pathways act antagonistically in Drosophila mesothorax bristle patterning. *Development* **128**, 299-308.

Dambly-Chaudière, C. and Ghysen, A. (1987). Independent subpatterns of sense organs require independent genes of the *achaete-scute* complex in *Drosophila* larvae. *Genes and Development* **1**, 297-306.

Dang, C. V., Dolde, C., Gillison, M. L. and Kato, G. J. (1992). Discrimination between related DNA sites by a single amino acid residue of Myc-related basic-helix-loop-helix proteins. *Proc Natl Acad Sci U S A* **89**, 599-602.

Davis, R. L., Weintraub, H. and Lassar, A. B. (1987). Expression of a single transfected cDNA converts fibroblasts to myoblasts. *Cell* **51**, 987-1000.

de Bruyne, M., Clyne, P. J. and Carlson, J. R. (1999). Odor coding in a model olfactory organ: the Drosophila maxillary palp. *J Neurosci* **19**, 4520-32.

de Bruyne, M., Foster, K. and Carlson, J. R. (2001). Odor coding in the Drosophila antenna. *Neuron* **30**, 537-52.

Doe, C. Q., Chu-LaGraff, Q., Wright, D. M. and Scott, M. P. (1991). The *prospero* gene specifies cell fates in the *Drosophila* central nervous system. **65**, 451-464.

Doe, C. Q. and Goodman, C. S. (1985). Early events in insect neurogenesis: I. The role of cell interactions and cell lineage in the determination of neuronal precursor cells. *Developmental Biology* **111**, 206-219.

Dokucu, M. E., Zipursky, S. L. and Cagan, R. L. (1996). Atonal, rough and the resolution of proneural clusters in the developing Drosophila retina. *Development* **122**, 4139-4147.

Domínguez, M., Wasserman, J. D. and Freeman, M. (1998). Multiple functions of the EGF receptor in *Drosophila* eye development. *Current Biology* **8**, 1039-1048.

Ellenberger, T., Fass, D., Arnaud, M. and Harrison, S. C. (1994). Crystal structure of transcription factor E47: E-box recognition by a basic region helix-loop-helix dimer. *Genes Dev* **8**, 970-80.

Ellis, H. M., Spann, D. R. and Posakony, J. W. (1990). extramacrochaetae, a negative regulator of sensory organ development in Drosophila, defines a new class of helix-loop-helix proteins. *Cell* **61**, 27-38.

Emerald, B. S., Curtiss, J., Mlodzik, M. and Cohen, S. M. (2003). Distal antenna and distal antenna related encode nuclear proteins containing pipsqueak motifs involved in antenna development in Drosophila. *Development* **130**, 1171-80.

Emery, J. F. and Bier, E. (1995). Specificity of CNS and PNS regulatory subelements comprising pan-neural enhancers of the deadpan and scratch genes is achieved by repression. *Development* **121**, 3549-60.

Fichelson, P. and Gho, M. (2003). The glial cell undergoes apoptosis in the microchaete lineage of Drosophila. *Development* **130**, 123-33.

Fisher, A. and Caudy, M. (1998). The function of hairy-related bHLH repressor proteins in cell fate decisions. *Bioessays* **20**, 298-306.

Fisher, A. L., Ohsako, S. and Caudy, M. (1996). The Wrpw Motif Of the Hairy-Related Basic Helix-Loop-Helix Repressor Proteins Acts As a 4-Amino-Acid Transcription Repression and Protein- Protein Interaction Domain. *Molecular and Cellular Biology* **16**, 2670-2677.

Fode, C., Gradwohl, G., Morin, X., Dierich, A., LeMeur, M., Goridis, C. and Guillemot, F. (1998). The bHLH protein NEUROGENIN 2 is a determination factor for epibranchial placode-derived sensory neurons. *Neuron* **20**, 483-94.

Fortini, M. E. and Artavanis-Tsakonas, S. (1994). The suppressor of hairless protein participates in notch receptor signaling. *Cell* **79**, 273-82.

Freeman, M. (1994). The *spitz* gene is required for photoreceptor determination in the *Drosophila* eye where it interacts with the EGF receptor. *Mechanisms of Development* **48**, 25-33.

Freeman, M. (1996). Reiterative use of the EGF receptor triggers differentiation of all cell types in the *Drosophila* eye. *Cell* **87**, 651-660.

Garrell, J. and Modolell, J. (1990). The Drosophila extramacrochaetae locus, an antagonist of proneural genes that, like these genes, encodes a helix-loop-helix protein. *Cell* **61**, 39-48.

Gautier, P., Ledent, V., Massaer, M., Dambly-Chaudiere, C. and Ghysen, A. (1997). tap, a Drosophila bHLH gene expressed in chemosensory organs. *Gene* **191**, 15-21.

Gho, M., Bellaiche, Y. and Schweisguth, F. (1999). Revisiting the Drosophila microchaete lineage: a novel intrinsically asymmetric cell division generates a glial cell. *Development* **126**, 3573-84.

Ghysen, A., Dambly-Chaudiere, C., Jan, L. Y. and Jan, Y. N. (1993). Cell interactions and gene interactions in peripheral neurogenesis. *Genes Dev* **7**, 723-33.

Ghysen, A. and O'Kane, C. (1989). Neural enhancer-like elements as specific cell markers in *Drosophila*. *Development* **105**, 35-52.

Giebel, B., Stuttem, I., Hinz, U. and Campos-Ortega, J. A. (1997). Lethal of scute requires overexpression of daughterless to elicit ectopic neuronal development during embryogenesis in Drosophila. *Mech Dev* **63**, 75-87.

Goding, C. R. (2000). Mitf from neural crest to melanoma: signal transduction and transcription in the melanocyte lineage. *Genes Dev* **14**, 1712-28.

Goldfarb, A. N., Lewandowska, K. and Pennell, C. A. (1998). Identification of a highly conserved module in E proteins required for in vivo helix-loop-helix dimerization. *J Biol Chem* **273**, 2866-73.

Gomez-Skarmeta, J. L., Diez del Corral, R., de la Calle-Mustienes, E., Ferre-Marco, D. and Modolell, J. (1996). Araucan and caupolican, two members of the novel iroquois complex, encode homeoproteins that control proneural and vein-forming genes. *Cell* **85**, 95-105.

Goriely, A., Dumont, N., Dambly-Chaudière, C. and Ghysen, A. (1991). The determination of sense organs in *Drosophila*: effect of the neurogenic mutations in the embryo. *Development* **113**, 1395-1404.

Goulding, S. E., White, N. M. and Jarman, A. P. (2000a). *cato* encodes a basic-helix-loop-helix transcription factor implicated in the correct differentiation of *Drosophila* sense organs. *Developmental Biology* **221**, 120–131.

Goulding, S. E., zur Lage, P. and Jarman, A. P. (2000b). amos, a proneural gene for Drosophila olfactory sense organs that is regulated by lozenge. *Neuron* **25**, 69-78.

Gowan, K., Helms, A. W., Hunsaker, T. L., Collisson, T., Ebert, P. J., Odom, R. and Johnson, J. E. (2001). Crossinhibitory activities of Ngn1 and Math1 allow specification of distinct dorsal interneurons. *Neuron* **31**, 219-32.

Gradwohl, G., Fode, C. and Guillemot, F. (1996). Restricted expression of a novel murine atonal-related bHLH protein in undifferentiated neural precursors. *Dev Biol* **180**, 227-41.

Guillemot, F., Lo, L. C., Johnson, J. E., Auerbach, A., Anderson, D. J. and Joyner, A. L. (1993). Mammalian achaete-scute homolog 1 is required for the early development of olfactory and autonomic neurons. *Cell* **75**, 463-76.

Guo, M., Bier, E., Jan, L. Y. and Jan, Y. N. (1995). tramtrack acts downstream of numb to specify distinct daughter cell fates during asymmetric cell divisions in the Drosophila PNS. *Neuron* **14**, 913-25.

Gupta, B. P. and Rodrigues, V. (1997). Atonal is a proneural gene for a subset of olfactory sense organs in Drosophila. *Genes Cells* **2**, 225-33.

Haenlin, M., Cubadda, Y., Blondeau, F., Heitzler, P., Lutz, Y., Simpson, P. and Ramain, P. (1997). Transcriptional activity of pannier is regulated negatively by heterodimerization of the GATA DNA-binding domain with a cofactor encoded by the u-shaped gene of Drosophila. *Genes Dev* **11**, 3096-108.

Hartenstein, A. Y., Rugendorff, A., Tepass, U. and Hartenstein, V. (1992). The Function Of the Neurogenic Genes During Epithelial Development In the Drosophila Embryo. *Development* **116**, 1203-1220.

Hartenstein, V. and Posakony, J. W. (1989). Development of adult sensilla on the wing and notum of Drosophila melanogaster. *Development* **107**, 389-405.

Hartenstein, V. and Posakony, J. W. (1990). A dual function of the Notch gene in Drosophila sensillum development. *Dev Biol* **142**, 13-30.

Hartenstein, V., Younossi-Hartenstein, A. and Lekven, A. (1994). Delamination and division in the Drosophila neurectoderm: spatiotemporal pattern, cytoskeletal dynamics, and common control by neurogenic and segment polarity genes. *Dev Biol* **165**, 480-99.

Hassan, B. A. and Bellen, H. J. (2000). Doing the MATH: is the mouse a good model for fly development? *Genes Dev* **14**, 1852-65.

Heitzler, P., Bourouis, M., Ruel, L., Carteret, C. and Simpson, P. (1996). Genes of the Enhancer of split and achaete-scute complexes are required for a regulatory loop between Notch and Delta during lateral signalling in Drosophila. *Development* **122**, 161-171.

Helms, A. W. and Johnson, J. E. (1998). Progenitors of dorsal commissural interneurons are defined by MATH1 expression. *Development* **125**, 919-28.

Henriksson, M. and Luscher, B. (1996). Proteins of the Myc network: essential regulators of cell growth and differentiation. *Adv Cancer Res* **68**, 109-82.

Henrique, D., Tyler, D., Kintner, C., Heath, J. K., Lewis, J. H., IshHorowicz, D. and Storey, K. G. (1997). cash4, a novel achaete-scute homolog induced by Hensen's node during generation of the posterior nervous system. *GENES & DEVELOPMENT* **11**, 603-615.

Hirsch, M. R., Tiveron, M. C., Guillemot, F., Brunet, J. F. and Goridis, C. (1998). Control of noradrenergic differentiation and Phox2a expression by MASH1 in the central and peripheral nervous system. *Development* **125**, 599-608.

Hitchcock, P. and Kakuk-Atkins, L. (2004). The basic helix-loop-helix transcription factor neuroD is expressed in the rod lineage of the teleost retina. *J Comp Neurol* **477**, 108-17.

Hsu, H. L., Huang, L., Tsan, J. T., Funk, W., Wright, W. E., Hu, J. S., Kingston, R. E. and Baer, R. (1994). Preferred sequences for DNA recognition by the TAL1 helix-loop-helix proteins. *Mol Cell Biol* **14**, 1256-65.

Hsu, H. L., Wadman, I. and Baer, R. (1994). Formation of in vivo complexes between the TAL1 and E2A polypeptides of leukemic T cells. *Proc Natl Acad Sci U S A* **91**, 3181-5.

Huang, F., Dambly-Chaudiere, C. and Ghysen, A. (1991). The emergence of sense organs in the wing disc of Drosophila. *Development* **111**, 1087-95.

Huang, H. P., Liu, M., El-Hodiri, H. M., Chu, K., Jamrich, M. and Tsai, M. J. (2000a). Regulation of the pancreatic islet-specific gene BETA2 (neuroD) by neurogenin 3. *Mol Cell Biol* **20**, 3292-307.

Huang, M. L., Hsu, C. H. and Chien, C. T. (2000b). The proneural gene amos promotes multiple dendritic neuron formation in the Drosophila peripheral nervous system. *Neuron* **25**, 57-67.

Inoue, T., Hojo, M., Bessho, Y., Tano, Y., Lee, J. E. and Kageyama, R. (2002). Math3 and NeuroD regulate amacrine cell fate specification in the retina. *Development* **129**, 831-42.

Isaka, F., Shimizu, C., Nakanishi, S. and Kageyama, R. (1996). GENETIC-MAPPING OF 4 MOUSE BHLH GENES RELATED TO DROSOPHILA PRONEURAL GENE ATONAL Download Full Text of Article. *Genomics* **37**, 400-402.

Jack, J. W. (1985). Molecular organization of the cut locus of Drosophila melanogaster. *Cell* **42**, 869-76.

Jan, L. Y. and Jan, Y. N. (1982). Antibodies to horseradish peroxidase as specific neuronal markers in Drosophila and in grasshopper embryos. *Proc Natl Acad Sci U S A* **79**, 2700-4.

Jan, Y. N. and Jan, L. Y. (1993). HLH proteins, fly neurogenesis, and vertebrate myogenesis. *Cell* **75**, 827-30.

Jan, Y. N. and Jan, L. Y. (1993). The peripheral nervous system. In *The Development of Drosophila melanogaster*, vol. 2 (ed. M. Bate and A. Martinez-Arias), pp. 1207-1244. New York: Cold Spring Harbor Press.

Jarman, A. P. (2002). Studies of mechanosensation using the fly. *Hum Mol Genet* **11**, 1215-8.

Jarman, A. P. and Ahmed, I. (1998). The specificity of proneural genes in determining Drosophila sense organ identity. *Mech Dev* **76**, 117-25.

Jarman, A. P., Brand, M., Jan, L. Y. and Jan, Y. N. (1993a). The regulation and function of the helix-loop-helix gene, asense, in Drosophila neural precursors. *Development* **119**, 19-29.

Jarman, A. P., Grau, Y., Jan, L. Y. and Jan, Y. N. (1993b). atonal is a proneural gene that directs chordotonal organ formation in the Drosophila peripheral nervous system. *Cell* **73**, 1307-21.

Jarman, A. P., Grell, E. H., Ackerman, L., Jan, L. Y. and Jan, Y. N. (1994). Atonal is the proneural gene for Drosophila photoreceptors. *Nature* **369**, 398-400.

Jarman, A. P. and Jan, Y. N. (1995a). Multiple roles for proneural genes in *Drosophila* neurogenesis. In *Neural Cell Specification: Molecular Mechanisms and Neurotherapeutic Implications*, vol. 3 (ed. B. H. J. Juurlink P. H. Krone W. M. Kulyk V. M. K. Verge and J. R. Doucette), pp. 97-104. New York: Plenum Press.

Jarman, A. P., Sun, Y., Jan, L. Y. and Jan, Y. N. (1995b). Role of the proneural gene, atonal, in formation of Drosophila chordotonal organs and photoreceptors. *Development* **121**, 2019-30.

Kanekar, S., Perron, M., Dorsky, R., Harris, W. A., Jan, L. Y., Jan, Y. N. and Vetter, M. L. (1997a). Xath5 participates in a network of bHLH genes in the developing Xenopus retina. *Neuron* **19**, 981-94.

Kanekar, S., Perron, M., Harris, W. A., Jan, L. Y., Jan, Y. N. and Vetter, M. L. (1997b). Xath5, a Xenopus homolog of the Drosophila proneural gene atonal, functions with Xash3 and NeuroD to regulate retinal neurogenesis. *Developmental Biology* **186**, A239-A239.

Kay, J. N., Finger-Baier, K. C., Roeser, T., Staub, W. and Baier, H. (2001). Retinal ganglion cell genesis requires lakritz, a Zebrafish atonal Homolog. *Neuron* **30**, 725-36.

Kim, P., Helms, A. W., Johnson, J. E. and Zimmerman, K. (1997). XATH-1, a vertebrate homolog of Drosophila atonal, induces a neuronal differentiation within ectodermal progenitors. *Dev Biol* **187**, 1-12.

Kumar, J. P., Tio, M., Hsiung, F., Akopyan, S., Gabay, L., Seger, R., Shilo, B. Z. and Moses, K. (1998). Dissecting the roles of the Drosophila EGF receptor in eye development and MAP kinase activation. *Development* **125**, 3875-85.

Kunisch, M., Haenlin, M. and Campos-Ortega, J. A. (1994). Lateral inhibition mediated by the Drosophila neurogenic gene delta is enhanced by proneural proteins. *Proc Natl Acad Sci U S A* **91**, 10139-43.

Kunne, A. G. and Allemann, R. K. (1997). Covalently linking BHLH subunits of MASH-1 increases specificity of DNA binding. *Biochemistry* **36**, 1085-91.

Lai, E. C. (2003). Drosophila Tufted Is a Gain-of-Function Allele of the Proneural Gene amos. *Genetics* **163**, 1413-25.

Lassar, A. B., Davis, R. L., Wright, W. E., Kadesch, T., Murre, C., Voronova, A., Baltimore, D. and Weintraub, H. (1991). Functional activity of myogenic HLH proteins requires hetero-oligomerization with E12/E47-like proteins in vivo. *Cell* **66**, 305-15.

Ledent, V. and Vervoort, M. (2001). The basic helix-loop-helix protein family: comparative genomics and phylogenetic analysis. *Genome Res* **11**, 754-70.

Lee, E. C., Hu, X., Yu, S. Y. and Baker, N. E. (1996). The scabrous gene encodes a secreted glycoprotein dimer and regulates proneural development in Drosophila eyes. *Molecular and Cellular Biology* **16**, 1179-1188.

Lee, J. E. (1997). NeuroD and neurogenesis. *Dev Neurosci* **19**, 27-32.

Lee, J. E., Hollenberg, S. M., Snider, L., Turner, D. L., Lipnick, N. and Weintraub, H. (1995). Conversion of *Xenopus* ectoderm into neurons by *NeuroD*, a basic helix-loop-helix protein. *Science* **268**, 836-844.

Leyns L, Gomez-Skarmeta JL, Dambly-Chaudiere C. (1996). iroquois: a prepattern gene that controls the formation of bristles on the thorax of Drosophila. *Mechanisms of Development* **59 (1)** 63-72.

Li, L. and Vaessin, H. (2000). Pan-neural Prospero terminates cell proliferation during Drosophila neurogenesis. *Genes Dev* **14**, 147-51.

Li, X., Veraksa, A. and McGinnis, W. (1999). A sequence motif distinct from Hox binding sites controls the specificity of a Hox response element. *Development* **126**, 5581-9.

Liao, J., He, J., Yan, T., Korzh, V. and Gong, Z. (1999). A class of neuroD-related basic helix-loop-helix transcription factors expressed in developing central nervous system in zebrafish. *DNA Cell Biol* **18**, 333-44.

Lo, L., Dormand, E., Greenwood, A. and Anderson, D. J. (2002). Comparison of the generic neuronal differentiation and neuron subtype specification functions of mammalian achaete-scute and atonal homologs in cultured neural progenitor cells. *Development* **129**, 1553-67.

Ma, P. C. M., Rould, M. A., Weintraub, H. and Pabo, C. O. (1994). Crystal structure of MyoD bHLH domain-DNA complex: perspectives on DNA recognition and implications for transcriptional activation. *Cell* 77, 451-459.

Ma, Q., Chen, Z., del Barco Barrantes, I., de la Pompa, J. L. and Anderson, D. J. (1998). neurogenin1 is essential for the determination of neuronal precursors for proximal cranial sensory ganglia. *Neuron* **20**, 469-82.

Ma, Q., Kintner, C. and Anderson, D. J. (1996). Identification of neurogenin, a vertebrate neuronal determination gene. *Cell* **87**, 43-52.

Martin-Bermudo, M. D., Gonzalez, F., Dominguez, M., Rodriguez, I., Ruiz-Gomez, M., Romani, S., Modolell, J. and Jimenez, F. (1993). Molecular characterization of the lethal of scute genetic function. *Development* **118**, 1003-12.

Massari, M. E. and Murre, C. (2000). Helix-loop-helix proteins: regulators of transcription in eucaryotic organisms. *Mol Cell Biol* **20**, 429-40.

McIver, S. B. (1985). Mechanoreception. In *Comprehensive Insect Physiology, Biochemistry and Pharmacology*, vol. 6 (ed. L. I. Gilbert and D. A. Kerkut), pp. 71-132. New York/London: Pergamon Press.

Merritt, D. J. (1997). Transformation of external sensilla to chordotonal sensilla in the cut mutant of Drosophila assessed by single-cell marking in the embryo and larva. *Microsc Res Tech* **39**, 492-505.

Merritt, D. J., Hawken, A. and Whitington, P. M. (1993). The role of the cut gene in the specification of central projections by sensory axons in Drosophila. *Neuron* **10**, 741-52.

Miyachi, T., Maruyama, H., Kitamura, T., Nakamura, S. and Kawakami, H. (1999). Structure and regulation of the human NeuroD (BETA2/BHF1) gene. *Brain Res Mol Brain Res* **69**, 223-31.

Miyata, T., Maeda, T. and Lee, J. E. (1999). NeuroD is required for differentiation of the granule cells in the cerebellum and hippocampus. *Genes Dev* **13**, 1647-52.

Mlodzik, M., Baker, N. E. and Rubin, G. M. (1990). Isolation and expression of scabrous, a gene regulating neurogenesis in Drosophila. *Genes Dev* **4**, 1848-61.

Molkentin, J. D. and Olson, E. N. (1996). Combinatorial control of muscle development by basic helix-loop-helix and MADS-box transcription factors. *Proc Natl Acad Sci U S A* **93**, 9366-73.

Moore, A. W., Jan, L. Y. and Jan, Y. N. (2002). hamlet, a binary genetic switch between single- and multiple- dendrite neuron morphology. *Science* **297**, 1355-8.

Morrow, E. M., Furukawa, T., Lee, J. E. and Cepko, C. L. (1999). NeuroD regulates multiple functions in the developing neural retina in rodent. *Development* **126**, 23-36.

Moulins, M. (1976). Ultrastructure of chordotonal organs. In *Structure and Function of Proprioceptors in the Invertebrates*, (ed. P. J. Mill), pp. 387-426. London: Chapman and Hall.

Murre, C., McCaw, P. S. and Baltimore, D. (1989). A new DNA binding and dimerization motif in immunoglobulin enhancer binding, daughterless, MyoD, and myc proteins. *Cell* **56**, 777-83.

Murre, C., McCaw, P. S., Vaessin, H., Caudy, M., Jan, L. Y., Jan, Y. N., Cabrera, C. V., Buskin, J. N., Hauschka, S. D., Lassar, A. B. et al. (1989). Interactions between heterologous helix-loop-helix proteins generate complexes that bind specifically to a common DNA sequence. *Cell* **58**, 537-44.

Nakada, Y., Hunsaker, T. L., Henke, R. M. and Johnson, J. E. (2004). Distinct domains within Mash1 and Math1 are required for function in neuronal differentiation versus neuronal cell-type specification. *Development* **131**, 1319-30.

Nieto, M., Schuurmans, C., Britz, O. and Guillemot, F. (2001). Neural bHLH genes control the neuronal versus glial fate decision in cortical progenitors. *Neuron* **29**, 401-13.

Okabe, M. and Okano, H. (1997). Two-step induction of chordotonal organ precursors in Drosophila embryogenesis. *Development* **124**, 1045-53.

Orgogozo, V., Schweisguth, F. and Bellaiche, Y. (2001). Lineage, cell polarity and inscuteable function in the peripheral nervous system of the Drosophila embryo. *Development* **128**, 631-43.

Orgogozo, V., Schweisguth, F. and Bellaiche, Y. (2002). Binary cell death decision regulated by unequal partitioning of Numb at mitosis. *Development* **129**, 4677-84.

Park, S. H., Yeo, S. Y., Yoo, K. W., Hong, S. K., Lee, S., Rhee, M., Chitnis, A. B. and Kim, C. H. (2003). Zath3, a neural basic helix-loop-helix gene, regulates early neurogenesis in the zebrafish. *Biochem Biophys Res Commun* **308**, 184-90.

Porcher, C., Liao, E. C., Fujiwara, Y., Zon, L. I. and Orkin, S. H. (1999). Specification of hematopoietic and vascular development by the bHLH transcription factor SCL without direct DNA binding. *Development* **126**, 4603-15.

Porcher, C., Swat, W., Rockwell, K., Fujiwara, Y., Alt, F. W. and Orkin, S. H. (1996). The T cell leukemia oncoprotein SCL/tal-1 is essential for development of all hematopoietic lineages. *Cell* **86**, 47-57.

Powell, L. M., zur Lage, P.I., Prentice, D.R.A., Senthinathan, B. and Jarman, A.P. (2004). The proneural proteins Atonal and Scute regulate neural target genes through different E-box binding sites. *Mol. Cell. Biol* **24**.

Quan, X. J., Denayer, T., Yan, J., Jafar-Nejad, H., Philippi, A., Lichtarge, O., Vleminckx, K. and Hassan, B. A. (2004). Evolution of neural precursor selection: functional divergence of proneural proteins. *Development* **131**, 1679-89.

Ramain, P., Heitzler, P., Haenlin, M. and Simpson, P. (1993). pannier, a negative regulator of achaete and scute in Drosophila, encodes a zinc finger protein with homology to the vertebrate transcription factor GATA-1. *Development* **119**, 1277-91.

Ramain, P., Khechumian, R., Khechumian, K., Arbogast, N., Ackermann, C. and Heitzler, P. (2000). Interactions between chip and the achaete/scute-daughterless heterodimers are required for pannier-driven proneural patterning. *Mol Cell* **6**, 781-90.

Ray, K. and Rodrigues, V. (1995). Cellular events during development of the olfactory sense organs in *Drosophila melanogaster*. *Developmental Biology* **167**, 426-438.

Reddy, G. V., Gupta, B., Ray, K. and Rodrigues, V. (1997). Development of the Drosophila olfactory sense organs utilizes cell-cell interactions as well as lineage. *Development* **124**, 703-12.

Rhyu, M. S., Jan, L. Y. and Jan, Y. N. (1994). Asymmetric distribution of numb protein during division of the sensory organ precursor cell confers distinct fates to daughter cells. *Cell* **76**, 477-91.

Roark, M., Sturtevant, M. A., Emery, J., Vaessin, H., Grell, E. and Bier, E. (1995). *scratch*, a pan-neural gene encoding a zinc finger protein related to Snail, promotes neuronal development. *Genes and Development* **9**, 2384-98.

Rodriguez, I., Hernandez, R., Modolell, J. and Ruiz-Gomez, M. (1990). Competence to develop sensory organs is temporally and spatially regulated in Drosophila epidermal primordia. *Embo J* **9**, 3583-92.

Romani, S., Campuzano, S., Macagno, E. R. and Modolell, J. (1989). Expression of achaete and scute genes in Drosophila imaginal discs and their function in sensory organ development. *Genes Dev* **3**, 997-1007.

Roztocil, T., Matter-Sadzinski, L., Alliod, C., Ballivet, M. and Matter, J. M. (1997). NeuroM, a neural helix-loop-helix transcription factor, defines a new transition stage in neurogenesis. *Development* **124**, 3263-72.

Sato, M. and Saigo, K. (2000). Involvement of pannier and u-shaped in regulation of decapentaplegic-dependent wingless expression in developing Drosophila notum. *Mech Dev* **93**, 127-38.

Schweisguth, F., Gho, M. and Lecourtois, M. (1996). Control of cell fate choices by lateral signaling in the adult peripheral nervous system of Drosophila melanogaster. *Dev Genet* **18**, 28-39.

Sen, A., Kuruvilla, D., Pinto, L., Sarin, A., and Rodrigues, V., (2004). Programmed cell death and context dependent activation of the EGF pathway regulate gliogenesis in the Drosophila olfactory system. *Mech Dev* **121**, 65-78.

Shanbhag, S. R., Müller, B. and Steinbrecht, R. A. (1999). Atlas of olfactory organs of Drosophila melanogaster 1. Types, external organization, innervation and distribution of olfactory sensilla. *International Journal of Insect Morphology and Embryology* **28**, 377-397.

Shao, D., Creasy, C. L. and Bergman, L. W. (1998). A cysteine residue in helixII of the bHLH domain is essential for homodimerization of the yeast transcription factor Pho4p. *Nucleic Acids Res* **26**, 710-4.

Shao, R., Karunagaran, D., Zhou, B. P., Li, K., Lo, S. S., Deng, J., Chiao, P. and Hung, M. C. (1997). Inhibition of nuclear factor-kappaB activity is involved in E1A-mediated sensitization of radiation-induced apoptosis. *J Biol Chem* **272**, 32739-42.

Shimizu, C., Akazawa, C., Nakanishi, S. and Kageyama, R. (1995). MATH-2, a mammalian helix-loop-helix factor structurally related to the product of Drosophila proneural gene atonal, is specifically expressed in the nervous system. *European Journal of Biochemistry* **229**, 239-248.

Simpson, P. (1997). Notch signalling in development: on equivalence groups and asymmetric developmental potential. *CURRENT OPINION IN GENETICS & DEVELOPMENT* **7**, 537-542.

Skeath, J. B. and Carroll, S. B. (1991). Regulation of achaete-scute gene expression and sensory organ pattern formation in the Drosophila wing. *Genes Dev* **5**, 984-95.
Skeath, J. B., Panganiban, G., Selegue, J. and Carroll, S. B. (1992). Gene regulation in two dimensions: the proneural achaete and scute genes are controlled by combinations of axis-patterning genes through a common intergenic control region. *Genes Dev* **6**, 2606-19.

Sommer, L., Ma, Q. and Anderson, D. J. (1996). neurogenins, a novel family of atonal-related bHLH transcription factors, are putative mammalian neuronal determination genes that reveal progenitor cell heterogeneity in the developing CNS and PNS. *Mol Cell Neurosci* **8**, 221-41.

Sommer, L., Ma, Q. F. and Anderson, D. J. (1996). neurogenins, a novel family of atonal-related bHLH transcription factors, are putative mammalian neuronal determination genes that reveal progenitor cell heterogeneity in the developing CNS and PNS Download Full Text of Article. *Molecular and Cellular Neuroscience* **8**, 221-241.

Stocker, R. F. (1994). The organization of the chemosensory system in Drosophila melanogaster: a review. *Cell Tissue Res* **275**, 3-26.

Stocker, R. F. (2001). Drosophila as a focus in olfactory research: mapping of olfactory sensilla by fine structure, odor specificity, odorant receptor expression, and central connectivity. *Microsc Res Tech* **55**, 284-96.

Stocker, R. F., Gendre, N. and Batterham, P. (1993). Analysis of the antennal phenotype in the Drosophila mutant lozenge. *J Neurogenet* **9**, 29-53.

Sun, X. and Artavanistsakonas, S. (1996). The Intracellular Deletions Of Delta and Serrate Define Dominant- Negative Forms Of the Drosophila Notch Ligands. *Development* **122**, 2465-2474.

Sun, Y., Kanekar, S. L., Vetter, M. L., Gorski, S., Jan, Y. N., Glaser, T. and Brown, N. L. (2003). Conserved and divergent functions of Drosophila atonal, amphibian, and mammalian Ath5 genes. *Evol Dev* **5**, 532-41.

Sun, Y., Nadal-Vicens, M., Misono, S., Lin, M. Z., Zubiaga, A., Hua, X., Fan, G. and Greenberg, M. E. (2001). Neurogenin promotes neurogenesis and inhibits glial differentiation by independent mechanisms. *Cell* **104**, 365-76.

Sun, Y., Jan, L. Y. and Jan, Y. N. (2000). Ectopic scute induces Drosophila ommatidia development without R8 founder photoreceptors. *Proc Natl Acad Sci U S A* **97**, 6815-9.

Takebayashi, K., Takahashi, S., Yokota, C., Tsuda, H., Nakanishi, S., Asashima, M. and Kageyama, R. (1997). Conversion of ectoderm into a neural fate by ATH-3, a vertebrate basic helix-loop-helix gene homologous to Drosophila proneural gene atonal. *Embo J* **16**, 384-95.

Tapscott, S. J., Davis, R. L., Thayer, M. J., Cheng, P. F., Weintraub, H. and Lassar, A. B. (1988). MyoD1: a nuclear phosphoprotein requiring a Myc homology region to convert fibroblasts to myoblasts. *Science* **242**, 405-11.

Thiem, S. M. and Miller, L. K. (1989). A baculovirus gene with a novel transcription pattern encodes a polypeptide with a zinc finger and a leucine zipper. *J Virol* **63**, 4489-97.

Tio, M., Ma, C. and Moses, K. (1994). *spitz*, a *Drosophila* homolog of transforming growth factor-a, is required in the founding photoreceptor cells of the compound eye facets. *Mechanisms of Development* **48**, 13-23.

Tomita, K., Nakanishi, S., Guillemot, F. and Kageyama, R. (1996). Mash1 Promotes Neuronal Differentiation In the Retina. *Genes to Cells* **1**, 765-774.

Tomlinson, A. and Ready, D. F. (1987). Cell Fate In the Drosophila Ommatidium. *Developmental Biology* **123**, 264-275.

Uemura, T., Shepherd, S., Ackerman, L., Jan, L. Y. and Jan, Y. N. (1989). numb, a gene required in determination of cell fate during sensory organ formation in Drosophila embryos. *Cell* **58**, 349-60.

Vaessin, H., Grell, E., Wolff, E., Bier, E., Jan, L. Y. and Jan, Y. N. (1991). prospero is expressed in neuronal precursors and encodes a nuclear protein that is involved in the control of axonal outgrowth in Drosophila. *Cell* **67**, 941-53.

Van De Bor, V. and Giangrande, A. (2001). Notch signaling represses the glial fate in fly PNS. *Development* **128**, 1381-90.

Van Doren, M., Powell, P. A., Pasternak, D., Singson, A. and Posakony, J. W. (1992). Spatial regulation of proneural gene activity: auto- and cross-activation of achaete is antagonized by extramacrochaetae. *Genes Dev* **6**, 2592-605.

Vervoort, M., Merritt, D. J., Ghysen, A. and Dambly-Chaudiere, C. (1997). Genetic basis of the formation and identity of type I and type II neurons in Drosophila embryos. *Development* **124**, 2819-28.

Vetter, M. L. and Brown, N. L. (2001). The role of basic helix-loop-helix genes in vertebrate retinogenesis. *Semin Cell Dev Biol* **12**, 491-8.

Villa-Cuesta, E., De Navascues, J., Ruiz-Gomez, M., Del Corral, R. D., Dominguez, M., De Celis, J. F. and Modolell, J. (2003). Tufted Is a Gain-of-Function Allele That Promotes Ectopic Expression of the Proneural Gene amos in Drosophila. *Genetics* **163**, 1403-12.

Voronova, A. and Baltimore, D. (1990). Mutations that disrupt DNA binding and dimer formation in the E47 helix-loop-helix protein map to distinct domains. *Proc Natl Acad Sci U S A* **87**, 4722-6.

Wang, V. Y., Hassan, B. A., Bellen, H. J. and Zoghbi, H. Y. (2002). Drosophila atonal fully rescues the phenotype of Math1 null mice: new functions evolve in new cellular contexts. *Curr Biol* **12**, 1611-1616.

Wang, X., Emelyanov, A., Korzh, V. and Gong, Z. (2003). Zebrafish atonal homologue zath3 is expressed during neurogenesis in embryonic development. *Dev Dyn* **227**, 587-92.

Wendt, H., Thomas, R. M. and Ellenberger, T. (1998). DNA-mediated folding and assembly of MyoD-E47 heterodimers. *J Biol Chem* **273**, 5735-43.

White, N. M. and Jarman, A. P. (2000). Drosophila atonal controls photoreceptor R8-specific properties and modulates both receptor tyrosine kinase and Hedgehog signalling. *Development* **127**, 1681-9.

Yan, R. T. and Wang, S. Z. (1998). neuroD induces photoreceptor cell overproduction in vivo and de novo generation in vitro. *J Neurobiol* **36**, 485-96.

Yan, R. T. and Wang, S. Z. (2004). Requirement of neuroD for photoreceptor formation in the chick retina. *Invest Ophthalmol Vis Sci* **45**, 48-58.

Yang, L. and Baker, N. E. (2001). Role of the EGFR/Ras/Raf pathway in specification of photoreceptor cells in the Drosophila retina. *Development* **128**, 1183-91.

Younossi-Hartenstein, A., Nassif, C., Green, P. and Hartenstein, V. (1996). Early neurogenesis of the Drosophila brain. *J Comp Neurol* **370**, 313-29.

Zhang, J. M., Chen, L., Krause, M., Fire, A. and Paterson, B. M. (1999). Evolutionary conservation of MyoD function and differential utilization of E proteins. *Dev Biol* **208**, 465-72.

Zhuang, Y., Cheng, P. and Weintraub, H. (1996). B-lymphocyte development is regulated by the combined dosage of three basic helix-loop-helix genes, E2A, E2-2, and HEB. *Mol Cell Biol* **16**, 2898-905.

Zhuang, Y., Soriano, P. and Weintraub, H. (1994). The helix-loop-helix gene E2A is required for B cell formation. *Cell* **79**, 875-84.

Zipursky, S. L., Venkatesh, T. R., Teplow, D. B. and Benzer, S. (1984). Neuronal development in the Drosophila retina: monoclonal antibodies as molecular probes. *Cell* **36**, 15-26.

zur Lage, P., Jan, Y. N. and Jarman, A. P. (1997). Requirement for EGF receptor signalling in neural recruitment during formation of *Drosophila* chordotonal sense organ clusters. *Current Biology* **7**, 166-175.

zur Lage, P. and Jarman, A. P. (1999). Antagonism of EGFR and notch signalling in the reiterative recruitment of Drosophila adult chordotonal sense organ precursors. *Development* **126**, 3149-57.

zur Lage, P. I., Powell, L.M. Prentice, D.R.A., McLaughlin, P. and Jarman, A.P. (2004). EGF receptor signalling triggers recruitment of *Drosophila* sense organ precursors by stimulating proneural gene autoregulation. *Dev. Cell.*

zur Lage, P. I., Prentice, D. R., Holohan, E. E. and Jarman, A. P. (2003). The Drosophila proneural gene amos promotes olfactory sensillum formation and suppresses bristle formation. *Development* **130**, 4683-93